THE
PHYSICAL REVIEW

A journal of experimental and theoretical physics established by E. L. Nichols in 1893

SECOND SERIES, VOL. 74, NO. 7 OCTOBER 1, 1948

On the β-Decay of Mesons

J. J. HOROWITZ,* O. KOFOED-HANSEN, AND J. LINDHARD
Institute for Theoretical Physics, University of Copenhagen, Denmark

(Received June 10, 1948)

The β-decay of cosmic-ray mesons is discussed. The possible process of decay into electron-neutrino plus a neutral particle is treated in some detail. This process is found to fit in well with the familiar formalism of β-decay of atomic nuclei. A comparison is made with present experimental data on mesons.

1. INTRODUCTION

RECENT cloud-chamber investigations of the β-decay of cosmic-ray mesons performed by Anderson *et al.*[1] and by Thompson[2] lead to values of the energy of the electron emitted lying predominantly in the neighborhood of 25 Mev. This result shows that the hypothesis of decay of the meson into an electron and a neutrino can hardly be upheld. Moreover, the experiments do not seem to exclude the possibility of a continuous spectrum of the energy of the electron, as would be the consequence of the introduction of a neutral recoil particle, of mass roughly half the mass of the decaying meson.

It is natural to consider the possibility that the neutral particle introduced in this way is the same as the neutral meson emitted in the μ-decay of the π-meson. The rather uncertain estimates of the mass of the neutral meson are so far in agreement with an assumption of this kind.

On the other hand, the spread in the value of the ratio $m_\pi/m_\mu=1.65\pm0.15$[3] could just permit a decay process in which the μ-meson decayed into an electron and a neutral meson, without emission of a neutrino. The latter process demands a definite energy of the electron, and a mass of the μ-meson $\cong 175m_e$, if $m_\pi=313m_e$.

In the present paper we shall discuss the former alternative, i.e,

$$\mu^\pm \rightarrow \mu^0 + e^\pm + \nu. \qquad (1)$$

A process of this kind may have interesting consequences as regards the interpretation of the β-decay of atomic nuclei. In fact, Klein[4] has suggested that the decay of the μ-meson should be regarded as the prototype of all β-decay processes.

Klein's proposal is primarily based on the following comparison of the decay constants; the product $f\cdot t$ of the half-life and the Fermi integral of the distribution in energy of the electron and the neutrino, as evaluated for a maximum energy of the electron of 2×25 Mev$\cong 100m_e$ (we put

* Attaché de recherches au Centre National de la Recherche Scientifique (Paris).

[1] C. D. Anderson, R. V. Adams, P. E. Lloyd, and R. R. Ran, Phys. Rev. **72**, 724 (1947).

[2] B. Rossi, Pocono Conference, March 30, 1948; see further E. C. Fowler, R. H. Cool, and J. C. Street, Phys. Rev. **74**, 101 (1948); J. L. Zar, J. Hershkowite, and E. Berezin, Phys. Rev. **74**, 111 (1948).

[3] C. F. Powell and G. P. S. Occhialini, Nature **161**, 551 (1948); C. M. G. Lattes, G. P. S. Occhialini, and C. F. Powell, Proc. Phys. Soc. **61**, 173 (1948).

[4] O. Klein, Nature **161**, 897 (1948). We are much indebted to Professor Klein for having communicated his manuscript to us before publication.

TABLE I.

	π	H^3	He^6
t	20^m	12^y	0.85^s
E (in units of m_e)	2.48	0.022	7.85
Uncertainty in E	0.03	0.004	1.00
$f\cdot t$	1700	200	800
Uncertainty in $f\cdot t$	?	a factor 2	a factor 2

$c=1$), and $t=1.5\cdot10^{-6}$ sec., is equal to

$$f\cdot t=E^5/30\cdot t\cong 500. \tag{2}$$

This value of $f\cdot t$ is just of the same order of magnitude as in the case of β-decay of the lightest nuclei.

In this connection it will be of importance to discuss the values of the decay constants of the lightest nuclei, and in particular the decay constant of H^3. The maximum energy of the electron in the β-decay of H^3 is so small that it becomes necessary to take into account the effect of the Coulomb field of the recoil nucleus. The best estimate of the half-life and the maximum energy seems to be $t=12$ years and $E^{\max}=11$ kev. We then find $f\cdot t=200$. The value of $f\cdot t$ is very sensitive to variations in the maximum energy, however. If the maximum energy is changed by 2 kev, $f\cdot t$ will change by a factor ~ 2. This calculation corresponds to zero mass of the neutrino. It was pointed out by Konopinski[5] that a non-vanishing mass of the neutrino can lead to a large increase in the value of f for H^3, and thus the $f\cdot t$ value calculated for zero mass of the neutrino may be an underestimate. Though the upper limit to the neutrino mass was recently found to be as low as 25 kev,[6] still the effect from a finite mass cannot definitely be ruled out.

On the other hand, arguments in favor of a larger value of $f\cdot t$ for H^3, as put forward on the basis of a comparison with $f\cdot t$ values of other elements, can hardly be considered as compelling, primarily because no exhaustive explanation of the variation of the $f\cdot t$ values has been found so far. But one should bear in mind also that H^3 represents an extreme case, where corrections on the Fermi theory of β-decay may be necessary because of the low maximum energy.

In Table I we shall use, with all due reservation, the tabulated $f\cdot t$ values for the lightest elements as a basis for a comparison with the β-decay of the meson.

The half-life of the neutron, $t\cong 20^m$, as found in recent experiments,[7] leads to a comparatively high $f\cdot t$ value, $f\cdot t\cong 1700$.

2. THE FERMI INTEGRAL AND THE ENERGY DISTRIBUTION

The estimate of the Fermi integral made above in the case of β-decay of the μ-meson may be improved because the neglect of the kinetic energy carried off by the recoil particle is by no means a satisfactory approximation. We shall find that a more correct evaluation of the Fermi integral leads to values which are considerably smaller than those found with neglect of the recoil.

Consider a β-decay process where a particle of mass M is transformed into a particle of mass m, an electron, and a neutrino. The available energy can for the present purpose be assumed to be so large that the extreme relativistic approximation holds for the electron and the neutrino. As to the recoil particle, however, the exact relativistic energy formula must be used. On these assumptions the maximum energy of the electron is found to be

$$E^{\max}=(M/2)(1-m^2/M^2). \tag{3}$$

The maximum energy of the electron is thus somewhat smaller than the mass difference $M-m$.

When the recoil energy is taken into account the Fermi integral can be written as

$$f_\alpha=\tfrac{1}{2}\int E_e^2dE_e\int E_\nu^2dE_\nu \times\int d\cos\vartheta\cdot(1+\alpha\cos\vartheta)\cdot\delta(M-E_e-E_\nu -[m^2+E_e^2+E_\nu^2+2E_eE_\nu\cos\vartheta]^{\frac{1}{2}}), \tag{4}$$

in the extreme relativistic approximation for the electron. Here ϑ is the angle between the directions of emission of the electron and the neutrino, and E_e and E_ν denote the energies of the electron

[5] E. J. Konopinski, Phys. Rev. **72**, 518 (1947).
[6] D. J. Hughes and C. Eggler, Phys. Rev. **73**, 809 (1948).
[7] Mr. Aage Bohr has kindly informed us of these measurements.

and the neutrino, respectively. In the factor $(1+\alpha\cos\vartheta)$ one has a choice between several values of α, all compatible with the invariance conditions imposed on the coupling between the heavy particles and the electron-neutrino field.[8] The value $\alpha=1$ corresponds to Fermi's original choice. It is noteworthy that the term $\alpha\cos\vartheta$ gives a considerable contribution to f and also affects the form of the energy spectrum of the electron, which is not the case for β-emitting nuclei, at least not for allowed transitions.

Besides the factor $(1+\alpha\cos\vartheta)$ in (4), similar expressions involving the recoil particle may be introduced as a consequence of the above-mentioned invariance conditions. The precise form of such expressions will depend on the character of the wave equation to be ascribed to the μ-meson and the neutral meson. Fortunately, it can be foreseen that these unknown terms will be of minor importance and may be neglected in the present approximation. Such a neglect is permissible if the velocity of the recoil particle is not too close to the velocity of light. This is illustrated by the following example: if the neutral meson and the μ-meson follow the Dirac wave equation, one has to introduce in (4) the extra factor $\frac{1}{2}(1+m/E_m)$, where E_m is the total energy of the recoil particle. If $m\sim\frac{1}{2}M$ the resulting correction on the Fermi integral will only amount to a few percent.

The integrations in (4) are easily performed, and lead to the formula

$$f_\alpha=(M^5/384)\{(1+\alpha)[(7/10)-5\beta+2\beta^2+2\beta^3+\tfrac{1}{2}\beta^4-\tfrac{1}{5}\beta^5+6\beta^2\log(1/\beta)]-\alpha[1-8\beta+8\beta^3-\beta^4+12\beta^2\log(1/\beta)]\},\quad(5)$$

with $\beta=m^2/M^2$. Equation (5) takes a very simple form when $\alpha=1$. Using (3) we find in this case

$$f_{+1}=E^{\max 5}/30.\quad(6)$$

The formula (6) is quite similar to the familiar extreme relativistic Fermi integral, where the recoil energy is neglected. Other values of α lead to somewhat more involved expressions for f_α. In the extreme case $\alpha=-1$, we put

$$f_{-1}=\varphi(\beta)\cdot f_{+1},\quad(7)$$

where $\varphi(\beta)$ can be found by a comparison of (5) and (6). In Fig. 1, φ is plotted as a function of β, and is in general somewhat larger than 1. For intermediate values of α the Fermi integral f_α can be found from an interpolation in Fig. 1, together with formula (6). It appears that if the masses are given, the choice $\alpha=1$ will lead to the lowest value of the Fermi integral.

In order to make a comparison with the observed β-energies one must find the form of the energy spectrum of the electron. It turns out that the spectrum is not symmetric with respect to $E^{\max}/2$, but slightly shifted towards higher energies, the shift being least pronounced for $\alpha=1$. The reason why the shift comes in is simply that the energy shared by the electron and the neutrino is not always equal to the maximum energy. If these two particles are not emitted in the same direction the sum of the energies of the electron and the neutrino will be larger than the maximum energy of the electron.

The differential contribution df_α to the Fermi integral from the energy interval E_e, E_e+dE_e is proportional to the probability of emission of an electron in this energy interval. From Eq. (4) we calculate df_α, and thus obtain the energy spec-

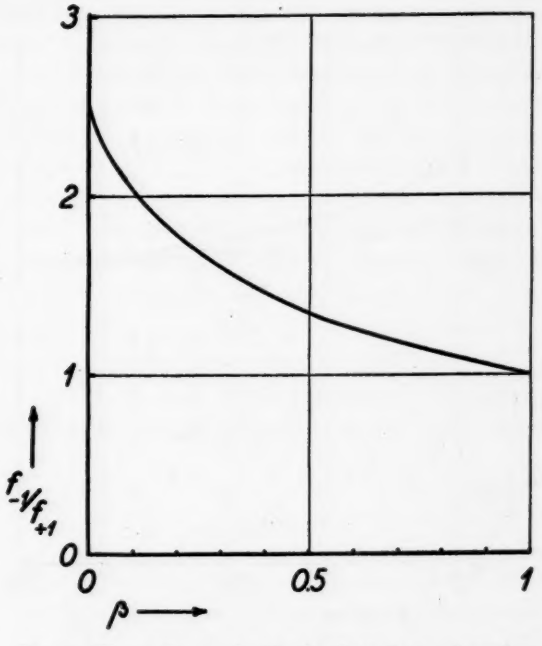

FIG. 1. The ratio $\varphi=f_{-1}/f_{+1}$ is plotted as a function of $\beta=m^2/M^2$. It is seen that $f_{-1}\approx f_{+1}$ when $\beta\approx 1$, i.e., when recoil effects can be neglected.

[8] Compare, e.g., D. R. Hamilton, Phys. Rev. **71**, 456 (1947).

TABLE II.

$\langle E\rangle$	α	E^{max}	M	m	m_π/M	$f\cdot t$
55	+1	98	216	67	1.45	450
55	−1	88	207	79	1.51	500
50	+1	90	208	77	1.50	300
50	−1	82	201	87	1.56	340
45	+1	82	201	87	1.56	190
45	−1	75	196	94	1.60	200

trum of the electron,

$$df_\alpha = dE_e \frac{E_e^2(E^{max}-E_e)^2}{6M(M-2E_e)^3} \times\{(1+\alpha)[3M^4+3M^2m^2 -E_e(12M^3+6Mm^2) +E_e^2(14M^2+4m^2)-4ME_e^3] -\alpha[3M^4+3M^2m^2-E_e(10M^3+2Mm^2) +8M^2E_e^2]\}. \quad (8)$$

The asymmetry of the β-spectrum is illustrated in Fig. 2, where the ratio of the average energy, $\langle E\rangle$, to the maximum energy, E^{max}, is plotted as a function of $\beta=m^2/M^2$, in the two extreme cases $\alpha=\pm1$.

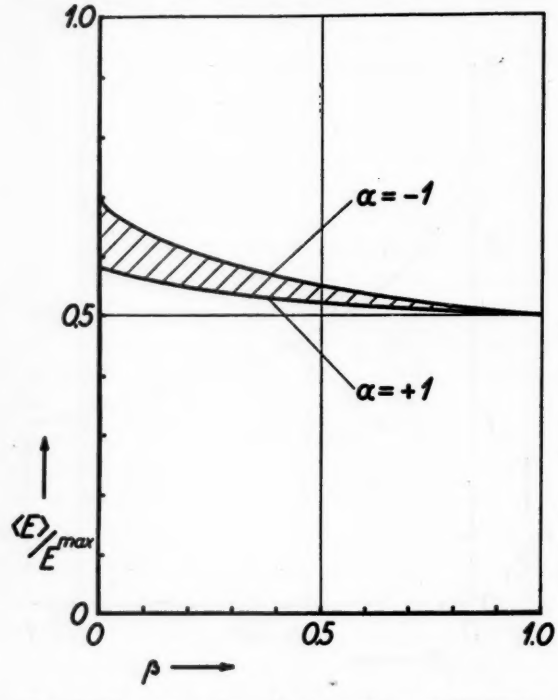

FIG. 2. The curves show the dependence of $\langle E\rangle/E^{max}$ on β, in the two extreme cases $\alpha=\pm1$. For intermediate values of α the ratio $\langle E\rangle/E^{max}$ will stay inside the hatched area.

3. COMPARISON WITH EXPERIMENTAL DATA

The observations on the β-decay of the cosmic-ray meson suggest a value of the average energy close to $50m_e$. From the average energy we can find the masses M, m if some further relations between the masses are known. As the supplementary relations we shall use the mass of the π-meson, $m_\pi=313m_e$, as measured in the artificial production of mesons in Berkeley,[9] together with the value of the kinetic energy of the μ-meson resulting from the decay of a π-meson, given by Powell and co-workers.[10] Together, these data give approximately the sum of the masses, $M+m$. We assume here that the heavy meson observed in the Berkeley experiments is the same as the π-meson found by the Bristol group. This assumption, though plausible, has not been confirmed beyond all doubt.

The values of M, m, E^{max}, m_π/M, and $f\cdot t$, as resulting from a given average energy, are listed in Table II in the two cases $\alpha=\pm1$. In order to show the dependence of these quantities on the average energy we have used three different values of the average energy, $\langle E\rangle=45$, 50, and $55m_e$.

We can compare the tabulated values of m_π/M with Powell's ratio,[3] $m_\pi/m_\mu=1.65\pm0.15$. Except for the case of $\langle E\rangle=55\cdot m_e$ the values agree fairly well with this mass ratio. For each energy the two possibilities $\alpha=\pm1$ lead to rather different mass values, while the product $f\cdot t$ remains less sensitive to the choice of α. The $f\cdot t$ values are in good accordance with those of the lightest elements, as given in Table I.

It seems probable that accurate determinations of the masses of mesons will be made in the near future. Then, the validity of the process discussed here may be tested directly, since the maximum energy is determined from the mass values, and the latitude left in the expression for the average energy as different values of α are assumed is then directly found from the two limiting curves for $\langle E\rangle/E^{max}$, as shown in Fig. 2.

[9] E. Gardner and C. M. G. Lattes, Science, March 12 (1948).

[10] C. M. G. Lattes, G. P. S. Occhialini, and C. F. Powell, Nature 160, 453 and 486 (1947).

Another way of testing the process (1) is to compare the theoretical expectations as regards the energy spectrum with the energy values actually found for the electron. It is found from (8) that the mean deviation from the average energy is, approximately,

$$\Delta E \equiv \{\langle E^2\rangle - \langle E\rangle^2\}^{\frac{1}{2}} \cong 0.2 \cdot E^{\max}, \qquad (9)$$

independent of the mass values and of the choice of α. This result contrasts strongly with the discrete energy value expected in the alternative decay process with emission of two particles instead of three.

In the case of decay of negative mesons an effect of a special kind can come in. If a slow meson is captured in an s-orbit around an atomic nucleus, the uncertainty of the momentum of the meson will be $\Delta p \sim m_\mu Ze^2/\hbar$. The uncertainty of momentum gives rise to a smearing out of the energy spectrum of the electron emitted, and the maximum energy available to the electron is increased by $\sim E^{\max} \cdot Z/137$. The change of the average energy is very small, however. In the same way, the Fermi integral and consequently the lifetime is approximately unchanged for a meson bound in medium nuclei; the small change in f tends to increase the half-life.

In this connection it should be remembered that as long as the properties of the different mesons are not known, the influence of the interaction of mesons with nuclei on the β-decay of the μ-meson cannot be appreciated. Accordingly, great caution should be observed in comparisons between experimental results and theoretical expectations as regards β-decay, in those cases where effects of interaction with nuclei may play a role.

4. EFFECT OF THE FINITE RANGE OF INTERACTION

In performing the above calculations we have assumed that the wave-lengths of the particles involved are sufficiently large to allow the transition probability to remain proportional to the volume available in phase space, i.e., the transition probability depends on the Fermi integral. Now, one cannot exclude the possibility of a departure from this simple picture. The wave-length of an electron of energy 25 Mev is $\lambda\!\!\!^{-} = 8 \cdot 10^{-13}$ cm. The three particles emitted in the β-decay will have wave-lengths of this order of magnitude, or even less. In the Fermi theory of β-decay one might expect corrections to the Fermi integral of the order of $a^2/\lambda\!\!\!^{-2}$, where a is a suitably defined range of interference of the wave functions of the particles. The value of a is possibly somewhat larger than 10^{-13} cm. A correction of this kind will probably not be so large as to affect essentially the present approximate evaluations.

On the other hand, if the β-decay is described by an intermediary mesonic coupling between the heavy particles and the electron-neutrino field as in the Yukawa theory, corrections to the Fermi integral will be of the type $a/\lambda\!\!\!^{-}$. More definitely, one obtains as a weight factor in the Fermi integral (4) a term of the type $m_1^2/(m_1 - E_e - E_\nu)^2$, where m_1 is the mass of the meson responsible for the coupling. If $m_1 \sim 300 m_e$ the result will be an increase of the Fermi integral by a factor ~ 2, while the energy spectrum of the electron remains nearly unchanged. Moreover it is seen that the Fermi integral is quite sensitive to the value of the mass m_1, and for small values of m_1 the energy spectrum is changed appreciably. However, the familiar description of the interaction of mesons with nucleons meets with well-known difficulties, and in the present treatment we have omitted corrections of the above kind, even though the corrections will seem to be of importance in mesonic descriptions of β-decay.

Our thanks are due Professor C. Møller for discussions on the subject of the present paper.

PHYSICAL REVIEW VOLUME 74, NUMBER 7 OCTOBER 1, 1948

Nuclear Quadrupole Interaction in CsF*

J. W. TRISCHKA
Columbia University, New York, New York
(Received June 4, 1948)

The electric resonance method of molecular beam spectroscopy has been used under high resolution conditions to study the rotational Stark spectrum of CsF for a single rotational state of the molecule, $J=1$. In this method polar molecules in a single rotational state and a particular state of space quantization are selected from a molecular beam by means of inhomogeneous electric fields which give the desired molecules a unique, sigmoid path in the apparatus. Changes in the beam intensity are observed when a change in the space quantization of the molecule is produced by an oscillating electric field transverse to a homogeneous, steady electric field. For weak electric fields the observed line widths agree well with the estimated uncertainty width of 10 kc/sec. At stronger fields inhomogeneities in the field cause a broadening of the lines. At sufficiently strong fields the spectrum for CsF contains several broad lines, each of which is due to transitions of molecules in a particular vibrational state. As the field strength is decreased the resolution improves and these lines reveal a complex fine structure, the principal features of which can be explained by the interaction of the electric quadrupole moment of the Cs nucleus, spin 7/2, with the molecular electrons and the F nucleus. The F nucleus, spin 1/2, has no quadrupole moment. A complete, quantitative explanation of the spectra requires the existence of a cosine type coupling between the nuclear spins and the molecular spin of the form $c\mathbf{I}\cdot\mathbf{J}$, and a correction for the spin-spin interaction of the two nuclei. At weak fields a different type of spectrum appears, permitting an independent evaluation of the nuclear-molecular interactions. The data allows a determination of both the magnitude and sign of the interaction constants. The quadrupole interaction, defined by $(e^2q'Q/2h)$, is $(+0.310\pm0.002)$ mc/sec. The constants, c/h, for the $\mathbf{I}\cdot\mathbf{J}$ interactions for F and Cs are, respectively, $(+16\pm2)$ kc/sec and (0 ± 1) kc/sec. The difference in the quadrupole interaction for the first two vibrational states is less than the experimental error; i.e., less than one percent. Application of the method to the measurement of various molecular constants is discussed briefly at the end of the paper.

I. INTRODUCTION

THE magnetic resonance method of molecular beam spectroscopy has been used for the measurement of the electric quadrupole moment of the deuteron[1] and the quadrupole interaction in the sodium halides.[2] A significant difference between these two experiments is that in HD and D_2 the spectra can be attributed to molecules having specific, small values of the rotational quantum number, J; whereas, in the sodium halide experiments a statistical analysis involving many $J\gg1$ is necessary to account for the spectra. This difference is a result of the large difference in the temperatures of the two molecular sources.

The advent of the electric resonance method[3] has now made possible measurements of the quadrupole interaction in molecules in a specific rotational state, even though the molecular beam is produced by a high temperature source. The essence of the method is that it selects for study only that part of the beam, about one part in ten thousand, which contains molecules in a particular J state. Its advantages for high temperature beams are the simplicity of interpretation of results and greater accuracy.

The electric resonance apparatus, shown schematically in Fig. 1,** makes use of the deflecting power of the inhomogeneous fields (A- and B-fields) to select for detection polar molecules with a particular J and a particular electric quantum number, m_J. The wire stop eliminates molecules with large values of J, as they are not appreciably deflected by the A- and B-fields. In passing through a homogeneous electric field (C-field) the molecules can change their state of space-quantization (change in m_J) through absorption or stimulated emission of radiation in the presence of a superposed oscillating electric field set at a frequency corresponding to the energy difference of the initial and final states. When this occurs they fail to reach the detector, as shown by the dashed line in Fig. 1, and the measured beam intensity drops.

* Publication assisted by the Ernest Kempton Adams Fund for Physical Research of Columbia University.

[1] J. M. B. Kellogg, I. I. Rabi, N. F. Ramsey, and J. R. Zacharias, Phys. Rev. 57, 677 (1940).

[2] W. A. Nierenberg and N. F. Ramsey, Phys. Rev. 72, 1075 (1947).

[3] H. K. Hughes, Phys. Rev. 72, 614 (1947).

** The author is indebted to Dr. H. K. Hughes for the use of this figure, which is Fig. 1 in reference 3.

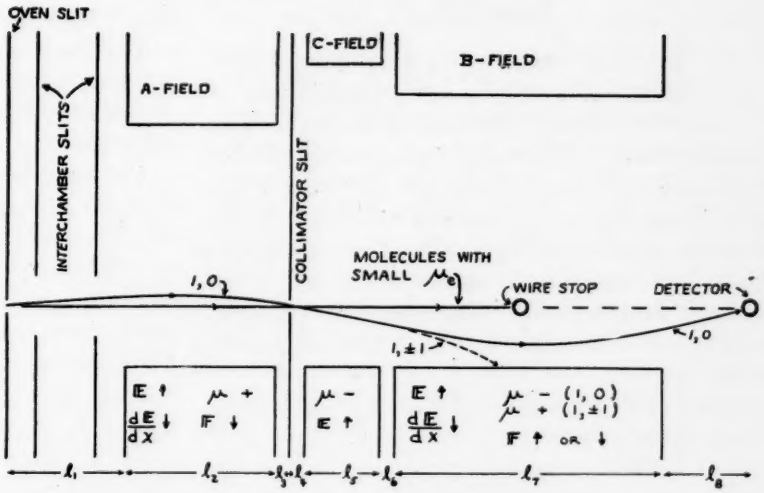

FIG. 1. Schematic diagram of electric resonance apparatus.

It has been shown[3] that the spectral lines in CsF resulting from such a change in m_J yield values of the electric dipole moment and moment of inertia of the molecules. The present paper is a report of an experimental study of these lines in CsF under high resolution conditions and an analysis of the spectra observed. With the present high resolution the single lines found by Hughes[3] show a fine structure which can be attributed to two principal causes: *viz.*, the presence in the beam of molecules in different vibrational states and the electric quadrupole moment of the Cs nucleus. Secondary details of this fine structure are explained by assuming that a cosine type coupling exists between the nuclear spins and the molecular rotation and by making a small correction arising from the magnetic dipole-dipole interaction of the Cs and F nuclei.

II. EXPERIMENTAL DETAILS

The apparatus used in these experiments is essentially the same as that used, and described in considerable detail, by Hughes,[3] with one important exception. This is the *C*-field, which is completely new.

C-Field

The component of the apparatus crucial for high resolution is the *C*-field. This must produce an electric field of great uniformity. Figure 2 shows the essential elements of the field used in these experiments. Two parallel, brass plates, $\frac{1}{4}$ inch thick, 1 and 2, are clamped together against three, ground, quartz spacers and mounted so that the molecular beam passes midway between them. Plate 2 is composed of two parts, 3 and 4, separated by a space of 0.016 inch. A steady, homogeneous electric field is produced over the length of 3 and over the height of the beam, about 5 mm, by applying a d.c. voltage from *B*-batteries to 1 and 2. Three and 4 are at the same d.c. potential. An oscillating electric field is superposed on the steady fields by connecting the output of a vacuum tube oscillator to 3 and 4. In this way the oscillating field has an appreciable strength only in the region where the steady field is uniform.

The field gap is 0.4983 cm. The overall length is 6 cm, and the length (along the beam) of 3 is 4 cm. The plates are ground flat to 0.00025 cm and gold-plated to eliminate changes in the contact potential difference from tarnishing of the brass.

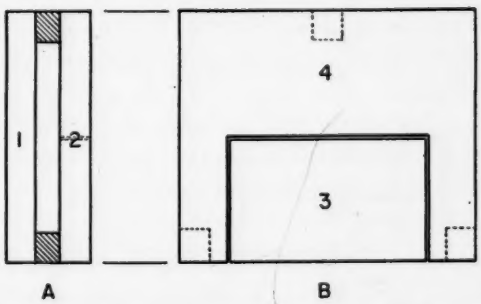

FIG. 2. Two views of the *C*-field, showing the basic features of the design. *A* is a view in the direction of the molecular beam. *B* is a side view of *A*.

Resolution

The resolution possible with the present *C*-field construction is determined by the uniformity of the electric field and by its effective length. The lower limit of resolution set by the non-uniformity of the field corresponds to 1 part in 2000 of the field strength or 1 part in one thousand of the frequency, since the frequency of the rotational Stark line varies as the square of the field. This gives an estimated line width (full width at half-maximum) of 7 kc/sec at a transition frequency of 3.7 mc/sec.

The width to be expected from the uncertainty relationship

$$\Delta\nu\Delta\tau\sim 1 \qquad (1)$$

is 10 kc/sec. $h\Delta\nu$ is the uncertainty in the energy and $\Delta\tau$ is the time spent by the molecules in the radiation field. In this case $\Delta\tau$ is computed using the most probable velocity of the molecules at an oven temperature of 800°K, 4×10^4 cm/sec, and an effective length of the field of 4 cm.

The effect of the magnitude of the oscillating field on the resolution can be calculated from the expression for the transition probability[3]

$$P=0.5/[1+(E_{dc}/E_{rms})^2(1-f/f_0)^2]. \qquad (2)$$

E_{rms} is the rms value of the oscillating field, while E_{dc} is the value of the steady field. For experiments with strong fields, where this formula is valid, typical values were $E_{dc}=100$ v/cm and $E_{rms}=0.16$ v/cm; $f_0=3.7$ mc/sec. These give a width of 12 kc/sec.

The theoretical width resulting from a combination of the above estimates was not calculated. However, the observed width of lines produced by a single transition in the vicinity of 3.7 mc/sec was 16 kc/sec, so that it is reasonable to conclude that the experimental limit of resolution was reached.

The line width at weak fields, $E_{dc}\sim 2$ v/cm, is in close agreement with the width calculated from (1). E_{rms} was 1 v/cm.

Beam Intensities

The CsF beam was detected with a hot W wire, 0.005 inch in diameter, at the surface of which the neutral molecules were ionized. The ion current was measured with a d.c. amplifier[4] employing an FP54 tube and a 5×10^{10} ohm grid resistor. The sensitivity of the amplifier was 50,000 mm/volt on a scale two meters from the galvanometer.

The total beam, with the stop-wire removed, gave an equivalent galvanometer deflection of 300,000 cm. The refocused beam in the (1,0) state produced a 30 to 40 cm deflection. The need for such a large beam arose from the fact that a great many lines are resolved; in fact the maximum change in beam strength corresponding to a single transition gave a deflection of only 2 to 3 cm.

Three factors contributed to the galvanometer deflection at any instant of time: (1) detector "noise", (2) a residual beam; i.e., a beam detected with the wire-stop in place, but with the *A*- and *B*-fields turned off, (3) the refocused beam. The residual beam was usually as large as, sometimes less than, the refocused beam. Unsteadiness in all of these factors, chiefly the detector "noise", required that measurements be made by noting the change in deflection produced by turning the oscillator on and off and averaging four successive readings. With this procedure the minimum detectable change in beam strength was 3 mm, under the best conditions. This corresponds to a change of about 10^4 molecules/sec or 10^6 molecules/cm^2/sec for a beam 5 mm high.

Procedure

The procedure for measuring changes in beam strength has been detailed above. In addition, measurements were made of the frequency of the oscillating field and the voltage applied to the homogeneous field. At strong fields the relative positions of the lines in the fine structure due to the nuclear-molecular interactions is independent of the field strength. Hence, it is possible to fix the frequency and vary the field, to scan the spectrum, or to fix the field and vary the frequency. The latter method was used in gathering all the important data reported on here. The voltage was measured with a type *K* potentiometer and held constant to 1 part in 5000. Frequency was measured with a General Radio Type 624A heterodyne frequency meter to 1 part in 10,000.

[4] D. B. Pennick, Rev. Sci. Inst. 6, 115 (1935).

Measurements at zero electric field would have been desirable both because of the simplicity of the line structure and as an independent check on the strong field measurements. However, the transition probability vanishes at zero field.[3] Thus it was necessary to work at a field strong enough so that transitions could be observed but not so strong that effects caused by the interaction of the molecule with the field were large.

In practice it was found that as the strength of the homogeneous field was decreased the strength of the refocused beam dropped because some of the molecules were undergoing nonadiabatic transitions[5] in the regions between the C-field and the two focusing fields. This effect set the lower limit of weak field operation.

III. THEORY

The Hamiltonian used as a basis for theoretical calculations was

$$\begin{aligned}\mathcal{H}=&(\hbar^2/2A)\mathbf{J}^2-\boldsymbol{\mu}\cdot\mathbf{E}\\&-e^2q'Q/I_1(2I_1-1)(2J-1)(2J+3)\\&\times[3(\mathbf{I}_1\cdot\mathbf{J})^2+\tfrac{3}{2}(\mathbf{I}_1\cdot\mathbf{J})\\&-I_1(I_1+1)J(J+1)]+c_1\mathbf{I}_1\cdot\mathbf{J}\\&+c_2\mathbf{I}_2\cdot\mathbf{J}+g_1g_2\mu_N^2/r^3(2J+3)(2J-1)\\&\times[3(\mathbf{I}_1\cdot\mathbf{J})(\mathbf{I}_2\cdot\mathbf{J})+3(\mathbf{I}_2\cdot\mathbf{J})(\mathbf{I}_1\cdot\mathbf{J})\\&-2\mathbf{I}_1\cdot\mathbf{I}_2J(J+1)].\end{aligned}\quad(3)$$

The first term, in which A is the moment of inertia of the molecule and J is the rotational quantum number, corresponds to the mechanical energy of rotation of the molecule. This remains unchanged in these experiments, since $J=1$ at all times. The second term gives the splitting produced by the interaction between the electric dipole moment, μ, and the electric field, E. Reference 3 gives a summary of the energy levels arising from this term alone. The third term is the operator for the interaction between the electric quadrupole moment of the Cs nucleus, Q, and the electric field gradient at this nucleus produced by the remaining charges in the molecule. Q and q' are defined by Nordsieck[6] and in reference 1. I_1 is the spin of the Cs nucleus. The theory of Fano[7] was used in calculating the matrix elements given by this term. Since the F spin is $\frac{1}{2}$, this nucleus has no electric quadrupole moment, whence the absence of a quadrupole term for it in (3). The third and fourth terms, where I_2 is the spin of the F nucleus, represent perturbations produced by a cosine coupling between the nuclear spins and the molecular rotation. They can be thought of as representing the interaction between the nuclear magnetic dipole moment and a magnetic field produced at the nucleus by a current set up by the molecular electrons as a result of the rotation of the molecule. A more detailed picture of this type of interaction is discussed by Foley[8] and by Wick.[9] Calculations for this interaction made use of the formulas presented by Nierenberg and Slotnick.[10] The last term comes from the small perturbation produced by the coupling of the two nuclear magnetic dipole moments. g_1 and g_2 are the nuclear gyromagnetic ratios of the Cs and F nuclei respectively; μ_N is the nuclear magneton and r is the internuclear distance of the molecule. The operator in this form is taken from reference 1. The matrix elements, calculated by Nierenberg,[11] are given in an appendix to this paper.

In analyzing the observed spectra it is necessary to take into account the fact that the refocused beam contains molecules in several different vibrational states. It is reasonable to assume that the main effect of vibration is to change the average electric dipole moment and the average moment of inertia of the molecule as the vibrational state changes. This means that the second term in (3) will be different for different vibrational states, and the observed spectrum will be a superposition of lines from molecules in different vibrational states. No theoretical estimates are available for the effect of vibration on the constants in the other terms of (3). However, from the data presented in this report it is possible to make an experimental estimate of the magnitude of such an effect.

In general the terms in (3) will be different for different isotopic species. However, CsF has only one isotopic species. This greatly simplified the experimental work and the analysis of the data.

In the application of the perturbation theory

[5] I. I. Rabi, Phys. Rev. **49**, 324 (1936).
[6] A. Nordsieck, Phys. Rev. **58**, 310 (1940).
[7] U. Fano, J. Res. Nat. Bur. Stand., Wash., **40**, 215 (1948). Energy level charts in this paper are directly applicable to CsF.
[8] H. Foley, Phys. Rev. **72**, 504 (1947).
[9] G. C. Wick, Phys. Rev. **73**, 51 (1948).
[10] W. A. Nierenberg and M. Slotnick, Phys. Rev. **73**, 1437 (1948).
[11] W. A. Nierenberg, private communication.

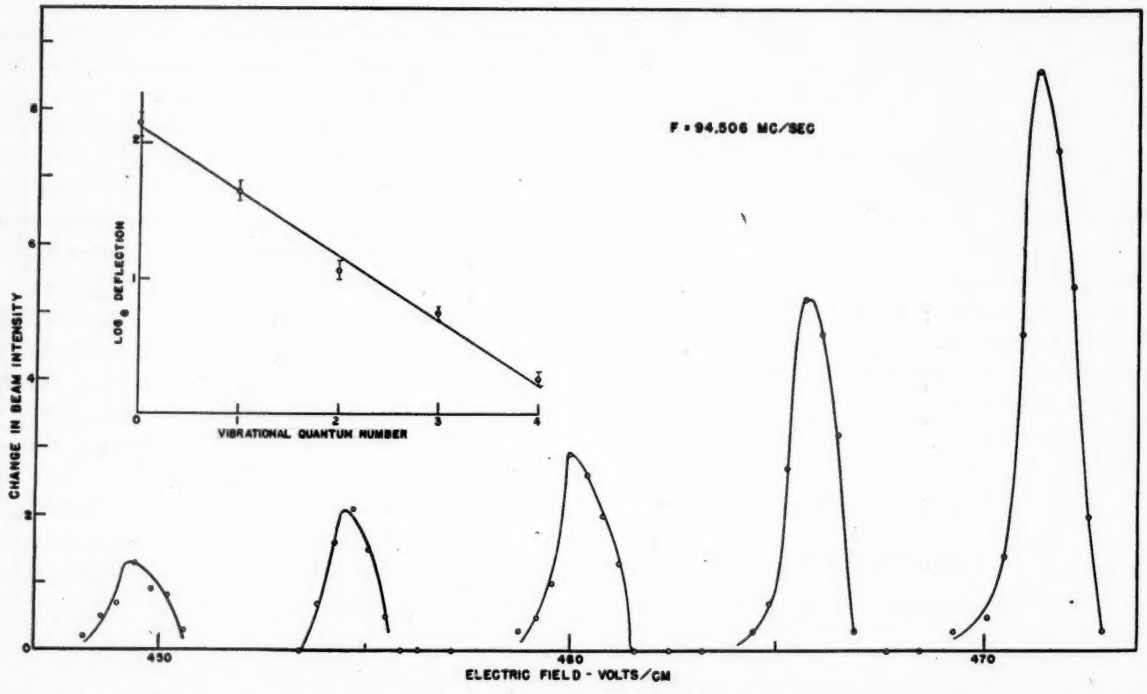

FIG. 3. Spectrum at strong fields, showing lines produced by molecules in five different vibrational states. The fine structure resulting from nuclear-molecular interactions is not resolved. The graph in the upper left corner is a semi-log plot showing the distribution of vibrational states. v is the vibrational quantum number.

to computing the characteristic values of (3) it is convenient to distinguish two cases for which the theory is relatively simple. "Strong fields" are defined for this purpose as fields for which

$$e^2q'Q \ll \mu^2E^2/\hbar^2/2A \ll \hbar^2/2A \times J(J+1). \quad (4)$$

In this case the electrical terms are diagonal in an m_J, m_{I_1} representation, i.e., the molecular and nuclear spins are effectively decoupled. It is noteworthy that in this instance, $\hbar^2/2A \times J(J+1) \gg \mu^2E^2/\hbar^2/2A$, there is a negligible mixing of J-states and therefore Casimir's expression for the quadrupole interaction, which is diagonal in J, is correctly applied. Hence, since I and J are in effect decoupled, the matrix elements in reference 1 are suitable. For CsF the errors in making this approximation are less than the errors of measurement, for $e^2q'Q/2h \sim 0.3$ mc/sec while $(\hbar^2/2Ah)J(J+1) \sim 10{,}000$ mc/sec.

An important consequence of the strong field theory is that the fine structure produced by the terms beyond the second one in (3) is independent of the value of the field, thus rendering unnecessary a knowledge of the magnitude of the field.

"Weak fields" are defined by

$$e^2q'Q \gg \mu^2E^2/\hbar^2/2A. \quad (5)$$

In this case I_1 and J are strongly coupled and an F_1, m_{F_1} representation is used, so that the quadrupole interaction will contribute only diagonal elements to the energy matrix. $\mathbf{F}_1 = \mathbf{I}_1 + \mathbf{J}$.

IV. ANALYSIS OF SPECTRA

Value of J

It was decided at the beginning of these experiments to obtain spectra from molecules for which $J=1$, this being the state easiest to refocus with the present apparatus. However, it is possible to refocus CsF molecules with several values of $J \geqslant 1$, depending on the A- and B-field voltages. In addition, more than one value of J may be represented in the beam refocused for a particular set of refocusing conditions. Two different methods were used for determining J.

The first method makes use of the uniqueness of the fine structure for a given $(J, m_J) \rightarrow (J, m_{J'})$ transition. This was not so easy as might be anticipated. For example, calculations showed

that the $(2, \pm 1) \rightarrow (2, \pm 2)$ and $(1,0) \rightarrow (1, \pm 1)$ transitions should give fine structure patterns which are identical at strong fields, except for a difference in sign, and small differences due to the $\mathbf{I} \cdot \mathbf{J}$ interaction not experimentally detectable. At weak fields the predicted patterns are different, but still not sufficiently different to make a distinction experimentally. However, when the value of the quadrupole interaction computed from the weak field data was compared with the value computed from the strong field data it was found that the two values disagreed by much more than the experimental error if the spectra were attributed to $J=2$. On the other hand, they agreed satisfactorily when the assumption was made that $J=1$.

In the second method observations of the $\boldsymbol{\mu} \cdot \mathbf{E}$ interaction were made for two different values of J and compared. Such a comparison permits an unambiguous identification of both J's. A brief review of the procedure follows.

The transition frequency corresponding to $(J, m_J) \rightarrow (J, m_J')$ is given by[3]

$$\nu = K_1(J, m_J, m_J')E^2 + K_2(J, m_J, m_J')E^4, \quad (6)$$

if only the $\boldsymbol{\mu} \cdot \mathbf{E}$ interaction is taken into account. This frequency can be readily calculated once the analysis of the fine structure produced by the other terms in (3) has been carried out.

The most precise way of comparing results for two different values of J is to obtain the ratio

$$K_1(J_1, m_J, m_J')/K_1(J_2, m_J'', m_J'''), \quad (7)$$

which can be predicted from the theory. K_1 was determined with a precision of 1 part in 3000 by plotting ν/E^2 *vs* E^2 and extrapolating the straight line so obtained to $E=0$. In this way the transitions $(1, 0) \rightarrow (1, \pm 1)$ and $(2, 0) \rightarrow (2, \pm 1)$ were identified. An additional check on the $(1, 0) \rightarrow (1, \pm 1)$ transition was also obtained by a comparison with Hughes'[3] results.

The spectra analyzed in this paper are all from molecules for which $J=1$. The spectra obtained for $J=2$ were observed at fields too high for good resolution, and were consequently of no value in evaluating the nuclear-molecular interactions.

Vibrational Effects

Figure 3 shows the spectrum obtained with an electric field so strong that the $(1, 0) \rightarrow (1, \pm 1)$ transitions are displayed for molecules in the first five vibrational states. In this run the fre-

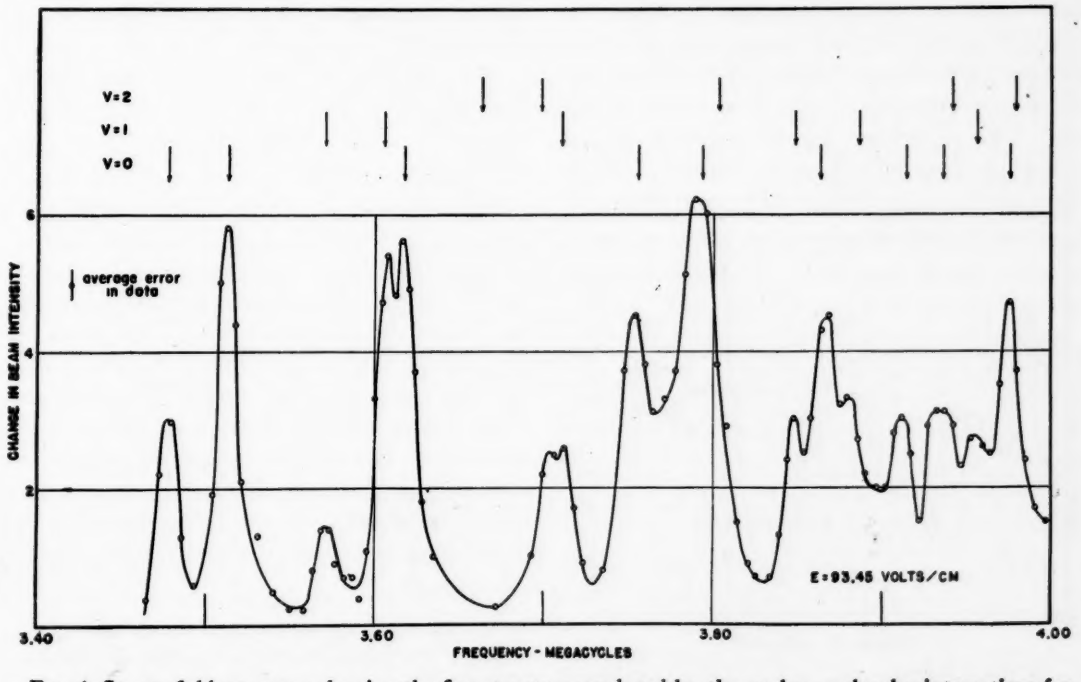

FIG. 4. Strong field spectrum showing the fine structure produced by the nuclear-molecular interactions for molecules in several vibrational states. Arrows at the top of the figure indicate theoretical line positions. v is the vibrational quantum number.

quency was held constant at 94.506 mc/sec and the field varied. That this spectrum does show the presence of several vibrational states can be demonstrated in two ways: (1) When spectra were observed at several different field strengths, a straight line resulted from a plot of ν/E^2 *vs* E^2 for each of the spectral lines. This would be expected from (6) if the individual lines arise from molecules having slightly different values of μ and A; (2) a plot of the logarithm of the peak intensities of the lines as a function of the vibrational quantum number, v, is a straight line (shown in the upper left hand corner of Fig. 3). Thus the distribution of the molecules producing the lines is the same as the distribution of vibrational states in a molecular gas.

Data was taken at larger fields than those shown in Fig. 3 to insure that the most intense line in the figure actually corresponded to $v=0$.

The width of the lines in Fig. 3 is produced by the unresolved fine structure, arising from the nuclear-molecular interactions and the field inhomogeneity. The latter alone would produce a line width of 0.5 v/cm.

Since the frequency separations of the "vibration" lines varies as E^2 while the fine structure produced by the nuclear-molecular interactions remains constant until intermediate fields are reached, it is evident that the spectra from the molecules in different vibrational states will eventually overlap as the field strength is decreased. This is the case for the results shown in Fig. 4 where the lines corresponding to various vibrational states are indicated by the arrows at the top of the figure for three different states. It is clear from the complexity of the spectra in Fig. 4 that the data presented in Fig. 3, where the vibrational effect is completely unambiguous, is invaluable in assigning the lines in Fig. 4 to molecules in the various vibrational states.

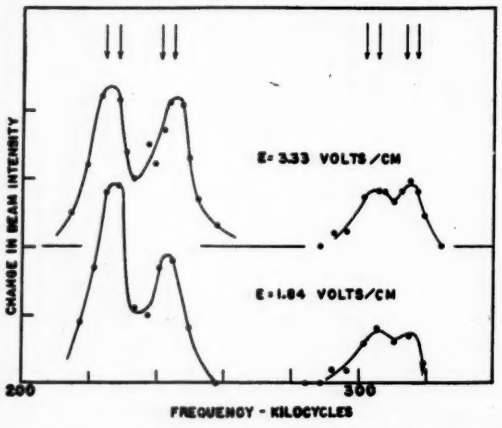

FIG. 5. Weak field spectra for two different values of the field. Arrows show the theoretical positions of lines at zero field.

For the weak fields indicated in Fig. 5 the spectral shift produced by the $\boldsymbol{\mu}\cdot\mathbf{E}$ interaction for molecules in different vibrational states is less than 1 kc. This is far below the resolution of the apparatus.

Structure At Strong Fields

Figure 4 shows the spectrum obtained at strong fields, but with sufficient resolution to reveal the fine structure produced by the nuclear-molecular interactions. Since the main features of this structure are due to the quadrupole interaction it is necessary to make certain that the "strong field" theory applies. Discussion, at this point, will center on the lines for which $v=0$. There are nine such lines, as indicated by the arrows in the figure. The total spread of the spectrum is a rough measure of the quadrupole interaction. This is 0.499 mc/sec. The frequency corresponding to the $\boldsymbol{\mu}\cdot\mathbf{E}$ interaction alone is 3.74 mc/sec, so that the ratio of the two is 7.5/1. Calculations show that this ratio is large enough to satisfy (4) very well.

The detailed calculations of the theoretical line positions are too lengthy to present here. Therefore, only pertinent aspects of the theory will be given. Since $I_1=7/2$, $I_2=1/2$ and $J=1$, at most 48 energy levels will be involved. The quadrupole interaction alone gives rise to 24 energy levels which are degenerate in such a way that 8 levels correspond to $m_J=\pm 1$ and 4 to $m_J=0$. If the oscillating field is perpendicular to the steady field the selection rules are $\Delta m_J=\pm 1$ and $\Delta m_{I_1}=0$, so that 14 lines are predicted. Of these, only 8 should be resolved. Since the oscillating field actually has components both parallel and perpendicular to the steady field, there is a small possibility of observing lines for which $\Delta m=0$, $(m=m_J+m_{I_1})$. No such lines were found, however.[12]

[12] The presence of corresponding lines was observed at intermediate fields. Results at these fields are not presented because the theoretical calculations are highly involved, and preliminary calculations showed that no new information was available from these measurements.

An examination of Fig. 4 reveals nine lines instead of eight. A detailed comparison of the experimental and theoretical lines gives good agreement for all of the lines except lines 7 and 8, counting from low to high frequencies. In this case the predicted line falls midway between 7 and 8. Hence, we conclude that the results cannot be explained by the quadrupole interaction alone, but the contributions of the other terms in (3) must be considered.

Calculations for the $\mathbf{I}\cdot\mathbf{J}$ interaction show that the effect of the Cs spin is to shift the quadrupole lines slightly, while the F spin produces a splitting of the levels for $m_J=\pm 1$. Because of the way in which some of the states for $m_J=\pm 1$ are mixed by the quadrupole interaction the effect of the $\mathbf{I}\cdot\mathbf{J}$ interaction for the F nucleus, is largely suppressed except for one of the quadrupole levels. It is precisely the transitions from this split level which correspond to lines 7 and 8. The theory shows that the constant c_2 is just equal to the energy separation of lines 7 and 8. As the result of several runs this separation is found to be 22 kc/sec. However, this must be corrected for the effect of the nuclear dipole-dipole interaction.

Calculations for the dipole-dipole interaction show that its observable effects in this case are indistinguishable from the effect of the $\mathbf{I}\cdot\mathbf{J}$ interaction. Fortunately the values of g_1, g_2 and r are known so that exact calculations can be made. The result is a correction of 4 kc/sec which makes the value of $c_2/h=18$ kc/sec.

An additional comparison between theory and experiment can be made by considering the line intensities. For example, the ratio of the intensities of lines 1 and 2 should be one to two according to the theory, and this agrees with the intensities shown in Fig. 4. Agreement also exists for line 3, theoretical weight two, on this scale. Lines 4 and 5 are made up of a number of unresolved lines, but the observed intensities seem to be in agreement with estimates made by combining the effects of the theoretical lines. Lines 6 and 9 should each have a weight of one, and their large, observed peak intensities are doubtless the result of the presence of so many nearby lines for $v=0$ and $v>0$. Intensity considerations also give striking confirmation of the predictions for the $\mathbf{I}\cdot\mathbf{J}$ interaction. The line predicted between 7 and 8, considering the quadrupole coupling alone, had a weight of one. Lines 7 and 8 are clearly much weaker than 6 and 9.

TABLE I. Comparison of experimental and theoretical relative positions of lines at strong fields for $v=0$. Frequencies in kc/sec. Lines counted from the low frequency end of the spectrum. (Cf. Fig. 4.)

Line	Exp.	Theor.
1	−263	−263
2	−228	−228
3	—	−123
4	+ 14	+ 15
5	+ 51	+ 53
6	+126	+123
7	+172	+174
8	+195	+196
9	+236	+236

The effect of vibration on the quadrupole interaction must be less than one percent for CsF, since the fine structure separations for higher vibrational states is in experimental agreement with the separations for $v=0$. The absence of line 1 for $v=2$ in Fig. 4 is due to the absence of data in this run. Other runs show the line to be present. Additional lines for $v>0$ beyond the high frequency end of Fig. 4 have also been observed and their positions agree with the theoretical predictions.

Structure at Weak Fields

Figure 5 shows the spectra obtained at two different, weak electric fields. According to the theory for the quadrupole interaction at weak fields there will be three levels corresponding to $F_1=9/2,\ 7/2,\ 5/2$. Thus two lines are predicted from $\Delta F_1=\pm 1$. Figure 5, however, shows two groups of lines, a pair of lines in the low frequency group and a broad line, presumably made up of several unresolved lines, at a higher frequency. If the $\mathbf{I}\cdot\mathbf{J}$ interaction is taken into account, this discrepancy is resolved. The theory predicts four lines, occurring in two closely spaced pairs in the low frequency group, and four lines nearly evenly spaced in the high frequency group. These lines are indicated by the arrows in Fig. 5. As was the case at strong fields the dipole-dipole interaction is indistinguishable from the $\mathbf{I}\cdot\mathbf{J}$ interaction experimentally. Again, a small correction must be made for it.

Although the effect of the $\boldsymbol{\mu}\cdot\mathbf{E}$ interaction is small in comparison with the quadrupole effect it is not entirely negligible for the fields indicated

TABLE II. Experimental positions of lines at weak fields. Frequencies are in kc/sec. Lines are counted from the low frequency end of the spectrum. (Cf. Fig. 5.)

Line	ν
1	226
2	243
3	310

in Fig. 5. Calculations using the appropriate formula in reference 10 show that only the level $F_1=5/2$ is measurably affected. The result is that there should be 14 unresolved lines in the high frequency group. Since the positions of these lines depend on field strength the experimental agreement at the two field values shown in Fig. 5 seems strange. However, the lines shift in relative positions with no appreciable change in their center of gravity in going from the smaller to the larger field.

No effort has been made in this case to calculate the relative intensities of the lines.

The complete explanation of these results by the analysis outlined above leaves no room for effects due to vibration of the molecules. The experimental upper limit set on the possible change of the quadrupole interaction with vibrational state is about 2 percent. Thus, the strong field data are more conclusive on this point than the weak field data.

V. RESULTS

Table I shows the experimental and theoretical positions of the lines in Fig. 4 for $v=0$. The center of reference is the frequency which would correspond to the $\mu\cdot\mathbf{E}$ transitions alone. In this table theoretical lines which would be experimentally unresolved have been "merged" in calculating the theoretical positions presented. Table II shows the experimental positions of the lines in Fig. 5. Table III shows the constants required to give the best fit between the theory and the experimental results. The magnetic fields at the Cs and F nuclei, H_1 and H_2, produced by the molecular rotation are computed from c_1 and c_2 by means of the formula

$$H=(hc/\mu_N g). \tag{8}$$

This is the field per unit rotation.

TABLE III. Interaction constants calculated from the strong and weak field spectra. Subscripts 1 and 2 refer to Cs and F nuclei respectively. See text for definitions of symbols.

Quantity	Strong field	Weak field	Average
$eq'Q/2h$, mc/sec	+0.312±0.002	+0.307±0.004	+0.310±0.002
c_1/h, kc/sec	−0.6±1	+0.5±1	0±1
c_2/h, kc/sec	+18±2	+14±3	+16±2
H_1, gauss	−1±2	+1±2	0±2
H_2, gauss	+4.6±0.5	+3.5±0.7	+4.0±0.5

The errors stated are a result of uncertainty in estimating line positions. The value of the quadrupole interaction constant at strong electric fields is based on the positions of all of the observed lines and is more accurate than the value determined at weak fields, where the error in determining the center of the line pattern for the high frequency group was relatively large.

It is important to note the relative merits of evaluating the constants in Table III from strong and weak field data. Besides the relative accuracies discussed above there are features unique to each case. The sign of the quadrupole interaction constant can be determined from the strong field data by observing the asymmetry of the fine structure pattern. The weak field data yields only the magnitude and not the sign of this constant. On the other hand the sign of c_2 can be determined only from the weak field data and not from the strong field data. c_1 is so small that its sign is in doubt in either case in these experiments, but theoretically the sign could be determined from either the strong or weak field results.

VI. DISCUSSION

It is of interest to compare the results presented here with results obtained by the magnetic resonance method. To make this comparison for the quadrupole interaction, unpublished data of Millman and Kusch on the Cs resonance in CsF was used. The theoretical shape for their resonance curve is given by Feld and Lamb in Fig. 6 of their paper.[13] This curve has a central maximum with six symmetrically placed "spikes" of decreasing intensity on either side of it. The experimental curve is a perfectly smooth, resonance curve, the "spikes" being unresolved. It is therefore difficult to make an accurate estimate of the quadrupole interaction constant without a detailed analysis of the resolution of the magnetic resonance apparatus. In lieu of this the half width of the experimental curve was taken arbitrarily to

[13] B. T. Feld and W. E. Lamb, Phys. Rev. 67, 15 (1945).

be the same as the distance between $1-2x$ and $1+2x$ on the theoretical curve. The result,

$$e^2q'Q/2h=0.31 \text{ mc/sec}$$

agrees even better than might be expected, considering the approximations made in the analysis, with the result reported here. The sign of the interaction cannot be determined from the magnetic resonance data.

It was not thought worth while to attempt an estimate of the constant c_1/h for the Cs $\mathbf{I}\cdot\mathbf{J}$ interaction from the magnetic resonance data, since the accuracy of such an estimate would be at least an order of magnitude less than the accuracy of this constant determined by the electric resonance method. However, the agreement between the two values of $e^2q'Q/2h$ indicates that the small value of c_1/h reported in this paper is consistent with the magnetic resonance results.

The value of H_2 presented in Table III can be compared with the value calculated by Wick[9] using the magnetic resonance data from reference 2; *viz.*, 1.8 gauss. The discrepancy between the two values, amounting to more than a factor of two, is far beyond the experimental error in both methods of measurement. If this discrepancy is real, it may indicate that the $\mathbf{I}\cdot\mathbf{J}$ interaction is given by $f(J)(\mathbf{I}\cdot\mathbf{J})$ instead of $c\mathbf{I}\cdot\mathbf{J}$, where $f(J)\rightarrow 1$ for $J\gg 1$. Further experiments are indicated in which the $\mathbf{I}\cdot\mathbf{J}$ interaction is studied as a function of J. It is important to note that the sign of the interaction is not given by the magnetic resonance method.

Since the measurements of the quadrupole interaction give neither the value of q' nor of Q, but only their product, the important problem of separating the two quantities still remains. However, if the same nucleus is present in different molecules, the product, $q'Q$, gives some information about the changes in molecular binding. In this connection it is interesting to note the striking difference between the present results and those deduced from measurements made by the magnetic resonance method on Cs_2;[14] *viz.*,

$$e^2q'Q/2h=0.074 \text{ mc/sec}$$

This difference is qualitatively the same as that already noted by Nierenberg and Ramsey[2] for the sodium halides and Na_2. The theory used as a basis for the above estimate for Cs_2 has been developed by Foley.[15]

This paper has been directed at understanding the nuclear-molecular interactions revealed in the fine structure observed in transitions of the type $(J, m_J)\rightarrow(J, m_J')$. However, with the present high resolution, valuable information about certain molecular constants can be obtained. In the first place, the electric dipole moment and moment of inertia of the molecule can be reevaluated with greater accuracy than was possible before.[3] Secondly, the variation of the product, μ^2A, with vibrational quantum number can be found and should yield some information about the shape of the potential energy curve for the molecule, especially if either μ or A can be determined separately with high accuracy. Thirdly, the slope of the straight line in the upper left corner of Fig. 3 gives the vibrational constant ω_e, although not with great accuracy, perhaps 10 percent in this instance, because of the large uncertainty in the source temperature.[16]

The author wishes to thank Professor I. I. Rabi for suggesting this research and for many helpful discussions. He also wishes to thank Mr. L. Grabner and Mr. S. Jacobson for their help in the laboratory. The help of Mr. M. Slotnick and Dr. W. A. Nierenberg in the theoretical work is gratefully acknowledged.

APPENDIX

The first order energy terms for the magnetic dipole-dipole interaction under weak field conditions are[11]

$$g_1g_2\mu_N^2/r^3(2J+3)(2J-1)\times[3g_J\{F_1(F_1+1)-I_1(I_1+1)-J(J+1)\}+2g_{I_1}J(J+1)]\mathbf{I}_2\cdot\mathbf{F}, \quad (9)$$

where

$$g_J=[F_1(F_1+1)+J(J+1)-I_1(I_1+1)]/2F_1(F_1+1), \quad (10)$$

$$g_{I_1}=[F_1(F_1+1)+I_1(I_1+1)-J(J+1)]/2F_1(F_1+1), \quad (11)$$

$$\mathbf{I}_2\cdot\mathbf{F}=1/2\times[F(F+1)-F_1(F_1+1)-I_2(I_2+1)], \quad (12)$$

$$\mathbf{F}_1=\mathbf{I}_1+\mathbf{J}, (F_1=I_1+J, I_1+J-1, \cdots|I_1-J|), \quad (13) \text{ and}$$

$$\mathbf{F}=\mathbf{F}_1+\mathbf{I}_2, (F=F_1+I_2, F_1+I_2-1, \cdots|F_1-I_2|). \quad (14)$$

The other symbols are defined in the text.

For strong electric fields the first order energy terms for this interaction are

$$2g_1g_2\mu_N^2/r^3(2J+3)(2J-1)\times[3m_J^2-J(J+1)]m_{I_1}m_{I_2}, \quad (15)$$

where

$$m_J=J, J-1, \cdots -J, \quad (16)$$

$$m_{I_1}=I_1, I_1-1, \cdots -I_1, \text{ and} \quad (17)$$

$$m_{I_2}=I_2, I_2-1, \cdots -I_2. \quad (18)$$

[14] P. Kusch, S. S. Millman, and I. I. Rabi, Phys. Rev. 55, 1176 (1939).

[15] H. M. Foley, Phys. Rev. 71, 747 (1947).

[16] The value of ω_e obtained from Fig. 3 is 270 ± 30 cm^{-1}. The oven temperature was 800°K.

PHYSICAL REVIEW VOLUME 74, NUMBER 7 OCTOBER 1, 1948

Short-Lived Isomers of Nuclei*

S. DEBENEDETTI AND F. K. MCGOWAN
Oak Ridge National Laboratory, Oak Ridge, Tennessee

(Received June 24, 1948)

A search for short-lived nuclear isomers of half-lives between 10^{-6} and 10^{-3} sec. has been performed using the method of delayed coincidences between two Geiger counters. A short-lived isomer is detected by the measurement of the time lapsed between β-decay and γ- (or internal conversion electron) emission. Out of 60 nuclei investigated, 4 short-lived isomeric states were found. These are: Ta^{181*} (22 μsec.), Re^{187*} (0.65 μsec.), Tm^{169*} (1 μsec.), and Tm^{171*} (2.5 μsec.).

THOUGH excited states of nuclei usually decay with a half-life too short to be directly measurable, the existence of numerous examples of metastable states with half-life long enough to be measured with the stop watch (*isomeric states*) is well established. It is therefore reasonable to assume that a number of metastable states of intermediate but directly measurable half-life (*short-lived isomers*) should exist; this paper summarizes a systematic search for the occurrence of nuclear excited states decaying with half-lives between 10^{-6} and 10^{-3} sec.

In order to detect such short-lived metastable states one has taken advantage of the fact that, when they are produced as a consequence of a β-disintegration, there is a time interval between the rays of the radioactive disintegration and the radiation emitted by the decay of the metastable state. The β- and γ-rays will not be, as usual, coincident, but will give two signals shifted in time, one corresponding to the formation of the metastable state, and the other to its decay.

Since the γ-rays of forbidden transitions are known to be strongly converted, it was thought that the decay of the metastable state could be detected efficiently through the observation of conversion electrons.

For the measurement of time intervals the method of delayed coincidences, which had proven successful in the measurement of the half-life of the mesotron, was chosen.

DESCRIPTION OF THE EQUIPMENT

For the detection of the radiations Geiger counters were used. The use of these instruments, though advisable because of their simplicity and reliability, involves two disadvantages. The first is their long dead-time, which prevents these counters from recording a ray following another after a time shorter than $\sim 10^{-4}$ sec.; and the second is the variation of the time lag between ionization and discharge which introduces an error in the measurement of the individual time intervals.

In order to circumvent the difficulty connected with the dead-time it is necessary to use two different counters, one for the detection of the immediate, the other for the detection of the delayed rays. The errors in the measurement of time intervals resulting from variations of counter lag times are estimated to be around 0.5 μsec. by some authors and are found to be much smaller by others. With the counters available at this laboratory they are of the order of 0.5 μsec. and cannot be reduced by improving the electronic circuits. For the moment we have limited our search to the measurement of time intervals of 1 μsec. or longer, and the shortest half-life detected is of this order of magnitude. However, Bittencourt and Goldhaber[1] have shown that, despite counter lag times of the same order as those observed by us, the method of delayed coincidences between Geiger counters can be refined and used for the measurement of half-lives as short as $5 \cdot 10^{-8}$ sec.

Three different counter sets were used during the experiments. Since the radiation from metastable states was expected to be in most cases strongly internally converted, two similar β-ray counters were used, one (counter 1) for the detection of the immediate radiation, the other (counter 2) for the detection of delayed conver-

* This work was done under Atomic Energy Project No. W-35-058eng. 71 at the Oak Ridge National Laboratory, Oak Ridge, Tennessee.

[1] P. T. Bittencourt and M. Goldhaber, Phys. Rev. 70, 780 (1946).

sion electrons. The first counter set (Fig. 1A) consists of two conventional mica window self-quenching counters, between which the source was introduced. Counter 2 of this set could be used for the detection of γ-rays by interposing between it and the source a convenient absorber. However, most of the effort was directed toward the detection of soft conversion electrons, and for this reason a second set of counters (Fig. 1B) was built in order to eliminate the absorption of the mica windows: it consisted of two counters contained in the same envelope, which is provided with a plug for the introduction of the source. This second set had the disadvantage of requiring evacuation and introduction of new gas in order to remove or change the source. To overcome this difficulty a third set (Fig. 1C) was prepared. In this set the counters are still contained in the same envelope, but this is provided with two arms, each containing a sliding magnetically operated source support. Each of these sets was provided with a small mica window W which was used to introduce canalized beta-rays through both counters in order to study their behavior when simultaneously traversed by a ray.

The block diagram of the coincidence circuit is shown in Fig. 2. The delay time T in the circuit of counter 1 is controlled by multivibrator 1, and can be varied from 1.5 μsec. to 975 μsec. in discontinuous steps, by changing the value of a condenser. The duration τ_1 and τ_2 of the pulses to be fed in coincidence is determined by multivibrators 2 and 3 and can be changed in a similar manner. Changes in resolving time $\tau=\frac{1}{2}(\tau_1+\tau_2)$ and in delay time could be effected by operating selector switches in the front panel of the instrument. Multivibrators 2 and 3 were always set to give pulses of nearly equal duration.

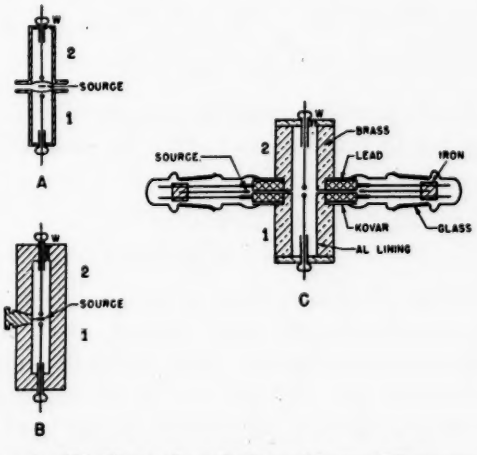

FIG. 1. (A) Two mica-window self-quenching counters; (B) Two self-quenching counters in the same envelope; (C) Similar to B but with magnetically controlled source supports.

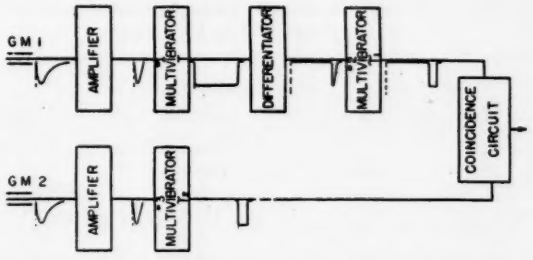

FIG. 2. Block diagram of coincidence circuit.

The length of the pulses from the multivibrators was measured on an oscilloscope (DuMont type 248) by comparison with the timing markers built in this instrument. The accuracy of the markers was checked with a calibrated wave generator. Finally, the value of τ was verified by counting delayed random coincidences.

DISCUSSION OF THE METHOD

Let us first consider the case of a source disintegrating with the emission of β-rays and neglect the corrections resulting from counter dead-time. Let N be the number of disintegrations per second of the source; if a fraction k of these disintegrations lead to a short-lived metastable state and if α is the conversion coefficient of the radiation from the metastable state, then there are $n_e=k\alpha/(1+\alpha)$ delayed electrons per disintegration, accompanied by the same number of atomic x-rays, and $n_\gamma=k/(1+\alpha)$ gamma-quanta per disintegration. One can assume that the efficiency of the counters, used without any absorber, is roughly equal to their useful solid angles ω_1 and ω_2 for electrons of all energies, while the efficiency for the detection of electromagnetic radiations is much smaller. Then, if α is large, the number of single counts per second in one of the counters (say counter 1) is

$$N_1=N\omega_1(1+n_e), \tag{1}$$

and the number of delayed coincidences per second is

$$D=2\tau N n_e\omega_1\omega_2\lambda\exp(-\lambda T), \tag{2}$$

TABLE I. Table of isotopes giving negative results in the range 10^{-6} to 10^{-3} sec.

Isotope investigated for short-lived isomeric state	Radio-active source	Half-life of the source	Mode of decay
$_{21}Sc^{45}$	$_{20}Ca^{45}$	180 d	β^-
$_{23}V^{51}$	$_{24}Cr^{51}$	26 d	K-capture
$_{25}Mn^{55}$	$_{24}Cr^{55}$	1.3 hr.	β^-
$_{26}Fe^{56}$	$_{25}Mn^{56}$	2.6 hr.	β^-
$_{27}Co^{59}$	$_{26}Fe^{59}$	46 d	β^-
$_{28}Ni^{60}$	$_{27}Co^{60}$	5.3 yr.	β^-
$_{29}Cu^{65}$	$_{28}Ni^{65}$	2.6 hr.	β^-
$_{28}Ni^{64}$ $_{30}Zn^{64}$	$_{29}Cu^{64}$	12.8 hr.	β^+, K, β^-
$_{32}Ge^{72}$	$_{31}Ga^{72}$	14 hr.	β^-
$_{31}Ga^{71}$	$_{32}Ge^{71}$	11 d	K-capture
$_{33}As^{75}$	$_{32}Ge^{75}$	1.5 hr.	β^-
$_{34}Se^{76}$	$_{33}As^{76}$	27 hr.	β^-
$_{33}As^{75}$	$_{34}Se^{75}$	115 d	K-capture
$_{36}Kr^{82}$	$_{35}Br^{82}$	34 hr.	β^-
$_{38}Sr^{86}$	$_{37}Rb^{86}$	19.5 hr.	β^-
$_{39}Y^{?}$	$_{38}Sr^{?}$	(fission product)	β^-
$_{39}Y^{89}$	$_{38}Sr^{89}$	55 d	β^-
$_{40}Zr^{90}$	$_{39}Y^{90}$	60 hr.	β^-
$_{41}Cb^{95}\rightarrow{}_{42}Mo^{95}$	$_{40}Zr^{95}$	65 d (fission prod.)	β^-
$_{41}Cb^{97?}$	$_{40}Zr^{97?}$	17 hr.	β^-
$_{45}Rh^{103}$	$_{44}Ru^{103}$	42 d	β^-
$_{45}Rh^{106}\rightarrow{}_{46}Pd^{106}$	$_{44}Ru^{106}$	1 yr. (fission prod.)	β^-
$_{45}Rh^{105}$	$_{44}Ru^{105}$	4.5 hr.	β^-
$_{46}Pd^{110}$	$_{47}Ag^{110}$	225 d	K-capture
$_{51}Sb^{?}$	$_{50}Sn^{?}$	26 hr.	β^-
$_{51}Sb^{?}$	$_{50}Sn^{?}$	long	β^-
$_{52}Te^{122}$	$_{51}Sb^{122}$	2.8 d	β^-
$_{52}Te^{124}$	$_{51}Sb^{124}$	60 d	β^-
$_{53}I^{127}$	$_{52}Te^{127}$	9.3 hr.	β^-
$_{54}Xe^{131}$	$_{53}I^{131}$	8 d	β^-
$_{55}Cs^{133}$	$_{54}Xe^{133}$	5 d	β^-
$_{55}Cs^{135}$	$_{54}Xe^{135}$	9 hr.	β^-
$_{56}Ba^{134}$	$_{55}Cs^{134}$	2.3 yr.	β^-
$_{57}La^{139}$	$_{56}Ba^{139}$	1.5 hr.	β^-
$_{58}Ce^{140}$	$_{57}La^{140}$	40 hr.	β^-
$_{59}Pr^{141}$	$_{58}Ce^{141}$	30 d	β^-
$_{59}Pr^{143}$	$_{58}Ce^{143}$	33 hr.	β^-
$_{59}Pr^{?}$	$_{58}Ce^{?}$	long (fission product)	β^-
$_{60}Nd^{142}$	$_{59}Pr^{142}$	19 hr.	β^-
$_{63}Eu^{153}$	$_{62}Sm^{153}$	46 hr.	β^-
$_{66}Dy^{160?}$	$_{65}Tb^{160?}$	73 d	β^-
$_{67}Ho^{165}$	$_{66}Dy^{165}$	2.5 hr.	β^-
$_{69}Tm^{169}$	$_{68}Er^{169}$	9.4 d	β^-
$_{71}Lu^{175}$	$_{70}Yb^{175}$	4 d	β^-
$_{71}Lu^{177}$	$_{70}Yb^{177}$	2.4 hr.	β^-
$_{74}W^{182}$	$_{73}Ta^{182}$	97 d	β^-
$_{75}Re^{185}$	$_{74}W^{185}$	74 d	β^-
$_{76}Os^{186}$	$_{75}Re^{186}$	92 hr.	β^-
$_{76}Os^{188}$	$_{75}Re^{188}$	18 hr.	β^-
$_{77}Ir^{191}$	$_{76}Os^{191}$	31 hr.	β^-
$_{77}Ir^{193}$	$_{76}Os^{193}$	17 d	β^-
$_{78}Pt^{192}$	$_{77}Ir^{192}$	60 d	β^-
$_{78}Pt^{194}$	$_{77}Ir^{194}$	19 hr.	β^-
$_{80}Hg^{198}$	$_{79}Au^{198}$	2.7 d	β^-
$_{82}Pb^{206}$	$_{81}Tl^{206}$	3.3 yr.	β^-
$_{84}Po^{210}$	$_{83}Bi^{210}$	5 d	β^-
$_{91}Pa^{231}$	$_{90}UY^{231}$	1 d	β^-

where λ is the disintegration constant of the metastable state, and where it has been assumed $\lambda\tau \ll 1$. From these equations it is possible to compute the number of delayed electrons per disintegration of the source from measurements of single counts and of delayed coincidences.

The number of random coincidences per second is expressed by

$$R = 2\tau N_1 N_2. \tag{3}$$

Within the limits of validity of Eqs. (1) and (2) one can evaluate the sensitivity of the method for the detection of delayed conversion electrons. Considering that the minimum detectible number of delayed coincidences is of the same order as the random coincidence rate, one obtains

$$n_{e\,\min} \approx \frac{N_1/\omega_1}{\lambda e^{-\lambda T} - N_1/\omega_1}, \tag{4}$$

where $n_{e\,\min}$ is the minimum number of delayed electrons which can be observed per disintegration.

In order to discuss the more general case, let us call *preceding radiation* that part of the radiation of the source which leads to the metastable state; *delayed radiation*, the radiation emitted by the metastable state itself; and *parallel radiation*, the radiation from the source which does not lead to the metastable state. The *immediate radiation* is then the sum of the preceding and parallel radiations. The fraction of source disintegrations through preceding and delayed rays is k, while the fraction through parallel rays is $1-k$. If ϵ_{1pr}, ϵ_{2pr} are the efficiencies (including geometric factors) of counters 1 and 2 for preceding rays as a whole, and if ϵ_{1d}, ϵ_{2d}, ϵ_{1par}, ϵ_{2par} are similarly defined, then

$$N_1 = N\{k\epsilon_{1pr} + k\epsilon_{1d} + (k-1)\epsilon_{1par}\}, \tag{5}$$

$$D = 2\tau N k \epsilon_{1pr}\epsilon_{2d}\lambda \exp(-\lambda T). \tag{6}$$

If the immediate, delayed, and parallel radiations are in turn complex, the efficiencies ϵ can be expressed as sums. For instance,

$$\epsilon_{2d} = n_{\mathrm{Kel}}\epsilon_{2\mathrm{Kel}} + n_{\mathrm{Lel}}\epsilon_{2\mathrm{Lel}} + \cdots + n_\gamma\epsilon_{2\gamma} + n_{KX}\epsilon_{2KX} + n_{LX}\epsilon_{2LX} + \cdots,$$

where n_{Kel} is the number of K conversion electrons per metastable state formed, $\cdots n_\gamma$ is the number of unconverted γ-rays, n_{KX} is the number of KX rays, $\cdots$, and the ϵ's are the efficiencies for these radiations. Equations (5) and (6) are, in general, too complicated to be of any use for the computation of k and α. However, they are important for the interpretation of the results,

in particular when the efficiency of the counters for different radiations is changed by the use of absorbers. For instance, they make clear that if absorbers are used in front of counter 1 and single counts are recorded, the measurement corresponds to the absorption of the total radiation from the source. By counting delayed coincidences with absorbers in front of counter 1, a measurement of the absorption of the preceding radiation is obtained; likewise, with absorbers in front of counter 2, a measurement of the absorption of the delayed radiation is obtained.

The sources used in the experiment were so weak that the corrections resulting from counter dead-time for pulses distributed at random (sometimes called coincidence correction) could be neglected. However, when a short-lived isomer is present there is a definite correlation between the time of emission of an immediate and of a delayed ray, and this requires special corrections for delay times shorter than counter dead-time. Both the expressions for single counts and for the number of delayed coincidences must be modified because the counters will miss the delayed ray after having detected a preceding one. Thus (1) and (2) become

$$N_1 = N\omega_1[1+(1-\omega_1)n_e], \qquad (1')$$

$$D = 2\tau(N\omega_1 - C)n_e\omega_2\lambda \exp(-\lambda T), \qquad (2')$$

where C is the number of simultaneous coincidences between the two counters. Similarly, (3) becomes

$$R = 2\tau(N_1 - C)(N_2 - C). \qquad (3')$$

NEGATIVE RESULTS

Sources of the 60 isotopes listed in the first column of Table I were tested for delayed coincidences with the windowless counter arrangement of Fig. 1B or 1C, and found not to give any appreciable number of delayed coincidences above the random background.

The sources were prepared either by neutron activation in the Oak Ridge Pile, or were obtained as products of uranium fission.[2] When necessary for the identification of the radioisotope, their decay was followed for a sufficient length of time. The active material was deposited on aluminum foil 1.5 mg/cm², with the thickness of the source never exceeding 1 mg/cm². The foil was introduced between the counters with the activity facing the counter used for the detection of the delayed radiation.

[2] We are indebted to members of the Chemistry Division of Oak Ridge National Laboratory for supplying us with many samples of separated fission products.

TABLE II. Experimental conditions.

Delay time T	Resolving time $\frac{1}{2}(\tau_1+\tau_2)$	Single counts $N_1 \approx N_2$	Expected random coincidences R
1.7 μsec.	0.75 μsec.	7500 c/m	1.4 c/m
13 μsec.	6.5 μsec.	4000 c/m	3.5 c/m
140 μsec.	70 μsec.	1000 c/m	2.3 c/m

For each isotope three different ranges of delays were investigated and sources of different strength were used for each range. Typical experimental conditions of these tests are shown in Table II.

The number of delayed random coincidences was obtained in each experiment by direct comparison with a source of nearly the same intensity prepared from an isotope known not to give any delayed coincidences. Initially, RaE was used for this purpose, but in later experiments any isotope previously tested with negative results (and in particular Tl^{206} and Ca^{40} which are convenient because of their long half-life) was used. Single counts and simultaneous coincidences were recorded for both sources and formula (3′) was used for the comparison of the random coincidences.

A negative result has to be interpreted as a failure to detect delayed conversion electrons emitted by a metastable state of the nucleus indicated in the first column of Table I.

The sensitivity of the method for the detection of delayed conversion electrons has been com-

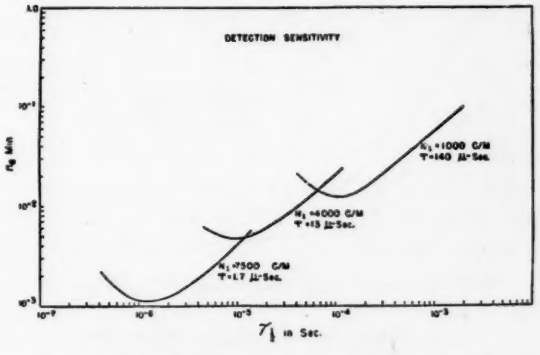

FIG. 3. Sensitivity of method for detection of delayed conversion electrons.

puted by means of (4) as a function of the half-life, assuming $\omega_1=0.5$ and using the figures of Table II. The results are plotted in Fig. 3; the curves of Fig. 3 indicate the maximum number of delayed electrons per β-disintegration which could have escaped observation.

The sensitivity for the detection of metastable states is obviously smaller than the sensitivity for the detection of delayed conversion electrons and will depend on the value of the conversion coefficient. Since this quantity increases with the third power of the atomic number and with decreasing energy, the method used is most sensitive for low energy metastable states in nuclei of high atomic number. For the detection of high energy metastable states in elements of low atomic number, it would be advantageous to measure also $\beta-\gamma$-delayed coincidences.

Independently from our work, and essentially at the same time, Hirzel, Stoll, and Wäffler[3] have used the method of delayed coincidences for the study of short-lived isomers. These authors report a 70-μsec. Pr^{141*} (daughter of Ce^{141}) and a 1200-μsec. Te^{124*} (daughter of Sb^{124}). Our attempts to verify their findings have failed, and we can state that there are less than 4×10^{-3} electron delayed with a half-life of 70 μsec. per disintegration of Ce^{141}, and less than 10^{-2} electron delayed with a half-life of 1200 μsec. per disintegration of Sb^{124}.

Several isomeric states of half-life considerably smaller than 1 μsec. have been reported by other authors. Our failure to detect these metastable states cannot be regarded as a disagreement since the sensitivity of our instrument decreases rapidly for half-lives smaller than 1 μsec.

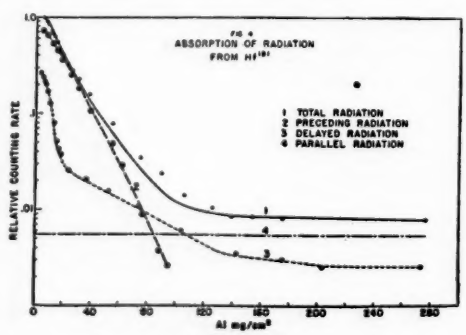

FIG. 4. Absorption of radiation from Hf^{181}.

[3] O. Hirzel, P. Stoll, and H. Wäffler, Helv. Phys. Acta 20, 241 (1947).

22 μsec. Ta^{181*}

It is known that isomeric states have been found in most nuclei of spin 9/2. Considering that the efficiency of the instrument described increases with atomic number, it seemed natural to start the experiments by looking for short isomeric states in heavy nuclei of spin 7/2.

In effect, the first short-lived isomer to be found[4] by the method of delayed coincidences was an excited state of Ta^{181} which is the heaviest nucleus of known spin 7/2. This state was detected using sources of Hf^{181}.

The decay curve of this metastable state corresponds to a half-life of 22 μsec. The decay curve was obtained by plotting delay times as the abscissae and the delayed coincidence counting rate, divided by the resolving time, as the ordinates.

From the number of single counts and delayed coincidences recorded it appears (using Eqs. (1′) and (2′) with $\omega_1=\omega_2=0.3$ as it is obtained by rough geometrical considerations) that there are around 0.5 delayed electrons per disintegration of Hf^{181}. Accordingly, 74 percent of the single counts are due to beta-disintegration electrons, and 26 percent to conversion electrons from Ta^{181*}.

Absorption curves of the radiations from Hf^{181} are plotted in Fig. 4. All these curves were obtained with the counter set of Fig. 1A whose high geometry, necessary for intensity reasons, is obviously poor for the purpose of energy determination. The full points indicate the absorption of the total radiation of this isotope, arbitrarily normalized to unity for no absorber, and were obtained by counting single counts with the absorber inserted between the source and the counter. The radiation of Hf^{181} appears to consist of soft radiations and of a hard γ-component, whose energy was found to be 0.5 Mev by absorption in Pb. Curve 2 is the absorption curve of the radiation preceding the metastable state and was measured by counting delayed coincidences (with constant T and τ) with absorbers between the source and counter 1; curve 2 is normalized to 0.74. Curve 3 is the absorption curve of the delayed radiation measured by counting delayed coincidences with absorbers in front of counter 2 and is normalized to 0.26.

[4] S. DeBenedetti and F. K. McGowan, Phys. Rev. 70, 569 (1946).

Curve 4 is obtained by extrapolating the absorption curve of the 0.5-Mev γ-rays.

Curve 1 is the result of the addition of curves 2, 3, and 4. Since this fits fairly closely the points obtained by absorbing the total radiation, we can consider that Hf^{181} emits a single beta-spectrum, whose absorption is given by curve 2. The maximum energy of the β-spectrum of Hf^{181} was estimated by applying Feather's method to curve 2, and the value $E_{max}=0.42$ Mev was obtained.[5] The γ-rays of 0.5 Mev, which are not found either in the preceding or in the delayed radiation, are emitted in parallel to the metastable state.

The radiation from the metastable state consists of K or L conversion electrons, x-rays, and possibly unconverted γ-rays. The maximum range in Al of the delayed electrons is 19 mg/cm^2. Their energy is therefore around 120 kev; if the maximum range measured corresponds to K conversion, the energy of the metastable state is about 185 kev, while, if mostly L electrons are present (as can be the case for a highly forbidden γ-transition), its energy can be estimated to 132 kev.

For the interpretation of these data one has to consider the other information available on the isotope considered. Cork, Shreffler, and Fowler[6] have studied the conversion lines from Hf^{181} by means of a photographic β-ray spectrograph. They report γ-rays of 0.478, 0.345, and 0.133 Mev, and suggest that the γ-rays of 0.345 and 0.133 Mev are in cascade, with the 0.478-Mev γ-radiation in parallel. If one assumes that the metastable state of 22 μsec. has an energy of 0.133 Mev, this scheme is in agreement with our observations. Our failure to detect the γ-rays of 0.345 Mev can be due to the low sensitivity of the counters for γ-rays. However, there is some evidence that the 0.345-Mev radiation is strongly converted. In effect, Cork *et al.* do not report any large difference in the intensities of the conversion lines of the 0.345- and 0.133-Mev gamma-radiations, and the 0.133-Mev radiation is known to be strongly converted. Furthermore, some careful absorption experiments of $\beta-\gamma$ immediate coincidences by Wiedenbeck and Chu[7] show

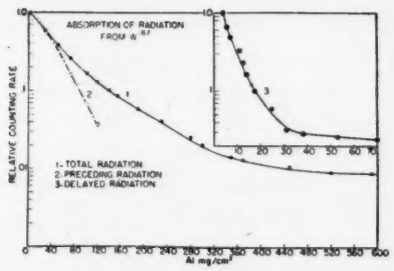

FIG. 5. Absorption of radiation from W^{187}.

the presence of a strong conversion line having an energy of 0.35 Mev. However, if the 0.345-Mev radiation is strongly converted, and therefore of high polarity, it would be difficult to explain why it should compete favorably with the γ-rays of 0.478 Mev.

Careful investigation of the continuous spectrum and of the conversion lines from Hf^{181} by means of a β-ray spectrometer is needed in order to elucidate these points and to confirm the present interpretation.

0.65 μsec. Re^{187*}

As previously reported,[8] sources of 24-hr. W^{187} give rise to delayed coincidences. From the decay curve the half-life of the metastable state (Re^{187*}) appears to be 0.65 μsec.

The absorption curves of the total (curve 1) and preceding (curve 2) radiations are shown in Fig. 5, indicating that the preceding radiation is softer than the total β-radiation from W^{187}. The delayed radiation (curve 3, Fig. 5) consists of electrons having a maximum energy of 0.13–0.15 Mev, accompanied by an electromagnetic radiation of less than 0.1 Mev. The mica window of counter set 1A absorbs a much larger percentage of the rays of Re^{187*} than of Ta^{181*}. This seems to show that the electrons from these two short-lived isomers, though of about the same maximum energy, have a different energy distribution, possibly due to a different ratio of K to L conversion. The β-spectrum of W^{187} is known to consist of two components of 1.31- and 0.62-Mev maximum energy and intensities 23 and 77 percent respectively, accompanied by a rather large number of conversion lines.[9] Though many authors have investigated this isotope, there is no general agreement as to the disintegration scheme.

[5] In a previous communication (see reference 4) this energy was erroneously reported as 0.8 Mev, because of an error in transcription superimposed on a different method of analyzing the curves.

[6] J. M. Cork, R. G. Shreffler, and C. M. Fowler, Phys. Rev. 72, 1209 (1947).

[7] M. L. Wiedenbeck and K. Y. Chu, Phys. Rev. 72, 1164 (1947).

[8] S. DeBenedetti and F. K. McGowan, Phys. Rev. 71, 380 (1947).

[9] P. W. Levy, personal communication of unpublished work.

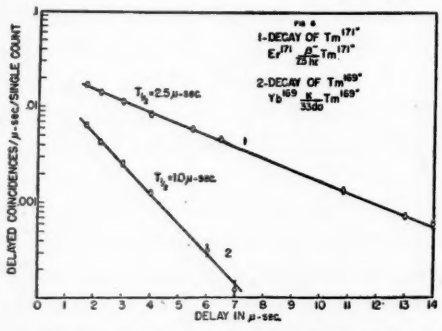

FIG. 6. Decay of Tm^{171*} and Tm^{169*}.

Analyzing the absorption curve of the preceding radiation by Feather's method, one obtains a maximum energy consistent with 0.62 Mev, indicating that the metastable state follows only the lower energy component of the β-spectrum. Some delayed coincidences, not numerous enough to permit the measurement of an absorption curve, were observed after absorbing all the preceding β-rays, indicating that some γ-rays are present in the preceding radiation.

A number of soft γ-rays which, within the accuracy of our absorption measurements, could be due to the decay of Re^{187*}, have been observed in the spectrum of W^{187}. However, one might feel inclined to associate this metastable state with a radiation of 0.130 Mev, since this is strongly internally converted.[10]

There are about 0.1 delayed electrons per disintegration of W^{187}, or around 0.13 delayed electrons per β-ray of the softer component of the continuous spectrum. However, the number of delayed electrons per metastable state could be higher, if there were other γ-rays in parallel.

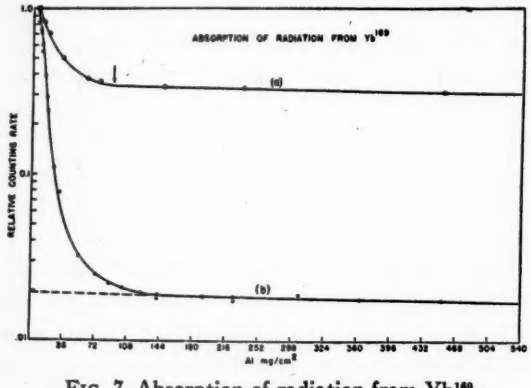

FIG. 7. Absorption of radiation from Yb^{169}.

[10] We are indebted to L. C. Miller and L. F. Curtiss for the communication of this result.

1 μsec. Tm^{169*}

Delayed coincidences corresponding to a half-life of 1 μsec. were observed with sources of 33-day Yb, which, according to Bothe,[11] decays by K capture to Tm^{169}. The assignment of the 33 days' activity to Yb was verified by the ion exchange technique of separating rare earths.[12] The fact that the decay process is K capture was confirmed by our absorption measurements; no positive electrons were found in a rough investigation.

Curve 2 of Fig. 6 is the decay curve of the metastable state of Tm^{169*}; the delayed radiation consists mostly of electrons having an energy of 0.12 Mev, and the excitation energy of the metastable state appears to be around 0.19 Mev (assuming that the observed electrons are K electrons) or around 0.13 Mev (if most delayed electrons are from L conversion).

Figure 7 shows the absorption of the total radiation of Yb^{169} (curve b) and that of the radiation preceding the 1-μsec. metastable state (curve a). It is evident from these curves that the metastable state is preceded by x-rays and, at least in certain cases, by conversion electrons of harder gamma-rays (around 0.4 Mev). The ratio of electronic to x-radiation is much larger in the total radiation than in the radiation preceding the metastable state, indicating that some electrons must be emitted in parallel to this state (it does not seem possible to account for the excess of electrons in the total radiation by attributing it to the delayed electrons alone). These "parallel" electrons are probably due to the conversion of some other γ-component.

2.5 μsec. Tm^{171*}

After the observations on Tm^{169*} we examined for delayed coincidences a number of Er activities in the hope that one of them would lead by β^--decay to the 1-μsec. metastable state. Evidence of delayed coincidences was found with a 7.5-hr. activity, but the half-life of the corresponding metastable state was 2.5 μsec. (curve 1, Fig. 6). In order to prove the difference of these two

[11] W. Bothe, Zeits. f. Naturf. 1, 173 (1946).

[12] B. H. Ketelle and G. E. Boyd, J. Am. Chem. Soc. 69, 2800 (1947). We are greatly indebted to Mr. Ketelle, of the Chemistry Division of Oak Ridge National Laboratory, for the preparation of all the separated rare earth sources used in these experiments.

half-lives (which were originally supposed to be due to the same isotope) they were compared with the arrangement of Fig. 1C. The values of 1 and 2.5 μsec. were confirmed in this way.

Some subsequent work by Ketelle and Peacock[13] showed that the 7.5-hr. Er activity cannot be assigned to the mass number 169, since it decays into a long-lived β-active daughter. Furthermore, these authors studied the spectrum of the 7.5-hr. Er and were led to assign this activity to mass 171 on the basis of its disintegration energy. This assignment seems to be confirmed by other thus far unpublished evidence.

From β-spectrographic work Ketelle and Peacock suggest a disintegration scheme for Er^{171}. The 2.5-μsec. metastable state is attributed to a 0.113-Mev transition, whose strongly converted L line appeared in the beta-spectrum.

An approximate evaluation of the number of delayed electrons per disintegration of Er^{171} from the number of delayed coincidences leads to the value of 0.4. Since only 71 percent of the beta-rays of Er^{171} lead to the isomeric state, the number of delayed electrons per disintegration of the metastable state is 0.56, and the total coefficient of internal conversion

$$\alpha=\frac{0.56}{1-0.56}=1.3.$$

DISCUSSION OF RESULTS

Practically the only information available about the four short-lived isomers observed is their half-life and a rough estimate of their energy. The radiation emitted is strongly converted, but from the experimental results it is not known (with the exception of Tm^{171*}) whether the conversion coefficients are high enough to change the order of magnitude of the half-life caused by γ-emission alone. It is therefore impossible to draw any definite conclusions on the nature of the transitions involved. Nevertheless, comparing the half-lives and energies experimentally determined with the theoretical estimates[14] of half-lives for γ-emission, it appears that the observed values fall between the theoretical predictions for changes in angular momentum of 2 and 3 units. The inclusion of internal conversion would lower the theoretically expected half-lives, and as a consequence one can consider that the observed transitions are more probably to be associated to a change of angular momentum of 3 units, rather than 2.

Though it is clear that any statistical consideration on the frequency of occurrence of isomeric states with half-lives between 10^{-6} and 10^{-3} sec. is premature, one cannot escape the impression that changes in angular momentum of 3 units occur less frequently than changes of 4 or 5 units, since a large number of isomeric states with half-lives ranging from 1 sec. to 10^{7} sec. (corresponding to the larger spin changes) are known, and only 4 short-lived isomers were found in these experiments.

One must keep in mind, however, that the method used in the present investigation cannot be expected to detect all the isomeric states of the 60 nuclei studied, with half-lives in the range covered in the present survey. A first requirement which has to be satisfied for a positive result is that the metastable state be reached as a product of β-disintegration; furthermore, the radiation from the metastable state must be strongly converted; and, finally, the efficiency of detection is not constant over the whole range explored, but increases for shorter lives.

These considerations might be sufficient to explain why only four cases were observed, and why these were found in heavy elements, with small excitation energy and with half-lives in the microsecond region. It is conceivable that using different techniques for the production of nuclear excited states and for the detection of their radiation, one could discover many more short-lived isomers in the range considered. The possibility of exciting nuclei by irradiation with x-rays, by capture of slow neutrons, or by particles bombardment is immediately apparent. Also, the newly discovered technique of efficient gamma-counting with organic scintillation counters might provide a method of detecting short-lived isomers whose radiation is only slightly converted, and some work along these lines has already been started.[15]

[13] B. H. Ketelle and W. C. Peacock, Phys. Rev. **73**, 1269 (1948).

[14] See, for instance, H. A. Bethe, Rev. Mod. Phys. 9, 226 (1937).

[15] S. DeBenedetti, F. K. McGowan, and J. E. Francis, Jr., Phys. Rev. **73**, 1404 (1948).

Molecular Orbital Method and Molecular Ionization Potentials*

ROBERT S. MULLIKEN
Department of Physics, The University of Chicago, Chicago, Illinois
(Received June 14, 1948)

(1) Empirical evidence indicates that, other things being equal, the atomic integral α of the LCAO molecular orbital method decreases in magnitude, (*a*), with increasing interatomic distance, (*b*), with increase in the number of atoms covered by a MO.

(2) Theoretical computations give a satisfactory account of effect (*a*), and (except for the absolute values of α in many-center cases) also of effect (*b*).

(3) It is reasonable to hope that further study of theoretical approximation methods of the MO type will make possible an increasingly quantitative theoretical understanding of molecular ionization potentials and of other molecular properties.

THE electronic structure of any well-organized molecular system, e.g., an atom, a molecule, or a single crystal, can usually be indicated by specifying an electron configuration and an electronic state. To this specification corresponds a wave function, antisymmetric in the electrons, which may be a rather good approximation to the accurate eigenfunction. If the electron configuration is stated in terms of orbitals of the complete system (i.e., non-localized molecular orbitals in the case of a molecule), a wave function of the self-consistent-field type can in principle be constructed, in which the MO's (molecular orbitals) used are all mutually orthogonal.

Each MO (say ϕ_f) is then an eigenfunction of a one-electron Schrödinger equation, $h\phi=e\phi$ in which the Hamiltonian h corresponds to the proper molecular self-consistent field. The corresponding energy eigenvalue (say e_f) is of particular importance in that $-e_f$ is rather closely equal to the ionization energy I_f for removal of an electron from ϕ_f—after certain corrections in case the electron configuration is not of closed shell type. This theorem was stated by Slater in 1928 explicitly for atoms, but implicitly also for molecules. It is no longer valid (or at least is less accurate) for a molecule if the electron configuration is given in terms of localized molecular orbitals or of atomic orbitals, since such orbitals cannot be orthogonal.

TABLE I.

	I	α
CH_3 (methyl radical)	10.07	−10.07
C_2H_2 (acetylene)	11.41	−9.2
C_2H_4 (ethylene)	10.50	−8.14
C_4H_6 (1,3-butadiene)	9.07	−7.42
C_6H_6 (benzene)	9.24	−7.18
graphite	4.39	−4.39

* This work was assisted by the Office of Naval Research under Task Order IX of Contract N6ori-20 with the University of Chicago.

Experimentally observed molecular ionization potentials involving removal of a single electron, after correction if necessary to the case of fixed nuclei, may then to a good approximation be set equal to the negatives of energy eigenvalues of whole-molecule, self-consistent-field MO's. On the other hand, approximate theoretical energy expressions such as

$$e_f=\alpha+b_f\beta \tag{1}$$

can be obtained by the well-known method of approximating the MO's of an m-center problem by LCAO forms ($f=1\cdots m$). (The symbol LCAO means "linear combination of atomic orbitals.") In the homopolar 2-center case, $m=2$, and in Eq. (1),

$$b=\pm 1/(1\pm S), \tag{2}$$

where S is the overlap integral $\int \chi_a\chi_b dv$ between the atomic orbitals χ_a and χ_b involved in the LCAO forms. The + and − signs in Eq. (2) correspond respectively to bonding and antibonding MO's.

The atomic integral α and the bond integral β are both negative, with $|\alpha|>|\beta|$.[1] If a and b are two adjacent-like atoms, α and β are defined by

$$\alpha=\int \chi_a h\chi_a dv,$$

and

$$\beta=\int \chi_b h\chi_a dv-S\alpha.$$

If h in the expression for α were replaced by the Hamiltonian h_a corresponding to the self-consistent field for an isolated atom a, then α would become e_a, the atomic one-electron energy eigenvalue corresponding to the atomic orbital χ_a. Thus since h is roughly equal to h_a, α should be roughly equal to e_a. The bond integral β is roughly a measure of the strength of the chemical bond between atoms a and b.

If more than one kind of atom is involved, there is more than one α and β, and Eq. (1) is replaced by more complicated expressions. In this event, the difference in the α values of two atoms is a measure of their difference in electronegativity.

In most MO work to date, β has been determined empirically, and little attention has been paid to α.

Setting $e_f = -I_f$, an empirical α can be determined from Eq. (1) if b_f and β are known. The largest body of I data for a set of related molecules is that for the unsaturated and aromatic hydrocarbons.[1,2] The coefficient b of Eq. (1) for the most loosely bound π-type MO can be computed fairly accurately for any such molecule by solving an appropriate secular equation, while β is known from spectroscopic data to be near -3 ev for C–C π-bonds.[2a,3] Using this information, it is found that $|\alpha|$ decreases with increase in the number of atoms in the conjugated system. Some examples are given in Table I (energies are in ev).

Substitution of a methyl or other alkyl group for a hydrogen atom causes a further decrease in $|\alpha|$.[1,2,3] Since the alkyl group may be regarded as part of the conjugated system (phenomenon of hyperconjugation), this effect may reasonably be considered, just as in the preceding examples, to be associated with an increase in the number of atoms in a conjugated system. The examples of Table II are illustrative. The α values for propylene and isoprene should be compared with those for ethylene and butadiene respectively. In a similar way, alkyl substitution for H atoms in CH_3 or other free radicals leads to marked decreases in I and $|\alpha|$.[1]

TABLE II.

	I	α
$C_2H_3CH_3$ (propylene)	9.70	−7.49
$C_4H_5CH_3$ (isoprene)	8.86	−7.24

Decrease in $|\alpha|$ with increase in number of participating atoms may thus be taken as an empirically well-established phenomenon characteristic of conjugated and hyperconjugated systems. How may this be understood theoretically? A suggested explanation[1,3] in the case of alkyl substitution is that the π-electron-bearing carbon atoms become negatively charged at the expense of the alkyl groups, causing a decrease in $|\alpha|$. (It is well known that such "charge transfer" effects are important in cases such as that of H_2O, where the first I corresponds to removal of a nonbonding O atom electron but is lower than for a free O atom because of the negative charge on the O atom in H_2O.) However, charge transfer obviously cannot explain the trends in the first of the two tables above.

Recently the writer has found it possible to make approximate theoretical computations of the parameters α and β.[4] In all cases so far considered, the computed β values agree rather well with those obtained empirically from spectroscopic and other data. In the cases so far treated which involve only two-center MO's (H_2, σ MO's; C_2H_2 and C_2H_4, π MO'S), the observed and computed α values agree extremely closely (see Table III).[5] These results are very encouraging with respect to the possibility of an understanding of observed ionization potentials in diatomic

TABLE III.

	$-\alpha_{obs}$	$-\alpha_{comp}$	I_a
H_2 (r=0.74A)	14.68	14.86	13.60
H_2 (for r=1.07A)	12.7	12.10	13.60
C_2H_2 (r=1.20A)	9.2	8.81	10.91
C_2H_4 (r=1.35A)	8.25	8.33	11.28

[1] Cf. W. C. Price, Chem. Rev. 41, 257 (1947).
[2] R. E. Honig, J. Chem. Phys. 16, 105 (1948).
[2a] The definition of β used here is that proposed by Mulliken and Rieke, J. Am. Chem. Soc. 63, 1770 (1941); see Roothaan and Mulliken, J. Chem. Phys. 16, 118 (1948) for a more explicit statement.
[3] R. S. Mulliken, Rev. Mod. Phys. 14, 265 (1942).
[4] Reported at international colloquium on "Theory of Chemical Binding" held at Paris April 12–16, 1948. To be published in part in J. de Chimie Physique (1948).
[5] The I_a values as given for carbon are for suitable tetravalent "valence states" of the atom (cf. R. S. Mulliken, J. Chem. Phys. 2, 792 (1934)).

and other two-center cases. In particular, the fact that the observed $-\alpha$ is *greater* than the corresponding atomic ionization potential $I_a \approx -e_a$ for closely spaced nuclei, but becomes increasingly *less* than the latter as the interatomic distance increases, is reproduced by the theoretical computation (see the last column of Table III).

Approximate theoretical formulas have also been obtained by means of which α and β values can be computed for π-type MO's extending over any number of centers. Thus far, these have been applied only to butadiene, benzene, and graphite. As in the two-center cases, they give β values in approximate agreement with experiment. For $-\alpha$, they are disappointing in that they give considerably larger values (10.83 ev for benzene, 6.29 ev for graphite) than those observed. On the other hand, they are encouraging in that the computed $|\alpha|$, like the observed $|\alpha|$ (see Table I above), diminishes with increasing molecule size.

PHYSICAL REVIEW VOLUME 74, NUMBER 7 OCTOBER 1, 1948

Quantum Theory of the Point Electron. I*

MARIO SCHÖNBERG
University of São Paulo, São Paulo, Brazil
(Received February 9, 1948)

A new treatment of the quantum theory of the electromagnetic field is discussed. The interactions between the particles and their interactions with the radiation field are treated according to the ideas of the author's classical theory. The radiation field is taken as a difference of two fields analogous to the field of the Heisenberg-Pauli electrodynamics. The commutation rules for the radiation field differ essentially from those of the Heisenberg-Pauli electrodynamics. In our formalism it is possible to avoid all the divergences by a suitable choice of the wave function of the system particles plus field. The physically relevant wave functions satisfy wave equations similar to those of systems with finite numbers of degrees of freedom, although they are also exact solutions of the Schrödinger equation of the system particles plus field which has an infinite number of degrees of freedom. There is also the possibility of getting finite non-vanishing self-energies.

I. INTRODUCTION

THE theory of point particles interacting with a field presents well-known difficulties, both in classical and quantum theories. We have shown[1–3] that it is possible to get a satisfactory classical theory of the point electron by modifying the usual ideas of the interactions between the point particles and their interactions with fields. We have also attempted a quantum generalization of our theory for the case of one electron.[4] in which there is only the interaction with the radiation field. The method we used in that paper has some basic points in common with the method we shall use in this paper (description of the radiation field by means of two fields of the Heisenberg-Pauli type) but it differs in some essential aspects, because in the present paper we shall not use anti-Hermitian operators in the description of the advanced waves.**

The essential point in our classical and quantum treatments lies in the modification of the field concepts of Faraday and Maxwell which underlie the quantum electrodynamics of Heisenberg and Pauli,[5,***] as well as more recent

* Revised form of a paper sent to The Physical Review in February, 1947.

[1] M. Schönberg, Phys. Rev. **69**, 211 (1946).

[2] M. Schönberg, Summa Brasiliensis Math. **1**, 41, 77 (1946).

[3] M. Schönberg, Summa Brasiliensis Phys. **1**, 51 (1947).

[4] M. Schönberg, Phys. Rev. **67**, 193 (1945).

** In that paper the advanced waves give negative contributions to the energy of the field in the classical formalism. The use of anti-Hermitian operators transforms the negative energy waves into positive energy photons so that the zero-point energy of the field is not canceled (see J. Leite Lopes, Anais Acad. Brasil. Ciencias **19**, 51 (1947).

[5] W. Heisenberg and W. Pauli, Zeits. f. Physik **56**, 1 (1929), and **59**, 168 (1930).

*** A more detailed discussion of the methods of field quantization and of the Heisenberg-Pauli electrodynamics will appear soon in the Anais da Academia Brasileirs de Ciencias.

treatments.[6–9] In our theory we distinguish the direct intercation between two electrons from their interactions with the photons. The direct interactions between the electrons are treated as relativistic actions at a distance; they are assumed to be half-retarded, half-advanced actions of the type considered in classical theory by Tetrode[10] and Fokker;[11] no field concepts are used in the description of the direct interactions between the electrons. The photons are described by a radiation field which is a field of the Faraday-Maxwell type. In our classical theory the radiation field is one-half the difference between the retarded and advanced fields of the system of electrons; it satisfies homogeneous Maxwell equations.

The interaction between the particles and the radiation field gives rise to the emission and absorption of radiation. In order to ensure the conservation of energy and momentum in the emission and absorption of radiation, the energy and momentum of the radiation field must not be defined as in Maxwell's theory: *The energy of the radiation field is not necessarily positive, even in classical theory.* It follows from that circumstance that in the quantum formalism there are photons with positive and negative energies.

The fundamental difference between our quantum theory and the Heisenberg-Pauli quantum electrodynamics lies in the commutation rules for the field which interacts with the particles. *The potentials of our radiation field taken at any two-world points do commute, whereas they do not commute in the Heisenberg-Pauli electrodynamics when one of the world-points belongs to the light cone of the other one.* It follows from the irrestricted commutability of the radiation field potentials that the Fourier coefficients of these potentials do commute with their complex conjugates, so that it is possible to get states of the radiation field in which any set of Fourier coefficients and their complex conjugates have the value zero. We call the degress of freedom of the radiation field corresponding to the aforementioned Fourier coefficients the "frozen" degrees of freedom. *The possibility of the "freezing" allows us to get rid of the divergences arising from the infinite number of degrees of freedom of the field.*

In our quantum formalism there are exact solutions of the Schrödinger equation of the system particles plus radiation field describing states of motion of the system in which the particles interact only with a finite number of degrees of freedom of the field, provided we enclose the field in a box and impose periodic boundary conditions. Those solutions correspond to states in which the degrees of freedom which do not interact with the particles are "frozen."

In order to compute the transition probabilities and other physically interesting values we need a "freezing" rule and a physical interpretation rule. The "freezing" rule indicates which particular solution of the Schrödinger equation of the system ought to be used in the computation of the experimentally measurable quantities. The physical interpretation rule is necessary because of the existence of photons with positive and negative energies in our formalism. There are several acceptable interpretation rules. *The simplest interpretation rule can be considered as the quantum analog of the time boundary conditions of the classical theory.*

There is no difficulty in setting up a "freezing" criterion in the computation of the transition probabilities. We have not been able to find a reasonable "freezing" rule for the computation of self-energies, there is a large arbitrariness which seems to require the introduction of some elementary length, although there is no difficulty in eliminating the infinite self-energies.

II. THE CLASSICAL VARIATIONAL PRINCIPLE

Let us consider a system of n charged point particles. The coordinates of the jth particle will be denoted by x_j^μ ($\mu=0, 1, 2, 3$), its electric charge and rest mass by e_j and m_j, respectively. The retarded and advanced fields of the jth particle will be denoted by $F_{j,\mathrm{ret}}^{\mu\nu}$ and $F_{j,\mathrm{adv}}^{\mu\nu}$. We shall introduce the attached fields of the particles

$$F_{j,\mathrm{at}}^{\mu\nu}=\tfrac{1}{2}(F_{j,\mathrm{ret}}^{\mu\nu}+F_{j,\mathrm{adv}}^{\mu\nu}) \qquad (1)$$

[6] P. A. M. Dirac, V. Fock, and B. Podolsky, Physik. Zeits. Sowjetunion 2, 468 (1932).
[7] P. A. M. Dirac, An. Inst. H. Poincaré 9, 13 (1939).
[8] P. A. M. Dirac, Proc. Roy. Soc. A180, 1 (1942).
[9] P. A. M. Dirac, Com. Dublin Inst. A, 3 (1946).
[10] H. Tetrode, Zeits. f. Physik. 10, 317 (1922).
[11] A. D. Fokker, Zeits. f. Physik 58, 386 (1929).

and the radiation field of the system

$$F_{\text{rad}}{}^{\mu\nu}=\tfrac{1}{2}\sum_{j=1}^{n}(F_{j,\text{ret}}{}^{\mu\nu}-F_{j,\text{adv}}{}^{\mu\nu}). \tag{2}$$

The equations of motion of the jth particle are

$$m_j c^2\frac{d^2x_j{}^{\mu}}{ds_j{}^2}=e_j\left[F_{\text{rad}}{}^{\mu\nu}(x_j)+\sum_{k\neq j}F_{k,\text{at}}{}^{\mu\nu}(x_j)\right]\frac{dx_{j,\nu}}{ds_j}, \tag{3}$$

with

$$ds_j=(g_{\mu\nu}dx_j{}^{\mu}dx_j{}^{\nu})^{\frac{1}{2}} \tag{4}$$

and

$$g_{00}=1,\quad g_{11}=g_{22}=g_{33}=-1,\quad g_{\mu\nu}=0\ (\mu\neq\nu). \tag{5}$$

We shall denote the potentials of a field F by the letter A.

$$F^{\mu\nu}=\partial A^{\nu}/\partial x_{\mu}-\partial A^{\mu}/\partial x_{\nu}. \tag{6}$$

The attached potentials $A_{j,\text{at}}{}^{\mu}$ can be conveniently represented by integrals

$$A_{j,\text{at}}{}^{\mu}(x)=e_j\int_{-\infty}^{+\infty}\frac{dx_j{}^{\mu}}{ds_j}\delta(x_j,x)ds_j, \tag{7}$$

$$\delta(x_j,x)=\delta((x_j{}^{\nu}-x^{\nu})(x_{j,\nu}-x_{\nu})). \tag{8}$$

$\delta(u)$ denotes the Dirac symbolic function of the argument u.

The radiation potentials are solutions of the homogeneous d'Alembert equation

$$\Box A_{\text{rad}}{}^{\mu}=0,\quad\left(\Box=g^{\mu\nu}\frac{\partial}{\partial x^{\mu}}\frac{\partial}{\partial x^{\nu}}\right). \tag{9}$$

They satisfy also the Lorentz condition

$$\frac{\partial}{\partial x^{\mu}}A_{\text{rad}}{}^{\mu}=0. \tag{10}$$

The equations of motion of the particles and the field can be derived from the variational principle

$$\delta\mathfrak{L}=0, \tag{11}$$

$$\mathfrak{L}=\mathfrak{L}_p+\mathfrak{L}_f. \tag{12}$$

$\mathfrak{L}_p$ is the Lagrangian integral of the particles

$$\mathfrak{L}_p=-\sum_{j=1}^{n}m_j c\int_{-\infty}^{+\infty}\left(\frac{dx_j{}^{\mu}}{ds_j}\frac{dx_{j,\mu}}{ds_j}\right)^{\frac{1}{2}}ds_j$$
$$-\sum_{j=1}^{n}\frac{e_j}{c}\int_{-\infty}^{+\infty}A_{\text{rad}}{}^{\mu}(x_j)\frac{dx_{j,\mu}}{ds_j}ds_j$$
$$-\frac{1}{2c}\sum_{j=1}^{n}\sum_{k\neq j}e_j e_k\int_{-\infty}^{+\infty}\int_{-\infty}^{+\infty}\frac{dx_j{}^{\mu}}{ds_j}\frac{dx_{k,\mu}}{ds_k}$$
$$\times\delta(x_j,x_k)ds_j ds_k. \tag{13}$$

$\mathfrak{L}_f$ is the Lagrangian integral of the field

$$\mathfrak{L}_f=-\frac{1}{32\pi c}\int_{-\infty}^{+\infty}[F^{(+)\mu\nu}F_{\mu\nu}{}^{(+)}-F^{(-)\mu\nu}F_{\mu\nu}{}^{(-)}]d_4x$$
$$-\frac{1}{16\pi c}\int_{-\infty}^{+\infty}\left[\left(\frac{\partial A^{(+)\mu}}{\partial x^{\mu}}\right)^2-\left(\frac{\partial A^{(-)\mu}}{\partial x^{\mu}}\right)^2\right]d_4x. \tag{14}$$

In the variational Eq. (11) the potentials $A^{(+)\mu}$ and $A^{(-)\mu}$ are treated as independent field variables. Their equations of motion are

$$\Box A^{(\pm)\mu}=4\pi\sum_{j=1}^{n}J_j{}^{\mu}, \tag{15}$$

$$J_j{}^{\mu}(x)=e_j\int_{-\infty}^{+\infty}\frac{dx_j{}^{\mu}}{ds_j}\prod_{\lambda=0}^{3}\delta(x_j{}^{\lambda}-x^{\lambda})ds_j. \tag{16}$$

We must assume that

$$\tfrac{1}{2}(A^{(+)\mu}-A^{(-)\mu})=A_{\text{rad}}{}^{\mu}, \tag{17}$$

so that we must have

$$\frac{\partial}{\partial x^{\mu}}(A^{(+)\mu}-A^{(-)\mu})=0. \tag{18}$$

In order to satisfy (18) we shall impose the Lorentz conditions

$$\frac{\partial}{\partial x^{\mu}}A^{(\pm)\mu}=0. \tag{19}$$

We could obviously take for $A^{(+)\mu}$ the potentials of the retarded field of the system of particles, and for $A^{(-)\mu}$ the corresponding advanced potentials.

III. CONJUGATED MOMENTA AND POISSON BRACKETS

We get at once the momenta conjugated to the particle and field variables from the Lagrangian integral $\mathfrak{L}$:

$$p_{j,\mu}=-\frac{\delta\mathfrak{L}}{\delta(dx_j{}^{\mu}/ds_j)}=m_j c\frac{dx_{j,\mu}}{ds_j}$$
$$+\frac{e_j}{c}\left[A_{\text{rad},\mu}(x_j)+\sum_{k\neq j}A_{k,\text{at},\mu}(x_j)\right], \tag{20}$$

$$\prod_0{}^{(\pm)}=-\frac{\delta\mathfrak{L}}{\delta(\partial A^{(\pm)0}/\partial x_0)}=\pm\frac{1}{8\pi c}\frac{\partial A^{(\pm)\mu}}{\partial x^{\mu}}, \tag{21}$$

$$\Pi_a^{(\pm)} = -\frac{\delta \mathfrak{L}}{\delta(\partial A^{(\pm)a}/\partial x_0)} = \mp\frac{1}{8\pi c} F_{a0}^{(\pm)} \qquad (a=1, 2, 3). \quad (22)$$

The Poisson brackets are defined in the usual way. We get

$$\left(A^{(+)\mu}(\mathbf{x}, x_0), \frac{\partial}{\partial x_0} A^{(+)\nu}(\mathbf{x}', x_0)\right) = -8\pi c g^{\mu\nu}\delta(\mathbf{x}-\mathbf{x}'), \quad (23)$$

$$\left(A^{(-)\mu}(\mathbf{x}, x_0), \frac{\partial}{\partial x_0} A^{(-)\nu}(\mathbf{x}', x_0)\right) = 8\pi c g^{\mu\nu}\delta(\mathbf{x}-\mathbf{x}'), \quad (24)$$

whence

$$\left(A_{\text{rad}}^{\mu}(\mathbf{x}, x_0), \frac{\partial}{\partial x_0} A_{\text{rad}}^{\nu}(\mathbf{x}', x_0)\right) = 0. \quad (25)$$

IV. ENERGY AND MOMENTUM OF THE FIELD

The four vector of energy and momentum of the field can be taken as

$$P_f^{\mu} = \int_{-\infty}^{+\infty} T_f^{\mu 0} d_3x + \frac{1}{c}\sum_{j=1}^{n} e_j A_{\text{rad}}^{\mu}(x_j), \quad (26)$$

with

$$T_f^{\mu\nu} = \frac{1}{16\pi c} g^{\mu\nu}\left[\frac{\partial A^{(+)\rho}}{\partial x^{\sigma}}\frac{\partial A_{\rho}^{(+)}}{\partial x_{\sigma}} - \frac{\partial A^{(-)\rho}}{\partial x^{\sigma}}\frac{\partial A_{\rho}^{(-)}}{\partial x_{\sigma}}\right] - \frac{1}{8\pi c}\left[\frac{\partial A^{(+)\rho}}{\partial x_{\mu}}\frac{\partial A_{\rho}^{(+)}}{\partial x_{\nu}} - \frac{\partial A^{(-)\rho}}{\partial x_{\mu}}\frac{\partial A_{\rho}^{(-)}}{\partial x_{\nu}}\right]. \quad (27)$$

cP_f^0 includes the potential energy of the particles with respect to the radiation field plus the energy of the radiation field. The Hamiltonian of the system particles plus radiation field is H:

$$H = H_p + H_f, \quad (28)$$

$$H_p = \sum_j m_j c^2 \frac{dx_j^0}{ds} + \sum_j e_j\left[A_{\text{rad}}^{0}(x_j) + \sum_{k\neq j} A_{k,\text{at}}^{0}(x_j)\right], \quad (29)$$

$$H_f = c\int_{-\infty}^{+\infty} T_f^{00} d_3x. \quad (30)$$

It is easily seen that

$$H_f = \frac{1}{16\pi}\int_{-\infty}^{+\infty}\left[\sum_{a=1}^{3}\{F_{a0}^{(+)2} - F_{a0}^{(-)2}\} + \sum_{a=1}^{3}\sum_{b>a}\{F_{ab}^{(+)2} - F_{ab}^{(-)2}\}\right] d_3x - \frac{1}{16\pi}\int_{-\infty}^{+\infty}\left[\left(\frac{\partial A^{(+)\mu}}{\partial x^{\mu}}\right)^2 - \left(\frac{\partial A^{(-)\mu}}{\partial x^{\mu}}\right)^2\right] d_3x. \quad (31)$$

The energy density of the radiation waves may be negative even when the Lorentz conditions (19) *are taken into account.*

V. COMMUTATION RULES FOR THE QUANTUM POTENTIALS

Equations (23)–(25) are still valid in quantum theory. The quantum Poisson bracket of two quantities B and C is proportional to their commutator

$$(B, C) = -\frac{i}{\hbar}[B, C], \quad (32)$$

$$[B, C] = BC - CB, \quad (33)$$

The commutation rules corresponding to the values of the classical Poisson brackets and the equations of motion of the potentials allow us to write the relativistic commutation rules. Let us put

$$\Delta(x, x') = 2\text{sig n}(x_0 - x_0')\delta(x, x'). \quad (34)$$

The relativistic commutation rules are

$$[A^{(+)\mu}(x), A^{(+)\nu}(x')] = 2i\hbar c g^{\mu\nu}\Delta(x, x'), \quad (35)$$

$$[A^{(+)\mu}(x), A^{(-)\nu}(x')] = 0, \quad (36)$$

$$[A^{(-)\mu}(x), A^{(-)\nu}(x')] = -2i\hbar c\Delta(x, x'), \quad (37)$$

whence we get

$$[A_{\text{rad}}^{\mu}(x), A_{\text{rad}}^{\nu}(x')] = 0. \quad (38)$$

If the A_{rad}^{μ} would be potentials of the Heisenberg-Pauli type we would have instead of (38)

$$[A_{\text{rad}}^{\mu}(x), A_{\text{rad}}^{\nu}(x')] = i\hbar c g^{\mu\nu}\Delta(x, x').$$

It is well known that in quantum electrodynamics the potentials which come in the interaction with the particles are Wentzel potentials.[6] From now on we shall always assume that our potentials are

Wentzel potentials, which depend on two time variables: the time of the field x^0 and the time of the particles $x_p{}^0$. The commutation rules (35)–(37) are also valid for the Wentzel potentials.

We shall now expand the Wentzel potentials in Fourier series by enclosing the field in a cubic box of volume V and imposing periodic boundary conditions

$$A^{(\pm)\mu}(x)=\left(\frac{4\pi\hbar c}{V}\right)^{\frac{1}{2}}\sum_k k_0{}^{-\frac{1}{2}} \times\{Q^{(\pm)\mu}(k)\exp[-ik^\rho x_\rho] +\bar{Q}^{(\pm)\mu}(k)\exp[ik^\rho x_\rho]\}, \quad (39)$$

$$k_0=|\mathbf{k}|. \quad (39a)$$

The commutation rules for the Fourier coefficients are

$$[Q^{(+)\mu}(k),\ \bar{Q}^{(+)\nu}(k')]=-g^{\mu\nu}\delta_{kk'}, \quad (40)$$

$$[Q^{(-)\mu}(k),\ \bar{Q}^{(-)\nu}(k')]=g^{\mu\nu}\delta_{kk'}. \quad (41)$$

The Fourier coefficients of the radiation potentials are the $Q_{\text{rad}}{}^\mu(k)$:

$$Q_{\text{rad}}{}^\mu(k)=\tfrac{1}{2}[Q^{(+)\mu}-Q^{(-)\mu}]. \quad (42)$$

It results from (40) and (41) that

$$[Q_{\text{rad}}{}^\mu(k),\ \bar{Q}_{\text{rad}}{}^\nu(k')]=0. \quad (43)$$

Let us consider now the operators $N_\mu{}^{(\pm)}(k)$:

$$N_a{}^{(+)}=\bar{Q}_a{}^{(+)}Q_a{}^{(+)},\quad N_0{}^{(+)}=Q_0{}^{(+)}\bar{Q}_0{}^{(+)}, \quad (44)$$

$$N_a{}^{(-)}=Q_a{}^{(-)}\bar{Q}_a{}^{(-)},\quad N_0{}^{(-)}=\bar{Q}_0{}^{(-)}Q_0{}^{(-)}. \quad (45)$$

The operators N have the eigenvalues $0, 1, 2, 3\cdots$. It is easily seen that the Hamiltonian of the radiation waves H_f has the following expression

$$H_f=\sum_k\left[\left\{\sum_{a=1}^{3}N_a{}^{(+)}(k)-N_0{}^{(+)}(k)\right\} -\left\{\sum_{a=1}^{3}N_a{}^{(-)}(k)-N_0{}^{(-)}(k)\right\}\right]\hbar k_0. \quad (46)$$

VI. THE QUANTUM EQUATIONS OF MOTION

(A.) In our quantum formalism we shall introduce a single time variable for all the particles because of the actions at a distance. Therefore, we will have two equations of motion for any quantity B which does not depend explicitly on the time variables

$$ihc\frac{\partial B}{\partial x_p{}^0}=[B, H_p], \quad (47)$$

$$ihc\frac{\partial B}{\partial x^0}=[B, H_f]. \quad (48)$$

(It is more satisfactory to consider (47) and (48) as supplementary conditions.) We shall assume that our particles have spin $\frac{1}{2}$. Therefore the Hamiltonian of the particles will be

$$H_p=\sum_j H_j+H_{\text{int}}, \quad (49)$$

$$H_j=(c\alpha_j\cdot\{\mathbf{p}_j-(e_j/c)\mathbf{A}_{\text{rad}}(x_j)\}) +\beta_j m_j c^2+e_j A_{\text{rad}}{}^0(x_j), \quad (50)$$

$$H_{\text{int}}=\tfrac{1}{2}\sum_j e_j\alpha_j{}^\mu\sum_{k\neq j}[A_{k,\text{at},\mu}(x_j)]_{(x_j{}^0=x_p)}. \quad (51)$$

The attached potentials can be defined in quantum theory by integrals analogous to the classical ones (Eq. (7)):

$$A_{j,\text{at}}{}^\mu(x)=e_j\int_{-\infty}^{+\infty}\alpha_j{}^\mu(\tau)[\delta(x, x_j(\tau))]_{(x_j{}^0=\tau)}d\tau. \quad (52)$$

The α and β are the well-known Dirac operators. The δ-function which appears under the integral is defined as a symbolic limit

$$\delta(x, x_j(\tau))=\frac{1}{(\pi)^{\frac{1}{2}}}\lim_{\epsilon\to 0}\epsilon^{-1}\exp[\epsilon^{-2}\{(x^\rho-x_j{}^\rho(\tau)) \times(x_\rho-x_{j,\rho}(\tau))\}^2]. \quad (53)$$

Hence

$$A_{j,\text{at}}{}^\mu(x)=\frac{1}{(\pi)^{\frac{1}{2}}}e_j\lim_{\epsilon\to 0}\epsilon^{-1}\int_{-\infty}^{+\infty}\alpha_j{}^\mu(\tau) \times\exp[\epsilon^{-2}\{(x_0-\tau)^2-|\mathbf{x}-\mathbf{x}_j(\tau)|^2\}^2]d\tau, \quad (54)$$

with

$$|\mathbf{x}-\mathbf{x}_j(\tau)|^2=\sum_{a=1}^{3}[x^a-x_j{}^a(\tau)]^2. \quad (54a)$$

It results from (47) that

$$\frac{\partial}{\partial x_p{}^0}A^{(\pm)\mu}(x) =\sum_j\alpha_j{}^\mu(x_p{}^0)[\Delta(x, x_j(x_p{}^0))]_{(x_j{}^0=x_p{}^0)}, \quad (55)$$

whence

$$\frac{\partial}{\partial x_p{}^0}A_{\text{rad}}{}^\mu(x)=0. \tag{56}$$

This equation is very important because it shows that the radiation potentials are pure field quantities since they do not depend on the time of the particles.

We can go over from the preceding formalism to the formalism with a single time variable by putting

$$x_p{}^0=x^0=x_s{}^0. \tag{57}$$

$x_s{}^0/c$ is the time of the system particles plus radiation field. We have, obviously,

$$i\hbar c\frac{\partial B}{\partial x_s{}^0}=i\hbar c\left(\frac{\partial B}{\partial x_p{}^0}+\frac{\partial B}{\partial x^0}\right)_{(x_p{}^0=x^0=x_s{}^0)}$$
$$=[B, H_p+H_f]. \tag{58}$$

(B.) In the preceding section we used the Heisenberg picture in which the state of the system does not vary with time. We shall now go over to the Schrödinger picture in which the state of the system varies with time. In this picture we have the Schrödinger equation for the wave function Ψ:

$$i\hbar\frac{\partial\Psi}{\partial t}=\mathfrak{H}\Psi, \quad (ct=x_s{}^0). \tag{59}$$

$\mathfrak{H}$ is the Hamiltonian in the Schrödinger picture; it cannot be taken as the Hamiltonian of the Heisenberg picture corresponding to a fixed value of t, $t=0$, for instance, because the attached potentials do depend explicitly on the time. $\mathfrak{H}$ is given in terms of H by the formula

$$\mathfrak{H}=U(t, 0)HU^{-1}(t, 0), \tag{60}$$

which is a particular case of the general formula (79). The state Ψ must satisfy the Dirac-Fock-Podolsky supplementary conditions

$$R^{(\pm)}(x)\Psi=0, \tag{61}$$

$$R^{(\pm)}(x)=\frac{\partial}{\partial x^\mu}A^{(\pm)\mu}(x)+\sum_j e_j\Delta(x, x_j). \tag{62}$$

It is remarkable that the supplementary condition for the radiation potentials is the Lorentz condition, as it results at once from (61).

It is more convenient to express the supplementary conditions in terms of the Fourier coefficients of the potentials. We have

$$\left\{k_\mu Q^{(\pm)\mu}(k)-\left(\frac{\pi}{\hbar cV}\right)^{\frac{1}{2}}\sum_j e_j k_0{}^{-\frac{1}{2}}\right.$$
$$\left.\times\exp[ik_\mu x_j{}^\mu]_{(x_j{}^0=ct)}\right\}\Psi=0, \tag{63}$$

$$\left\{k_\mu \bar{Q}^{(\pm)\mu}(k)-\left(\frac{\pi}{\hbar cV}\right)^{\frac{1}{2}}\sum_j e_j k_0{}^{-\frac{1}{2}}\right.$$
$$\left.\times\exp[-ik_\mu x_j{}^\mu]_{(x_j{}^0=ct)}\right\}\Psi=0. \tag{64}$$

VII. ELIMINATION OF THE LONGITUDINAL WAVES

Let us put

$$Q_T{}^{(\pm)a}(k)=Q^{(\pm)a}(k)+\frac{k^a}{k_0{}^2}[Q^{(\pm)b}(k)k_b]. \tag{65}$$

The $Q_T{}^a(k)$ are components of transversal vectors $\mathbf{Q}_T(k)$ which can be conveniently decomposed along the directions of two unit vectors $\mathbf{u}_s(k)$ $(s=1, 2)$ mutually orthogonal and orthogonal to $\mathbf{k}$.

$$[\mathbf{Q}_T{}^{(\pm)}(k)]_{(t=0)}=\sum_{s=1}^{2}Q_s{}^{(\pm)}(k)\mathbf{u}_s(k). \tag{66}$$

By taking into account the supplementary conditions (63) and (64), we get

$$\mathfrak{H}_f\Psi=\sum_k \hbar ck_0\left[\sum_{s=1}^{2}\{N_s{}^{(+)}(k)-N_s{}^{(-)}(k)\}\right]\Psi$$
$$-\sum_{j=1}^{n}e_j[A_{\text{rad}}{}^0(x_j)]_{(x_j{}^0=0)}\Psi. \tag{67}$$

$\mathfrak{H}_f$ is the Hamiltonian of the photons in the Schrödinger picture

$$\mathfrak{H}_f=U(t, 0)H_fU^{-1}(t, 0). \tag{68}$$

The N are the numbers of positive and negative energy photons

$$N_s{}^{(+)}=\bar{Q}_s{}^{(+)}Q_s{}^{(+)}, \quad N_s{}^{(-)}=Q_s{}^{(-)}\bar{Q}_s{}^{(-)}. \tag{69}$$

It results from (67) that

$$\mathcal{H}\Psi=\sum_j\left\{-c\alpha_{j,a}\left(p_j{}^a-\frac{e_j}{c}A_{\text{rad}}{}^a(x_j)\right)+m_jc^2\beta_j\right.$$
$$\left.+\frac{e_j}{2}\sum_{l\neq j}\alpha_{j,\mu}A_{l,\text{at}}{}^\mu(x_j)\right\}_{\text{Schröd}}\Psi$$
$$+\left\{\sum_k\hbar ck_0\left[\sum_{s=1}^{2}(N_s{}^{(+)}(k)-N_s{}^{(-)}(k))\right]\right\}\Psi. \quad (70)$$

All the operators in the right-hand side of (70) are taken in the Schrödinger picture. Let us introduce now the gauge invariant momenta $\mathbf{p}_j{}^\dagger$:

$$\mathbf{p}_j{}^\dagger=\mathbf{p}_j-\frac{e_j}{c}\mathbf{A}_{\text{rad},\,L}(x_j). \quad (71)$$

$\mathbf{A}_{\text{rad},\,L}$ is the longitudinal part of the vector potential $\mathbf{A}_{\text{rad}}$. By taking into account that the curl of $\mathbf{A}_{\text{rad},\,L}$ vanishes, we see that the components of the gauge invariant momenta do commute. The commutation rules between the gauge invariant momenta and the coordinates of the particles are of the same type as those for the ordinary momenta $\mathbf{p}$. The $\mathbf{p}^\dagger$ are gauge invariant because

$$[p_j{}^{\dagger a},\,R^{(\pm)}(x)]=0. \quad (72)$$

By introducing the gauge invariant momenta we can eliminate completely the longitudinal photons from the expression of $\mathcal{H}\Psi$:

$$\mathcal{H}\Psi=\sum_j\left\{-c\alpha_{j,a}\left(p_j{}^{\dagger a}-\frac{e_j}{c}A_{\text{rad},\,T}{}^a(x_j)\right)+m_jc^2\beta_j\right.$$
$$\left.+\frac{e_j}{2}\sum_{l\neq j}\alpha_{j,\mu}A_{l,\text{at}}{}^\mu(x_j)\right\}_{\text{Schröd}}\Psi$$
$$+\left\{\sum_k\hbar ck_0\left[\sum_{s=1}^{2}(N_s{}^{(+)}(k)-N_s{}^{(-)}(k))\right]\right\}\Psi. \quad (73)$$

$\mathbf{A}_{\text{rad},\,T}$ is the transverse part of $\mathbf{A}_{\text{rad}}$

$$\mathbf{A}_{\text{rad},\,T}(x)=\left(\frac{4\pi\hbar c}{V}\right)^{\frac{1}{2}}\sum_k k_0{}^{-\frac{1}{2}}$$
$$\times\{\mathbf{Q}_{\text{rad},\,T}(k)\exp[-ik^\rho x_\rho]$$
$$+\bar{\mathbf{Q}}_{\text{rad},\,T}(k)\exp[ik^\rho x_\rho]\}, \quad (74)$$
$$\mathbf{Q}_{\text{rad},\,T}=\tfrac{1}{2}[\mathbf{Q}_T{}^{(+)}-\mathbf{Q}_T{}^{(-)}]. \quad (75)$$

VIII. THE MÖLLER INTERACTION

We shall now establish first approximation formulas for the attached potentials which show that the direct interaction between particles coincides, in a first approximation, with the Möller interaction.

In the Heisenberg picture the time variation of a physical quantity B which does not depend explicitly on the time is given by a contact transformation

$$B(t)=U^{-1}(t,t')B(t')U(t,t'). \quad (76)$$

When the Hamiltonian does not depend explicitly on the time, we have

$$U(t,t')=\exp\left[-\frac{i}{\hbar}H(t-t')\right]. \quad (77)$$

We have in the Heisenberg picture, because of (52) and (76),

$$A_{j,\text{at}}{}^\mu(x)=ce_j\int_{-\infty}^{+\infty}U^{-1}(t',0)$$
$$\times[\alpha_j{}^\mu(0)\delta(x,x_j(0))]U(t',0)dt'. \quad (78)$$

We go over from the Heisenberg to the Schrödinger picture by a contact transformation

$$B_{\text{Schröd}}(t)=U(t,0)B(t)U^{-1}(t,0), \quad (79)$$

whence

$$[A_{j,\text{at}}{}^\mu(x)]_{\text{Schröd}}=ce_j\int_{-\infty}^{+\infty}U(t,t')$$
$$\times[\alpha_j{}^\mu\delta(x,x_j)]_{\text{Schröd}}U^{-1}(t,t')dt'. \quad (80)$$

In order to determine the first approximation expressions of the attached potentials we shall use the operator U corresponding to an unperturbed motion in which the interactions between the particles and their interactions with the radiation field are neglected. We shall denote the U of the unperturbed motion by U_0:

$$U_0(t,t')=\exp[-(i/\hbar)(\textstyle\sum_j H_j{}^0+H_f)(t-t')], \quad (81)$$
$$H_j{}^0=c(\boldsymbol{\alpha}_j\cdot\mathbf{p}_j)+\beta_jm_jc^2. \quad (82)$$

In the approximation we are using

$$[A_{j,\text{at}}{}^\mu(x)]_{\text{Schröd}}=ce_j\int_{-\infty}^{+\infty}\exp[-(i/\hbar)H_j{}^0(t-t')]$$
$$\times[\alpha_j{}^\mu\delta(x,x_j)]_{\text{Schröd}}$$
$$\times\exp[(i/\hbar)H_j{}^0(t-t')]dt'. \quad (83)$$

Let us denote by H_d the direct interaction between the particles in the Schrödinger picture

$$H_d=\tfrac{1}{2}\sum_j\sum_{l\neq j} e_j[\alpha_{j,\mu}A_{l,\mathrm{ret}}{}^{\mu}(x_j)]_{\mathrm{Schröd}},\ (x_j{}^0=ct). \quad (84)$$

In order to derive Möller's formula for the matrix elements of the interaction between the particles, we shall consider two states of the system particles plus field $\Psi^{(r)}$ $(r=1, 2)$, whose wave functions are of the form

$$\Psi^{(r)}=\prod_j \psi_j{}^{(r)}\psi_f. \quad (85)$$

The $\psi_j{}^{(r)}$ are solutions of the Dirac equations

$$H_j{}^0\psi_j{}^{(r)}=E_j{}^{(r)}\psi_j{}^{(r)}, \quad (86)$$

representing free particles with momenta $\mathbf{p}_j{}^{(r)}$. ψ_f is the wave function of the radiation field; we assume that ψ_f does not depend on the variables of the particles. By taking into account that

$$\exp[-(i/\hbar)H_j{}^0(t-t')]\psi_j{}^{(r)}=\exp[-(i/\hbar)E_j{}^{(r)}(t-t')]\psi_j{}^{(r)}, \quad (87)$$

we get the first approximation value of the matrix element of H_d:

$$(1|H_d|2)=-\tfrac{1}{2}h^{3n}(h\pi)^{-1}\sum_j\sum_{l\neq j} e_je_l(1|\alpha_j{}^{\mu}\alpha_{l,\mu}|2)_{\mathrm{Schröd}}\times\delta(\mathbf{p}_j{}^{(1)}-\mathbf{p}_j{}^{(2)}+\mathbf{p}_l{}^{(1)}-\mathbf{p}_l{}^{(2)})\prod_{k\neq l,j}\delta(\mathbf{p}_k{}^{(1)}-\mathbf{p}_k{}^{(2)})\times\left[\frac{1}{c^2}(E_j{}^{(1)}-E_j{}^{(2)})^2-|\mathbf{p}_j{}^{(1)}-\mathbf{p}_j{}^{(2)}|^2\right]^{-1}, \quad (88)$$

corresponding to a transition between the two states (Möller's formula).

IX. THE "FREEZING" OF THE DEGREES OF FREEDOM OF THE FIELD

In our formalism the number of degrees of freedom of the field corresponding to each wave number vector $\mathbf{k}$ is larger than in the Heisenbergs Pauli electrodynamics, because we have photon-with negative energies. In this point our formalism is analogous to those introduced by Dirac.[8,9] There are, however, essential differences between Dirac's treatments and ours. Dirac uses the Wentzel potentials of the Heisenberg-Pauli field and introduces redundant variables by splitting the Heisenberg-Pauli field into two parts, whereas we use the potentials of the radiation field. In Dirac's formalism the interaction between the particles results from their interactions with the Heisenberg-Pauli field, whereas in our theory the main part of the interaction between the particles cannot be derived from their interactions with the radiation field.

Let us introduce the variables $p_s{}^{\pm}(k)$ and $q_s{}^{\pm}(k)$:

$$\left.\begin{aligned} Q_s{}^{(+)}(k)+Q_s{}^{(-)}(k)&=p_s{}^{+}(k)+ip_s{}^{-}(k)\\ \bar{Q}_s{}^{(+)}(k)+\bar{Q}_s{}^{(-)}(k)&=p_s{}^{+}(k)-ip_s{}^{-}(k)\end{aligned}\right\}(s=1, 2); \quad (89)$$

$$\left.\begin{aligned} Q_s{}^{(+)}(k)-Q_s{}^{(-)}(k)&=q_s{}^{-}(k)-iq_s{}^{+}(k)\\ &=2Q_{\mathrm{rad},s}(k)\\ \bar{Q}_s{}^{(+)}(k)-\bar{Q}_s{}^{(-)}(k)&=q_s{}^{-}(k)+iq_s{}^{+}(k)\\ &=2\bar{Q}_{\mathrm{rad},s}(k)\end{aligned}\right\}. \quad (90)$$

The commutation rules for the new variables are

$$[q_s{}^{+}(k), p_{s'}{}^{+}(k')]=[q_s{}^{-}(k), p_{s'}{}^{-}(k')]=i\delta_{ss'}\delta_{kk'}, \quad (91)$$

$$[q_s{}^{\pm}(k), q_{s'}{}^{\pm}(k')]=[p_s{}^{\pm}(k), p_{s'}{}^{\pm}(k')]=0, \quad (92)$$

$$[q_s{}^{+}(k), p_{s'}{}^{-}(k')]=[q_s{}^{-}(k), p_{s'}{}^{+}(k')]=0. \quad (93)$$

It results from Eqs. (90) *that the interaction between a particle and the radiation field does not involve the variables* $p_s{}^{\pm}$.

It is easily seen that

$$N_s{}^{(+)}(k)-N_s{}^{(-)}(k)=p_s{}^{+}(k)q_s{}^{-}(k)-p_s{}^{-}(k)q_s{}^{+}(k). \quad (94)$$

We can take as variables of the radiation field in the wave function Ψ the $p_s{}^{\pm}(k)$. If the wave function Ψ does not depend on the $p_s{}^{\pm}(k)$ corresponding to a definite value of $\mathbf{k}$, we will have

$$[N_s{}^{(+)}(k)-N_s{}^{(-)}(k)]\Psi=0, \quad (95)$$

$$[\mathbf{Q}_{\mathrm{rad},r}(k)\exp(-ik^{\rho}x_{\rho})+\bar{\mathbf{Q}}_{\mathrm{rad},r}(k)\exp(ik^{\rho}x_{\rho})]\Psi=0. \quad (96)$$

Therefore, in the state described by such a wave function the degrees of freedom of the field corresponding to the value of $\mathbf{k}$ *do not give any contribution to the energy of the field and to the interaction with the particles.* We shall call "frozen" degrees of freedom of the field the degrees of freedom corresponding to values of $\mathbf{k}$ and s whose

$p_s^{\pm}(k)$ are not involved in the wave function Ψ of the system field plus particles.

The numbers of positive and negative energy photons corresponding to a "frozen" set of values of $\mathbf{k}$ and s are not determined but they are equal, as it results from (95).

It is obviously possible to impose on the solution of the Schrödinger equation of the system field plus particles the condition of not involving the $p_s^{\pm}(k)$ corresponding to as many values of $\mathbf{k}$ as we want, because the freezing conditions

$$Q_{\text{rad.}\,s}(k)\Psi=0, \quad \bar{Q}_{\text{rad.}\,s}(k)\Psi=0 \qquad (97)$$

will be satisfied at any time if they are fullfiled for $t=0$. *We could, for instance, "freeze" all the degrees of freedom of the radiation field and thus obtain solutions of the Schrödinger equation representing states of motion in which the particles do not interact with the radiation field. The existence of such solutions is of fundamental importance because it shows that the existence of negative energy photons in our formalism does not exclude the existence of stationary states of motion of the particles.*

The "freezing" of degrees of freedom opens new possibilities in the quantum theory of fields. Thus, for instance, if we consider the one-electron problem, we will get an infinite self-energy if we define the vacuum as the state of the field in which there are no positive or negative energy photons. But, if we define the vacuum as the state of the field in which all its degrees of freedom are "frozen," we will get a vanishing self-energy. *It is also possible to get a finite self-energy by "freezing" only the degrees of freedom corresponding to frequencies above a certain limit (in the rest system of the electron which is supposed to have a definite momentum).*

X. THE PHYSICAL INTERPRETATION RULE

In the computation of the probability of a transition in which are involved r photons (the photons which appear in the initial and final states) with momenta $\hbar\mathbf{k}_r$ $(r=1, 2, \cdots l)$, we shall use a wave function of the system particles plus field involving only the field variables corresponding to $\mathbf{k}$'s in the relevant ranges $(\mathbf{k}_r-\frac{1}{2}\Delta\mathbf{k}, \mathbf{k}_r+\frac{1}{2}\Delta\mathbf{k})$, $\Delta\mathbf{k}$ being a small vector with a length of the order of the line breadths. The degrees of freedom corresponding to values of $\mathbf{k}$ outside the relevant ranges will be "frozen." The "frozen" wave function will satisfy the Schrödinger equation of the system but it will also satisfy the reduced Schrödinger equation, which is obtained by dropping in the Hamiltonian all the terms corresponding to "frozen" degrees of freedom. We shall assume that: *The reduced Schrödinger equation must be treated as the wave equation of a system with a finite number of degrees of freedom. Its solutions will be normalized as if the "frozen" degrees of the field would not exist.* It would not be possible to normalize the "frozen" wave function by treating it as the wave function of a system with an infinite number of degrees of freedom, but it can be normalized as the wave function of a system with a finite number of degrees of freedom.

We shall now take as field variables in the "frozen" wave function the $N_s^{(\pm)}(k)$ corresponding to the "unfrozen" degrees of freedom. Let the initial and final states of the field in the physical world be characterized by the occupation numbers $n_i(k, s)$ and $n_f(k, s)$. We shall associate to that transition in the physical world the transition of the formalism between the states characterized by the occupation numbers $[N_s^{(\pm)}(k)]_i$ and $[N_s^{(\pm)}(k)]_f$.

$$[N_s^{(+)}(k)]_i=n_i(k, s), \quad [N_s^{(-)}(k)]_i=0, \qquad (98)$$

$$[N_s^{(+)}(k)]_f=n_f(k, s), \quad [N_s^{(-)}(k)]_f=0. \qquad (99)$$

We shall denote by N the total number of emitted and absorbed photons in the physical world. The physical interpretation rule is the following one:

The probability of the transition $n_i \to n_f$, in the physical world, is equal to the probability of the transition $[N]_i \to [N]_f$ in the formalism—computed according to the usual quantum rules—multiplied by 2^N.

The preceding interpretation rule does not use the negative energy photons. It is possible to give an interpretation rule in which no use is made of the positive energy photons, by interpreting the emission of a negative energy photon as an absorption in the physical world, and conversely the absorption of a negative energy photon as an emission in the physical world. It is also possible to give an interpretation rule in which the ab-

sorptions and emissions of photons in the physical world do correspond to emissions of negative energy and positive energy photons, respectively, in the formalism. The arbitrariness in the physical interpretation rule is analogous to that existing in Dirac's form of the Heisenberg-Pauli electrodynamics (see W. Pauli[12]). The interpretation rule we have formulated is the simplest one and can be justified by a correspondence argument as we shall see.

The existence of positive and negative energy photons in our quantum formalism gives rise to the multiplicity of the possible interpretation rules and seems to be an inconvenience of the theory. The negative energy photons are not introduced by a device of quantization, their existence is a consequence of the fact that the classical expression of the energy of the radiation field is not necessarily positive. The multiplicity of the possible physical interpretations will presumably disappear when the problem of the negative energy states for both electrons and photons will be better understood. We have shown that in classical theory it is necessary to assume that a particle with negative kinetic energy creates an advanced field,[1,2] in order that the reaction of radiation be a damping force, because the advanced field gives rise to a Larmor "gain." In quantum theory such a Larmor "gain" corresponds to an emission of negative energy photons, therefore, it may be unavoidable to introduce negative energy photons, because of the existence of negative energy states for the electrons.

Our physical interpretation rule was chosen by a criterion of simplicity, but it corresponds to the classical time boundary conditions. In the classical theory of the point electron the time boundary conditions are introduced in order to get rid of the motions with indefinite self-acceleration of the particles, as it was shown by Dirac[13] and Schönberg.[1,2] The indefinite self-acceleration is due to an indefinite decrease of the potential energy of a particle with respect to the radiation field, which is included in the energy of the radiation field. The classical time boundary conditions select the motions in which the potential energy of a particle with respect to the radiation field (acceleration energy) remains constant on the average, so that on the average there is an increase of the energy of the radiation field in the physically possible motions, because of the Larmor loss of the particles. *The emission of negative energy photons is the quantum equivalent of the classical self-acceleration and, thus, our physical interpretation which does not take into account the emission and absorption of negative energy photons corresponds to the classical exclusion of the self-accelerations on the average by means of the time boundary conditions.*

[12] W. Pauli, Rev. Mod. Phys. 15, 175 (1943).

[13] P. A. M. Dirac, Proc. Roy. Soc. A167, 148 (1938).

PHYSICAL REVIEW VOLUME 74, NUMBER 7 OCTOBER 1, 1948

Elimination of Divergences in the Meson Theory. I

MARIO SCHÖNBERG
University of São Paulo, São Paulo, Brazil

(Received March 15, 1948)

The divergences of the meson theory are avoided by using a method introduced by the author in quantum electrodynamics; the method is worked out for the case of pseudoscalar charged mesons. The quasi-static forces between the nucleons are treated as relativistic actions at a distance; two independent complex pseudoscalars are used in the description of the meson field. It is shown that it is possible to choose separately the type of nuclear forces and the interaction with the meson field, because of the action at a distance treatment. The formalism, associated to special rules of interpretation, leads to finite transition probabilities; it can also be applied to self-energy problems and leads to finite self-energies and magnetic moments. In the computation of the self-energies and magnetic moments two constants appear, which may be chosen in such a way as to give different masses to the proton and neutron.

I. INTRODUCTION

IN this paper we shall extend to the meson theory the methods applied by us to the quantum theory of the electromagnetic field.[1,2] Our treatment of the electromagnetic field is based on a combination of the ideas of actions at the distance of Tetrode[3] and Fokker[4] with the field concepts of Faraday and Maxwell[5] (in quantum theory these concepts correspond to the quantum theory of fields of Heisenberg and Pauli[6]). The separation of the actions at a distance from the radiative actions (actions through the field) is closely related to the separation of the static forces from the radiative actions, which is usually done by means of a contact transformation (in the meson theory such a treatment was systematically developed by Möller and Rosenfeld[7]). The actions at a distance are a relativistic generalization of the static forces; they are half-advanced, half-retarded forces, not instantaneous ones. The actions at a distance include the static actions plus a part of the forces which are usually derived from the interaction between the particles and the radiation field (interaction with the transverse waves, in the electromagnetic case). In order to separate the actions at a distance from the true radiation field, which is classically one-half the difference between the retarded and advanced fields, it is necessary to modify the method of quantization of the fields by using two sets of field quantities, which correspond to the quantities of the classical retarded and advanced fields. The commutation rules for the quantities of the two independent fields, which correspond to the classical retarded and advanced fields, are not the same, because of the structure of the classical Lagrangian, but they are not very different. On the other hand, the commutation rules for the quantities of the true radiation field are essentially different from those of the usual forms of the field theories. Since the particles interact only with the true radiation field, because the actions at a distance are introduced separately, the description of the interaction between the particles and the fields, given by our formalism, is essentially different from the usual one and allows us to avoid the divergences.

In order to describe the actions at a distance we define particle operators for the half-retarded, half-advanced quantities analogous to the half-retarded, half-advanced classical potentials. The method of defining those operators, in the quantum formalism, is similar to that used in the classical theory; it is analogous to the method used by Möller and Rosenfeld in their definition of the static potentials. Instead of the Green function of the static Yukawa equation, used by Möller and Rosenfeld, we use the Green function

[1] M. Schönberg, "Quantum theory of the point electron. I." Phys. Rev. 74, 738 (1948).
[2] M. Schönberg, "Quantum theory of the electromagnetic field. I." Anais Acad. Brasil. Cienc. (in print).
[3] H. Tetrode, Zeits. f. Physik 10, 317 (1922).
[4] A. D. Fokker, Zeits. f. Physik 58, 386 (1929).
[5] M. Schönberg, "Classical theory of the point electron," Phys. Rev. 69, 211 (1946).
[6] W. Heisenberg und W. Pauli, Zeits. f. Physik 56, 1 (1929), and 59, 168 (1930).
[7] C. Möller and L. Rosenfeld, Kgl. Danske Vid. Sels. Math.-Fys. Medd 17, 8 (1940).

of the Klein-Gordon equation which corresponds to half-advanced, half-retarded solutions. The essential difference between our treatment and the Möller and Rosenfeld one lies in the fact that they can obtain the static forces by means of a contact transformation applied to the Hamiltonian of the system nucleons plus meson field, whereas we do not get the actions at a distance from the interaction between the nucleons and the meson field, but do introduce them directly and independently. Our treatment allows us to associate actions at a distance corresponding to the symmetrical Möller-Rosenfeld mixture to an arbitrary type of meson field. In this part of the paper we consider only a field of pseudoscalar charged mesons, for the sake of simplicity, but we could associate the same actions at a distance with a charged vector meson field or to a field of charged mesons with spin $\frac{1}{2}$. The interaction constants which appear in the actions at a distance can be taken independently. Our particle operators for the potentials allow us to get the static forces, by neglecting all the relativistic corrections; they lead to relativistic interactions of the type considered by Leite Lopes[8] and Tamm,[9] by taking into account the retardation effects in a first approximation.

The treatment of the nuclear forces as actions at a distance offers new possibilities. From the point of view of the actions at a distance it is not necessary to use the Green functions of the Klein-Gordon equation in the derivation of the nuclear forces. We may replace those Green functions by other relativistic functions in such a way as to modify the form of the nuclear forces for small distances and thus avoid the difficulties arising from the high singularity of the dipole interactions as well as from those involved in the non-static part of the interaction. Thus we get a relativistic "radius" for the nucleons which does not come in the interactions between the nucleons and the meson or electromagnetic fields but does introduce a relativistic cut-off of the forces at small distances.

The special nature of the commutation rules of the radiation meson field allows us to get exact solutions of the Schrödinger equation of the system nucleons plus meson field, in which the nucleons interact only with the degrees of freedom corresponding to some arbitrarily chosen momenta of the mesons. We call those solutions "frozen" solutions and the degrees of freedom of the meson field, which do not interact with the nucleons in those "frozen" solutions, the "frozen" degrees of freedom. By using "frozen" solutions it becomes possible to get rid of the divergences both in the computation of the transition probabilities and the self-energies. The possibility of the "freezing" results from the fact that, in our formalism, the field has twice as many degrees of freedom as in the usual treatment, because we introduce two sets of field quantities. Our method of quantization has some points in common with Dirac's method,[10,11] but the two methods differ fundamentally because in Dirac's treatment the particles interact with a field which does not have the same commutation rules as our radiation field, so that it is not possible to "freeze" the irrelevant degrees of freedom of the field. The duplication of the degrees of freedom of the meson field leads to the existence of mesons with positive and negative energies. It is important to notice that the negative energy mesons which appear in our quantum formalism correspond to the waves with negative energy of the underlying *c*-number theory. The existence of the negative energy mesons is not due to a special method of quantization, but it follows from the fact that the *c*-number energy of the radiation field is not necessarily positive as the total energy of the field-including the potential energy of the actions at a distance—in the usual *c*-number field theories.

The existence of negative energy mesons and the necessity of using "frozen" solutions, in order to avoid divergences, require a physical interpretation rule and a "freezing" criterion. The physical interpretation rule can be chosen in many different ways—as it happens in Dirac's formalism with an indefinite metric in Hilbert space (see W. Pauli[12]). In the electromagnetic case it is possible to justify the choice of the simplest interpretation rule by correspondence considerations, presumably the same thing can

[8] J. Leite Lopes, Anais Acad. Brasil. Ciencias **17**, 273 (1945).
[9] Ig. Tamm, J. Physics, **9**, 449 (1945).
[10] P. A. M. Dirac, Proc. Roy. Soc. **A180**, 1 (1942).
[11] P. A. M. Dirac, Com. Dublin Inst. Adv. Stud. A, No. 3 (1946).
[12] W. Pauli, Rev. Mod. Phys. **15**, 175 (1943).

also be done in meson theory, so that our choice of a definite interpretation rule seems justified. In the computation of transition probabilities there is a very natural "freezing" criterion; the degrees of freedom which must be kept "unfrozen" are indicated by the mesons which appear before and after the transition. Thus the application of our formalism to the computation of transition probabilities is quite straightforward and does not lead to any real arbitrariness, because the "freezing" criterion is natural and the physical interpretation rule has a classical analog.

The application of our formalism to self-energy problems is less satisfactory than in the case of the transition probabilities, because we lack a natural "freezing" criterion. Presumably a further development of the theory will improve the situation. We applied the formalism to the computation of the self-energies and magnetic moments of the nucleons, by assuming that the degrees of freedom of the field corresponding to momenta of the mesons above certain limits, in the rest system of the nucleon, are "frozen." The "freezing" in the case of the meson field presents a difference, with respect to the electromagnetic case, arising from the existence of positive and negative mesons: It is possible to introduce two radiation meson fields, one giving rise to the emission and absorption of positive mesons with positive energy and negative mesons with negative energy, another giving rise to the emission and absorption of negative mesons with positive energy and positive mesons with negative energy. The two radiation meson fields can be "frozen" separately in the computation of the self-energies and magnetic moments, with the introduction of two different upper limits for the "unfrozen" meson momenta. If the two limits are equal, the self-energies of the proton and the neutron will become equal, and the contributions of the meson field to the magnetic moments will be opposite. By taking two different limits, the self-energy of the neutron can be made larger than the self-energy of the proton, in agreement with the experimental evidence.

II. QUANTIZATION OF THE MESON FIELD

We shall consider a system of n point nucleons interacting with a field of pseudoscalar charged mesons, described by two independent pseudoscalars, $\phi^{(+)}$ and $\phi^{(-)}$. The equations of motion of the field will be derived from the action principle

$$\delta\int L d_4x=0, \tag{1}$$

$$\begin{aligned}L=&-\frac{1}{2}\left(\frac{\partial\phi^{(+)*}}{\partial x^\mu}\frac{\partial\phi^{(+)}}{\partial x_\mu}-K^2\phi^{(+)*}\phi^{(+)}\right)\\&-\frac{1}{2}\left(\frac{\partial\phi^{(-)*}}{\partial x^\mu}\frac{\partial\phi^{(-)}}{\partial x_\mu}-K^2\phi^{(-)*}\phi^{(-)}\right)\\&+\tfrac{1}{2}g_0\sum_{j=1}^{n}\Gamma_j\delta(\mathbf{x}-\mathbf{x}_j)[T_j(\phi^{(+)}-\phi^{(-)})\\&+T_j^*(\phi^{(+)*}-\phi^{(-)*})]+\frac{i}{2}f_0\sum_{j=1}^{n}\Gamma_j\gamma_j^\mu\delta(\mathbf{x}-\mathbf{x}_j)\\&\times\left[T_j\left(\frac{\partial\phi^{(+)}}{\partial x^\mu}-\frac{\partial\phi^{(-)}}{\partial x^\mu}\right)\right.\\&\left.+T_j^*\left(\frac{\partial\phi^{(+)*}}{\partial x^\mu}-\frac{\partial\phi^{(-)*}}{\partial x^\mu}\right)\right].\end{aligned} \tag{2}$$

K is related to the mass of the meson m.

$$K=mc/h. \tag{3}$$

g_0 and f_0 are interaction constants. The index j denotes the nucleons. The tensor index μ takes the values 0, 1, 2, 3. The operators γ_j^μ and Γ_j are

$$\gamma_j^0=\beta_j,\quad \gamma_j^a=\beta_j\alpha_j^a,\quad (a=1,2,3). \tag{4}$$

$$\Gamma_j=\gamma_j^1\gamma_j^2\gamma_j^3=-\beta_j\alpha_j^1\alpha_j^2\alpha_j^3. \tag{5}$$

The α and β are the well-known operators of the Dirac wave equation. The operators T and T^* transform neutrons into protons and protons into neutrons, respectively. We are taking as metrical tensor the tensor $g_{\mu\nu}$ whose components are

$$g_{00}=1,\quad g_{11}=g_{22}=g_{33}=-1,\quad g_{\mu\nu}=0,\quad (\mu\neq\nu). \tag{6}$$

$\phi^{(+)}$ and $\phi^{(-)}$ satisfy the same wave equation

$$\begin{aligned}\left(\frac{\partial^2}{\partial x^\mu\partial x_\mu}+K^2\right)\phi=&g_0\sum_{j=1}^{n}\Gamma_jT_j^*\delta(\mathbf{x}-\mathbf{x}_j)\\&-if_0\sum_{j=1}^{n}\frac{\partial}{\partial x^\mu}[\Gamma_j\gamma_j^\mu T_j^*\delta(\mathbf{x}-\mathbf{x}_j)].\end{aligned} \tag{7}$$

The conjugated momenta of the ϕ are the Π

$$\Pi^{(\pm)}(x)=\pm\frac{1}{2c}\frac{\partial}{\partial x_0}\phi^{(\pm)*}(x) \pm\frac{i}{2c}f_0\sum_j\Gamma_j\beta_jT_j\delta(\mathbf{x}-\mathbf{x}_j). \quad (8)$$

The only non-vanishing commutators between the ϕ and their derivatives are the following ones

$$\left[\phi^{(+)}(\mathbf{x},x_0),\frac{\partial}{\partial x_0}\phi^{(+)*}(\mathbf{x}',x_0)\right] =\left[\phi^{(+)*}(\mathbf{x},x_0),\frac{\partial}{\partial x_0}\phi^{(+)}(\mathbf{x}',x_0)\right] =2i\hbar c\delta(\mathbf{x}-\mathbf{x}'). \quad (9)$$

$$\left[\phi^{(-)}(\mathbf{x},x_0),\frac{\partial}{\partial x_0}\phi^{(-)*}(\mathbf{x}',x_0)\right] =\left[\phi^{(-)*}(\mathbf{x},x_0),\frac{\partial}{\partial x_0}\phi^{(-)}(\mathbf{x}',x_0)\right] =-2i\hbar c\delta(\mathbf{x}-\mathbf{x}'). \quad (10)$$

The commutation rules between quantities taken at different times can be derived in the usual way

$$[\phi^{(+)}(x),\phi^{(+)*}(x')]=-2i\hbar cD(x,x'), \quad (11)$$

$$[\phi^{(-)}(x),\phi^{(-)*}(x')]=2i\hbar cD(x,x'). \quad (12)$$

$D(x,x')$ is the symbolic function defined by the following equations:

$$\left(\frac{\partial^2}{\partial x^\mu\partial x_\mu}+K^2\right)D(x,x')=0, \quad (13)$$

$$D(x,x')_{(x_0=x_0')}=0,$$

$$\left[\frac{\partial}{\partial x_0}D(x,x')\right]_{(x_0=x_0')}=\delta(\mathbf{x}-\mathbf{x}'). \quad (14)$$

Let us put

$$\phi_{\text{rad}}=\tfrac{1}{2}[\phi^{(+)}-\phi^{(-)}]. \quad (15)$$

The radiation field ϕ_{rad} satisfies the homogeneous Klein-Gordon equation

$$\left(\frac{\partial^2}{\partial x^\mu\partial x_\mu}+K^2\right)\phi_{\text{rad}}=0. \quad (16)$$

The commutation rules of the radiation field and its complex conjugated are

$$[\phi_{\text{rad}}(x),\phi_{\text{rad}}(x')]=[\phi_{\text{rad}}{}^*(x),\phi_{\text{rad}}{}^*(x')]=0 \quad (17)$$

and

$$[\phi_{\text{rad}}(x),\phi_{\text{rad}}{}^*(x')]=0. \quad (18)$$

We shall enclose the field in a cubic box of volume V and impose periodic boundary conditions. It results from (16) that we may expand ϕ_{rad} in free waves

$$\phi_{\text{rad}}(x)=(\hbar c/V)^{\frac{1}{2}}\sum_k k_0^{-\frac{1}{2}}\{A_{\text{rad}}{}^p(k)\exp(-ik^\rho x_\rho) +A_{\text{rad}}{}^{n*}(k)\exp(ik^\rho x_\rho)\}. \quad (19)$$

$$k_0=(|\mathbf{k}|^2+K^2)^{\frac{1}{2}}. \quad (20)$$

We shall now introduce the two partial radiation fields $\phi_{\text{rad}}{}^p$ and $\phi_{\text{rad}}{}^n$

$$\phi_{\text{rad}}{}^{p,n}=(\hbar c/V)^{\frac{1}{2}}\sum_k k_0^{-\frac{1}{2}}A_{\text{rad}}{}^{p,n}(k) \times\exp(-ik^\rho x_\rho). \quad (21)$$

We have

$$[(\partial^2/\partial x^\mu\partial x_\mu)+K^2]\phi_{\text{rad}}{}^{p,n}=0, \quad (22)$$

and

$$[\phi_{\text{rad}}{}^{p,n}(x),\phi_{\text{rad}}{}^{p,n}(x')] =[\phi_{\text{rad}}{}^{p,n}(x),\phi_{\text{rad}}{}^{p,n*}(x')]=0. \quad (23)$$

The energy of the meson waves is H_m.

$$H_m=\tfrac{1}{2}\int\left(4c^2\Pi^{(+)*}\Pi^{(+)} -\frac{\partial\phi^{(+)*}}{\partial x^a}\frac{\partial\phi^{(+)}}{\partial x_a}+K^2\phi^{(+)*}\phi^{(+)}\right)d_3x -\tfrac{1}{2}\int\left(4c^2\Pi^{(-)*}\Pi^{(-)} -\frac{\partial\phi^{(-)*}}{\partial x^a}\frac{\partial\phi^{(-)}}{\partial x_a}+K^2\phi^{(-)*}\phi^{(-)}\right)d_3x. \quad (24)$$

The interaction energy between the nucleons and the mesons is H'.

$$H'=-g_0\sum_j[\Gamma_j\{T_j\phi_{\text{rad}}(x_j)+T_j{}^*\phi_{\text{rad}}{}^*(x_j)\}] -if_0\sum_j\left[\Gamma_j\gamma_j{}^\mu\left\{T_j\frac{\partial}{\partial x_j{}^\mu}\phi_{\text{rad}}(x_j) +T_j{}^*\frac{\partial}{\partial x_j{}^\mu}\phi_{\text{rad}}{}^*(x_j)\right\}\right]. \quad (25)$$

In our formalism the contact forces between nucleons arising from the two fields $\phi^{(\pm)}$ cancel each other, and there is no ambiguity as in the one field theories (see Kemmer[13]). The total momentum of the meson field is $\mathbf{G}_m$

$$\mathbf{G}_m=-\int[\text{grad}\phi^{(+)*}\cdot\Pi^{(+)*}+\Pi^{(+)}\,\text{grad}\phi^{(+)}]d_3x$$
$$-\int[\text{grad}\phi^{(-)*}\Pi^{(-)*}$$
$$+\Pi^{(-)}\,\text{grad}\phi^{(-)}]d_3x. \quad (26)$$

The four vector of charge and current density of the meson field is $S_m{}^\mu$.

$$S_m{}^\mu=\frac{ie}{2\hbar c}\left(\phi^{(+)*}\frac{\partial\phi^{(+)}}{\partial x_\mu}-\phi^{(+)}\frac{\partial\phi^{(+)*}}{\partial x_\mu}\right)$$
$$-\frac{ie}{2\hbar c}\left(\phi^{(-)*}\frac{\partial\phi^{(-)}}{\partial x_\mu}-\phi^{(-)}\frac{\partial\phi^{(-)*}}{\partial x_\mu}\right)$$
$$+\frac{e}{\hbar c}f_0\sum_j\Gamma_j\gamma_j{}^\mu\delta(\mathbf{x}-\mathbf{x}_j)$$
$$\times[T_j\phi_{\text{rad}}(x)-T_j{}^*\phi_{\text{rad}}{}^*(x)]. \quad (27)$$

III. THE WENTZEL MESON FIELDS

In quantum theory it is necessary to introduce different time variables for the particles and the field, as it was shown in the case of the electromagnetic field by Dirac, Fock, and Podolsky.[14] We shall introduce only two time variables, $x_m{}^0$ and $x_N{}^0$, the time variables of the meson field and the nucleons, respectively. The field quantities $\phi_W{}^{(\pm)}$ which depend on the two time variables are the Wentzel meson fields; the $\phi_W{}^{(\pm)}$ go over into the $\phi^{(\pm)}$ by putting $x_m{}^0=x_N{}^0$. For the sake of simplicity we shall denote the time variable of the meson field by x_0 and the time of the whole system nucleons plus meson field by t. Let us put

$$H_p=\sum_j H_j+H'+H_{\text{int}}, \quad (28)$$

$$H_j=c(\boldsymbol{\alpha}_j\cdot\mathbf{p}_j)+\beta_j m_j c^2, \quad (29)$$

$$m_j=\tfrac{1}{2}[M_N(1+\tau_j{}^3)+M_P(1-\tau_j{}^3)]. \quad (30)$$

$\mathbf{p}_j$ is the momentum of the jth particle, and $\tau_j{}^3$ the third component of its isotopic spin. We assume that the isotopic spin component τ^3 has the value 1 in the neutron state and -1 in the proton state. H_{int} is the potential energy of the actions at a distance between the nucleons; it commutes with the meson field quantities. M_N and M_P are the rest masses of the neutron and the proton, respectively. We have the equations of motion of the Wentzel fields $\phi_W{}^{(\pm)}$:

$$i\hbar c\frac{\partial\phi_W{}^{(\pm)}}{\partial x^0}=[\phi_W{}^{(\pm)},H_m(x_0)], \quad (31)$$

$$i\hbar c\frac{\partial\phi_W{}^{(\pm)}}{\partial x_N{}^0}=[\phi_W{}^{(\pm)},H_p(x_N{}^0)]$$
$$=[\phi_W{}^{(\pm)},H'(x_N{}^0)]$$
$$=i\hbar c\left\{\sum_j\Gamma_jT_j{}^*\left[g_0-if_0\gamma_j{}^\mu\frac{\partial}{\partial x^\mu}\right]\right.$$
$$\left.\times D(x,x_j)\right\}_{(x_j{}^0=x_N{}^0)}, \quad (32)$$

$$i\hbar c\frac{\partial\phi_{\text{rad},W}}{\partial x_N{}^0}=[\phi_{\text{rad},W},H_p(x_N{}^0)]=0, \quad (32a)$$

$$i\hbar c\frac{\partial^2\phi_W{}^{(\pm)}}{\partial x_0{}^2}=\left[\frac{\partial\phi_W{}^{(\pm)}}{\partial x_0},H_m\right]$$
$$=-i\hbar c\left(\frac{\partial^2}{\partial x^a\partial x_a}+K^2\right)\phi_W{}^{(\pm)}. \quad (33)$$

From now on we shall denote the Wentzel fields by $\phi^{(\pm)}$. It results from Eq. (33) that we can expand the Wentzel fields in terms of free meson waves. We shall assume that the field is enclosed in a cubic box of volume V, and impose periodic conditions in order to get Fourier series

$$\phi^{(+)}=(\hbar c/V)^{\frac{1}{2}}\sum_k k_0{}^{-\frac{1}{2}}\{A_p{}^{(+)}(k)\exp[-ik^\rho x_\rho]$$
$$+A_n{}^{(+)*}(k)\exp[ik^\rho x_\rho]\}. \quad (34)$$

$$\phi^{(-)}=(\hbar c/V)\sum_k k_0{}^{-\frac{1}{2}}\{A_n{}^{(-)}(k)\exp[-ik^\rho x_\rho]$$
$$+A_p{}^{(-)*}(k)\exp[ik^\rho x_\rho]\}. \quad (35)$$

It results from (32a) that the radiation field does not depend on the time of the nucleons so that

[13] N. Kemmer, Proc. Roy. Soc. A166, 127 (1938).
[14] P. A. M. Dirac, V. Fock, and B. Podolski, Physik. Zeits. Sowjetunion 2, 468 (1932).

$\phi_{\text{rad},W}=\phi_{\text{rad}}$ and

$$A_{\text{rad}}{}^{p}(k)=\tfrac{1}{2}[A_p{}^{(+)}(k)-A_n{}^{(-)}(k)],$$
$$A_{\text{rad}}{}^{n}(k)=\tfrac{1}{2}[A_n{}^{(+)}(k)-A_p{}^{(-)}(k)]. \quad (36)$$

The only non-vanishing commutators are those of a Fourier coefficient and its conjugate

$$[A_p{}^{(+)}(k), A_p{}^{(+)*}(k')]$$
$$=[A_n{}^{(+)}(k), A_n{}^{(+)*}(k')]=\delta_{kk'}, \quad (37)$$

$$[A_p{}^{(-)}(k), A_p{}^{(-)*}(k')]$$
$$=[A_n{}^{(-)}(k), A_n{}^{(-)*}(k')]=-\delta_{kk'}. \quad (38)$$

Let us introduce the operators N which give the numbers of mesons

$$N_{p,n}{}^{(+)}(k)=A_{p,n}{}^{(+)*}(k)A_{p,n}{}^{(+)}(k),$$
$$N_{p,n}{}^{(-)}(k)=A_{p,n}{}^{(-)}(k)A_{p,n}{}^{(-)*}(k). \quad (39)$$

We have

$$H_m=\hbar c\sum_k k_0[N_p{}^{(+)}(k)+N_n{}^{(+)}(k)$$
$$-N_p{}^{(-)}(k)-N_n{}^{(-)}(k)]. \quad (40)$$

$$Q_m=\int S_0 d_3x=e\sum_k[N_p{}^{(+)}(k)-N_n{}^{(+)}(k)$$
$$+N_p{}^{(-)}(k)-N_n{}^{(-)}(k)]. \quad (41)$$

Q_m is the total charge of the meson field. Equation (40) shows that the mesons of the field $\phi^{(+)}$ have positive energies and those of the field $\phi^{(-)}$ negative energies. Mesons with the same wave number vector $\mathbf{k}$ belonging to different fields have opposite momenta, since

$$\mathbf{G}_m=\hbar\sum_k \mathbf{k}[N_p{}^{(+)}(k)+N_n{}^{(+)}(k)$$
$$-N_p{}^{(-)}(k)-N_n{}^{(-)}(k)]. \quad (42)$$

IV. THE ACTIONS AT A DISTANCE BETWEEN THE NUCLEONS

In the preceding section we did not give the explicit form of the potential energy of the actions at a distance H_{int}. In our theory the nature of the actions at a distance is not determined by the choice of the meson field interacting with the nucleons. We shall investigate the actions at a distance which would result from theories of the Heisenberg-Pauli type corresponding to pseudoscalar and vector symmetrical fields (charged and neutral mesons).

In order to get the actions at a distance of the symmetrical pseudoscalar type let us consider the following equations

$$\left(\frac{\partial^2}{\partial x^\mu \partial x_\mu}+K_0{}^2\right)\phi_j{}^s=\tfrac{1}{2}g_0{}^\dagger\tau_j{}^s\Gamma_j\delta(\mathbf{x}-\mathbf{x}_j)$$
$$-\frac{i}{2}f_0{}^\dagger\frac{\partial}{\partial x^\mu}[\Gamma_j\gamma_j{}^\mu\tau_j{}^s\delta(\mathbf{x}-\mathbf{x}_j)]; \quad (s=1,2,3). \quad (43)$$

K_0 is a constant related to the range of the static forces; $g_0{}^\dagger$ and $f_0{}^\dagger$ are real interaction constants. The $\tau_j{}^s$ are the components of the isotopic spins of the jth nucleon. We shall consider the half-retarded, half-advanced solution of Eqs. (43):

$$\phi_j{}^s(x)=\tfrac{1}{2}g_0{}^\dagger\int_{-\infty}^{+\infty}\Gamma_j(x_j{}^0)\tau_j{}^s(x_j{}^0)$$
$$\times G(x, x_j(x_j{}^0); K_0)dx_j{}^0$$
$$+\frac{i}{2}f_0{}^\dagger\int_{-\infty}^{+\infty}\Gamma_j(x_j{}^0)\gamma_j{}^\mu(x_j{}^0)\tau_j{}^s(x_j{}^0)$$
$$\times\frac{\partial}{\partial x_j{}^\mu}G(x, x_j(x_j{}^0); K_0)dx_j{}^0. \quad (44)$$

$G(x, x'; K_0)$ is the Green function of the Klein-Gordon equation corresponding to the value K_0 of the constant. G is related to the function D corresponding to the same value of the constant K_0.[15,16]

$$G(x, x'; K_0)=\tfrac{1}{2}\operatorname{sign}(x_0-x_0')D(x, x')_{(K=K_0)}. \quad (45)$$

We shall use the expression of G as a Fourier integral

$$G(x, x'; K_0)$$
$$=\frac{1}{(2\pi)^4}\int_{-\infty}^{+\infty}\exp[iu^\rho(x_\rho-x_\rho')]\frac{d_4u}{\omega_0{}^2-u_0{}^2}, \quad (46)$$

$$\omega_0=(K_0{}^2+|\mathbf{u}|^2)^{\frac{1}{2}}. \quad (47)$$

Let χ be any function of the type of the wave function of the system in consideration. We

[15] M. Schönberg, Physica, 5, 553, 961 (1938).
[16] M. Schönberg, Rev. Union Matem. Argentina 12, 238 (1947).

shall take

$$G(x, x_j(x_j^0); K_0)\chi = \frac{1}{(2\pi)^4}\int_{-\infty}^{+\infty} \exp[iu^\rho(x_\rho - x_{j,\rho}(x_j^0))]\chi \frac{d_4u}{\omega_0^2 - u_0^2}, \tag{48}$$

$$\frac{\partial}{\partial x_j^\mu} G(x, x_j(x_j^0); K_0)\chi = -\frac{i}{(2\pi)^4}\int_{-\infty}^{+\infty} \exp[iu^\rho(x_\rho - x_{j,\rho}(x_j^0))]\chi \frac{u_\mu d_4u}{\omega_0^2 - u_0^2}. \tag{49}$$

In a similar way we can define the operators $G(x_j(x_j^0), x_l(x_l^0); K_0)$ and $(\partial/\partial x_l^\mu)G(x_j(x_j^0), x_l(x_l^0); K_0)$, which we need in order to compute the operators $\phi_l^s(x_j)$ by means of (44).

The potential energy of the actions at a distance of the symmetrical pseudoscalar type is $H_{\text{int}}^{(0)}$.

$$H_{\text{int}}^{(0)}(x_0) = -\tfrac{1}{2}g_0^\dagger \sum_j \sum_{l\neq j} \sum_{s=1}^{3} [\Gamma_j(x_0)\tau_j^s(x_0)\phi_l^s(x_j)]$$
$$-\frac{i}{2}f_0^\dagger \sum_j \sum_{l\neq j} \sum_{s=1}^{3} \left[\Gamma_j(x_0)\gamma_j^\mu(x_0)\tau_j^s(x_0)\frac{\partial}{\partial x_j^\mu}\phi_l^s(x_j)\right]. \tag{50}$$

In order to compute the potential energy of the actions at a distance of the symmetrical vector type let us consider the real four vectors $\phi_j^{(s)\mu}$ which are half-retarded, half-advanced solutions of the equations

$$\left(\frac{\partial^2}{\partial x^\mu \partial x_\mu} + K_1^2\right)\phi_j^{(s)\mu} = \tfrac{1}{2}g_1^\dagger \alpha_j^\mu \delta(\mathbf{x}-\mathbf{x}_j) + \frac{i}{2}f_1^\dagger \sum_{\nu\neq\mu}\frac{\partial}{\partial x^\nu}[\alpha_j^\nu \gamma_j^\mu \tau_j^s \delta(\mathbf{x}-\mathbf{x}_j)], \tag{51}$$

$$\phi_j^{(s)\mu}(x) = \tfrac{1}{2}g_1^\dagger \int_{-\infty}^{+\infty} \alpha_j^\mu(x_j^0)\tau_j^s(x_j^0)G(x, x_j(x_j^0); K_1)dx_j^0$$
$$-\frac{i}{2}f_1^\dagger \sum_{\nu\neq\mu}\int_{-\infty}^{+\infty} \alpha_j^\nu(x_j^0)\gamma_j^\mu(x_j^0)\tau_j^s(x_j^0)\frac{\partial}{\partial x_j^\nu}G(x, x_j(x_j^0); K_1)dx_j^0. \tag{52}$$

$g_1^\dagger$ and $f_1^\dagger$ are interaction constants. K_1 is the range constant.

The potential energy of the actions at a distance of the symmetrical vector type is $H_{\text{int}}^{(1)}$.

$$H_{\text{int}}^{(1)}(x_0) = -\tfrac{1}{2}g_1^\dagger \sum_j \sum_{l\neq j} \sum_{s=1}^{3} \tau_j^s(x_0)\alpha_{j,\mu}(x_0)\phi_l^{(s)\mu}(x_j)$$
$$-\frac{i}{4}f_1^\dagger \sum_j \sum_{l\neq j} \sum_{s=1}^{3} \tau_j^s(x_0)\beta_j(x_0)\gamma_j^\mu(x_0)\gamma_j^\nu(x_0)\phi_{l,\mu\nu}^{(s)}(x_j), \tag{53}$$

$$\phi_l^{(s)\mu\nu}(x) = \frac{\partial}{\partial x_\mu}\phi_l^{(s)\nu}(x) - \frac{\partial}{\partial x_\nu}\phi_l^{(s)\mu}(x). \tag{54}$$

V. STATIC FORCES BETWEEN NUCLEONS

In order to get the static forces between nucleons we assume in (44) and (52) that the variables of the nucleons are constant. Since

$$\int_{-\infty}^{+\infty} G(x, x'; K_0)dx_0'$$
$$= \frac{1}{(2\pi)^3}\int_{-\infty}^{+\infty} \exp[i(\mathbf{u}\cdot\{\mathbf{x}-\mathbf{x}'\})]\frac{d_3u}{\omega_0^2}$$
$$= \frac{1}{4\pi}|\mathbf{x}-\mathbf{x}'|^{-1}\exp(-K_0|\mathbf{x}-\mathbf{x}'|) \tag{55}$$

and

$$\int_{-\infty}^{+\infty}\frac{\partial}{\partial x'^0}G(x, x'; K_0)dx_0' = 0, \tag{56}$$

we have in the static case

$$\phi_j^s(x_l) = \frac{g_0^\dagger}{8\pi}\tau_j^s\Gamma_j R_{jl}^{-1}\exp(-K_0R_{jl})$$
$$-\frac{f_0^\dagger}{8\pi}\tau_j^s(\sigma_j\cdot\operatorname{grad}_j)R_{jl}^{-1}\exp(-K_0R_{jl}), \tag{57}$$

$$R_{jl} = |\mathbf{x}_j - \mathbf{x}_l|. \tag{58}$$

σ_j denotes, as usual, the spin of the jth particle divided by $\frac{1}{2}\hbar$. We have also

$$\phi_j^{(a)\mu}(x_l)=\frac{g_1^\dagger}{8\pi}\tau_j^a\alpha_j^\mu R_{jl}^{-1}\exp(-K_1R_{jl})$$

$$-\frac{if_1^\dagger}{8\pi}\tau_j^a\sum_{\nu\neq\mu}\alpha_j^\nu\gamma_j^\mu\frac{\partial}{\partial x_j^\nu}[R_{jl}^{-1}\exp(-K_1R_{jl})]. \quad (59)$$

By neglecting all the relativistic corrections we get

$$\phi_j^a(x_l)_{st}=\frac{f_0^\dagger}{8\pi}\tau_j^a(\sigma_j\cdot\mathrm{grad}_j)\times[R_{jl}^{-1}\exp(-K_0R_{jl})], \quad (60)$$

$$\phi_j^{(a)0}(x_l)_{st}=\frac{g_1^\dagger}{8\pi}\tau_j^aR_{jl}^{-1}\exp(-K_1R_{jl}), \quad (61)$$

$$\phi_j^{(a)}(x_l)_{st}=-\frac{f_1^\dagger}{8\pi}\tau_j^a[\sigma_j\times\mathrm{grad}_j]\times[R_{jl}^{-1}\exp(-K_1R_{jl})]. \quad (62)$$

By introducing the preceding expressions of the ϕ in Eqs. (50) and (53), we get the usual expressions for the static interactions.

We shall now derive explicit expressions of the ϕ_j^a which take into account the retardation effects in a first approximation. In the Heisenberg picture the operators which represent a non-variable physical quantity at two different times are related by a contact transformation

$$B(x_0')=U^{-1}(x_0',x_0)B(x_0)U(x_0',x_0). \quad (63)$$

U is an unitary operator related to the Hamiltonian. When the Hamiltonian does not depend explicitly on the time,

$$U(x_0',x_0)=\exp\left[-\frac{i}{\hbar c}H(x_0'-x_0)\right]. \quad (64)$$

By taking into account (63), we may write

$$\phi_j^a(x)=\tfrac{1}{2}g_0^\dagger\int_{-\infty}^{+\infty}U_j^{-1}(x_j^0,0)[\tau_j^a(0)\Gamma_j(0)\times G(x,x_j(0);K_0)_{(x_j^0(0)=x_j^0)}]U(x_j^0,0)dx_j^0$$
$$+\frac{i}{2}f_0^\dagger\int_{-\infty}^{+\infty}U^{-1}(x_j^0,0)\left[\tau_j^a(x_j^0)\Gamma_j(x_j^0)\times\gamma_j^\mu(x_j^0)\frac{\partial}{\partial x_j^\mu}G(x,x_j(0);K_0)\right]\times U(x_j^0,0)dx_j^0. \quad (65)$$

In our approximation treatment we shall use the operator U corresponding to an unperturbed motion in which the nucleons do not interact with the meson fields and the actions at a distance are neglected. We shall denote the operator U of the unperturbed motion by U_0:

$$U_0(x_0',x_0)=\exp\left[-\frac{i}{\hbar c}H_m(x_0'-x_0)\right]\times\exp\left[-\frac{i}{\hbar c}\{\textstyle\sum_j H_j\}(x_0'-x_0)\right], \quad (66)$$

so that

$$\phi_j^a(x)=\tfrac{1}{2}g_0^\dagger\int_{-\infty}^{+\infty}\exp\left[\frac{i}{\hbar c}H_jx_j^0\right]\times\{\tau_j^a(0)\Gamma_j(0)G(x,x_j(0);K_0)\}\times\exp\left[-\frac{i}{\hbar c}H_jx_j^0\right]dx_j^0+\frac{i}{2}f_0^\dagger\int_{-\infty}^{+\infty}\times\exp\left[\frac{i}{\hbar c}H_jx_j^0\right]\left\{\tau_j^a(0)\Gamma_j(0)\gamma_j^\mu(0)\frac{\partial}{\partial x_j^\mu}\times G(x,x_j(0);K_0)\right\}\exp\left[-\frac{i}{\hbar c}H_jx_j^0\right]dx_j^0. \quad (67)$$

The operator which represents a physical quantity in the Schrödinger picture is related to the corresponding operator in the Heisenberg picture

$$B(x_0)_{\mathrm{Schröd}}=U(x_0,0)B(x_0)U^{-1}(x_0,0). \quad (68)$$

In our approximation

$$\phi_j^s(x)_{\text{Schröd}} = \exp\left[-\frac{i}{\hbar c}H_j x_0\right]\phi_j^s(x)\exp\left[\frac{i}{\hbar c}H_j x_0\right]$$

$$= \tfrac{1}{2}g_0^\dagger \int_{-\infty}^{+\infty} \exp\left[\frac{i}{\hbar c}H_j z_j^0\right]\{\tau_j^s \Gamma_j G(x, x_j; K_0)\}_{\text{Schröd}} \exp\left[-\frac{i}{\hbar c}H_j z_j^0\right] dz_j^0$$

$$+\frac{i}{2}f_0^\dagger \int_{-\infty}^{+\infty} \exp\left[\frac{i}{\hbar c}H_j z_j^0\right]\left\{\tau_j^s \Gamma_j \gamma_j^\mu \frac{\partial}{\partial x_j^\mu} G(x, x_j; K_0)\right\}_{\text{Schröd}} \exp\left[-\frac{i}{\hbar c}H_j z_j^0\right] dz_j^0, \quad (69)$$

$$z_j^0 = x_j^0 - x^0. \quad (70)$$

It is worth while to remark that $\phi_j^s(x)_{\text{Schröd}}$ does not depend on x_0, because $G(x, x'; K_0)$ is a function of $x_0 - x_0'$. The matrix element $(I|H_{\text{int}}^{(0)}|II)_{\text{Schröd}}$ of $H_{\text{int}}^{(0)}$ between two states in which the nucleons are free and have the momenta $(\mathbf{p}_j^I, \mathbf{p}_j^{II})$ and the energies (cp_j^{I0}, cp_j^{II0}) can be easily computed by using (69).

$$(I|H_{\text{int}}^{(0)}|II)_{\text{Schröd}} = \tfrac{1}{4}h^{3(n-1)} \sum_j \sum_{l\neq j} \sum_s \delta(\mathbf{p}_j^I - \mathbf{p}_j^{II} + \mathbf{p}_l^I - \mathbf{p}_l^{II}) \prod_{r\neq l,j} \delta(\mathbf{p}_r^I - \mathbf{p}_r^{II})$$

$$\times \{\hbar^{-2}(p_l^{I\rho} - p_l^{II\rho})(p_{l,\rho}^I - p_{l,\rho}^{II}) - K_0^2\}^{-1}[(g_0^\dagger)^2(I|\tau_j^s\tau_l^s\Gamma_j\Gamma_l|II)$$

$$-(f_0^\dagger)^2\hbar^{-2}(I|\tau_j^s\tau_l^s\Gamma_j\gamma_j^\mu\Gamma_l\gamma_l^\mu|II)(p_{l,\mu}^I - p_{l,\mu}^{II})(p_{l,\nu}^I - p_{l,\nu}^{II})$$

$$+g_0^\dagger f_0^\dagger \hbar^{-1}(p_{l,\mu}^I - p_{l,\mu}^{II})(I|\tau_j^s\tau_l^s\Gamma_j\Gamma_l(\gamma_l^\mu - \gamma_j^\mu)|II)]. \quad (71)$$

This expression of the matrix element of the interaction corresponds to Möller's formula[17] in the electromagnetic case. Leite Lopes[8] and Tamm[9] have derived expressions of the matrix element of the relativistic interactions between nucleons analogous to (71), by using the usual field theories of the nuclear forces. The nature of the retardation effects does not appear clearly in their derivations because they come in through the recoil of the nucleons in the virtual emissions and absorptions of mesons.

VI. DISCUSSION

In the preceding section we derived approximate expressions for the relativistic interactions, of the same type as those derived from the field theory of the nuclear forces. Nevertheless our formalism and the field theory do not lead to the same description of the nuclear forces. We obtained linear operators for the relativistic interactions analogous to those of Leite Lopes and Tamm, in an approximation treatment. *But, in an exact treatment of the relativistic interactions, the fundamental equations we must solve are not linear.*

The fundamental equations of the exact theory are those which determine the operator U:

$$i\hbar c\frac{\partial}{\partial x_0}U(x_0, x_0') = U(x_0, x_0')H(x_0), \quad (72)$$

$$U(x_0, x_0) = 1, \quad (73)$$

because we cannot use the Schrödinger equation unless we know beforehand the explicit expression of H_{int}, and we cannot compute H_{int} without knowing U.

We do not know whether the exact expression of $[H_{\text{int}}]_{\text{Schröd}}$ is time independent, as it is in the approximation considered at the end of the preceding section. Thus it is not certain whether it is possible to obtain stationary states in the exact treatment, at least with the usual definition of a stationary state. It may be necessary to use indirect methods, such as that of the Heisenberg S-matrix, in order to get the energy levels of the closed stationary states.

The approximation method we have used to investigate the retardation effects differs essen-

[17] C. Möller, Zeits. f. Physik **70**, 786 (1931).

tially from the perturbation method. That method may be considered satisfactory in the case of collisions of high energy nucleons, but it is not certain whether it describes correctly the retardation effects in the case of the nuclei, because of the small energy of the nucleons. It is important to take into account the preceding remark because of the difficulties which exist in the relativistic treatment of the nuclear forces; in this case we ought rather to start from an unperturbed motion in which the retardation effects are neglected and use its operator U in the computation of the first approximation values of the ϕ_j^s and $\phi_j^{(s)\mu}$, instead of the operator U_0 which corresponds to non-interacting nucleons.

We have developed the formalism of the actions at a distance between nucleons by analogy with the corresponding formalism for the electromagnetic case (references 1 and 2). We have replaced the inhomogeneous d'Alembert equation by the inhomogeneous Klein-Gordon equations (43) and (51) and, by taking their half-retarded, half-advanced solutions, we obtained actions at a distance which coincide in a first approximation with those given by the field theory. It is important to notice that the method of the actions at a distance allows many other possibilities. For instance, we may replace the Green function $G(x, x'; K_0)$ by some other invariant function in Eqs. (44) and (52). By a convenient choice of that function we can give a finite radius to the nucleons, from the point of view of the actions at a distance, without changing their point interaction with the meson field or the electromagnetic field. We shall now examine in some detail the introduction of such a radius. Let us replace the Green function G by the function G_Λ:

$$G_\Lambda(x, x'; K_0) = \frac{1}{4\pi} F_\Lambda'(s^2) J_0(K_0 s) - \frac{K_0}{8\pi s} F_\Lambda(s^2) J_1(K_0 s), \quad (74)$$

$$s = [(x^\mu - x'^\mu)(x_\mu - x_\mu')]^{\frac{1}{2}}, \quad (75)$$

$$F_\Lambda(s^2) = \frac{1}{\Lambda^2 \pi^{\frac{1}{2}}} \int_{-\infty}^{s^2} \exp\left(-\frac{t^2}{\Lambda^4}\right) dt. \quad (76)$$

J_0 and J_1 are Bessel functions, Λ is a constant with the dimension of a length. We have

$$\lim_{\Lambda \to 0} G_\Lambda(x, x'; K_0) = G(x, x'; K_0). \quad (77)$$

$G_\Lambda(x, x'; K_0)$ depends only on the variable s^2 and is free of singularities. In the computation of the static forces G_Λ can be replaced by $\mathbf{G}_\Lambda$.

$$\mathbf{G}_\Lambda(x, x'; K_0) = \delta(x_0 - x_0') K_\Lambda(\mathbf{x}, \mathbf{x}'; K_0), \quad (78)$$

$$K_\Lambda(\mathbf{x}, \mathbf{x}'; K_0) = \int_{-\infty}^{+\infty} G_\Lambda(x, x'; K_0) dx_0. \quad (79)$$

$K_\Lambda(\mathbf{x}, \mathbf{x}', K_0)$ and its derivatives of the first and second order are finite for $\mathbf{x} = \mathbf{x}'$. Thus we can get rid of the singularities in the interaction between nucleons.

VII. THE "FREEZING" OF THE DEGREES OF FREEDOM OF THE MESON FIELD

Let us introduce new variables for the description of the meson field:

$$P_{p,n}^2(k) + iP_{p,n}^1(k) = [A_{p,n}^{(+)}(k) + A_{n,p}^{(-)}(k)], \quad (80)$$

$$P_{p,n}^2(k) - iP_{p,n}^1(k) = [A_{p,n}^{(+)*}(k) + A_{n,p}^{(-)*}(k)], \quad (81)$$

$$Q_{p,n}^1(k) - iQ_{p,n}^2(k) = [A_{p,n}^{(+)}(k) - A_{n,p}^{(-)}(k)], \quad (82)$$

$$Q_{p,n}^1(k) + iQ_{p,n}^2(k) = [A_{p,n}^{(+)*}(k) - A_{n,p}^{(-)*}(k)]. \quad (83)$$

The only non-vanishing commutators between the new variables are those between a P and the corresponding Q:

$$[P_p^r(k), Q_p^{r'}(k')] = [P_n^r(k), Q_n^{r'}(k')] = -i\delta_{rr'}\delta_{kk'}. \quad (84)$$

We have

$$N_{p,n}^{(+)}(k) - N_{n,p}^{(-)}(k) = Q_{p,n}^1(k) P_{p,n}^2(k) - Q_{p,n}^2(k) P_{p,n}^1(k). \quad (85)$$

Let us consider the Fourier expansions of the

fields $\phi_{\text{rad}}^{p,n}$.

$$\phi_{\text{rad}}^{p,n}(x)=(\hbar c/V)^{\frac{1}{2}}\sum_k k_0^{-\frac{1}{2}}A_{\text{rad}}^{p,n}(k)\times\exp(-ik^\rho x_\rho). \quad (86)$$

It results from (82) and (83) that

$$A_{\text{rad}}^{p}(k)=\tfrac{1}{2}[Q_p^1(k)-iQ_p^2(k)], \quad (87)$$

$$A_{\text{rad}}^{n}(k)=\tfrac{1}{2}[Q_n^1(k)-iQ_n^2(k)]. \quad (88)$$

Since the only fields that come in the interaction between nucleons and mesons are the $\phi_{\text{rad}}^{p,n}$, it follows that the interaction can be expressed in terms of the field variables Q.

The wave function χ of the system nucleons plus field is a function of the variables of the nucleons and variables of the field which we may take as the P. If χ does not depend on the P corresponding to a given wave vector $\mathbf{k}$, we have

$$[N_{p,n}^{(+)}(k)-N_{n,p}^{(-)}(k)]\chi=0, \quad (89)$$

$$A_{\text{rad}}^{p,n}(k)\chi=0, \quad A_{\text{rad}}^{p,n*}(k)\chi=0. \quad (90)$$

Therefore:

In the state of the system represented by the wave function we consider those degrees of freedom of the field do not give any contribution to the energy of the field and to the interaction energy between the nucleons and the field.

We shall call "frozen" degrees of freedom those which correspond to values of $\mathbf{k}$ whose P are not involved in the wave function of the state in considerations. *By using the "freezing" method we can get rid of the divergences.*

The simplest application of the "freezing" is the elimination of the infinite self-energies. *If we assume that the wave function of the system free nucleon plus meson field is described, in the rest system of the nucleon, by a wave function in which all the degrees of freedom corresponding to values of* $|\mathbf{k}|$ *above a given limit are "frozen", we will get a finite self-energy of the nucleon.*

It is important to remark that there are exact solutions of the Schrödinger equation of the system nucleons plus field in which the degrees of freedom of the field corresponding to any given set of vectors $\mathbf{k}$ *are "frozen."* Indeed the freezing conditions

$$Q_{p,n}^{r}(k)\chi=0 \quad (91)$$

will be fulfilled at any time if they are satisfied at the initial time.

It is possible to introduce a more general kind of "freezing" which we shall need later. The freezing conditions (91) are equivalent to (90) which can be split into two groups of conditions

$$A_{\text{rad}}^{p}(k)\chi=A_{\text{rad}}^{p*}(k)\chi=0, \quad (92a)$$

$$A_{\text{rad}}^{n}(k)\chi=A_{\text{rad}}^{n*}(k)\chi=0. \quad (92b)$$

The conditions (92a) and (92b) "freeze" the interaction between the nucleons and the degrees of freedom corresponding to the wave vector $\mathbf{k}$ in the two radiation fields ϕ_{rad}^{p} and ϕ_{rad}^{n}, respectively. We can associate with the conditions (92a) and (92b) the following ones, respectively,

$$[N_p^{(+)}(k)-N_n^{(-)}(k)]\chi=0, \quad (93a)$$

$$[N_n^{(+)}(k)-N_p^{(-)}(k)]\chi=0, \quad (93b)$$

which will be satisfied as a consequence of conditions (92a) and (92b). Therefore, if we impose the conditions (92a)–(93a) the degrees of freedom of the field ϕ_{rad}^{p} will not give any contribution to the energy of the system nucleons plus total meson field in the state in consideration. It is therefore possible to "freeze" separately the degrees of freedom of the two partial radiation fields ϕ_{rad}^{p} and ϕ_{rad}^{n}. The possibility of "freezing" separately degrees of freedom of the two radiation fields is not necessary in order to eliminate the divergences, but it may play an important part in the explanation of the anomaly of the magnetic moments of the proton and neutron as well as in the explanation of the difference of their masses.

VIII. THE PHYSICAL INTERPRETATION RULE

Let us assume that we want to compute the probability of a transition in which are involved l_p positive mesons and l_n negative mesons with the momenta $\hbar\mathbf{k}_r$ $(r=1, 2, \cdots l_p)$ and $\hbar\mathbf{k}_s$ $(s=1, 2, \cdots l_n)$, respectively. We shall use a wave function χ_{fr} of the system particles plus field involving only the P_p corresponding to the $\mathbf{k}_r$ in the ranges $(\mathbf{k}_r-\frac{1}{2}\Delta\mathbf{k}, \mathbf{k}_r+\frac{1}{2}\Delta\mathbf{k})$ and the P_n corresponding to the $\mathbf{k}$ in the ranges $(\mathbf{k}_s-\frac{1}{2}\Delta\mathbf{k}, \mathbf{k}_s+\frac{1}{2}\Delta\mathbf{k})$ and $\Delta\mathbf{k}$ is a small vector with a length of the order of $V^{-\frac{1}{3}}$. We can satisfy the Schrödinger equation of the system nucleons plus

meson field with such a wave function because the terms of the Hamiltonian of the system, which involve field variables corresponding to $\mathbf{k}$'s outside the relevant ranges, give vanishing contributions when applied to our "frozen" wave function. The "frozen" wave function χ_{fr} satisfies a reduced Schrödinger equation which results from the exact one by dropping all the terms involving the frozen degrees of freedom. We shall now make an assumption:

The reduced Schrödinger equation must be treated in the same way as the usual Schrödinger equation of a dynamical system with a finite number of degrees of freedom, the degrees of freedom of the nucleons, and the meson field which it involves.

It results from this general assumption that the wave function χ_{fr} must be normalized as the wave function of a system with a finite number of degrees of freedom. It would not be possible to normalize χ_{fr}, if we would consider it as the wave function of the nucleons plus the "unfrozen" meson field. In order to formulate the rule of physical interpretation we shall take as variables, in the reduced Schrödinger equation, the numbers of mesons $N_{p,n}^{(\pm)}(k)$. The initial state of the observable meson fields is characterized by the occupation numbers $\mathfrak{N}_p(k_r)_I$ and $\mathfrak{N}_n(k_s)_I$; the final state of the observable meson field is characterized by the occupation numbers $\mathfrak{N}_p(k_r)_F$ and $\mathfrak{N}_n(k_s)_F$. We shall associate with these observable states the states of our formalism characterized by the occupation numbers $N_p^{(+)}(k_r)_I$, $N_n^{(-)}(k_r)_I$, $N_n^{(+)}(k_s)_I$, $N_p^{(-)}(k_s)_I$ (initial state) and $N_p^{(+)}(k_r)_F$, $N_n^{(-)}(k_r)_F$, $N_n^{(+)}(k_s)_F$, $N_p^{(-)}(k_s)_F$ (final state).

$$N_p^{(+)}(k_r)_I=\mathfrak{N}_p(k_r)_I, \quad N_n^{(+)}(k_s)_I=\mathfrak{N}_n(k_s)_I, \quad N_n^{(-)}(k_r)_I=N_p^{(-)}(k_s)_I=0, \tag{94a}$$

$$N_p^{(+)}(k_r)_F=\mathfrak{N}_p(k_r)_F, \quad N_n^{(+)}(k_s)_F=\mathfrak{N}_n(k_s)_F, \quad N_n^{(-)}(k_n)_F=N_p^{(-)}(k_s)_F=0. \tag{94b}$$

Let us denote by Δ the total number of absorbed and emitted mesons in the physical world (observed number). We shall assume the following rule of physical interpretation:

The probability of the transition $\mathfrak{N}_I \to \mathfrak{N}_F$, in the physical world, is equal to the product of 2^Δ by the probability of the associated transition computed with the reduced Schrödinger equation.

This interpretation rule is similar to the rule introduced in the electromagnetic case by Schönberg,[1,2] it is also similar to one of the interpretation rules given by Pauli[12] in his extension of Dirac's method of quantization[10] to the meson field. There are other possible interpretation rules, similar to those considered by Pauli, but they are more complicated than the one we have formulated. Moreover, Schönberg has shown that the corresponding interpretation rule for the electromagnetic case can be justified by considerations of correspondence with the classical theory; a similar justification could also be given if we would develop a formalism analogous to the one given in this paper for pseudoscalar neutral mesons, by considering the classical theory of point nucleons interacting with a pseudoscalar neutral meson field. The interpretation rules which do not use the negative energy particles, in our type of quantum formalism, correspond to the time boundary conditions of the classical theory of point particles which exclude the indefinitely self-accelerated motions of the particles.[5]

IX. SELF-ENERGIES AND MAGNETIC MOMENTS

The application of the "freezing" method to the computation of the self-energies and magnetic moments is not so straightforward as its application to the computation of transition probabilities. We shall introduce the following "freezing" criterion:

In the computation of the self-energies, magnetic moments, and other similar effects in which a nucleon interacts with the meson field in vacuum, we shall use wave functions of the system nucleon plus meson field in which the degrees of freedom of the two radiation fields, ϕ_{rad}^p and ϕ_{rad}^n, corresponding to momenta of the mesons above $\hbar K_p$ and $\hbar K_n$, respectively, are "frozen," in the rest system of the nucleon. K_p and K_n are two constants of the order of K.

The quantities we are considering can be computed as average values of operators O of the form $O^{(+)}+O^{(-)}$, $O^{(+)}$ involving only the field $\phi^{(+)}$, and $O^{(-)}$ involving only the field $\phi^{(-)}$. In the case of the self-energy the operator O is

$$\tfrac{1}{2}H'=\tfrac{1}{2}(H'^{(+)}+H'^{(-)}).$$

$$H'^{(\pm)}=\mp\tfrac{1}{2}g_0\Gamma\{T\phi^{(\pm)}(x_N)+T^*\phi^{(\pm)*}(x_N)\}$$
$$\mp\frac{i}{2}f_0\Gamma\gamma^\mu\left\{T\frac{\partial}{\partial x_{N^\mu}}\phi^{(\pm)}(x_N)\right.$$
$$\left.+T^*\frac{\partial}{\partial x_{N^\mu}}\phi^{(\pm)*}(x_N)\right\}. \quad (95)$$

The x_N are the coordinates of the nucleon in consideration. In the case of the magnetic moments the operators $O^{(\pm)}$ are the $M_{\mu\nu}{}^{(\pm)}$.

$$M_{\mu\nu}{}^{(\pm)}=\tfrac{1}{2}\int(x_\mu S_\nu{}^{(\pm)}-x_\nu S_\mu{}^{(\pm)})d_3x, \quad (96)$$

$$S_\mu{}^{(\pm)}(x)=\pm\frac{ie}{2\hbar c}\left(\phi^{(\pm)*}(x)\frac{\partial\phi^{(\pm)}(x)}{\partial x^\mu}\right.$$
$$\left.-\phi^{(\pm)}(x)\frac{\partial\phi^{(\pm)*}(x)}{\partial x^\mu}\right)$$
$$\pm\frac{ef_0}{2\hbar c}\Gamma\gamma^\mu\delta(\mathbf{x}-\mathbf{x}_N)$$
$$\times\{T\phi^{(\pm)}(x)-T^*\phi^{(\pm)*}(x)\}. \quad (97)$$

Besides the preceding "freezing" rule, we shall use the following computation rule which is obviously related to the physical interpretation rule of the preceding section:

In the computation of quantities such as the self-energies and magnetic moments of the nucleons, we must take the average of $2O^{(+)}$ instead of the average of $O^{(+)}+O^{(-)}$, in the state of the system nucleon plus "frozen" meson field in which there are no mesons in the "unfrozen" states.

Thus the self-energies are given by the following formula

$$\Delta E=(H'^{(+)})_{Av}, \quad (100)$$

and the corrections of the magnetic moments by a formula analogous to that given by Jauch[18] in the one-field theory

$$\Delta\mu_3=2(M_{12}{}^{(+)})_{Av}, \quad (101)$$

assuming that the spin of the nucleon is directed along the x^3 axis. For the sake of simplicity we shall put $g_0=0$ and neglect the recoil of the nucleons. Thus we get

$$(\Delta M)_P=-\frac{f_0{}^2}{4\pi^2c^2}\int_0^{K_P}\left(\frac{k}{k_0}\right)^2k^2dk, \quad (102)$$

$$(\Delta M)_N=-\frac{f_0{}^2}{4\pi^2c^2}\int_0^{K_N}\left(\frac{k}{k_0}\right)^2k^2dk, \quad (103)$$

$$(\Delta\mu_3)_P=\frac{ef_0{}^2}{12\pi^2\hbar c}\int_0^{K_P}\left(\frac{k}{k_0}\right)^4dk, \quad (104)$$

$$(\Delta\mu_3)_N=-\frac{ef_0{}^2}{12\pi^2\hbar c}\int_0^{K_N}\left(\frac{k}{k_0}\right)^4dk. \quad (105)$$

The existence of the two "freezing" limits, K_P and K_N allows us to get different self-energies for the proton and the neutron.

---

[18] J. M. Jauch, Phys. Rev. 63, 334 (1943).

Radioactive Kr Isotopes

L. L. WOODWARD,* D. A. MCCOWN,** AND M. L. POOL
The Ohio State University, Columbus, Ohio

(Received June 21, 1948)

A radioactive isotope of 1.1-hour half-life has been produced in krypton by alpha-particle bombardment of Se^{74}, enriched electromagnetically from 0.9 percent to 14.1 percent. Assignment of the isotope is made to Kr^{77}. Aluminum absorption measurements indicate a positron end point of 1.7 Mev. In addition to annihilation radiation, gamma-rays and K-capture have been observed. The ratio of K-capture to positron emission from the $Se^{74}(\alpha, n)$ reaction is computed as 2.6. The krypton 1.42-day isotope has been produced by an (α, n) reaction on electromagnetically enriched Se^{76}. The isotope is located as Kr^{79} and its half-life confirmed. A positron end point of 1.0 Mev is determined by aluminum absorption measurements. In addition to annihilation radiation, gamma-rays and K-capture have been observed. The ratio of K-capture to positron emission from the $Se^{76}(\alpha, n)$ reaction is computed to be 50. The cross-section ratio for formation of Kr^{77} compared to Kr^{79} by alpha-particle bombardment of selenium is computed as 1.4. The 4.6-hour Kr^{85} isotope has been produced by a $Se(\alpha, n)$ reaction.

I. INTRODUCTION

CYCLOTRON bombardments have been made with alpha-particles on electromagnetically enriched selenium.† Table I shows the percentages of stable selenium isotopes present in the two samples used. For comparison purposes, abundances of selenium isotopes of natural concentration are included in the table. Bombardments were also made with Hilger selenium.

As a result of these bombardments, a previously unreported radioactive krypton isotope has been found. The location and characteristic radiations of this isotope will be presented in this paper. The location and characteristic radiations of the Kr^{79} isotope, and production of the Kr^{85} isotope by alpha-particle bombardment of selenium will also be reported.

II. THE 1.1-HOUR Kr^{77} ISOTOPE

Samples of enriched Se^{74} and Se^{76} were prepared for simultaneous alpha-particle bombardment by pressing equal amounts by weight of the finely ground metallic selenium into the bottom of aluminum target holders under approximately 5000 pounds pressure. The two targets were then bombarded simultaneously in the cyclotron by means of a rotating probe.

In order to obtain separately the decay characteristics of positively and negatively charged particle activity, the samples were placed in a reversible electromagnetic field. A counter tube was located in such a position as to intercept β^-- or β^+-radiation, as desired.

Figure 1 shows a comparison between the decay of β^-- and β^+-activity in the two enriched selenium samples after simultaneous alpha-particle bombardment. β^--activity of similar characteristics and a β^+-activity of 1.4-day half-life were observed in both samples. In addition, as shown in the figure, a strong β^+-activity of 1.1-hour half-life was observed in the enriched Se^{74} sample but not in the enriched Se^{76} sample. This indicated that the 1.1-hour activity was formed by alpha-particle bombardment from the stable Se^{74} isotope. The activity was not observed in the Se^{76} sample because there was only 0.5 percent of stable Se^{74} in the Se^{76} sample.

TABLE I. Percentages of abundance of stable selenium isotopes in natural selenium and in the electromagnetically enriched selenium samples.

Se isotope	Percentages of abundance: Enriched Se^{74} sample	Enriched Se^{76} sample	Natural Se
74	14.1±1.0	0.5±0.2	0.9
76	9.4±0.5	41.5±1.0	9.5
77	7.1±0.3	6.8±0.5	8.3
78	21.4±1.0	16.1±0.8	24.0
80	40.4±1.0	30.2±1.0	48.0
82	7.5±0.5	5.0±0.5	9.3

* Lieutenont Colonel, USAF. Research under auspices of Air University, Maxwell Air Force Base, Montgomery, Alabama.

** Captain, USAF. Research under auspices of Air University, Maxwell Air Force Base, Montgomery, Alabama.

† Supplied by the Y-12 plant, Carbide and Carbon Chemicals Corporation, through the Isotopes Division, U. S. Atomic Energy Commission, Oak Ridge, Tennessee.

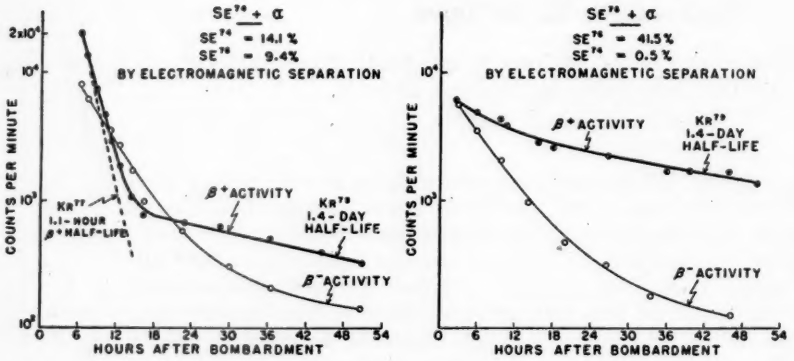

FIG. 1. A comparison of decay curves of separated β^-- and β^+-activity from alpha-particle bombardment of electromagnetically enriched Se^{74} and Se^{76}. The 1.1-hour Kr^{77} β^+-activity appears in the Se^{74} sample but not in the Se^{76} sample.

In order to determine whether the activity was due to a radioactive bromine or krypton isotope, a sample of Hilger selenium, laboratory No. 12006, was bombarded with alpha-particles. The target was prepared as in the first experiment. After bombardment, the radioactive krypton gas was removed by application of low heat to a mixture of the selenium, Na_2CO_3, $NaNO_3$, and KBr, and swept into a glass collector tube to one end of which a 2.0-mil aluminum foil window was attached.

Figure 2 shows the decay separately of β^+- and β^--activity in the krypton gas. A β^--activity of 4.4-hour half-life, and a strong β^+-activity of 1.1-hour half-life were observed. The 1.1-hour activity was thus established as a krypton isotope. Since it had been previously determined that the activity was also produced by alpha-particle bombardment of stable Se^{74}, assignment is made to Kr^{77}.

Figure 3 shows aluminum absorption measurements of the total activity obtained from an alpha-particle bombardment of enriched Se^{74}. Measurements were taken on a Wulf electrometer attached to a Freon-filled ionization chamber. Absorption measurements taken when the activity was in the 1.1-hour Kr^{77} period indicated a beta-end point of 0.74 g/cm², corresponding to 1.7 Mev as determined by the Sargent range-energy relation.

Measurements of electromagnetic radiation from the 1.1-hour activity were also taken. For this purpose the sample was placed between the pole faces of an electromagnet and a magnetic field applied of sufficient strength to prevent all beta-particles from entering the ionization chamber. Measurements of activity taken under these conditions were then measurements of the electromagnetic radiation from the sample. Measurements of activity were also taken with a $\frac{1}{4}$-inch aluminum absorber inserted between the sample and the ionization chamber. Since this amount of absorber was sufficient to stop any x-ray radiation present, these measurements were measurements of the gamma-ray activity of the sample.

From such data it was concluded that in the 1.1-hour Kr^{77} period there is gamma-ray activity in addition to that necessary to account for annihilation radiation, and also x-ray activity.

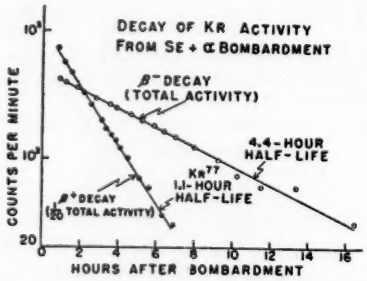

FIG. 2. Decay curves of β^-- and β^+-activity in krypton from alpha-particle bombardment of selenium. This shows that the strong 1.1-hour β^+-activity is a krypton isotope.

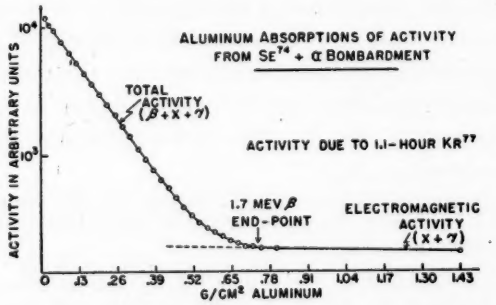
ALUMINUM ABSORPTIONS OF ACTIVITY FROM Se^{74} + α BOMBARDMENT
TOTAL ACTIVITY (β+X+γ)
ACTIVITY DUE TO 1.1-HOUR Kr^{77}
1.7 MEV β END-POINT
ELECTROMAGNETIC ACTIVITY ½(X+γ)
ACTIVITY IN ARBITRARY UNITS
G/CM² ALUMINUM

FIG. 3. Aluminum absorption measurements showing the 1.7-Mev positron end point of the 1.1-hour Kr^{77} activity.

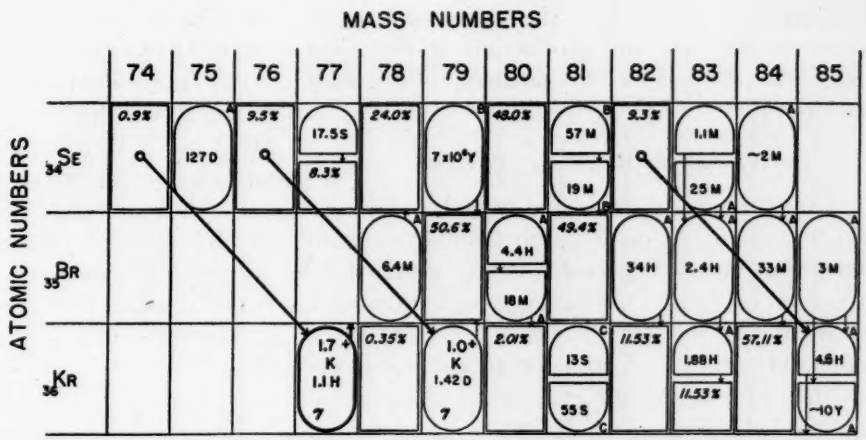

FIG. 4. The Se, Br, Kr section of the periodic table. The new Kr^{77} isotope, new reactions, and characteristic radiations found are shown in heavy lines.

The presence of x-ray activity was shown by subtracting the curve representing gamma-ray activity from the curve representing decay of total electromagnetic radiation. From considerations of the amount of x-ray radiation that would be expected from the "bremsstrahlung" effect, it was concluded that this x-ray radiation is a result of the *K*-capture process.

The ratio of *K*-capture processes to positron emissions in Kr^{77} from the $Se^{74}(\alpha, n)$ reaction is computed to be 2.6. This ratio was determined by a computation of saturation intensities and correcting for the relative ionization produced by the different forms and energies of radiation involved.

III. THE 1.4-DAY Kr^{79} ISOTOPE

A krypton activity of 18 ± 2 hours resulting from deuteron bombardment of krypton was first reported by Snell.[1] Assignment of the activity was made to either Kr^{79} or Kr^{81}. The same assignment of a 34.5 ± 1-hour krypton activity was made by Creutz *et al.*,[2] who obtained the period by proton bombardment of bromine. A positron end point of about 0.4 Mev was determined by cloud-chamber measurements. A krypton period of about 33-hour half-life was also reported by Clancy[3] as the result of alpha-particle bombardments of selenium, and assignment of the activity was made to either Kr^{79} or Kr^{81}. Beta end-point energies in the $Kr^{79,81}$ activity of 0.6 Mev (70 percent) and 0.9 Mev (30 percent) from Kr^{78} and Kr^{80} as target nuclei, respectively, have been reported.[4]

The location of the 1.4-day krypton period may be readily made as a result of alpha-particle bombardments of enriched Se^{74} and Se^{76}. Figure 1 shows that in the activity from such bombardments a period of 1.4-day half-life appeared in the Se^{76} sample in considerably larger intensity than in the Se^{74} sample. These curves indicate that the 1.4-day krypton period is formed from stable Se^{76}. If the activity had been formed from stable Se^{78} by alpha-particle bombardment, a smaller intensity of the 1.4-day period would have been expected in the Se^{76} sample than in the Se^{74} sample, since the former contained 16.1 percent of stable Se^{78}, which would produce Kr^{81}, while the latter contained 21.4 percent of Se^{78}. The 1.4-day krypton activity is then assigned to Kr^{79}.

Aluminum absorption measurements of the 1.4-day Kr^{79} activity indicate a beta-end point of 1.0 Mev. Beta-emission was determined to be entirely positrons.

Gamma-ray activity in addition to that produced by annihilation radiation has been observed. X-ray radiation resulting from the *K*-capture process is also present in the activity. The ratio of *K*-capture processes to positron emissions in the Kr^{79} activity from the $Se^{76}(\alpha, n)$ reaction is computed to be 50.

[1] A. H. Snell, Phys. Rev. **52**, 1007 (1937).
[2] E. C. Creutz, L. A. Delsasso, R. B. Sutton, M. G. White, and W. H. Barkas, Phys. Rev. **58**, 481 (1940).
[3] E. P. Clancy, Phys. Rev. **60**, 87 (1941).
[4] U. S. Atomic Energy Commission Abstracts of Declassified Documents, Vol. 1, No. 6, MDDC-614L, p. 380.

From the above data the ratio of reaction cross sections for the production of Kr^{77} and Kr^{79} by alpha-particle bombardment of selenium is determined to be 1.4.

IV. THE 4.6-HOUR Kr^{85} ISOTOPE

The 4.6-hour Kr^{85} period was reported by Snell[1] as a result of deuteron bombardment of krypton. The Kr^{85} period was not obtained by Clancy[3] as a result of alpha-particle bombardment of selenium. In the latter bombardments, only a 114-minute krypton period, assigned to the excited level of stable Kr^{83}, and a 33-hour krypton period, assigned to $Kr^{79, 81}$, were observed. The Kr^{85} period was then considered by Clancy to be long or fairly short, and a 4-hour krypton activity obtained from deuteron bombardment of krypton was presumed to be caused by Kr^{87}. The 4.6-hour Kr^{85} activity has been reported by Seelmann-Eggebert and Born[5] as a result of uranium fission by decay of the 3-minute Br^{85} siotope, and also as a result of $Sr(n, \alpha)$ and $Rb(n, p)$ reactions.[6]

A 4.4 ± 0.2-hour half-life of β^--activity appears in Fig. 2, which shows the decay curves of separated β^- and β^+ krypton activity from alpha-particle bombardment of Hilger selenium. This curve indicates that the Kr^{85} isotope is produced by alpha-particle bombardment of selenium.

Figure 4 shows the Se, Br, Kr part of the periodic table. The new Kr^{77} isotope and new reactions found are noted by heavy lines.

ACKNOWLEDGMENTS

The support received from the Ohio State University Development Fund and the Graduate School is gratefully acknowledged. All chemical separations were performed by Mr. H. L. Finston and Mr. R. M. Dyer. The successful technique developed by them for the separation and collection of the radioactive krypton gas used in these experiments is especially worthy of mention.

[5] W. Seelmann-Eggebert and H. J. Born, Naturwiss. **31**, 59 (1943).

[6] H. J. Born and W. Seelmann-Eggebert, Naturwiss. **31**, 86 (1943).

PHYSICAL REVIEW VOLUME 74, NUMBER 7 OCTOBER 1, 1948

On the Angular Distribution in Nuclear Reactions and Coincidence Measurements

C. N. YANG
Department of Physics, University of Chicago, Chicago, Illinois
(Received June 9, 1948)

Theorems concerning the general form of the angular distribution of products of nuclear reactions and distintegrations are derived. These theorems are based only on the invariance properties of the physical process under space rotation and under inversion. The following examples are studied in detail: (i) angular correlation between the electron and the neutrino in β-decay; (ii) angular correlation between a β-ray and a γ-ray emitted in succession by a nucleus; and (iii) angular correlation between two γ-rays emitted in succession by a nucleus.

INTRODUCTION

IN the calculation of the angular distribution in nuclear reactions and of the angular correlation in processes involving β- and γ-decay it often happens that many terms cancel out at the end of a laborious computation. The consistency of the occurrence of such cancellation leads one to suspect that some general reasons quite independent of the particular form of interaction are at work. In this paper we shall show that this is indeed the case. In fact, the general form of the angular distribution in many cases can be obtained directly from the theorems derived in this paper.

For nuclear reactions between spinless particles the existence of a limitation on the complexity of the angular distribution for fixed orbital angular momentum of the incoming particles is well known. That the same result holds *with the spin* taken into consideration (for un-

polarized incoming beam) was first pointed out by Critchfield and Teller.[1] A proof of this statement was recently given by Eisner, Sachs, and Wolfenstein.[2] We shall in this paper formulate a new proof that lends itself easily to generalization to the case in which the particles involved have relativistic velocities.

It will be shown in general that in studying the angular correlation between two particles, as long as one of them has a wave-length long compared to the size of the nucleus, the process can be classified into different orders and for a process of given order the general form of the angular correlation is essentially known. In case both of the particles have long wave-lengths, particularly simple conclusions may be reached, as in the case of β-neutrino correlation in β-decay.

Experimentally the angular correlations β-neutrino and γ–γ have been studied by many authors. Various calculations of these correlations based on different kinds of interactions have also been made. These will be separately discussed in the different sections.

NUCLEAR REACTION

Consider the following reaction,

$$A+P\rightarrow B+Q, \tag{1}$$

and suppose both the target nucleus A and the bombarding beam of particles P are unpolarized. The complexity of the angular distribution of the outgoing particles is limited by the following theorem: *If only incoming waves of orbital angular momentum L contribute appreciably to the reaction, the angular distribution of the outgoing particles in the center of mass system is an even polynomial of $\cos\theta$ with maximum exponent not higher than $2L$.* Here θ is the angle between the incoming and the outgoing particles in the center-of-mass system of reference.

To prove this let us consider the collision between two particles A and P with definite ($=a$ and p) components of spin along the z axis, and definite total and z component relative orbital angular momenta L and m. (We use the center-of-mass system throughout.) The incoming wave function is, at large distances r_{AP} between A and P:

$$\frac{1}{r_{AP}}\sin(k_{AP}r_{AP}-\tfrac{1}{2}L\pi)\psi_A{}^a\psi_P{}^p Y_{Lm}(\theta_P,\phi_P), \tag{2}$$

where $\psi_A{}^a$, $\psi_P{}^p$ are normalized internal wave functions of particles A and P; θ_P, ϕ_P describe the direction of motion of the particle P; and $Y_{Lm}(\theta,\phi)$ is the normalized spherical harmonics of order Lm.

The asymptotic behavior of the wave function at large values of r_{BQ} is of the form

$$\frac{1}{r_{BQ}}\exp(ik_{BQ}r_{BQ})\sum_{b,q}\psi_B{}^b\psi_Q{}^q f_{bq}{}^{apm}(\theta_Q,\phi_Q). \tag{3}$$

In reaction (1), if we choose as the z axis the direction of motion of particle P, it is clear that when the incoming wave is expanded into partial waves with definite total and z component orbital angular momenta L and m, only terms with $m=0$ occur. Under the assumption stated in the theorem we can neglect all terms except the spherical harmonic Y_{L0}. The differential cross section of reaction (1) is, therefore,

$$d\sigma=(\text{constant})d\Omega_Q\sum_{b,q}|f_{bq}{}^{ap0}(\theta_Q,\phi_Q)|^2. \tag{4}$$

For unpolarized incoming particles we get

$$d\sigma=(\text{constant})d\Omega_Q\sum_{apbq}|f_{bq}{}^{ap0}(\theta,\phi)|^2. \tag{5}$$

The requirement of invariance under rotation will now be introduced. Consider a new coordinate system (primed system) obtained from the old by a rotation of the coordinate axis. Let $(m'/m)^{(L)}$ be the matrix element[3] of the irreducible representation $\mathfrak{D}^L$ of the three-dimensional rotation group. We have

$$\begin{aligned} Y_{Lm'}(\theta',\phi')&=\textstyle\sum_m(m'|m)^{(L)}Y_{Lm}(\theta,\phi),\\ \psi_A{}'{}^{a'}&=\textstyle\sum_a(a'|a)^{(S_A)}\psi_A{}^a, \end{aligned} \tag{6}$$

where $S_A=$spin of particle A, which may be an integer or a half-odd integer. By $\psi'_A{}^{a'}$ is meant the function $\psi_A{}^{a'}$ of the *primed* internal coordinates. The proof of our theorem consists in showing that

[1] C. L. Critchfield and E. Teller, Phys. Rev. **60**, 10 (1941).

[2] E. Eisner and R. G. Sachs, Phys. Rev. **72**, 680 (1947); L. Wolfenstein and R. G. Sachs, Phys. Rev. **73**, 528 (1948).

[3] E. Wigner, *Gruppentheorie und ihre Anwsndung auf die Quantenmechanik der Atomspektren* (Braunschweig, 1931), p. 180.

(a) the superposition principle requires that f be transformed according to $\mathfrak{D}^{S_A}\times\mathfrak{D}^{S_P}\times\mathfrak{D}^{L}\times\mathfrak{D}^{S_B*}\times\mathfrak{D}^{S_Q*}$ and (b) the expression

$$I^{mm'}(\theta,\phi)=\sum_{apbq}[f_{bq}{}^{apm}(\theta,\phi)]^*f_{bq}{}^{apm'}(\theta,\phi) \tag{7}$$

transforms according to

$$\mathfrak{D}^{L^*}\times\mathfrak{D}^{L}=\mathfrak{D}^{2L}+\mathfrak{D}^{2L-2}+\cdots.$$

The linear combinations of (7) that transform according to $\mathfrak{D}^{2L-1}$, $\mathfrak{D}^{2L-3}$, etc., vanish identically.

(a) Consider the following incoming wave

$$\frac{1}{r_{AP}}\sin(k_{AP}r_{AP}-\tfrac{1}{2}L\pi)\psi_A{}'^{a'}\psi_P{}'^{p'}Y_{Lm'}(\theta_P',\phi_P'). \tag{2'}$$

To an observer in the primed coordinate system this has exactly the same form as (2). Hence the outgoing wave must be

$$\frac{1}{r_{BQ}}\exp(ik_{BQ}r_{BQ})\sum_{b'q'}\psi_B{}'^{b'}\psi_Q{}'^{q'}f_{b'q'}{}^{a'p'm'}(\theta_Q',\phi_Q'). \tag{3'}$$

Notice that we use the *same* f instead of an f', because there is *no physically observable distinction* between the two coordinate systems. Using (6) one can express (2') as a superposition of waves (2)

$$\sum_{apm}(a'|a)(p'|p)(m'|m)\left[\frac{1}{r_{AP}}\sin(k_{AP}r_{AP}-\tfrac{1}{2}L\pi)\times\psi_A{}^{a}\psi_P{}^{p}Y_{Lm}(\theta_P,\phi_P)\right].$$

Here we have omitted the superscripts S_A, S_P, L from $(a'|a)^{(S_A)}$, $(p'|p)^{(S_P)}$, $(m'|m)^{(L)}$ for simplicity. The outgoing wave must therefore be a corresponding superposition of waves (3) with the same coefficients:

$$\sum_{apm}(a'|a)(p'|p)(m'|m)\left[\frac{1}{r_{BQ}}\exp(ik_{BQ}r_{BQ})\times\sum_{bq}\psi_B{}^{b}\psi_Q{}^{q}f_{bq}{}^{apm}(\theta_Q,\phi_Q)\right].$$

Equating this to (3') and using (6) to express $\psi_B{}'^{b'}$, $\psi_Q{}'^{q'}$ in terms of $\psi_B{}^{b}$, $\psi_Q{}^{q}$, we get finally, by identifying the coefficient of $\psi_B{}^{b}\psi_Q{}^{q}$,

$$\sum_{apm}(a'|a)(p'|p)(m'|m)f_{bq}{}^{apm}(\theta,\phi)=\sum_{b'q'}(b'|b)(q'|q)f_{b'q'}{}^{a'p'm'}(\theta',\phi').$$

This reduces to the following form

$$f_{b'q'}{}^{a'p'm'}(\theta',\phi')=\sum_{apmbq}(a'|a)(p'|p)(m'|m)\times(b'|b)^*(q'|q)^*f_{bq}{}^{apm}(\theta,\phi) \tag{8}$$

through the orthogonality relations

$$\textstyle\sum_m(m'|m)(m''|m)^*=\delta_{m'm''}. \tag{9}$$

Equation (8) expresses the transformation property of f.

(b) To obtain the transformation property of expression (4) we investigate the behavior of expression (7) under rotation. By (8) and (9)

$$I^{m''m'}(\theta',\phi')=\sum_{abpq}\sum_{mm'''}(m''|m''')^*(m'|m)\times[f_{bq}{}^{apm'''}(\theta,\phi)]^*f_{bq}{}^{apm}(\theta,\phi)=\sum_{mm'''}(m''|m''')^*(m'|m)I^{m'''m}(\theta,\phi). \tag{10}$$

Now the differential cross section is proportional to I^{00}. If we put in (10) $m''=m'=0$ and take the rotation from the unprimed to the primed coordinate system to be a rotation around the z axis by an angle ξ we have $\theta'=\theta$ and $\varphi'=\varphi+\xi$. Since then $(0|m)=\delta_{0m}$ it is evident that

$$I^{00}(\theta,\varphi+\xi)=I^{00}(\theta,\varphi),$$

showing that I^{00} is independent of φ. To study its dependence on θ we put in (10) $m'=m''=0$. It is well known[4] that if $\theta=\varphi=0$,

$$(0|m)=Y_{L,-m}(\theta',\varphi').$$

Hence (10) becomes

$$I^{00}(\theta',\varphi')=\sum_{mm'''}Y_{L,-m'''}{}^*(\theta',\phi')\times Y_{L,-m}(\theta',\varphi')I^{m'''m}(0,0).$$

On application of the reduction theorem[4] of products of spherical harmonics this leads directly to our theorem.

If instead of a rotation we had chosen an inversion of the coordinates, it is evident that (8)

[4] H. Bethe, *Handbuch der Physik*, (Springer, 1933) Vol. 24/1, Chapter 3, Section 65.

would become

$$f_{bq}{}^{apm}(\pi-\theta, \pi+\phi) = P_A P_P P_B P_Q (-1)^L f_{bq}{}^{apm}(\theta, \varphi), \quad (11)$$

where P_A, P_P, etc., are the intrinsic parities of the nuclei. This shows that

$$|f(\pi-\theta, \pi+\varphi)|^2 = |f(\theta, \varphi)|^2,$$

and it follows that the angular dependence must be an even function of $\cos\theta$, a fact that is already established by (10). Equation (11) further shows that any odd power of $\cos\theta$ in the angular dependence must come from an interference term between orbital wave functions of opposite parity.

The symmetry requirements of the wave function under interchanges of the nucleons do not, in general, lead to any new conclusions about the properties of f.[5] However, in the special case in which the two incoming particles or the two outgoing particles are identical, more detailed consideration is necessary. An example of such a case is the reaction

$$Li^7+H^1 \rightarrow He^4+He^4.$$

Since the outgoing particles are spinless and satisfy Bose-Einstein statistics and since Li^7 has an odd parity, the value of L must be odd in order to have a balance of parity. This means that $f=0$ unless L is odd. At low energies, therefore, the effective orbital angular momentum is 1.

Another example is the D^2+D^2 reaction:

$$D^2+D^2 \rightarrow n'+He^3,$$
$$D^2+D^2 \rightarrow H^1+H^3.$$

This reaction has recently been considered theoretically by Konopinski and Teller.[6] Because of the symmetry nature of the deuterons it is no longer convenient to specify the spin of the two incoming particles separately. Instead we should group the nine possible incoming states into a quintet, a triplet, and a singlet. The space-wave functions for the quintet and the singlet states are symmetrical with respect to the exchange of the two deuterons, and those for the triplet states are antisymmetrical. Strictly speaking, the proof of our theorem does not apply to such a case where the space-wave function depends on the orientation of the spins of the particles. But since all the states in the same multiplet have the same *a priori* probability, it is evident that the difference of the space-wave function for the different multiplets does not affect the validity of our theorem.

The Coulomb field affects the waves of different orbital angular momenta in such a way as to favor those with higher angular momenta at low energies.[7] This accounts for the reason why at bombarding energies as low as 20 kev the angular distribution in the D+D reaction is not spherically symmetrical.[6,8] We shall not go into this point in any further detail here.

We conclude this section by stating a variation of the theorem proved above: *When contributions from incoming waves with orbital angular momenta $>L$ are neglected, the angular distribution in reaction* (1) *in the center-of-mass system is a polynomial of $\cos\theta$ with maximum exponent not higher than $2L$. This holds even if the contributing compound nuclear states have angular momenta $>L$.*

It will be noticed that when both even and odd values of the orbital angular momenta in the incoming beam are effective in producing the reaction, the angular distribution contains odd powers of $\cos\theta$. This, however, will not happen when either (a) the reaction goes through a *single* compound nuclear state (e.g. near a strong resonance level); or (b) symmetry requirements exclude even (or odd) L values as in the $Li^7+H^1 \rightarrow He^4+He^4$ reaction discussed above.

RELATIVISTIC CASE

We shall in this section generalize the result of the last section to the case when the particle P is an electron and has relativistic velocities. (The nuclei A, B, and Q are still supposed to be non-relativistic.) No such process has been experimentally realized. We shall, however,

[5] To understand this it is best to introduce the idea of *channels* in the configuration space which was first discussed by G. Breit, Phys. Rev. **58**, 1068 (1940); J. A. Wheeler, Phys. Rev. **52**, 1107 (1937). An interchange of the nucleons in general results in an interchange of the channels, except for the case when either A and P or B and Q are identical.

[6] E. J. Konopinski and E. Teller, Phys. Rev. **73**, 822 (1948).

[7] H. Bethe and E. J. Konopinski, Phys. Rev. **54**, 130 (1938).

[8] E. Bretscher, A. P. French, and F. G. P. Seidl, Phys. Rev. **73**, 815 (1948).

discuss it to illustrate our method. It will be proved that *if only partial waves of orbital angular momentum L in the electron wave function contribute to the reaction, the angular distribution is a polynomial of $\cos\theta$ with maximum exponent not higher than* $2L+1$.

Instead of the stationary picture used in the last section, we shall here use a non-stationary description of the process. The electron wave function at time $t=0$ is a product of a spin wave function with four components and a space-wave function e^{ikz}. The spin of the electron along the z axis is a constant of motion and is denoted by $p(=\pm\frac{1}{2})$. If we expand the space-wave function into partial waves of definite orbital angular momenta L, the first term ($L=0$) would give rise to allowed transitions, the second term ($L=1$) first forbidden transitions, etc. To study the angular distribution arising from the contribution of the partial wave of orbital angular momentum L we need to decompose it again into normalized waves ψ_{LJPm} of definite L, J (total angular momentum of the electron), $\boldsymbol{P}$ (parity), and m (z component of $\mathbf{J}$).* The advantage of using these ψ's is that they have simple transformation properties under rotation. The possible values of J are $L\pm\frac{1}{2}$. Under the assumption that we are considering only the contribution from a definite L value, the wave function at $t=0$ can be replaced by

$$\sum_{P=\pm1}\sum_{J=L\pm\frac{1}{2}}\alpha_{LJPp}\psi_{LJPp}. \tag{12}$$

We have put $m=p$ because the z component of the orbital angular momentum is zero.

Let us now first study the reaction arising from the electron wave ψ_{LJPm}. Starting at $t=0$ with ψ_{LJPm} and nucleus A with a definite value a for the z component of spin, we shall denote by $f_{bq}{}^{LJPam}(\theta_Q, \varphi_Q)$ the *probability amplitude* at any later time $t>0$ for that outgoing state in which the z component of spin of the particles B and Q are b and q, and in which the momentum of Q is in the direction θ_Q, φ_Q. The absolute value of the outgoing momentum (which is not fixed because the energy is not necessarily conserved when t is small) should also enter the function f as an independent variable, but has been omitted for the sake of simplicity in writing.

Now the probability amplitudes are additive when we superpose states. Since under a rotation the different waves ψ_{LJPm} with the same LJP values combine linearly, the argument which led to (8) in the last section would now lead to

$$f_{b'q'}{}^{LJPa'm'}(\theta', \varphi') = \sum_{ambq}(a'|a)(b'|b)^*\times(m'|m)(q'|q)^* f_{bq}{}^{LJPam}(\theta, \varphi). \tag{13}$$

Returning now to the wave (12) at $t=0$, we see that the differential cross section is proportional to

$$d\Omega_Q\Big|\sum_{PJ}\alpha_{LJPp}f_{bq}{}^{LJPap}(\theta, \varphi)\Big|^2.$$

This will have to be summed over a, b, p, and q. Since the coefficients in (12′) are independent of a, b and q, the final expression is

$$d\Omega_Q\sum_{JPJ'P'}\sum_{p}\alpha_{LJPp}\alpha^*{}_{LJ'P'p}\times\Big[\sum_{a,b,q}\{f_{bq}{}^{LJ'P'ap}(\theta, \phi)\}^* f_{bq}{}^{LJPap}(\theta, \phi)\Big]. \tag{14}$$

By (13) the individual terms under the summation sign $\sum_{abq}$ transform under a rotation according to $\mathfrak{D}^{S_A}\times\mathfrak{D}^{S_A*}\times\mathfrak{D}^{S_B}\times\mathfrak{D}^{S_B*}\times\mathfrak{D}^{S_Q}\times\mathfrak{D}^{S_Q*}\times\mathfrak{D}^{J}\times\mathfrak{D}^{J'*}$. But after the summation over a, b, and q is carried out, the sum transforms more simply according to

$$\mathfrak{D}^{J}\times\mathfrak{D}^{J'*}=\mathfrak{D}^{J+J'}+\mathfrak{D}^{J+J'-1}+\cdots.$$

This means that the expression in the square bracket in (14) is a sum of spherical harmonics of order $\mathfrak{LM}$ with $\mathfrak{L}\leqq J+J'$. But both J and J' are $\leqq L+\frac{1}{2}$. The theorem stated at the beginning of this section follows immediately.

If we introduce the requirement of invariance under inversion, Eq. (14) shows that those terms with $\boldsymbol{P'P}=+1$ give rise to angular correlation functions that are even under the transformation $\theta\to\pi-\theta$, and those with $\boldsymbol{P'P}=-1$ give rise to odd angular correlation functions. A consequence of this is the following. If the velocity v of the electron is small compared to the velocity of light c, and if the spin wave function of the electron is expanded in powers of v/c, the first term, i.e., the term that does not

* The parity can be either 1 or -1 for any given L, J, and m. However, for slow electrons the amplitude of waves with $P=-(-1)^L$ is very small. Cf. end of this section.

vanish as $v\to 0$, is invariant under an inversion. This term would therefore give rise to terms with $P=(-1)^L$. The opposite parity first appears in the next term of the expansion and is proportional to v/c. Hence those terms in (14) with $PP'=-1$ contain a factor v/c. Thus *the odd powers of $\cos\theta$ in the angular correlation have coefficients smaller than the even powers by a factor of v/c.*

β-NEUTRINO CORRELATION

In β-decay we have the particularly simple situation in which both the electron and the neutrino have wave-lengths long compared to the dimension of the nucleus. The argument of the last section can now be applied to both these particles and we can prove that *the angular correlation between the electron and the neutrino emitted in a β-decay is a polynomial of $\cos\theta$ up to a maximum exponent $K+1$, where*[9] *$K=0$ for allowed transitions, $K=1$ for first forbidden transitions, etc.*

The idea of the proof is that for first forbidden transitions one has either $L=1$ for the electron and $L_1=0$ for the neutrino or $L=0$ for the electron and $L_1=1$ for the neutrino. The waves $L=1$ and $L_1=1$ occur together only in second forbidden processes. Now the intensity produced by the $L=0$, $L_1=1$ waves has an angular correlation function that goes up to $\cos\theta$ to the first power, according to the theorem of the last section. Similarly, fixing our attention on the neutrino wave function we can draw the same conclusion about the $L=1$, $L_1=0$ waves. The interference term of the $L=1$, $L_1=0$ waves with the $L=0$, $L_1=1$ waves, however, gives an angular distribution that contains $\cos^2\theta$, which is the highest power of $\cos\theta$ possible for this case.

The proof is as follows. Consider the β-decay

$$A\to B+e+\nu.$$

Let a and b be the z components of the spin of the nuclei A and B, θ_e, ϕ_e and θ_ν, ϕ_ν the directions of motion of the electron and the neutrino, and s and s_1 the spin components of the electron and the neutrino in their respective directions of motion. Starting with the nucleus A at $t=0$, the probability amplitude at any later time t of the β-decay for given θ_e, ϕ_e, θ_ν, ϕ_ν, s, s_1, a, and b will be denoted by

$$f_{bss_1}{}^a(\theta_e, \varphi_e, \theta_\nu, \phi_\nu). \tag{15}$$

Now let the electron wave function be expanded into waves Φ_{LJP_s}, as done before in (12), with the only difference that here Φ_{LJP_s} represents a wave function with total angular momentum along the direction θ_e, ϕ_e (instead of along the z axis), equal to s. The coefficients α in (12) remain unchanged. Now Φ_{LJP_s} can be further expanded into waves ψ_{LJPm} with definite total angular momentum along the z axis. The final result is

$$\sum_{LJPm}\alpha_{LJP_s}(s|m)_e\psi_{LJPm}, \tag{16}$$

where e represents a rotation of the coordinate axes so that the z axis changes from the direction of motion of the electron (i.e., the direction specified by θ_e, ϕ_e) into the laboratory z axis. It is evident that the choice of the x and y axes perpendicular to the direction θ_e, ϕ_e affects only the phase of Φ_{LJP_s} and would not in any way influence our final result. In (16) $(s|m)_e$ is the only factor that depends on θ_e, ϕ_e. A similar expansion of the neutrino wave will now be made

$$\sum_{L_1J_1P_1n}\beta_{L_1J_1P_1S_1(s_1|n)_\nu}\psi_{\nu L_1J_1P_1n}. \tag{17}$$

The wave amplitude (15) is evidently given by

$$f_{bss_1}{}^a(\theta_e, \phi_e, \theta_\nu, \phi_\nu)=\sum_{LJPL_1J_1P_1}\sum_{mn}$$
$$\times\alpha_{\lambda s}{}^*\beta_{\lambda_1 s_1}{}^*(s|m)_e{}^*(s_1|n)_\nu{}^*F^a_{\lambda\lambda_1 bmn}, \tag{18}$$

where λ and λ_1 are abbreviations for LJP and $L_1J_1P_1$. We have taken the complex conjugates of the waves (16) and (17) because they represent final states. In (18) F represents the probability amplitude of the final state specified by b, $\psi_{\lambda m}$, and $\psi_{\nu\lambda_1 n}$, the initial state being specified by a.

The probability of the β-decay is proportional to

$$\sum_{abss_1}|f^a_{bss_1}(\theta_e, \varphi_e, \theta_\nu, \varphi_\nu)|^2. \tag{19}$$

Writing

$$\sum_{a,b}F^a_{\lambda\lambda_1 bmn}(\overline{F^a_{\lambda\lambda_1 b\bar m\bar n}})^*=G_{\lambda m\bar m n\bar n}, \tag{20}$$

[9] Notice that when the interaction involves derivatives of the wave function, as in the Konopinski-Uhlenbeck type of interaction, we always expand the wave function *before* taking the derivatives.

and

$$\alpha_\lambda S^* \beta \lambda_1 s_1{}^* \alpha_{\bar\lambda} S \beta \bar\lambda_1 s_1 = \Gamma_{\Lambda s s_1}, \tag{21}$$

where Λ is an abbreviation for λ, λ_1, $\bar\lambda$, $\bar\lambda_1$, expression (19) becomes

$$\sum_{\Lambda s s_1} \Gamma_{\Lambda s s_1} \sum_{m\bar m n \bar n} G_{\Lambda m \bar m n \bar n} (s|m)_e{}^* \times (s|\bar m)_e (s_1|n)_\nu{}^* (s_1|\bar n)_\nu. \tag{22}$$

We shall show later that

$$\sum_{m\bar m n \bar n} G_{\Lambda m \bar m n \bar n} (s|m)_e{}^* (s|\bar m)_e \times (s_1|n)_\nu{}^* (s_1|\bar n)_\nu \tag{23}$$

is a polynomial of $\cos\theta$ with maximum exponent $\leqq$ both $J+\bar J$ and $J_1+\bar J_1$, θ being the angle between the directions of motion of the electron and the neutrino. But $J=L\pm\frac{1}{2}$, $J_1=L_1\pm\frac{1}{2}$. Hence expression (23), which represents the (cross) term in the probability of the β-decay between waves LL_1 and $\bar L\bar L_1$, is a polynomial of $\cos\theta$ with maximum exponent $\leqq$ both $L+\bar L+1$ and $L_1+\bar L_1+1$.

The classification of β-decays into allowed, first forbidden, etc., processes consists of an expansion in powers of $r/\lambda_e \sim r/\lambda_\nu$ $(\sim \frac{1}{10})$, λ_e, λ_ν being the wave-lengths of the electron and the neutrino, and r the dimension of the nucleus. In an allowed transition only the waves $L=0$, $L_1=0$ are effective for the process. Contributions from other waves are negligible because with increasing values of L the amplitude of the wave ψ_{LJPm} inside the nucleus decreases as $(r/\lambda_e)^L$. In a first forbidden process $F^a{}_{\lambda\lambda_1 b m n}\,|_{L=L_1=0}$ vanishes because of selection rules and the contributing waves are the following two:[10] $L=1$, $L_1=0$ and $L=0$, $L_1=1$, In general, for a Kth forbidden transition only waves with $L+L'\leqq K$ are important.[9] This means that in the summation over Λ in (22) only $L+L_1\leqq K$, $\bar L+\bar L_1\leqq K$ terms need be retained. Hence $L_1+\bar L_1\leqq 2K-(L+\bar L)$. Thus the maximum exponent of $\cos\theta$ is $\leqq$ both $L+\bar L+1$ and $2K-(L+\bar L)+1$; hence it is $\leqq K+1$, which proves our theorem.

It remains to be proved that the above statement about (23) is true. This we do by noticing first that F represents the probability amplitude of the final state b, $\psi_{\lambda m}$, $\psi_{\nu\lambda_1 n}$ if the initial state is represented by a. If R is any rotation of coordinates, $\sum_a (a'/a)_R F^a{}_{\lambda\lambda_1 b m n}$ would give the probability amplitude of these *same* final states resulting from an initial state obtained by rotating nucleus A in state a' by R^{-1}. Thus

$$\sum_a (a'/a)_R F^a{}_{\lambda\lambda_1 b m n} = \sum_{b'MN} F^{a'}{}_{\lambda\lambda_1 b' M N} \times (b'|b)_R (M|m)_R (N|n)_R, \tag{24}$$

which means that $F_{\lambda\lambda_1}$ is invariant under $\mathfrak{D}^{S_A} \times \mathfrak{D}^{S_B{}^*} \times \mathfrak{D}^{J^*} \times \mathfrak{D}^{J_1{}^*}$. The definition (20) therefore shows that G_Λ is invariant under $\mathfrak{D}^{J^*} \times \mathfrak{D}^{J_1{}^*} \times \mathfrak{D}^{\bar J} \times \mathfrak{D}^{\bar J_1}$. That is,

$$G_{\Lambda m \bar m n \bar n} = \sum_{M\bar M N \bar N} G_{\Lambda M \bar M N \bar N} (M|m)_R \times (\bar M|\bar m)_R{}^* (N|n)_R (\bar N|\bar n)_R{}^*.$$

Hence

$$\sum_{m\bar m} (M|m)_R{}^* (\bar M|\bar m)_R G_{\Lambda m \bar m n \bar n} = \sum_{N\bar N} G_{\Lambda M \bar M N \bar N} (N|n)_R (\bar N|\bar n)_R{}^*.$$

Putting $R=e$, $M=\bar M=S$, we see that (23) can be written

$$\begin{aligned} &\sum_{N\bar N n \bar n} G_{\Lambda s s N \bar N} (N|n)_e (\bar N|\bar n)_e{}^* (s_1|n)_\nu{}^* (s_1/\bar n)_\nu \\ &= \sum_{N\bar N n \bar n} G_{\Lambda s s N \bar N} (n|N)_{e^{-1}}{}^* (\bar n|\bar N)_{e^{-1}} \times (s_1|n)_\nu{}^* (s_1|\bar n)_\nu \\ &= \sum_{N\bar N} G_{\Lambda s s N \bar N} (s_1|N)_{\nu e^{-1}}{}^* (s_1|\bar N)_{\nu e^{-1}}. \end{aligned} \tag{23'}$$

This is evidently independent of the choice of the laboratory coordinate system. If these be so chosen that $\theta_e=\phi_e=0$, the rotation represented by e becomes the identity and (23′) shows that (23) is a polynomial of $\cos\theta$ with maximum exponent $\leqq J_1+\bar J_1$. A similar argument shows that it is also $\leqq J+\bar J$. This completes the proof.

If we fix our attention on one end of the spectrum where the electron momentum p is $\ll$ the neutrino momentum q, the waves that contribute most in a Kth order forbidden transition are those with $L=0$, $L_1\leq K$. By the theorem proved in the last section we see that *the maximum exponent of $\cos\theta$ in the angular coorelation is 1.* This evidently applies also when $q\ll p$.

If $p\ll mc$ the spin function of the electron can be separated from the space-wave function.

[10] It may happen that $F^a{}_{\lambda\lambda_1 b m n}\,|_{L=L_1=0}$ is not zero but is $\sim F^a{}_{\lambda\lambda_1 b m n}\,|_{L=1,\ L_1=0}$. This happens in the usual interactions because of the presence of terms $\sim$nucleon velocity. In such cases we should include the $L=0$, $L_1=0$ wave. The conclusions are, however, unchanged as far as they concern only the complexity of the angular correlation.

Hence, after summation over the spin directions of the electron, the maximum exponent is both $\leqq L+\bar{L}$ and $J_1+\bar{J}_1\leqq 2K-(L+\bar{L})+1$. We have $L+\bar{L}$ instead of $J+\bar{J}$, as in all non-relativistic cases. Thus *the maximum exponent is* K.

In case $p\ll q$ *and* $p\ll mc$, *only* $L=0$ *wave is effective and the angular correlation is spherically symmetrical for transitions of any order.* Thus when $p\to 0$ the angular correlation becomes spherically symmetrical. On the other hand, when $q\to 0$ the angular correlation becomes $1+\alpha\cos\theta$ or 1 according as the mass of the neutrino is zero or otherwise.

Actual calculations of the angular correlation between the electron and the neutrino emitted in β-decays of different orders have been carried out by Hamilton,[11] using all the five usual types of interactions. The results, of course, conform with the theorems discussed above. Experimentally,[12] information about the angular correlation has been obtained by measuring the energy spectrum of the recoil nuclei or by coincidence measurements of the electrons and the recoil nuclei. Because of the indirect nature of these experiments, the results are not as yet very quantitative.

β-γ AND γ-γ CORRELATIONS

The method used in the last three sections evidently applies also to γ-rays. The rectangular components A_x, A_y, and A_z of the vector potential of the electromagnetic field is expanded into spherical harmonics. As is well known, the term $L=0$ leads to electric dipole processes, the term $L=1$ to magnetic dipole and electric quadrupole processes, etc. For each direction of propagation of the light quantum there are two possible waves with $L=0$, corresponding to the two different polarizations. Changing the direction of propagation we obtain other waves. But altogether there are only three linearly independent waves with $L=0$, and they transform among themselves under a rotation like a vector. Hence *the angular correlation between the* γ*-ray and any other particle in a nuclear process is of the form* $1+\alpha\cos^2\theta$ *if the* γ*-ray process is of the electric dipole type.*

[11] D. R. Hamilton, Phys. Rev. **71**, 456 (1947).

[12] J. S. Allen, Phys. Rev. **61**, 692 (1942); J. C. Jacobsen, and Kofoed-Hansen, Kgl. Danske Vid. Sels. Math.-Fys. Medd **23**, No. 12 (1945); J. S. Allen, H. R. Paneth, and A. H. Morrish, Bull. Am. Phys. Soc. **23**, No. 3 (1948); C. N. Sherwin, Phys. Rev. **73**, 216 (1948).

TABLE I.

		Nuclear particle	Electron or neutrino	Photon
Name for different approximations	$L=0$	S wave	Allowed	El. dipole
	$L=1$	P wave	First forbidden	Mag. dipole and el. quadrupole
	$L=2$	D wave	Second forbidden	Mag. quadrupole and el. octapole
Power of $\cos\theta$		Even	Even and odd	Even
Max. exponent of $\cos\theta$		$2L$	$2L+1$	$2L+2$

The odd power of $\cos\theta$ does not appear because the photon wave has a definite parity. This conclusion can be immediately generalized into *magnetic dipole and electric quadrupole processes where the angular correlation is* $1+\alpha\cos^2\theta+\beta\cos^4\theta$. This holds even when *both* the magnetic dipole and the electric quadrupole transitions are present. Similar theorems obtain in higher multipole processes.

In general, we can study a process with any number of incoming and outgoing particles. We assume that the incoming particles are unpolarized. If one of the particles (whether incoming or outgoing), say P, has a wave-length long compared to the dimension of the space-region in which it interacts with the other particles, the process can be classified according to to the effective orbital angular momentum L of P. The angular correlation between P and any other particle Q in the process would then be a polynomial of $\cos\theta$ with a maximum exponent determined by L, θ being the angle between the directions of propagation of P and Q. The presence of other particles in the process does not affect the result because a summation over the directions of motion and over the spin of these "redundant" particles must always be carried out. We may say that these particles do not produce any preferential direction in space. The general results when P is a nucleon, an electron, or a photon are summarized in Table I.

The application to the angular correlation between successive γ-rays emitted by a nucleus is straightforward. Actual calculations of this correlation for dipole-dipole, dipole-quadrupole, and quadrupole-quadrupole transitions (all electric poles) have been published.[13] They have the

[13] D. R. Hamilton, Phys. Rev. **58**, 122 (1940); experimental evidence has been reported by L. Brady and M. Deutsch, Phys. Rev. **72**, 870 (1947).

form

$$1+\alpha\cos^2\theta \text{ (dipole-dipole, dipole-quadrupole)}, \quad (25)$$
$$1+\alpha\cos^2\theta+\beta\cos^4\theta \text{ (quadrupole-quadrupole)},$$

agreeing with our results. In these calculations the line width of the second γ-ray process is assumed to be large compared to the hyperfine splitting of the atom, so that the lifetime of the intermediate nucleus is small compared to the time required for the nuclear spin to precess appreciably. Also the assumption is made that there is no magnetic dipole transition mixed with the electric quadrupole. It is evident that neither of these assumptions is necessary for the validity of our theorems, and that the angular correlation is quite generally of the form (25). It should be remarked, of course, that in case either of these two assumptions is violated the coefficients α and β in (25) may not have the values tabulated by Hamilton.

Another application is found in the problem of the angular correlation between the electron and the γ-ray emitted by a nucleus in succession. Since one of the particles is a photon, only even powers of $\cos\theta$ can occur in the correlation function. Using Table I, taking the electron to be P, we conclude that *for all allowed β-transitions the correlation is spherically symmetrical.* This appears at first sight very strange because, e.g., for the Gamow-Teller type of interaction the matrix element involves the spin of the nucleus and one would expect that the emission of an electron in a definite direction would result in a preferential distribution of the spin orientation of the intermediate nucleus and hence would affect the angular distribution of the γ-rays. *For first forbidden β-transitions the correlation is $1+\alpha\cos^2\theta$.* Falkoff and Uhlenbeck have made actual calculations for the first forbidden electric dipole process, using various types of β-interactions.[14] As in the γ–γ case discussed above, we remark here that our conclusions hold independently of any assumption about the lifetime of the intermediate nucleus, and independently of the multipole nature of the γ-radiation. Also it is not necessary to neglect the term in the β-interaction that is proportional to the nucleon velocity.

[14] D. L. Falkoff and G. E. Uhlenbeck, Bull. Am. Phys. Soc. **22**, No. 5 (1947).

REMARKS ABOUT OTHER PARTICLES

Table I can be extended to include mesons of spin 0 and 1. The treatment is very similar to the treatment of the electron if we use Kemmer's[15] representation of the meson wave functions. In this representation a scalar meson has a five-component and a vector meson a ten-component wave function. We shall assume that the rest mass is not zero. Let us take a plane wave

$$\psi=\phi\exp((i/\hbar)(\mathbf{p}\cdot\mathbf{x}-Et)) \quad (26)$$

and expand it into waves with definite orbital angular momentum L. Under a rotation the spin function ϕ is transformed by a matrix S. The total angular momentum can go as high as $L+1$. Notice that this is true for scalar mesons as well as vector mesons.[15] Thus if only orbital wave L contribute to the reaction the angular correlation between a meson and any other particle is a polynomial of $\cos\theta$ with maximum exponent $\leqq 2L+2$.

If further the meson has non-relativistic velocities v, as must actually be the case in order that the wave-length of the meson may be long compared to nuclear dimensions, we can expand ϕ into a power series in v/c.

$$\phi=\phi_0+\frac{|v|}{c}\phi_1+\cdots. \quad (27)$$

It can be readily proved that the following points are true:

(a) ϕ_0 has a definite parity and can be made independent of the direction of the velocity. The theorem proved in the section about nucleons can therefore be applied here and we see that to the order $(v/c)^0$ the angular correlation is an even polynomial of $\cos\theta$ with maximum exponent $\leqq 2L$.

(b) ϕ_1 has a definite parity which is the opposite of that of ϕ_0. Thus the interference term between ϕ_0 and ϕ_1 gives rise to odd powers of $\cos\theta$ only and we have the result that the terms in the angular correlation to the first order of v/c is an odd polynomial of $\cos\theta$.

The author wishes to take this opportunity to thank Professor E. Teller for invaluable discussions and advice.

[15] N. Kemmer, Proc. Roy. Soc. **A173**, 91 (1939).

The Isotopic Constitution of Europium, Gadolinium, and Terbium

DAVID C. HESS, JR.
Department of Physics, University of Chicago, Chicago, Illinois*

(Received June 21, 1948)

The isotopic abundances of europium, gadolinium, and terbium have been determined electrometrically by means of a mass spectrometer. The abundances of europium isotopes of masses 151 and 153 were found to be 47.77 and 52.23 percent, respectively. For gadolinium, masses 152, 154, 155, 156, 157, 158, and 160 were found to have abundances of 0.20, 2.15, 14.78, 20.59, 15.71, 24.78, and 21.79 percent, respectively. Upper limits for the existence of other isotopes of these elements were determined.

I. INTRODUCTION

THE previous measurements of the isotopic abundances of europium, gadolinium, and terbium were made photometrically.[1–5] This method is subject to several difficulties which may be eliminated by the use of electrometric measurements. Perhaps the most serious shortcoming of the photographic method is the unknown relation between the image density and the total numbers of ions producing the developable images. Attempts to produce standard densities on the plate by the use of x-rays,[6] light,[7] or ions other than those being measured[7,8] leave one in doubt as to the reliability of assuming that the connection between density and number of ions is the same for the "standard" as for the unknown. For example, the "reciprocity" law connecting time and intensity of exposure holds for x-rays but not for light.[9] For the second expedient, the use of light to produce standard densities, Dempster and Hayden[7] have shown that the slope of the exposure-density curve is much steeper for light than for ions. If different ions are used, the slope varies with the mass of the ion and also with its energy.[7] Dempster and Hayden have shown that the exposure-density curve is steeper for Sr^+ than for Ba^{++}, and that the curve is even steeper for light. Aston has found similar effects[8] with light and heavy ions. When exposure-density curves are made with the ions which are being studied by making exposures for different times,[10] the assumption must be made that the ion current is constant for the different exposures. The ion current may be integrated in some manner, but this forces us back to an electrometric method. In addition, errors may arise from the fact that the ions of different mass traverse different paths in a spectrograph and may produce lines of different widths. Aston discusses compensation for such factors.[11]

A scanning method of mass spectrometric determination of isotopic constitution as described herein has some difficulties which should be noted. One is the requirement that the ion source be reasonably steady. This can be accomplished in several ways, one of which is used here. Another is that the precision of the information that may be obtained with a given ion supply depends on the number of isotopes. For example, it was possible to make a great many more readings of the isotope ratio with a given sample of europium than with a given sample of gadolinium because it was necessary to scan only three mass units, 151, 152, and 153 with europium, whereas for gadolinium the number is nine. In addition, since the intensity range is greater for gadolinium, a larger total emission must be used. This means that, since the

* These experiments were carried out at the Argonne National Laboratory, Chicago, Illinois.

[1] F. W. Aston, Proc. Roy. Soc. **A146**, 46 (1934).
[2] H. Lichtblau, Naturwiss. **27**, 260 (1939).
[3] A. J. Dempster, Phys. Rev. **53**, 727 (1938).
[4] W. Wahl, Soc. Sci. Fenn. **11**, 1 (1941).
[5] R. E. Lapp, J. R. Van Horn, and A. J. Dempster, Phys. Rev. **71**, 745 (1947).
[6] According to a paper by J. Mattauch and H. Ewald, Zeits. f. Physik **122**, 321 (1944), the standard intensity marks used by Wahl (reference 4) were made by x-rays and a rotating sector.
[7] A. J. Dempster and R. J. Hayden, Metallurgical Laboratory Report MUC-AJD-41, December (1944).
[8] F. W. Aston, *Mass Spectra and Isotopes* (Edward Arnold & Company, London, 1942), pp. 90 ff.
[9] A. H. Compton and S. K. Allison, *X-Rays in Theory and Experiment* (D. Van Nostrand Company, Inc., New York, 1935), p. 6.
[10] J. Mattauch and V. Hauk, Naturwiss. **25**, 780 (1937).
[11] See page 93 of reference 8.

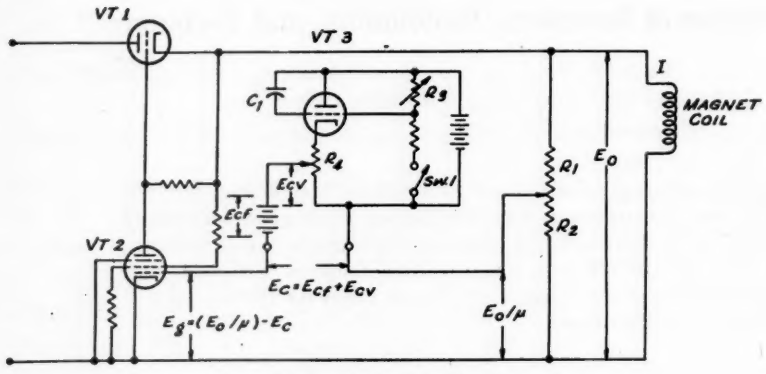

Magnetic Sweep Circuit

FIG. 1. Circuit used to stabilize the current through the analyzer magnet against random fluctuation and to vary it periodically to scan the mass range being studied.

recording speed is limited by the time constant of the input circuit and also by the mechanical recorder, three or more ratios can be obtained for europium in the time required for one set of readings with gadolinium. More of the ions are "wasted" with the latter. However, the accuracy which can be obtained is much greater than with a photographic method.

Electrometric determination of the isotopic constitution of europium, gadolinium, and terbium, together with upper limits for the existence of possible rarer isotopes of these elements, are given in this paper.

II. MASS SPECTROMETER AND MAGNET CONTROL

The mass spectrometer used in this investigation was a 60°, six-inch radius of curvature, single-focusing instrument which has been used in other investigations.[12–14] Ions were produced by thermionic emission from a heated anode consisting of a tungsten ribbon coated with an oxide of the element under study. Emission began at temperatures ranging from 1200° to 1600°C. The highest temperature was associated with terbium, while gadolinium was intermediate and europium lowest. The pressure in the tube varied from about 2×10^{-7} to 4×10^{-6} mm of mercury as measured by an ionization gauge.

Magnet Control

The different isotopes were focused on the collector by variation of the deflecting magnetic field. This variation was brought about as a function of time by the control circuit shown in Fig. 1. In this figure, $VT1$ is a series regulator tube that controls the current, I, through the magnet coil by varying the voltage, E, across the resistor network, $R1$, $R2$, which is the voltage across the coil. The voltage drop across the tube $VT1$ depends on the plate voltage of $VT2$ which, in turn, depends on the grid voltage of $VT2$. This is supplied by a fraction of the coil voltage, E_0/μ, minus the voltage E_c. If E_c is a fixed (say, battery) voltage, the circuit is merely a conventional degenerative voltage stabilizer with a battery standard.[15,16] If, however, E_c is represented by a fixed (battery) voltage E_{cf} in series with a varying voltage E_{cv}, the output voltage will vary with this latter voltage and the variation will have a magnitude μ' times the signal E_{cv}. It is apparent that this circuit is simply a two-stage amplifier with feedback obtained from the cathode circuit of the output stage. The gain, μ', of such an amplifier with feedback, if the gain without feedback is sufficiently high, is approximately $\mu' \approx (R_1+R_2)/R_2 = \mu$. We will replace μ' by μ, as the gain without feedback is high enough to permit this approximation. In the present case, the signal voltage is E_c where E_c may be fixed or variable since the amplifier is direct-coupled. If the variable part of E_c, E_{cv}, is a sawtooth wave such as is obtained by charging or discharging a capacitor through a resistor, it is seen that the current through the magnet and, therefore, the magnetic field will change smoothly

[12] M. G. Inghram, R. J. Hayden, and D. C. Hess, Jr., Phys. Rev. 72, 967 (1947).
[13] M. G. Inghram, D. C. Hess, Jr., and R. J. Hayden, Phys. Rev. 73, 180 (1948).
[14] M. G. Inghram, D. C. Hess, Jr., and R. J. Hayden, Phys. Rev. 74, 98 (1948).
[15] F. V. Hunt and R. W. Hickman, Rev. Sci. Inst. 10, 6 (1939).
[16] A. Abate, Proc. I.R.E. 33, 478 (1945).

with time though the variation of E_c may not be exactly linear with time.

The sawtooth wave was obtained by discharging $C1$ through $R3$. The variable voltage was applied to the grid of a cathode follower tube, $VT3$, for the purpose of isolating the capacitor-resistor circuit which necessarily has high impedance since the time constant may be of the order of hundreds of seconds. The fact that the sawtooth voltage variation so formed is not strictly linear with time is of little consequence in this application since the variation of B with I is not linear, and also the mass observed is not a linear function of the magnetic flux density B.

In the actual circuit, the value of resistance $R3$ was adjustable to allow the rate of mass sweep to be varied while the output tap on resistor $R4$ was adjustable to permit the range to be controlled. The measurement could be repeated by charging $C1$ through a limiting resistor by means of $SW1$.

III. ION SOURCE AND ION DISCRIMINATIONS

The ions used in these measurements were produced by thermionic emission from a hot filament. In this type of source, the efficiency of ionization depends on the ionization potential of the material and the work function of the support,[17–19] so it would be expected that the yield should not depend on the mass of the ion. Theoretically, evaporation from the surface of a liquid would give a change in abundance ratio of the evaporated isotopes proportional to the square root of the ratio of their masses, because the light atoms have greater velocity and therefore greater probability of escaping the surface.[19,20] Thus, initially there will be a preponderance of light ions.[21] This effect will continue only if there is sufficient mixing to maintain the normal ratio at the surface. If the rate of mixing in the liquid is low, there will be a developing scarcity of lighter atoms near the surface and therefore, although the probability of emission will continue to be higher for the light than for the heavy atoms, the fraction of the ions that are light will no longer be greater than the average fractional abundance in the mass of the material because of the depletion in the number per cubic centimeter relative to the heavier isotope. The rare-earth oxides remain solid at the temperatures used and since diffusion rates in solids are low,[22] it may be concluded that the effective mixing rate in the experiments is too low for an error due to this cause. An experimental check of this possibility was made by comparing the ratio of mass 151 to 153 in europium at various times in a complete run. No significant variation was observed. Furthermore, no trend in the ratio of Nd^{146} to Nd^{150} was observed,[14] and a similar constancy in the Gd^{160} to Gd^{155} ratio gives support to this conclusion.

The condition for no discrimination between light and heavy ions in their passage through a mass spectrometer is that the paths for different ions be identical.[23] In order to achieve this condition, it is not only necessary that ions of different masses be collected at the same point, but also that they originate from the same point in the source. Since the accelerating voltage is held constant in these experiments and the magnetic field varied, the path of the ions will be the same whatever ions are being observed. This is apparent when it is considered that although there is a stray field acting on the ions from the time they are emitted,[24] this stray field is proportional to the analyzer field only,[25] since there is no source magnet and the source is not ferromagnetic, and therefore will produce a deflection which will vary inversely as the square root of the mass. If, then, the whole region from source to collector is considered as the analyzer, it is seen that the focusing condition $Bm^{-\frac{1}{2}}=K=R^{-1}(2Ve^{-1})^{\frac{1}{2}}$, holds if B and R are considered as "integrated" values.[24]

[17] I. Langmuir and K. H. Kingdon, Proc. Roy. Soc. **A107**, 61 (1925).
[18] M. J. Copley and T. E. Phipps, Phys. Rev. **45**, 344 (1934).
[19] A. K. Brewer, J. Chem. Phys. **4**, 350 (1936).
[20] L. B. Loeb, *Kinetic Theory of Gases* (McGraw-Hill Book Company, Inc., New York, 1934).
[21] R. S. Mulliken and W. D. Harkins, J. Am. Chem. Soc. **44**, 37 (1922).
[22] For example, the diffusion rate of cerium oxide in tungsten at 2000°K is of the order of 10^{-9} cm²/sec. according to Dushman and Langmuir [Phys. Rev. **20**, 113 (1922)]. The ion currents used in the present measurements would correspond to current densities of 10^{15} ions/cm²/sec.
[23] E. B. Jordan and N. D. Coggeshall, J. App. Phys. **13**, 539 (1942).
[24] N. D. Coggeshall, J. App. Phys. **18**, 855 (1947).
[25] In the source region the magnitude of the constant field due to the earth was less than three percent of the stray field due to the magnet of the spectrometer.

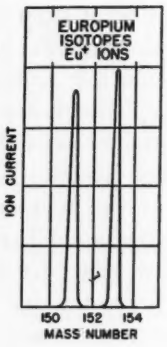

FIG. 2. Typical trace of the recorder chart when scanning the europium ion currents. Both isotopes are recorded at the same sensitivity.

Since the accelerating voltage was constant, there was no error due to "voltage effect" in the source. Emission was temperature-limited so that possible space-charge discriminations are negligible. Secondary electron emission was suppressed by a retarding field surrounding the collector.

IV. ION MEASUREMENTS

Since the observations were made by repeated scanning of the mass region of interest, slow variations in ion emission could be observed by the variation in height of the peaks corresponding to a given mass at different times. This permitted interpolation to obtain the height of one peak at the instant that another was being recorded and did not require the assumption that conditions remained constant while different masses were measured. Measurements were made from the peak heights as recorded, since care was taken to ensure that the collector-defining slit was sufficiently wide to accommodate all the ions corresponding to one mass. Only singly charged ions were observed with the source used.

A final source of error to be considered is the possibility of non-linearity of response of the recording system with variations of input current. The system consisted of a vibrating reed electrometer,[26] the output of which was recorded by a Brown Electronik Strip Chart Recorder. The ion current from the collector produced a voltage drop across a high resistance, 2×10^{9} ohms and 10^{10} ohms Victoreen resistors were used, and this voltage, from a high impedance generator, was transformed to the same voltage but from a lower impedance generator by the vibrating reed electrometer and amplifier. The linearity of the electrometer and amplifier and of the Brown Recorder were not checked individually but only the effect of the whole system was considered. The over-all response of the system was measured by plotting the discharge of a polystyrene capacitor through the high resistor. The slope of the exponential was measured by determining the time interval for the signal to drop to half of a given value. This measurement was repeated from a maximum voltage of 1.4 volts across the resistor down to 0.3 millivolt. The values observed were plotted and showed a variation of less than one-half percent. The range of ion currents used extended from about 1×10^{-9} ampere to 1×10^{-14}, corresponding to from 2.0 volts to 0.1 millivolt across the resistors. Therefore, measurements of isotopes of very different abundances were not in error due to the measuring system by greater than one-half percent.

In view of the elimination of or compensation for the systematic errors discussed above, we may conclude that the observed peak heights are proportional to the isotopic abundances to an accuracy of greater than one percent.

V. EUROPIUM ABUNDANCES

Europium was first studied by Aston[1] who found that it consisted of two isotopes of masses 151 and 153 with mass 151 more abundant in the ratio 1.024:1. It was later measured by Lichtblau[2] who found mass 151 to be less abundant in the ratio 0.963:1. The europium sample used was Hilger laboratory number 1772.

Europium oxide heated on the filament liberated primarily Eu^{+} ions. The EuO^{+} ions detected at any time during the measurements amounted to less than 0.1 percent of the Eu^{+} ions. The ratio of ion intensity of mass 151 to that of 153 was found to be 0.9145:1, giving the percentage abundances 47.77 for the mass at 151, and 52.23 for mass 153. These values are the result of 119 measurements. No other isotopes were found. The upper limits for the abundance of other isotopes, according to the present measurements, are 0.002 percent for masses 147, 148, 149, 156, and 157; 0.004 percent for mass 155; 0.005 percent for mass 150; 0.007 percent for mass 154; and 0.01 percent for mass 152. Limits on the masses 150, 152, 154, and 155 are

[26] H. Palevsky, R. K. Swank, and E. Grenchik, Rev. Sci. Inst. 18, 298 (1947).

TABLE I. Percent abundances of gasolinium isotopes, upper limits for possible weak isotopes, and location of known activities.

Mass	149	150	151	152	153	154	155	156	157	158	159	160	161	162
Aston[a]				—		—	21	23	17	23		16		
Dempster[b] and Aston				0.2		1.5	21	22	17	22		16		
Wahl[c]				0.2		2.86	15.61	20.59	16.42	23.45		20.87		
This measurement:	<.005	<.005	<.005	0.20	<.005	2.15	14.78	20.59	15.71	24.78	<0.01	21.79	<.02	<.02

[a] See reference 1. [b] See reference 3. [c] See reference 4.

not as low as on the other masses because of the less perfect resolution which resulted from the large amount of gas evolved when the filament temperature was increased to produce the high ion currents necessary in searching for the possible faint isotopes. A typical trace of the recorder chart is shown in Fig. 2. This trace was made at low intensity so there is no indication of any other masses due to impurities.

Radioactive europium isotopes are known to exist at masses 150, 152, 154, 155, and 156. Existence of an active isotope does not preclude existence of a stable isomer, but it decreases the likelihood for the element being studied.

Using the observed ratio, a packing fraction of -2.2, and dividing by the factor 1.000275 to convert the physical atomic weight to the chemical scale, the atomic weight is 151.97, which agrees well with the internationally accepted value of 152.0 (1940).

VI. GADOLINIUM ABUNDANCES

Gadolinium was first studied by Aston[1] who found it to consist principally of masses 155, 156, 157, 158, and 160. Later Dempster[3] found the weak isotopes at masses 154 and 152, and estimated their abundances relative to the other isotopes but did not give a photometric measurement of his plates. Later Wahl[4] gave new values to the abundances.

Gadolinium oxide, Hilger laboratory number 1073, heated on the filament gave rise at first to GdO^+ ions. After a short time, Gd^+ ions began to appear but were less than ten percent of the corresponding GdO^+ ions. This is to be contrasted with the behavior of europium where practically no oxide ions were detected. By the time the emission had been increased to a value where the peaks were high enough to give good measurements, the GdO^+ ions predominated although the Gd^+ ions were still present. The ratio of GdO^+ ions to Gd^+ ions remained roughly constant throughout the run. Later when the intensity was increased to look for weak isotopes, the Gd^+ ion current was still too small to be useful for this purpose. For these reasons the measurements reported were made in the oxide position.

A typical trace is shown in Fig. 3. The peak heights of masses 168, 175, 177, and 178 have been multiplied by 10, and that of 170 by 5, relative to the heights of the other peaks. Peaks were observed for masses 168, 170, 171, 172, 173, 174, 175, 176, 177, and 178, corresponding to the known gadolinium isotopes at masses 152, 154, 155, 156, 157, 158, and 160. The heights of the peaks at 177 and 178 are accounted for to a good approximation by the assumption that they are due to $Gd^{160}O^{17}$ and $Gd^{160}O^{18}$, using the value of the abundances of O^{17} and O^{18} due to Murphey.[27] The peak at 175 could be composed of $Gd^{157}O^{18}$ plus $Gd^{158}O^{17}$, plus $Gd^{159}O^{16}$, plus $Tb^{159}O^{16}$. Since

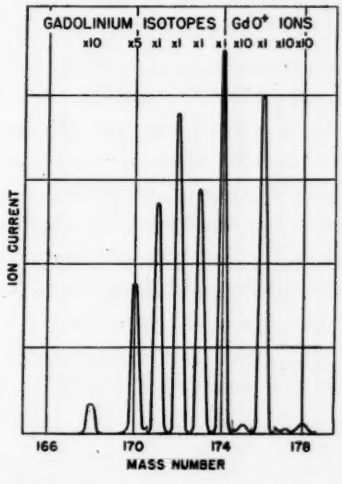

FIG. 3. Typical trace of the recorder chart when scanning the gadolinium ion currents. The relative sensitivities of the electrometer circuit for each isotope are indicated above the trace.

[27] B. Murphey, Phys. Rev. 59, 320 (1941).

the peak is very small, it is not possible to assign it to a gadolinium isotope of mass 159, as a very small amount of terbium impurity, together with the other oxide components, could easily account for it.

The measured abundances of the gadolinium isotopes are shown in Table I. These values are the averages of over three hundred measurements. The table also shows the previous values of the abundances. The row credited to Dempster and Aston is a superposition of Dempster's weak isotope abundances on Aston's previous observations. The upper limits obtained for the presence of weak isotopes of gadolinium are indicated. Some of the limits are not as low as for europium because of the poorer ionization efficiency of gadolinium and the consequent low ion currents obtainable consistent with maintaining a useful resolution. When the filament temperature was increased to increase the emission, the amount of gas emitted degraded the resolution. Attempts to bake out the gas at the high temperature necessary for operation in order to improve the resolution obtainable resulted in loss of the sample while the outgassing process was going on. Outgassing at lower temperatures was not effective. The filaments themselves were well outgassed after assembly before being coated with the nitric acid solution.

Using the measured isotopic composition, a packing fraction of -1.5, and the conversion factor 1.000275, the calculated atomic weight is 157.26, in disagreement with the internationally accepted value of 156.9 (1940).

It is interesting to note that the upper limit assigned to the existence of Gd^{150} is less than one-tenth that of some other weak isotopes which are known to exist, such as Ce^{136} and Ce^{138},[28] and Gd^{152}, and Gd^{154},[3] although comparable to K^{40}.[29] A radioactive gadolinium isotope is known at mass 153.

[28] A. J. Dempster, Phys. Rev. **49**, 947 (1936).
[29] A. O. Nier, Phys. Rev. **50**, 1041 (1936).

VII. TERBIUM ISOTOPES

Aston[1] found an isotope of mass 159 for terbium, but placed no limits on the existence of other isotopes. Terbium oxide, like gadolinium, showed both metal and oxide ions. However, TbO^+ became predominant early in the measurement so that the oxide position was used in the search for other isotopes. The principal peak found was at mass 175, corresponding to terbium of mass 159. The best sample obtainable from Hilger, laboratory number 1073, contained a considerable amount of gadolinium, so the limits placed on the other isotopes of terbium were obtained by measuring the observed gadolinium abundances in the sample and allowing for a deviation from previous gadolinium measurements. According to present measurements, terbium is monisotopic. No other isotopes were observed to have abundances greater than 0.03 percent of mass 159. Again, the lower ionization efficiency raises the upper limits for rare isotopes, while the presence of gadolinium contributes to the large limits given. A radioactive isotope of mass 160 is known.

Using a packing fraction of -1.0, and the conversion factor of 1.000275, the atomic weight is calculated to be 158.94, which is somewhat lower than the internationally accepted value of 159.2 (1940).

CONCLUSION

The isotopic constitution of europium, gadolinium, and terbium has been determined electrometrically. The results are believed to be accurate to better than one percent. The method used avoids the disadvantages of a photographic method.

The author wishes to express his sincere appreciation to Professor A. J. Dempster, Doctor M. G. Inghram, and Doctor R. J. Hayden for their help and encouragement in carrying out this work.

A First-Order Variational Principle for Classical Electrodynamics

F. J. BELINFANTE
*The University of British Columbia, Vancouver, British Columbia, Canada**

(Received April 21, 1948)

The fact that the Schrödinger and the Dirac equations for the wave function of an electron are differential equations of the first order with respect to time, while in classical theories differential equations of the second order are common, has necessitated a slightly different setup of the canonical theory in both fields. Under influence of the classical methods, second-order equations are also often used in the quantum theory of particles of integer spin, thus causing a difference between the treatment of Fermi-Dirac and of Einstein-Bose particles.

It is shown here that conformity between classical and quantum-mechanical methods can be achieved easily by use of first-order equations throughout, thus avoiding a superfluous distinction between integral and half-odd-integral spin fields. The classical theory of a point charge in an electromagnetic field of force is set up here from this point of view.

IN classical mechanics, it is usual to derive the equations of motion from a variational principle $\delta\int\mathfrak{L}(q_k, \dot{q}_k)dt=0$ of such a type that the differential equations obtained are of the second order. When the Hamiltonian, $\mathfrak{H}=\sum p_k\dot{q}_k-\mathfrak{L}$, is expressed in terms of the variables q_k and their canonical conjugates $p_k=\partial\mathfrak{L}/\partial\dot{q}_k$ afterwards, the $\dot{q}_k$ are eliminated then by expressing them in terms of the momenta p_k. A similar procedure is also used for Maxwell's theory, when $(1/8\pi)\int\int\int\int(\mathbf{E}^2-\mathbf{H}^2)dxdydzdt$ or some other convenient expression is used as a Lagrangian, with the equations $\mathbf{H}=\text{curl}\mathbf{A}$ and $\mathbf{E}=-\nabla\Phi-\dot{\mathbf{A}}/c$ added as definitions of $\mathbf{H}$ and of $\mathbf{E}$.

In wave mechanics, the procedure is slightly different. The variational principle used is here $\delta\int dt\mathfrak{L}(Q_k(x), \dot{Q}_k(x))=0$, where the functional $\mathfrak{L}$ is given by $\mathfrak{L}=\int\psi\dagger(i\hbar\partial/\partial t-\mathrm{H})\psi$. (The symbol $\int$ means integration over x, y, and z and summation over components.) This variational principle gives equations of motion $i\hbar\partial\psi/\partial t=\mathrm{H}\psi$ and $-i\hbar\partial\psi\dagger/\partial t=(\mathrm{H}\psi)\dagger$, which are of the *first* order, at least in t. (In Dirac's relativistic theory H is also linear in the gradient operator ∇.) Further, the "momentum" (P) canonically conjugate to the "variable" $(Q\equiv)\psi$ is here $(P\equiv)i\hbar\psi\dagger$, which is one of the variables, on which the Lagrangian $\mathfrak{L}$ itself depends. The Hamiltonian is now $\mathfrak{H}=\int P\dot{Q}-\mathfrak{L}=\int\psi\dagger\mathrm{H}\psi$, so that the $\dot{Q}$ drop out automatically. (Remark also that P is no longer some simple function of $\dot{Q}$.)

It seems surprising that there is so much difference between the wave mechanical and the classical procedure. This has led many authors, in particular when a field of particles of integral spin had to be described, to the use of a "second-order Lagrangian" also in wave mechanics, in close analogy with the procedure commonly used for Maxwell's theory. In the case of particles of spin $\frac{1}{2}$, however, this method remains unsatisfactory, so that a complete unification of methods would seem impossible.

This note serves to point out that the unification can be sought and found in the opposite direction. The application of first-order Lagrangians to the description of wave fields of particles with integral as well as with half-odd-integral spin has been recommended and demonstrated by the author several times.[1] Here I want to point out that this method is not confined to wave mechanics, but can be used just as well in classical point mechanics. The interesting point is the close resemblance one finds between the Hamiltonian in this classical formalism and the Hamiltonian of Dirac's theory of electrons.

We shall show here this method for a classical electron (for the sake of simplicity considered here as a point charge e at the position $\mathbf{x}_0$ at the time t) in an arbitrary Maxwell field. We start from the relativistic variational principle

$$\delta\{\int\Delta d\tau+\int\int L_f dxdydzdt\}=0, \qquad (1)$$

* Now at Purdue University, Lafayette, Indiana, U. S. A.

[1] F. J. Belinfante, *Theory of Heavy Quanta* (thesis) (M. Nijhoff, The Hague, 1939). See also: F. J. Belinfante, Physica **6**, 887 (1939); Physica **7**, 449, 765 (1940); Physica **12**, 1 (1946). Also: H. A. Kramers, F. J. Belinfante, and J. K. Lubański, Physica **8**, 597 (1941).

with

$$-c^2d\tau^2=dx^\mu dx_\mu,\quad (x^0=-x_0=ct,\quad x^1=x_1=x_e,\quad x^2=x_2=y_e,\quad x^3=x_3=z_e), \tag{2}$$

$$\left.\begin{aligned}\Lambda&=-mc(-u^\lambda u_\lambda)^{\frac{1}{2}}+p_\lambda dx^\lambda/d\tau\\&\quad-(p_\lambda-[e/c]A_\lambda{}^e)u^\lambda,\\ L_f&=(1/4\pi)(\tfrac{1}{4}F^{\mu\lambda}F_{\mu\lambda}-F^{\mu\lambda}\nabla_\mu A_\lambda),\\ &\text{with}\qquad F_{\mu\lambda}=-F_{\lambda\mu}.\end{aligned}\right\} \tag{3}$$

Here u_λ and p_λ are four-vectors, the meaning of which will be found later. $A_\lambda{}^e$ is the value of the potential four-vector of the (external) electromagnetic field at the point x^μ of the electron.

We introduce three-dimensional notation by $F_{10}=F^{01}=\mathbf{E}_x$, $F_{12}=\mathbf{H}_z$, $A^0=-A_0=\Phi$, $p^0=-p_0=E/c$, etc., while $\mathbf{x}_e$, $\mathbf{p}$, and $\mathbf{A}$ denote the spatial parts of the vectors x^λ, p^λ, and A^λ, respectively. Then, by $d\tau=(1-\dot{\mathbf{x}}_e^2/c^2)^{\frac{1}{2}}dt$, and also putting

$$\mathbf{u}(1-\dot{\mathbf{x}}_e^2/c^2)^{\frac{1}{2}}=\mathbf{v},\quad u^0(1-\dot{\mathbf{x}}_e^2/c^2)^{\frac{1}{2}}=cv_t, \tag{4}$$

one can write (1) in the form $\delta\int\mathfrak{L}dt=0$ with

$$\left.\begin{aligned}\mathfrak{L}&=\Lambda\cdot(d\tau/dt)+\int L_f=-mc^2(v_t{}^2-v^2/c^2)^{\frac{1}{2}}\\&\quad+\mathbf{p}\cdot\dot{\mathbf{x}}_e-E-\mathbf{p}\cdot\mathbf{v}+Ev_t+(e/c)\mathbf{v}\cdot\mathbf{A}^e\\&\quad-ev_t\Phi^e+(1/8\pi)\int\{(\mathbf{H}^2-\mathbf{E}^2)\\&\quad-2(\mathbf{H}\cdot\mathrm{curl}\mathbf{A}+\mathbf{E}\cdot\nabla\Phi+\mathbf{E}\cdot\dot{\mathbf{A}}/c)\}\\&=-mc^2(v_t{}^2-v^2/c^2)^{\frac{1}{2}}+\mathbf{p}\cdot(\dot{\mathbf{x}}_e-\mathbf{v})\\&\quad+E(v_t-1)+(1/4\pi)\int\{\tfrac{1}{2}\mathbf{H}^2\\&\quad-\mathbf{A}\cdot(\mathrm{curl}\mathbf{H}-4\pi\mathbf{i}/c)-\mathbf{E}\cdot\dot{\mathbf{A}}/c-\tfrac{1}{2}\mathbf{E}^2\\&\qquad+\Phi(\mathrm{div}\mathbf{E}-4\pi\rho)\}.\end{aligned}\right\} \tag{5}$$

Here, we put $\rho(\mathbf{x})=ev_t\delta^{(3)}(\mathbf{x}-\mathbf{x}_e)$ and $\mathbf{i}(\mathbf{x})=e\mathbf{v}\delta^{(3)}(\mathbf{x}-\mathbf{x}_e)$.

In this variational principle we shall now consider the variables $\mathbf{p}$, E, $\mathbf{x}_e$, $\mathbf{v}$, v_t, $\mathbf{A}(\mathbf{x})$, $\Phi(\mathbf{x})$, $\mathbf{H}(\mathbf{x})$, and $\mathbf{E}(\mathbf{x})$ as functions of t **to be varied independently** in $\delta\int\mathfrak{L}dt=0$. Thus, we get the following first-order equations:

$$\dot{\mathbf{x}}_e-\mathbf{v}=0;\quad v_t-1=0; \tag{6}$$

$$-dp_x/dt+(e/c)\mathbf{v}\cdot\partial\mathbf{A}^e/\partial x_e-ev_t\partial\Phi^e/\partial x_e=0; \tag{7}$$

$$m\mathbf{v}(v_t{}^2-v^2/c^2)^{-\frac{1}{2}}-\mathbf{p}+(e/c)\mathbf{A}^e=0; \tag{8a}$$

$$-mc^2v_t(v_t{}^2-v^2/c^2)^{-\frac{1}{2}}+E-e\Phi^e=0; \tag{8b}$$

and $(1/4\pi)$ times the equations

$$-\mathrm{curl}\mathbf{H}+\dot{\mathbf{E}}/c+4\pi\mathbf{i}/c=0;\quad \mathrm{div}\mathbf{E}-4\pi\rho=0; \tag{9}$$

$$\mathbf{H}-\mathrm{curl}\mathbf{A}=0\quad\text{and}\quad -(\mathbf{E}+\nabla\Phi+\dot{\mathbf{A}}/c)=0. \tag{10}$$

The first two equations give the meaning of the vector $\mathbf{v}$ and v_t, (thus indirectly the meaning of the four-vector u^λ which obviously is now $dx^\lambda/d\tau$). The third Eq. (7) is the equation of motion for the electron. The next two Eqs. (8a–b) determine $\mathbf{p}$ and E in the usual way as functions of the velocity $\mathbf{v}$ and the potentials Φ and $\mathbf{A}$. The last four equations, (9) and (10), give Maxwell's equations and the expressions of the field strengths in terms of the potentials. The equation of motion of the electron (7) can be written in the more usual form

$$\frac{d}{dt}\left\{\frac{m\mathbf{v}}{(1-v^2/c^2)^{\frac{1}{2}}}\right\}=e\mathbf{E}+\frac{e}{c}[\mathbf{v}\times\mathbf{H}], \tag{11}$$

if use is made of $\mathbf{v}\cdot\partial\mathbf{A}^e/\partial x_e=[\mathbf{v}\times\mathrm{curl}\mathbf{A}^e]_x+\mathbf{v}\cdot\nabla A_x{}^e$, of $dA_x{}^e/dt=\nabla A_x{}^e\cdot d\mathbf{x}_e/dt+\partial A_x{}^e/\partial t$ and of Eqs. (6), (8a), and (10). Thus we see that Maxwell's equations and the usual classical equations of motion for a point charge can be obtained from one "first-order" variational principle.

From the Lagrangian (5) we obtain the Hamiltonian in the usual way. The canonical conjugates of $\mathbf{x}_e$ and of $\mathbf{A}(\mathbf{x})$ are given by

$$\frac{\partial\mathfrak{L}}{\partial\dot{\mathbf{x}}_e}=\mathbf{p}\quad\text{and}\quad\frac{\delta\mathfrak{L}}{\delta\dot{\mathbf{A}}(\mathbf{x})}=-\frac{\mathbf{E}(\mathbf{x})}{4\pi c}, \tag{12}$$

respectively. Hence

$$\mathfrak{H}=\mathbf{p}\cdot\dot{\mathbf{x}}_e-\int(\mathbf{E}\cdot\dot{\mathbf{A}}/4\pi c)-\mathfrak{L}. \tag{13}$$

The derivatives of variables with respect to time drop out automatically, and one obtains

$$\mathfrak{H}=mc^2(v_t{}^2-v^2/c^2)^{\frac{1}{2}}+\mathbf{p}\cdot\mathbf{v}+E(1-v_t)+\mathfrak{W}+(1/4\pi)\int\{\mathbf{A}\cdot\mathrm{curl}\mathbf{H}-\tfrac{1}{2}\mathbf{H}^2+\tfrac{1}{2}\mathbf{E}^2-\Phi\mathrm{div}\mathbf{E}\}, \tag{14a}$$

with

$$\mathfrak{W}=ev_t\Phi(\mathbf{x}_e)-[e/c]\mathbf{A}(\mathbf{x}_e)=e\int\{\Phi v_t-\mathbf{A}\cdot\mathbf{v}/c\}\delta^{(3)}(\mathbf{x}-\mathbf{x}_e). \tag{14b}$$

The canonical equations

$$\frac{dP}{dt}=-\frac{\delta\mathfrak{H}}{\delta Q}\quad(15a)\qquad\text{and}\qquad\frac{dQ}{dt}=\frac{\delta\mathfrak{H}}{\delta P}\quad(15b)$$

are now easily verified as far as their right-hand members have a meaning. That is, for $Q=\mathbf{x}_e$ or $=\mathbf{A}(\mathbf{x})$, and $P=\mathbf{p}$ or $=\{-\mathbf{E}(\mathbf{x})/4\pi c\}$, respectively, both (15a) and (15b) are valid. But, if we take for Q one of the quantities $\mathbf{v}$, v_t, E, $\Phi(\mathbf{x})$, or $\mathbf{H}(\mathbf{x})$, the Eqs. (15b) are obviously meaningless, as the canonical conjugates P of these variables are zero. The Eqs. (15a) remain

valid; they give the so-called "identities"[2]

$$\mathbf{p}=m\mathbf{v}(v_t^2-v^2/c^2)^{-\frac{1}{2}}+[e/c]\mathbf{A}^e,$$
$$E=mc^2v_t(v_t^2-v^2/c^2)^{-\frac{1}{2}}+e\Phi^e,$$
$$v_t=1,\quad \mathrm{div}\mathbf{E}=4\pi\rho,\quad \text{and}\quad \mathbf{H}=\mathrm{curl}\mathbf{A}. \tag{16}$$

They do not contain any differentiation with respect to time and, when the equations of motion (15a–b) are to be integrated say from $t=0$, the initial conditions for the variables have to be such that Eqs. (16) are satisfied at $t=0$.

The Hamiltonian (14) can be simplified by elimination of some of the redundant ("derived") variables that have no canonical conjugate. For instance, by substitution of $v_t\equiv 1$ and $\mathbf{H}\equiv\mathrm{curl}\mathbf{A}$ one gets

$$\begin{aligned}\mathcal{H}=&mc^2(1-v^2/c^2)^{\frac{1}{2}}+\mathbf{p}\cdot\mathbf{v}\\&+(1/8\pi)\int\{\mathbf{E}^2+(\mathrm{curl}\mathbf{A})^2\}\\&-(e/c)\int(\mathbf{A}\cdot\mathbf{v})\delta^{(3)}(\mathbf{x}-\mathbf{x}_e)\\&+\int\Phi\{e\delta^{(3)}(\mathbf{x}-\mathbf{x}_e)-\mathrm{div}\mathbf{E}/4\pi\},\end{aligned} \tag{17}$$

which gives again canonical Eqs. (15a) for $Q=$ one of the variables $\mathbf{x}_e$, $\mathbf{A}(\mathbf{x})$, $\mathbf{v}$ or $\Phi(\mathbf{x})$, while (15b) is valid again for $\mathbf{x}_e$ and $\mathbf{A}(\mathbf{x})$ only. Expression (17) is remarkable for its resemblance to the Hamiltonian of Dirac's relativistic wave-mechanical theory of the electron. There, the Dirac matrix β simply replaces $(1-v^2/c^2)^{\frac{1}{2}}$ in the first term of (17), while $c\boldsymbol{\alpha}$ replaces $\mathbf{v}$ in the other terms. This is in complete accordance with the expectation values, which these Dirac matrices have in a situation in which the electron possesses a definite momentum.

A corresponding simplification can be made in the Lagrangian:

$$\begin{aligned}\mathfrak{L}=&-mc^2(1-v^2/c^2)^{\frac{1}{2}}+\mathbf{p}\cdot(\dot{\mathbf{x}}_e-\mathbf{v})\\&+e\int\{(\mathbf{A}\cdot\mathbf{v}/c)-\Phi\}\delta^{(3)}(\mathbf{x}-\mathbf{x}_e)\\&-(1/4\pi)\int\{\tfrac{1}{2}(\mathrm{curl}\mathbf{A})^2+\mathbf{E}\cdot\dot{\mathbf{A}}/c\\&\qquad+\tfrac{1}{2}\mathbf{E}^2+\mathbf{E}\cdot\nabla\Phi\},\end{aligned} \tag{18}$$

where E, v_t and $\mathbf{H}(\mathbf{x})$ have been eliminated, so that only $\mathbf{x}_e$, $\mathbf{p}$, $\mathbf{v}$, $\mathbf{A}(\mathbf{x})$, $\mathbf{E}(\mathbf{x})$, and $\Phi(\mathbf{x})$ are to be varied independently. Equations (6)–(10) following from (18) can obviously be made relativistically covariant by adding to them the missing Eqs. (6b), (8b), and (10a) as definitions for v_t, E, and $\mathbf{H}(\mathbf{x})$. The expression (18) may have the advantage of being simpler than (5), but, on the other hand, this Lagrangian (18) cannot be written in a covariant form as (5) was in Eqs. (1)–(3), without re-introducing the quantities eliminated.

Further elimination of redundant variables would call for substitution of

$$\mathbf{v}\equiv\frac{c\mathbf{p}-e\mathbf{A}^e}{(m^2c^2+(\mathbf{p}-[e/c]\mathbf{A}^e)^2)^{\frac{1}{2}}}.$$

This would make the Hamiltonian a rather complicated expression, and does not lead to any simplification.

Finally, the variable Φ cannot be eliminated in a similar way, as among the identities (16) there is no equation that gives $\Phi(\mathbf{x})$ in terms of the other variables. In quantum electrodynamics, this fact necessitates the introduction of a new variable S, canonically conjugate to Φ. This quantity S has no physical meaning, of course. It is, therefore, usually stated that the "situation functions" χ, that describe situations which can occur in nature, must satisfy the additional condition $S\chi=0$. This, however, makes it impossible to normalize χ in the usual way.[3] It is, therefore, then necessary to revise the definition of the method of normalization of a situation function and of calculation of matrix elements of observables in general. It has been shown that, when this is done, then the condition $S\chi=0$ even becomes superfluous.[3]

[2] The variables $\mathbf{v}$, v_t, E, and $\mathbf{H}(\mathbf{x})$ can be regarded as so-called "derived variables." Compare F. J. Belinfante, Physica **7**, 765 (1940).

[3] F. J. Belinfante, Physica **12**, 17 (1946).

Polarization and Direction of Propagation of Successive Quanta*

DONALD R. HAMILTON
Palmer Physical Laboratory, Princeton University, Princeton, New Jersey
(Received May 28, 1948)

The correlation between the direction of propagation of one quantum and the polarization of another quantum, when the two are emitted successively (in any order) by a radiating system, is investigated theoretically. This direction-polarization correlation is found to be capable of determining the relative parities of all three levels of the radiating system. The correlation is simply related to the already investigated correlation between the directions of propagation of two successive quanta. Results are given explicitly for the possible combinations of dipole and quadrupole radiation. The discussion applies also to certain types of resonance radiation.

I. INTRODUCTION

THE experimental observation[1] of the predicted[2,3] correlation in the directions of propagation of two successive gamma-rays emitted by a radiating nucleus, and the usefulness of this correlation in providing information on gamma-ray multipolarity and on the spins of the relevant nuclear levels, have stimulated interest in further correlations involving the polarizations of two such successive quanta. It has been pointed out by Falkoff[4] that while only the orders of multipolarity of the gamma-quanta enter into the directional correlation, the electric or magnetic nature of the radiating multipole of given order influences the polarization correlation. Falkoff has calculated the polarization correlation for two quanta emitted at an angle of 180° with each other. He finds, in particular, that when the two transitions involve one electric and one magnetic multipole, the correlation differs from that to be expected when both of a given pair of multipoles are electric or both magnetic; the experiment thus determines the relative parity of the initial and final levels of the three levels involved. Along somewhat different lines the present author has treated[5] the case where successive electric dipole quanta are emitted at an arbitrary angle to each other. However, this treatment, which may easily be generalized to arbitrary combinations of magnetic and electric dipoles, was a by-product of a discussion of resonance radiation, and hence specific results are given only for transitions in which the initial and final levels have the same angular momenta.

The present discussion provides the theoretical background for an experiment in which one measures the correlation between the direction of propagation of one quantum and the direction of polarization of another quantum emitted at an angle θ to the first. Just as there is a close relation between resonance radiation and the successive emission of two quanta from a single system, the existence of the correlation under discussion is to be expected by analogy with the polarization of the resonance radiation excited by unpolarized light.

For applications to gamma-radiation, the elimination of one of the polarization-measuring counters is an obvious advantage since polarization-sensitive counters for gamma-radiation[6] involve counting the gamma-quantum after a scattering process. In addition to this saving of one polarization measurement, the present arrangement in many cases allows one to determine enough about the electric or magnetic nature of the two successive transitions to specify the relative parity of all three nuclear levels involved. This is possible in all cases if by some means one may discriminate in favor of detecting coincidences in which the first quantum goes to an arbitrarily chosen, particular one of the counters.

II. THEORY AND CALCULATIONS

It will be noted immediately that since the two successive quanta are not detected in iden-

* This work supported in part by Navy contract N6ori-105, Task I.
[1] E. L. Brady and M. Deutsch, Phys. Rev. **72**, 870 (1947).
[2] D. R. Hamilton, Phys. Rev. **58**, 122 (1940).
[3] G. Goertzel, Phys. Rev. **70**, 897 (1946).
[4] D. L. Falkoff, Phys. Rev. **73**, 518 (1948).
[5] D. R. Hamilton, Astrophys. J., **106**, 457 (1947).
[6] H. S. Snyder, S. Pasternack, and J. Hornbostel, Phys. Rev. **73**, 440 (1948).

tical counters, the experiment under discussion possesses a dissymmetry in comparison to the 180° polarization-polarization correlation experiment of reference 4. One might thus expect the results to depend on whether the first or the second quantum is detected in the polarization-insensitive counter. Such a dependence in fact arises in exactly half the cases considered; this situation can be covered, however, by a simple generalization from the case where the first quantum is assumed to go to the polarization-insensitive counter. Therefore, this assumption will be the basis of discussion until further notice.

The details of the calculations follow very closely reference 2, with which a familiarity is assumed. There the directional correlation of the two quanta is specified in terms of the probability, $W(\theta)$, that the second quantum will come off with a direction of propagation making an angle θ with that of the first quantum. Formally, the direction of propagation of the first quantum is taken as the axis of quantization; $W(\theta)$ is then the angular distribution of the second quantum with respect to this axis, and the discussion is formulated in terms of the transitions between the various magnetic sub-states A_l, B_n, C_p of the initial, intermediate, and final levels (A, B, C) of the radiating system. With the above choice of axis of quantization and with the first quantum unpolarized, the phases of the intermediate states B_n are random; the specific multipoles which radiate the second quantum in the transitions B_nC_p are randomly phased and therefore radiate independently, with an intensity proportional to the (unequal) populations of the states B_n and to the B_nC_p transition probabilities. The details of the radiation of the second quantum from this assemblage of multipoles will now be summarized.

Given the electric or magnetic multipole associated with the line BC, the polarization of the quantum emitted in a given direction in the transition B_nC_p is determined by $\Delta m \equiv p-n$. The polarization is (for dipole and quadrupole and presumably for higher multipoles) elliptical with the principal axes of the ellipse parallel to the unit vectors $\boldsymbol{\theta}_0$ and $\boldsymbol{\phi}_0$ which in turn lie along the directions of increasing θ and φ in the usual spherical coordinate system. With the transitions B_nC_p and $B_{-n}C_{-p}$ there are associated equal transition probabilities, and polarization ellipses identical in shape and orientation but opposite in sense of traversal. Since the multipoles associated with B_nC_p and $B_{-n}C_{-p}$ are randomly phased (for the conditions assumed here, i.e., no knowledge of the polarization of first quantum) these two randomly phased ellipses are equivalent to two randomly phased waves linearly polarized along $\boldsymbol{\theta}_0$ and $\boldsymbol{\phi}_0$. Thus all the information about the polarization of the second quantum may be expressed by stating the intensities J_θ and J_φ in the linear polarizations $\boldsymbol{\theta}_0$ and $\boldsymbol{\phi}_0$.

In a notation analogous to that of reference 2, the relative values of the J_θ and J_φ associated with a given Δm may be denoted by $f_{|\Delta m|\theta}$ and $f_{|\Delta m|\varphi}$ for electric dipole radiation and by $g_{|\Delta m|\theta}$ and $g_{|\Delta m|\varphi}$ for electric quadrupole radiation; similarly, $f_{|\Delta m|} \equiv f_{|\Delta m|\theta} + f_{|\Delta m|\varphi}$ and $g_{|\Delta m|} \equiv g_{|\Delta m|\theta} + g_{|\Delta m|\varphi}$. The dependence of these functions on the angle θ between the axis of quantization and the direction of propagation of the quantum in question is given[7] by

$$
\begin{array}{lll}
f_{1\theta}=\tfrac{1}{2}\cos^2\theta & f_{1\varphi}=\tfrac{1}{2} & f_1=\tfrac{1}{2}(1+\cos^2\theta) \\
f_{0}\theta=1-\cos^2\theta & f_{0\varphi}=0 & f_0=1-\cos^2\theta \\
g_{2\theta}=\tfrac{1}{2}(\cos^2\theta-\cos^4\theta) & g_{2\varphi}=\tfrac{1}{2}(1-\cos^2\theta) & g_2=\tfrac{1}{2}(1-\cos^4\theta) \\
g_{1\theta}=\tfrac{1}{2}(4\cos^4\theta-4\cos^2\theta+1) & g_{1\varphi}=\tfrac{1}{2}\cos^2\theta & g_1=\tfrac{1}{2}(4\cos^4\theta-3\cos^2\theta+1) \\
g_{0\theta}=3(\cos^2\theta-\cos^4\theta) & g_{0\varphi}=0 & g_0=3(\cos^2\theta-\cos^4\theta).
\end{array}
\tag{1}
$$

It will be noted that

$$
2f_{1\theta}+f_{0\theta}=2f_{1\varphi}+f_{0\varphi}=2g_{2\theta}+2g_{1\theta}+g_{0\theta}
$$
$$
=2g_{2\varphi}+2g_{1\varphi}+g_{0\varphi}=2,
$$

corresponding to the fact that if transitions with the various Δm occur with equal intensity, the resulting radiation is isotropic and unpolarized.

[7] E. U. Condon and G. H. Shortley, *Theory of Atomic Spectra* (Cambridge University Press, New York, 1935); for example, Chap. IV.

The analogous equations for magnetic dipole and magnetic quadrupole radiation are obtained from Eq. (1) by interchanging θ and φ where they occur in the subscripts. This corresponds to the fact that the radiation fields of the electric and magnetic multipoles associated with a given Δm differ only by the interchange of E and H; their angular distributions of radiation are identical, their polarizations orthogonal. Thus, for any given line BC with given multipole order one will have $(J_\theta)_{\text{elec}}=(J_\varphi)_{\text{mag}}$ and $(J_\varphi)_{\text{elec}}=(J_\theta)_{\text{mag}}$.

If the relative number of transitions in the various Δm is denoted by $\beta_{|\Delta m|}$ for dipole radiation and by $\gamma_{|\Delta m|}$ for quadrupole radiation, then the total radiated intensity (all polarizations) is given for dipole radiation by

$$W(\theta)=\beta_0 f_0+2\beta_1 f_1, \tag{2}$$

and for quadrupole radiation by

$$W(\theta)=\gamma_0 g_0+2\gamma_1 g_1+2\gamma_2 g_2. \tag{3}$$

In terms of the foregoing β and γ, the J's are given for dipole radiation by

$$(J_\theta)_{\text{elec}}=(J_\varphi)_{\text{mag}}=\beta_0 f_{0\theta}+2\beta_1 f_{1\theta},$$

$$(J_\varphi)_{\text{elec}}=(J_\theta)_{\text{mag}}=\beta_0 f_{0\varphi}+2\beta_1 f_{1\varphi}, \qquad \text{(dipole)} \tag{4}$$

and for quadrupole radiation by

$$(J_\theta)_{\text{elec}}=(J_\varphi)_{\text{mag}}=\gamma_0 g_{0\theta}+2\gamma_1 g_{1\theta}+2\gamma_2 g_{2\theta},$$

$$(J_\varphi)_{\text{elec}}=(J_\theta)_{\text{mag}}=\gamma_0 g_{0\varphi}+2\gamma_1 g_{1\varphi}+2\gamma_2 g_{2\varphi}. \qquad \text{(quadrupole)} \tag{5}$$

The function $W(\theta)$ of Eqs. (2) and (3) is, of course, simply the angular correlation function of reference 2, there expressed as a power series in $\cos^2\theta$:

$$W(\theta)=1+\alpha_2\cos^2\theta+\alpha_4\cos^4\theta. \tag{6}$$

(Here α_2 and α_4 are the quantities R/Q and S/Q of the earlier work.) From Eqs. (1), (2), (3), and (6) the values of the β and γ may be found directly in terms of the α_2 and α_4 which have already been calculated in reference 2. The $W(\theta)$ of Eq. (6) has no particular normalization. However, in the later discussion of the case where the two transitions have different multipole order it is useful to have $W(\theta)$, when expressed in the form of Eqs. (2) or (3), normalized in some way, e.g.,

$$\int W(\theta)d(\text{solid angle})=\int(J_\theta+J_\varphi)d(\text{solid angle})=8\pi.$$

With this condition, the β and γ are found from Eqs. (1), (2), (3), and (6) to be given by

$$(3+\alpha_2)\beta_0=3(1-\alpha_2),$$
$$(3+\alpha_2)\beta_1=3(1+\alpha_2), \tag{7a}$$

$$(15+5\alpha_2+3\alpha_4)\gamma_0=5(3+5\alpha_2+3\alpha_4),$$
$$(15+5\alpha_2+3\alpha_4)\gamma_1=15(1+\alpha_2+\alpha_4), \tag{7b}$$
$$(15+5\alpha_2+3\alpha_4)\gamma_2=15(1-\alpha_2-\alpha_4).$$

From Eqs. (1), (4), (5), and (7) we then find directly for dipole radiation

$$(3+\alpha_2)(J_\theta)_{\text{elec}}=3(1+\alpha_2\cos2\theta),$$
$$(3+\alpha_2)(J_\varphi)_{\text{elec}}=3(1+\alpha_2), \qquad \text{(dipole)} \tag{8a}$$

and for quadrupole radiation

$$(15+5\alpha_2+3\alpha_4)(J_\theta)_{\text{elec}}=15[(1+\alpha_2+\alpha_4)-\tfrac{1}{2}\alpha_4\sin^2 2\theta],$$
$$(15+5\alpha_2+3\alpha_4)(J_\varphi)_{\text{elec}}=15[1+(\alpha_2+\alpha_4)\cos2\theta]. \qquad \text{(quadrupole)} \tag{8b}$$

It will be recalled now that the "dipole" and "quadrupole" labels in Eq. (8) refer to the second quantum only, corresponding to the assumption that the first quantum goes to the polarization-insensitive detector; the properties of this first quantum enter Eq. (8) only through their influence on α_2 and α_4. One might conceivably, although with some difficulty, arrange an experiment to correspond to this assumption; but, in general, one will want to know what happens when each counter is able to detect either the first or the second quantum, but not with the same efficiency. As a necessary preliminary to this more general question it turns out that we must first consider a question complementary to that answered by Eq. (8): What happens when the only observed coincidences are those in which the second quantum goes to the polarization-insensitive detector?

A proposition very relevant to this question concerns the directional correlation function

$W(\theta)$ discussed in reference 2. In that reference it is shown that if two pairs of transitions are each other's inverses—i.e., differ by an interchange of initial and final angular momenta and of first and second radiation processes—then $W(\theta)$ has the same dependence on θ for both pairs of transitions. To state this more formally for purposes of extension, let $W_{ABC}(\kappa_1\mathbf{e}_1\kappa_2\mathbf{e}_2)$ be the probability of emission of a quantum with unit propagation and polarization vectors κ_1 and $\mathbf{e}_1$ in the line AB, followed by a quantum $\kappa_2\mathbf{e}_2$ in the line BC; then a statement from p. 128 of reference 2 may be expressed in the form

$$\sum_{e'e''} W_{ABC}(\kappa'\mathbf{e}'\kappa''\mathbf{e}'') = \sum_{e'e''} W_{CBA}(\kappa''\mathbf{e}''\kappa'\mathbf{e}') = W(\theta),$$

where θ is, of course, the angle between κ' and κ''. Here the state A is alternately the initial and final state, but in both cases has the same angular momentum and is connected to the state B by a radiative transition of the same nature. If the reasoning used in obtaining the above theorem is interrupted short of the above result, one finds that it is also true that

$$W_{ABC}(\kappa'\mathbf{e}'\kappa''\mathbf{e}'') = W_{CBA}(\kappa''\mathbf{e}''\kappa'\mathbf{e}'). \quad (9)$$

Now, the values of J_φ when the first or the second quantum goes along the z-axis to the polarization-insensitive detector are proportional, respectively, to

$$\sum_{e'} W_{ABC}(\mathbf{k}\mathbf{e}'\kappa''\phi_0) \quad \text{and} \quad \sum_{e'} W_{ABC}(\kappa''\phi_0\mathbf{k}\mathbf{e}');$$

and it is apparent from Eq. (9) that

$$\sum_{e'} W_{ABC}(\kappa''\phi_0\mathbf{k}\mathbf{e}') = \sum_{e'} W_{CBA}(\mathbf{k}\mathbf{e}'\kappa''\phi_0). \quad (10)$$

This says, in words, that to find J_φ when the second quantum, instead of the first, goes to the polarization-insensitive detector one finds what J_φ would be if the first quantum of the inverse process $C\rightarrow B\rightarrow A$ were to go to this detector. A similar statement, of course, holds for J_θ.

Let us now return to the more general situation in which neither detector can distinguish completely between the first and second quanta. We may denote by a_{BC} the relative over-all efficiency for detection of the first (AB) quantum in the unpolarized detector and the second (BC) in the polarization-sensitive detector (a_{BC} will thus be simply the product of the individual counter efficiencies for these quanta); and let a_{AB} denote relative over-all efficiency for the converse process (second quantum to unpolarized detector). Similarly, let $J_{\theta BC}$ be the expected value of J_θ when $a_{BC}=1$ and $a_{AB}=0$ (the case to which Eq. (8) corresponds), and $J_{\theta AB}$ the same for $a_{BC}=0$ and $a_{AB}=1$. In the notation of Eq. (10),

$$\begin{aligned} J_{\theta BC} &\sim \sum_{e'} W_{ABC}(\mathbf{k}\mathbf{e}'\kappa''\theta_0), \\ J_{\theta AB} &\sim \sum_{e'} W_{ABC}(\kappa''\theta_0\mathbf{k}\mathbf{e}') \\ &= \sum_{e'} W_{CBA}(\mathbf{k}\mathbf{e}'\kappa''\theta_0) \end{aligned} \quad (11a)$$

If the total relative intensities observed in the θ_0 and ϕ_0 polarizations are I_θ and I_φ, then

$$\begin{aligned} I_\theta &= a_{AB}J_{\theta AB} + a_{BC}J_{\theta BC}, \\ I_\varphi &= a_{AB}J_{\varphi AB} + a_{BC}J_{\varphi BC}. \end{aligned} \quad (11b)$$

A notable simplification may be made when both the transitions AB and BC have the same multipole order. Recalling that the $W(\theta)$ of Eq. (4) is always the same for the sequence ABC and its inverse, CBA, it is apparent that the β and γ of Eqs. (2) and (3) must be the same for ABC and its inverse. If now the transitions AB and BC not only have the same multipole order but also are both electric or both magnetic, the J_θ and J_φ of Eqs. (4) and (5) must be the same for ABC and its inverse, i.e., $J_{\theta AB}=J_{\theta BC}$, $J_{\varphi AB}=J_{\varphi BC}$; and the total I_θ and I_φ are therefore the same as the J_θ and J_φ of Eqs. (4) and (5), no matter which quantum goes to which counter and *entirely independently of counter efficiencies:*

$$\begin{aligned} (I_\theta)_{ED,\,ED} &= (I_\varphi)_{MD,\,MD} = 1+\alpha_2\cos 2\theta, \\ (I_\varphi)_{ED,\,ED} &= (I_\theta)_{MD,\,MD} = 1+\alpha_2, \end{aligned} \quad (12a)$$

$$\begin{aligned} (I_\theta)_{EQ,\,EQ} &= (I_\varphi)_{MQ,\,MQ} \\ &= 1+\alpha_2+\alpha_4-\tfrac{1}{2}\alpha_4\sin^2 2\theta, \end{aligned} \quad (12b)$$

$$(I_\varphi)_{EQ,\,EQ} = (I_\theta)_{MQ,\,MQ} = 1+(\alpha_2+\alpha_4)\cos 2\theta.$$

Here and in Eqs. (13), (14), and (15) the first and second pairs of subscripts indicate, respectively, the multipole nature of the first and second quanta—i.e., ED for electric dipole, etc.

The next convenient category to consider comprises those pairs of transitions for which the multipole orders are different (i.e., one dipole, one quadrupole) and for which one multipole is electric, one magnetic. It is shown in reference 2

that with one dipole and one quadrupole transition there is no $\cos^4\theta$ term in $W(\theta)$—i.e., $\alpha_4=0$. It will be noted that in this case the functions of Eq. (8b) become very similar to those of Eq. (8a). This latter fact has the happy consequence that when the values of I_θ and I_φ are worked out in accordance with Eq. (11b), the relative efficiencies enter I_θ and I_φ only through a multiplicative function of α_2 which is independent of θ and is the same for I_θ and I_φ and hence irrelevant; and we have, *independently of the counter efficiencies*,

$$\begin{aligned}(I_\varphi)_{MD,EQ}&=(I_\varphi)_{EQ,MD}=(I_\theta)_{ED,MQ}\\&=(I_\theta)_{MQ,ED}=1+\alpha_2\cos 2\theta,\\(I_\theta)_{MD,EQ}&=(I_\theta)_{EQ,MD}=(I_\varphi)_{ED,MQ}\\&=(I_\varphi)_{MQ,ED}=1+\alpha_2.\end{aligned}\tag{13}$$

An analogous simplification does not result when Eq. (11b) is applied to pairs of transitions in which one transition is dipole, one quadrupole, but both are magnetic or both electric. In this case we have

$$\begin{aligned}(I_\theta)_{MD,MQ}&=(I_\theta)_{MQ,MD}=(I_\varphi)_{ED,EQ}=(I_\varphi)_{EQ,ED}\\&=a_D(1+\alpha_2)+a_Q(1+\alpha_2\cos 2\theta),\\(I_\varphi)_{MD,MQ}&=(I_\varphi)_{MQ,MD}=(I_\theta)_{ED,EQ}=(I_\theta)_{EQ,ED}\\&=a_D(1+\alpha_2\cos 2\theta)+a_Q(1+\alpha_2).\end{aligned}\tag{14}$$

Here a_D is the earlier a_{AB} or a_{BC}, according as the quantum AB or BC is the dipole quantum; and similarly for a_Q, with Q for "quadrupole."

The only remaining case to be covered is that of both quanta having the same multipole order, with one multipole electric and one magnetic. Here we find

$$\begin{aligned}(I_\theta)_{ED,MD}&=(I_\theta)_{MD,ED}\\&=a_E(1+\alpha_2\cos 2\theta)+a_M(1+\alpha_2),\\(I_\varphi)_{ED,MD}&=(I_\varphi)_{MD,ED}\\&=a_E(1+\alpha_2)+a_M(1+\alpha_2\cos 2\theta),\\(I_\theta)_{EQ,MQ}&=(I_\theta)_{MQ,EQ}\\&=a_E\left(1+\alpha_2+\alpha_4-\frac{\alpha_4}{2}\sin^2 2\theta\right)\\&\quad+a_M[1+(\alpha_2+\alpha_4)\cos 2\theta],\\(I_\varphi)_{EQ,MQ}&=(I_\varphi)_{MQ,EQ}\\&=a_E[1+(\alpha_2+\alpha_4)\cos 2\theta]\\&\quad+a_M[1+\alpha_2+\alpha_4-\tfrac{1}{2}\alpha_4\sin^2 2\theta].\end{aligned}\tag{15}$$

Here a_E is the earlier a_{AB} or a_{BC}, according as the quantum AB or BC is emitted by the electric multipole; the same holds for a_M. It will be observed that when $a_E=a_M$, then for all the pairs of transitions considered in this paragraph $I_\theta=I_\varphi\sim W(\theta)$.

III. DISCUSSION

Equations (12)–(15) cover all the possible sixteen combinations of dipole and quadrupole transitions. These equations simply extend the results on directional correlation[2] to include the effects of observing the polarization of one quantum; hence for all the cases considered it will be noted that $I_\theta+I_\varphi\sim W(\theta)$, independently of the efficiencies a_{AB} and a_{BC}. The most information is extracted from a given experiment by observing I_θ and I_φ as functions of θ; but for exploratory work it may be noted that in every case the ratio I_θ/I_φ has its maximum deviation from unity at $\theta=90°$, and is always unity at 180°.

For the eight cases covered by Eqs. (12) and (13) the relative counter efficiencies are completely irrelevant as far as any effect on the functional form of the results is concerned. Of these eight cases the sequences EQ,EQ and MQ,MQ may be identified individually by their characteristic dependences of I_θ and I_φ on θ; however, the experiment makes no distinction (for a given value of α_2) within the groups (ED,ED; ED,MQ; MQ,ED) and (MD,MD; MD,EQ; EQ,MD). It will, of course, often turn out in such an indeterminate case that knowledge of the spin of the ground state, or some auxiliary data such as lifetimes or internal conversion coefficients, will make a given value of α_2 consistent with only one of the three possibilities. But even if this were not so, it should be noted that within each of these groups the changes in the parity of the nuclear states are identical. We may recall that the parity relations for these various transitions are as follows:

ED: yes,	MD: no,
EQ: no,	MQ: yes,

in which "yes" indicates that the parity of the nuclear state must change in the radiative transition, and analogously for "no." Then for the group (ED,ED; ED,MQ; MQ,ED) (yes, yes) states A and C have the same parity, B a parity

different from A and C. For the group (MD,MD; MD,EQ; EQ,MD) (no, no) states A, B, and C all have the same parity. For many purposes (as, for example, determining certain selection rules in beta-decay) knowledge of these parity relations is more important than being able to make a choice within the group.

In this same connection, it will be noted that for the eight cases covered by Eqs. (14) and (15) the parities of states A and C are different, with state B varying. It will also be noted that the counter efficiencies do enter these latter equations, in contrast to the case just discussed. It will be recalled that the a's occurring in Eqs. (14) and (15) are products of the individual counter efficiencies; if both quanta have the same energy, or if both counters have the same dependence of efficiency on energy, then the a's are equal. In Eqs. (14) and (15), equal a's make $I_\theta = I_\varphi \sim W(\theta)$, affording no differentiation between the eight sequences covered by these equations; thus with equal a's, unless auxiliary evidence is available, one is not able for these eight cases to measure the parity of the intermediate state B relative to states A and C.

Suppose, however, that discrimination exists and that one knows which of the two possible types of coincidence is being discriminated against —e.g., knows that the relative coincidence-counting efficiency is higher when the first quantum goes to the polarization-sensitive counter, which would correspond to $a_{AB} > a_{BC}$. The inequality of the a's means that $I_\theta \neq I_\varphi$. Here, as before, the sequences EQ,MQ and MQ,EQ will have a characteristic dependence on θ which identifies them individually. The other six sequences fall into the two groups (MQ,MD; ED,EQ; ED,MD) and (MD,MQ; EQ,ED; MD,ED) within each of which no further distinction may be made; at $\theta = 90°$ one of these groups will have $(I_\theta/I_\varphi) > 1$, one group $(I_\theta/I_\varphi) < 1$, and which is which depends on which a is greater. Unless one of the a's is zero (a rather unlikely situation) the deviation of I_θ/I_φ from unity will be less (for a given α_2) than is the case for Eqs. (12) and (13). But the most relevant comment about the above two groups of sequences is that all the sequences of the first group correspond to states B and C having different parity from A, while the sequences of the second group have states A and B differing from C in parity.

Assuming the existence of some means for even partial discrimination, the procedure for identification of successive transitions of dipole and quadrupole character may be summarized as follows:

(*i*) A directional correlation experiment distinguishes[2] between the 12 sequences (dipole-dipole and dipole-quadrupole) for which $\alpha_4 = 0$ and the four quadrupole-quadrupole sequences for which $\alpha_4 \neq 0$; it also provides definite values of α_2 and α_4 which are necessary for use in further identification of sequences in what follows.

(*ii*) When neither are the a's equal nor is one of them zero, any one of the four quadrupole-quadrupole sequences may be identified.

(*iii*) The two groups (ED,ED; ED,MQ; MQ,ED) and (MD,MD; MD,EQ; EQ,MD) have, independently of counter efficiencies, (I_θ/I_φ) at $\theta = 90°$ equal to $(1-\alpha_2)/(1+\alpha_2)$ and $(1+\alpha_2)/(1-\alpha_2)$, respectively. To each of these groups corresponds a unique relative parity assignment of states A, B, C.

(*iv*) For the two groups (MQ,MD; ED,EQ; ED,MD) and (MD,MQ; EQ,ED; MD,ED) I_θ/I_φ deviates from unity less than for the previous two groups, this deviation depending on the coincidence-counting efficiency and providing a means of identifying within which of these two groups a sequence falls. To each of these groups corresponds a unique relative parity assignment of the states A, B, C.

The assignment of relative parities of states A, B, and C is thus unique; but no more light is shed on assignments of multipole orders alone than is available from a directional correlation experiment.

The basis of the present discussion actually does not depend on both quanta being emitted quanta; the discussion applies equally well to the polarization and intensity distribution of resonance radiation excited by unidirectional unpolarized or circularly polarized light, or to the angular variation of intensity (but not polariza-

tion) of the resonance radiation excited by linearly polarized light. These cases will correspond to one of the a's being unity, one zero.

Goertzel's discussion[3] of the effect of a magnetic field upon correlation experiments may be extended[3] to the present case. It is found that when no polarization measurements are made, a strong enough magnetic field parallel to the direction of propagation of either quantum should preserve the angular correlation against the perturbing effect of other fields such as those arising from the atomic electrons; a magnetic field in any other direction will to a varying degree wash out the correlation, the effect being complete when a strong enough field is perpendicular to the plane determined by the directions of the two quanta. When, on the other hand, a polarization measurement is made on one quantum, the correlation between this polarization and the direction of propagation of the other quantum is preserved only when the strong magnetic field is parallel to the direction of propagation of the unpolarized quantum. Since this statement holds true no matter whether the unpolarized quantum is the first or second to be emitted, magnetic field effects should not provide a means of discriminating between the first and second quanta.

[3] Private communication from Dr. Goertzel.

PHYSICAL REVIEW VOLUME 74, NUMBER 7 OCTOBER 1, 1948

The Use of Phase Space in Classical and Quantum Theory

H. C. CORBEN
Carnegie Institute of Technology, Pittsburgh, Pennsylvania
(Received March 22, 1948)

It is suggested that the symmetry between position and momentum space in classical and quantum mechanics may be extended by closer consideration of the concept of phase space. The discussion is limited to the kinematics of a single particle in phase space, to which is associated a metric which describes both the gravitational and the electromagnetic fields acting on the particle. The formulation is applicable only to a charged particle, and implies that for such a particle in an electromagnetic field the Poisson bracket of two position coördinates does not vanish in general, so that in quantum theory these coordinates do not commute. A fundamental constant is introduced as the ratio of the natural and Gaussian units of electromagnetic field strengths and, expressing this constant in terms of $\hbar$ and a length l, the theory satisfies a correspondence principle with present theory in the limit $l\rightarrow 0$. By postulating that $l\sim 10^{-13}$ cm, one is led to the basis of a theory which is indistinguishable from present theory for field strengths small compared with $(137)^{\frac{1}{2}}el^{-2}$, but which leads to essential modifications for the interaction of charged particles separated by distances of the order of nuclear dimensions.

I. CLASSICAL FORMULATION

SOME of the difficulties of present quantum theory appear to arise in the process of quantization, while others trace their origin to the classical theory. Therefore, attempts have been made to modify classical theory, but, unfortunately, such modifications suffer from the defect that they are not gauge invariant,[1] or not unique,[2] or difficult to quantize,[3] or possess some other disadvantage. Dirac's theory of the electron represents a close approximation to the truth, provided that the wave-lengths involved are large compared with $l\sim r_e=e^2/mc^2$. The possibility it admits of extremely large, even infinite energies and frequencies is clearly incorrect. In fact, it has been suggested by Bethe and Oppenheimer[4] that a new constant exists of the dimensions of a frequency, so that for frequencies below

[1] For example, G. Mie, Ann. d. Physik **37**, 511 (1912); **39**, 1 (1912); **40**, 1 (1913).
[2] M. Born and L. Infeld, Proc. Roy. Soc. **A144**, 425 (1934).
[3] J. A. Wheeler and R. P. Feynman, Rev. Mod. Phys. **17**, 157 (1945).
[4] H. Bethe and J. R. Oppenheimer, Phys. Rev. **70**, 451 (1946).

this limit present theory is valid, while for higher frequencies the theory must become essentially modified.

It is likely that many of the known difficulties of the theories of atomic and nuclear phenomena are related and that a number of them may be resolved at once in the light of some new general principle of physics. With the theory of elementary particles beset with so many difficulties at the present time, it is perhaps of interest to re-examine classical theory in the light of these difficulties in search of such a principle.

In this paper we examine a generalization of classical theory based on the remarkably symmetrical roles played by momentum and position coordinates in fundamental physical theory. This symmetry was first demonstrated in non-relativistic theory by Hamilton's equations and the theory of contact transformations, and relativity theory has extended it to include a symmetry between energy and time. In statistical mechanics the use of phase space in representing ensembles is widely known, and in quantum theory this symmetry has been emphasized in the uncertainty relations, in the expression for the wave function describing a plane wave, and in the use of Fourier transforms to connect the p- and x-representations. In quantum mechanics, too, the state of a system is of fundamental significance; corresponding to this we have, in classical theory, the representation of a system by a point in phase space.

Indeed, an attempt has been made by Born[5] to extend the symmetry between position and momentum by a principle of reciprocity and the application of the concepts of general relativity theory to momentum space. In this way it is possible to introduce a closed momentum space, with corresponding finite values for the self-energy of the electron, etc.

In this paper we consider the possibility that this symmetry may be pushed even further by examining the classical general relativistic motion of the representative point of a particle in eight-dimensional phase space. It has been pointed out[6] that the equations of classical non-relativistic dynamics assume a particularly simple form if expressed in terms of coordinates in phase space, $Q_\alpha=(q_k, p_k)(k=1\cdots n, \alpha=1\cdots 2n)$. Introducing $P_\alpha=(p_k, -q_k)$, it follows that all of the canonical equations may be written thus: $\dot{Q}_\alpha=\partial H/\partial P_\alpha$. We proceed to generalize this by defining contravariant and covariant coordinates in eight-dimensional phase space for a particle, thus:

$$\begin{aligned} Q^\alpha&=(X^k, a^{-1}P^k), \quad \alpha=1\cdots 8,\\ Q_\alpha&=(X_k, a^{-1}P_k), \quad k=1\cdots 4, \end{aligned} \tag{1.1}$$

where the X's and P's denote position and momentum coordinates associated with the particle, and a is a constant, of dimensions MT^{-1}, which may be characteristic of the particle. The introduction of a is analogous to the introduction of c in extending the formalism of non-relativistic dynamics to relativity theory.

We later identify a with the charge of the particle expressed in certain units which appear naturally (Eq. (2.21)), so that the formalism applies only to a charged particle. We then assume that the state of a particle in classical mechanics may be represented by a point in an eight-dimensional space, where the first four coordinates refer to its position and the time at which it is observed, and the second four, in appropriate units, denote the ratio of its four-momentum to its charge.

We postulate that phase space is characterized by a symmetrical metric $G_{\alpha\beta}=G_{\beta\alpha}$, so that

$$dQ_\alpha=G_{\alpha\beta}dQ^\beta; \quad dQ^\alpha=G^{\alpha\beta}dQ_\beta, \tag{1.2}$$

where

$$G_{\alpha\gamma}G^{\beta\gamma}=\delta_\alpha{}^\beta=G_\alpha{}^\beta. \tag{1.3}$$

The $G_{\alpha\beta}$ may, of course, be functions of all eight coordinates, i.e., of position and time and of momentum and energy. Throughout this paper suffixes α, β, etc., assume the values $1\cdots 8$; suffixes k, l, etc., go from 1 to 4.

We now define an eight-vector P_α which may be called the momentum eight-vector

$$\begin{aligned} P^\alpha&=(P^k, -aX^k),\\ P_\alpha&=(P_k, -aX_k), \end{aligned} \tag{1.4}$$

so that the P_α are essentially the Q_α arranged in different order:

$$P_\alpha=\pm aQ_{\alpha\pm 4},$$

the top signs to be taken for $\alpha\leqslant 4$, the bottom

[5] M. Born, Proc. Roy. Soc. **A165**, 291 (1938).
[6] H. C. Corben, Phys. Rev. **73**, 1270 (1948).

for $\alpha>4$. The negative sign has been introduced into the definitions (1.4) of P_α, because the nature of the reciprocity between position X^k and momentum P_k is analogous to that between position and time in relativity theory; cf. the form of the canonical equations or the representation of P_k by $-ih(\partial/\partial X^k)$ in wave mechanics, but the representation of X^k by $ih(\partial/\partial P_k)$ when the P_k are diagonal.

Thus, although the Q_α specify only the ratio of momenta to charge, the P_α specify the momenta and the electric moment of the particle about the origin. Two coincident particles, one with double the charge of the other but also with double the four-momentum, would be represented by the same set of values for Q_α; the P_α for the first would, however, be double that of the second. Thus between them the P_α, Q_α specify uniquely the position, time, energy, momentum, and charge of the particle.

We postulate that the differentials of P_α, P^α are related as in Eq. (1.2); i.e.,

$$dP_\alpha=G_{\alpha\beta}dP^\beta;\quad dP^\alpha=G^{\alpha\beta}dP_\beta. \tag{1.5}$$

Thus

$$dP_\alpha dQ^\alpha=-dQ_\alpha dP^\alpha=0.$$

We write

$$G_{\alpha\beta}=\begin{pmatrix} g_{kl}, & f_{kl} \\ h_{kl}, & k_{kl}\end{pmatrix}, \tag{1.6}$$

where f, g, h, k are four (4×4) matrices. Equations (1.2), (1.5) then become

$$\left.\begin{aligned} dX_k&=g_{kl}dX^l+a^{-1}f_{kl}dP^l\\ dP_k&=ah_{kl}dX^l+k_{kl}dP^l\\ dP_k&=g_{kl}dP^l-af_{kl}dX^l\\ dX_k&=-a^{-1}h_{kl}dP^l+k_{kl}dX^l\end{aligned}\right\}, \tag{1.5'}$$

from which it follows that $h_{kl}=-f_{kl}$, $k_{kl}=g_{kl}$.

If it be postulated that the metric is symmetric, it then follows that $f_{kl}=-f_{lk}$; $g_{kl}=g_{lk}$ and

$$G_{\alpha\beta}=\begin{pmatrix} g_{kl} & f_{kl} \\ -f_{kl} & g_{kl}\end{pmatrix}. \tag{1.6'}$$

We shall identify g_{kl}, f_{kl}, respectively, with the gravitational potentials and electromagnetic field strengths, but remember that in addition to being functions of position they may also depend on momentum and energy. More exactly, we write f_{kl} as proportional to the field strengths F_{kl} (Eq. (2.20)), the constant of proportionality ϵ, thereby relating the usual unit of field strength with the natural unit. In this way there appears in the theory a fundamental constant which may be written by Eq. (2.22) in terms of Planck's constant, and a length l which we postulate is of the order of nuclear dimensions.

The dependence of the g_{kl}, f_{kl} on momentum and energy as well as position and time means that, for example, the infinitesimal change in potential energy of a particle moving in a field depends not only on the change in position of the particle but also on the corresponding change of momentum. This latter dependence is important only when the rate of change of momentum of the particle along its path is extremely high ($\sim(137)^{\frac{1}{2}}e^2l^{-2}$ for an electron) so that the modifications which the theory offers to present theories are important only for the interaction of particles separated by distances of order l. For such small distances we show that the electromagnetic interactions possess quite a different character, being then represented by non-integrable complex potentials.

We may define

$$G^{\alpha\beta}=\begin{pmatrix} g^{kl}, & -f^{kl} \\ f^{kl}, & g^{kl}\end{pmatrix}; \tag{1.7}$$

i.e.,

$$\begin{aligned} G_{k,\,l+4}&=f_{kl}, & G_{kl}&=g_{kl}=G_{k+4,\,l+4},\\ G^{k,\,l+4}&=-f^{kl}, & G^{kl}&=g^{kl}=G^{k+4,\,l+4},\end{aligned}$$

so that, from (1.3)

$$\left.\begin{aligned} g_{km}g^{ml}+f_{km}f^{ml}&=\delta_k{}^l\\ f_{km}g^{ml}&=g_{km}f^{ml}\end{aligned}\right\}. \tag{1.3'}$$

The second of these equations is an identity in general relativity theory; the first implies that in the presence of an electromagnetic field the g_{kl}, g^{kl} may not assume exactly their special relativistic values ±1. In the next section, however, it appears that the extra term $f_{km}f^{ml}$ should be negligible except for fields of the order of those on the surface of the classical electron.

Introducing the reciprocal tensor to g_{kl}, and dropping suffixes and denoting contravariant tensors by a dagger, we have

$$g^\dagger=g^{-1}(1-ff^\dagger)$$

and

$$f^\dagger=g^{-1}fg^\dagger. \tag{1.3''}$$

If a dot denotes differentiation with respect to a parameter which labels the path of a particle, we may rewrite Eqs. (1–5′) thus:

$$\left.\begin{aligned}\dot{X}_k &= g_{kl}\dot{X}^l + a^{-1}f_{kl}\dot{P}^l \\ \dot{P}_k &= g_{kl}\dot{P}^l - af_{kl}\dot{X}^l\end{aligned}\right\}. \tag{1.8}$$

These equations represent the rules for raising and lowering suffixes. In the absence of an f field they clearly reduce to the usual rules. In general, it is not permissible to raise and lower suffixes without reversing the sign of the f terms, since these appear in $G^{\alpha\beta}$ and $G_{\alpha\beta}$ with reversed signs. Thus Eqs. (1.8) may be written

$$\begin{aligned}\dot{X}^k &= g^{kl}\dot{X}_l - a^{-1}f^{kl}\dot{P}_l, \\ \dot{P}^l &= g^{kl}\dot{P}_l + af^{kl}\dot{X}_l.\end{aligned} \tag{1.8′}$$

The invariant interval in phase space is

$$\begin{aligned}d\tau^2 &= dQ_\alpha dQ^\alpha = a^{-2}dP_\alpha dP^\alpha, \\ &= dX_k dX^k + a^{-2}dP_k dP^k, \\ &= g_{kl}(dX^k dX^l + a^{-2}dP^k dP^l) \\ &\qquad + 2a^{-1}f_{kl}dX^k dP^l.\end{aligned} \tag{1.9}$$

We shall denote differentiation with respect to τ by a dot.

II. POISSON BRACKET RELATIONS

In this paper it is our purpose merely to examine the underlying structure of any theory based on phase space, so that we do not limit ourselves here to the choice of a particular Lagrangian or Hamiltonian. We may, however, establish a few general results involving Poisson brackets. If H be an 8-invariant Hamiltonian function of the P_α, we may write *all* of the canonical equations in the form

$$\dot{Q}^\alpha = \partial H/\partial P_\alpha, \tag{2.1}$$

since, from the definitions (1.1) and (1.4), these may be written

$$\dot{X}^k = \partial H/\partial P_k; \quad \dot{P}^k = -\partial H/\partial X_k. \tag{2.1′}$$

Alternatively, all of the canonical equations are contained in

$$\dot{P}^\alpha = -\partial H/\partial Q_\alpha. \tag{2.1″}$$

We may define the Poisson bracket of two dynamical variables A, B thus:

$$\begin{aligned}(A, B) &= (\partial A/\partial Q^\alpha)(\partial B/\partial P_\alpha) \\ &= -(\partial A/\partial P^\alpha)(\partial B/\partial Q_\alpha) \\ &= (\partial A/\partial X^k)(\partial B/\partial P_k) \\ &\qquad - (\partial A/\partial P^k)(\partial B/\partial X_k),\end{aligned} \tag{2.2}$$

although, in general, this is not a tensor relation unless the A, B are 8-invariants. We have, however, the special case

$$(Q^\alpha, P_\beta) = \delta_\beta{}^\alpha, \tag{2.3}$$

which summarizes all of the Poisson bracket relations in the form

$$\begin{aligned}(X^k, X_l) &= 0, \\ (P^k, P_l) &= 0, \\ (X^k, P_l) &= \delta_l{}^k.\end{aligned} \tag{2.3′}$$

Further,

$$(A, H) = (\partial A/\partial Q^\alpha)\dot{Q}^\alpha = \dot{A}. \tag{2.4}$$

However, the P. B. of two covariant coordinates or momenta is given by

$$(Q_\alpha, P_\beta) = \partial Q_\alpha/\partial Q^\beta \tag{2.5}$$

from (2.2). Since the relations between the covariant and the contravariant coordinates are defined only in terms of their differentials by non-integrable relations of the form (1.2), we may regard the Q_α, for instance, as quasicoordinates[7] and define the right-hand side of (2.5) as the partial derivative of the invariant time derivatives

$$\partial Q_\alpha/\partial Q^\beta \equiv \partial\dot{Q}_\alpha/\partial\dot{Q}^\beta = G_{\alpha\beta}. \tag{2.6}$$

Then also

$$\partial P_\alpha/\partial P^\beta = G_{\alpha\beta},$$

and

$$\left.\begin{aligned}(Q_\alpha, P_\beta) &= G_{\alpha\beta} = -(P_\beta, Q_\alpha) \\ (Q^\alpha, P^\beta) &= G^{\alpha\beta} = -(P^\beta, Q^\alpha)\end{aligned}\right\}. \tag{2.7}$$

I.e.,

$$\left.\begin{aligned}(X^k, P^l) &= g^{kl} \\ (P^k, P^l) &= af^{kl} \\ (X^k, X^l) &= a^{-1}f^{kl}\end{aligned}\right\}. \tag{2.7′}$$

In the absence of any field these relations reduce to the usual ones, but they suggest that in the corresponding quantum theory the X^k, P^l would be operators, the non-commutation of which would be associated with the values of the local gravitational and electromagnetic fields. The Lagrange bracket of Q^α, P^β then becomes $[Q^\alpha, P^\beta] = G_{\alpha\beta}$.

We shall be continually writing expressions of the form $\partial Q_\alpha/\partial Q^\beta$, and it is important to remember that they are to be interpreted, in general, by the first part of Eq. (2.6).

[7] Cf. L. Boltzmann, Wien. Sitz. 111, 1603 (1902); E. T. Whittaker, *Analytical Dynamics* (Dover Publications, New York, 1944), p. 41.

The first of Eqs. (2.7′) is the familiar generalization to general relativity theory of the P. B. relation between position and momentum. In quantum theory it becomes

$$X^kP^l-P^lX^k=i\hbar g^{kl}.$$

The symmetry of g^{kl} then implies that

$$L^{kl}=X^kP^l-X^lP^k=P^lX^k-P^kX^l,$$

so that the order of the P^k and X^l is immaterial in the definition of the orbital angular momentum operator.

The second of Eqs. (2.7′) is closely analogous to the P. B. relation between two velocities in classical electromagnetic theory,

$$m^2(v^k, v^l)=(e/c)F^{kl},$$

and suggests that the P^k are to be identified with the *kinetic* momenta of the particle. In the corresponding quantum theory the P^k do not commute among themselves. The third of Eqs. (2.7′) is, however, entirely unfamiliar. It suggests a complementarity between position observations in the presence of an f field, and implies that in the corresponding quantum theory the X^k do not commute with each other.

The reason for the limited applicability of phase space to quantum mechanics is, of course, that since the X^k, P^l do not commute, phase space has strictly no meaning. In the above theory this situation is aggravated by the fact that not only do the X^k, P^l fail to commute with each other, they do not commute among themselves. It would seem, then, impossible to formulate a quantum theory which satisfied P. B. relations of the form (2.7′).

This difficulty may be partially overcome by introducing the complex variables

$$x^\alpha=Q^\alpha+ia^{-1}P^\alpha, \tag{2.8}$$

as in the theory of the harmonic oscillator, so that as $x^{k+4}=-ix^k$, the x^α consist of only four distinct complex variables. Then, from (2.7′)

$$(x^\alpha, x^\beta)=0, \tag{2.9}$$

so that the x^k commute among themselves. One may similarly define

$$x_k=X_k+ia^{-1}P_k, \tag{2.8′}$$

so that, from Eqs. (1.8), (1.8′),

$$dx_k=dx^lh_{lk},$$
$$dx^k=dx^l\bar{h}^{lk}=h^{kl}dx_l, \tag{2.10}$$

where

$$h_{kl}=g_{kl}+if_{kl}, \tag{2.11}$$

and the bar denotes conjugate complex

$$\bar{h}^{kl}=g^{kl}-if^{kl}=h^{lk}.$$

Thus

$$h_{km}\bar{h}^{ml}=h_{km}h^{lm}=\delta_k{}^l, \tag{2.12}$$

which is an alternative method of writing Eqs. (1.3), (1.3′). Thus h_{kl} is Hermitian and $\bar{h}_{kl}$ is obtained from it either by changing the sign of i or by interchanging rows and columns. The invariant interval in x^k space is

$$d\tau^2=dx_kd\bar{x}^k=dx^lh_{lk}d\bar{x}^k$$
$$=dX_kdX^k+a^{-2}dP_kdP^k, \tag{2.13}$$

which is identical with the interval (1.9) in the phase space Q^α. The complex metric h_{kl} is identical with that introduced by Einstein in his recent generalization of general relativity theory.[8] Here, however, the coordinates are also complex, the real part of x^k being the position coordinates X^k, the imaginary part of x^k being proportional to the kinetic momenta of the particle. It is clear that the interval $d\tau^2$ reduces to the interval

$$ds^2=dX_kdX^k$$

for

$$(dP_k/ds)(dP^k/ds)\ll a^2.$$

We have, from (2.6),

$$\partial x_l/\partial x^k\equiv\partial\dot{x}_l/\partial\dot{x}^k=h_{kl}, \tag{2.14}$$

which is the complex metric of the x^k space. Hence

$$(\partial x_l/\partial x^k)-(\partial x_k/\partial x^l)=2if_{kl}, \tag{2.15}$$

so that

$$(\partial f_{kl}/\partial x^m)+(\partial f_{lm}/\partial x^k)+(\partial f_{mk}/\partial x^l)=0. \tag{2.16}$$

We may introduce complex momenta conjugate to the x^k:

$$p_k=\tfrac{1}{2}(P_k+iaX_k)=\tfrac{1}{2}ia\bar{x}_k, \tag{2.17}$$

the P. B. of any two of which is also zero. Then

$$\dot{p}_k=-\partial H/\partial x^k;\quad \dot{x}_k=\partial H/\partial p^k,$$

[8] A. Einstein, Ann. Math. **46**, 578 (1945); A. Einstein and E. G. Straus, Ann. Math. **47**, 731 (1946). Cf. also E. Schrödinger, Proc. Roy. Irish Acad. **51A**, 41 (1946); H. C. Corben, Phys. Rev. **72**, 156 (1947).

and, if $p^k=\frac{1}{2}ia\bar{x}^k$,

$$(x^k, p^l)=h^{kl}. \tag{2.18}$$

Thus

$$\left.\begin{aligned} P_k&=p_k-\tfrac{1}{2}iax_k \\ X_k&=\tfrac{1}{2}x_k-ia^{-1}p_k \end{aligned}\right\}. \tag{2.19}$$

It is convenient to introduce a fundamental constant ϵ which relates the f_{kl} expressed in natural units to the electromagnetic field strengths F_{kl} expressed in Gaussian units:

$$f_{kl}=\epsilon F_{kl}. \tag{2.20}$$

Then, assuming that the constant a is proportional to the charge of the particle, we may write

$$a=e/\epsilon c. \tag{2.21}$$

We may express ϵ in terms of a length l, and from considerations of dimensions it is clear that we may write

$$\epsilon=l^2/(\hbar c)^{\frac{1}{2}}. \tag{2.22}$$

We now assume quite arbitrarily that l is a length of order 10^{-13} cm. We shall further write

$$x_k=-2i\epsilon A_k. \tag{2.23}$$

Substitution of these results into the above equations yields:

I
$$\dot{P}_k=g_{kl}\dot{P}^l-(e/c)F_{kl}\dot{X}^l, \tag{1.8}$$
$$(P^k, P^l)=(e/c)F^{kl}, \tag{2.7'}$$
$$F_{kl}=(\partial A_k/\partial x^l)-(\partial A_l/\partial x^k), \tag{2.15}$$
$$P_k=p_k-(e/c)A_k, \tag{2.19}$$
$$(A_k, A_l)=(p_k, p_l)=0, \tag{2.9}$$
$$(p_k, A_l)-(p_l, A_k)=F_{kl}; \tag{2.24}$$

II
$$g_{km}g^{ml}+(l^4/\hbar c)F_{km}F^{ml}=\delta_k{}^l, \tag{1.3'}$$
$$\dot{X}_k=g_{kl}\dot{X}^l+(l^4/\hbar e)F_{kl}\dot{P}^l, \tag{1.8}$$
$$d\tau^2=dX_kdX^k+(cl^4/\hbar e^2)dP_kdP^k, \tag{1.9}$$
$$(X^k, X^l)=(l^4/e\hbar)F^{kl}, \tag{2.7'}$$
$$x^k=X^k+i\frac{l^2}{e}\left(\frac{c}{\hbar}\right)^{\frac{1}{2}}P^k, \tag{2.8'}$$
$$dx_k=\left(g_{kl}-\frac{il^2}{(\hbar c)^{\frac{1}{2}}}F_{kl}\right)dx^l; \tag{2.10}$$

III
$$(p_k, A_l)+(p_l, A_k)=-i\frac{(\hbar c)^{\frac{1}{2}}}{l^2}g_{kl}. \tag{2.25}$$

III. DISCUSSION OF RESULTS AND APPLICATION TO QUANTUM THEORY

In group I of the equations given above the length l does not appear. Apart from the first of this group, these equations are formally very familiar. However, it is to be remembered that in general the covariant coordinates P_k, A_k, p_k are non-integrable. They are approximately integrable, however, for $g_{kl}=\pm\delta_{kl}$, $|f_{kl}|\ll 1$, i.e., in the absence of gravitational fields and for

$$|F_{kl}|\ll\epsilon^{-1}=(\hbar c)^{\frac{1}{2}}/l^2. \tag{3.1}$$

For $l\sim 10^{-13}$ cm this condition is satisfied for all fields except those within nuclear distances of an elementary charged particle. In the presence of fields weak compared with (3.1) the correspondence between the equations of group I and familiar equations of electromagnetic theory is therefore direct. When condition (3.1) is violated, however, the correspondence is purely formal and the consequences of the theory quite different in character from those of present electrodynamics.

The first of the equations of group I may be written

$$\dot{P}_k=\partial L/\partial X^k=g_{kl}\dot{P}^l-(e/c)F_{kl}\dot{X}^l.$$

If the dependence of the Lagrangian on X^k may be neglected, this becomes the Lorentz force equation.

As an example of the stringency of condition (3.1) we may consider an electron moving in a circle of radius r about a proton. The condition becomes then, approximately, $r\gg l/(137)^{\frac{1}{2}}$ and is therefore satisfied for atomic electrons.

The equations of group II contain l explicitly, and in the limit $l\to 0$ each of them transforms into a familiar equation of general relativity theory. The interval $d\tau$ in phase space then becomes identical with the interval ds in coordinate space and the real non-commuting X^k become, in this limit, indistinguishable from the complex commuting x^k of the more general theory. A theory formulated in terms of phase space in this manner thus satisfies a correspondence principle with relativity theory in that it reduces to the latter in the limit $l\to 0$. The equations of group III, however, exhibit a singularity as $l\to 0$. This

arises from the complex nature of the p_k and has no obvious counterpart in present theory.

The Poisson bracket relation (2.7′) implies that in the corresponding quantum theory the coordinates X^k are represented by operators which do not commute:

$$X^kX^l-X^lX^k=i(l^4/e)F^{kl}. \tag{3.2}$$

It then follows that it is impossible to measure simultaneously two position coordinates of a charged particle in an electromagnetic field. The predicted effect is extremely small, and even for fields which approach the value (3.1)

$$\Delta X^k\Delta X^l\sim(137)^{\frac{1}{2}}l^2, \tag{3.3}$$

i.e., the product of the errors is of the order of nuclear cross sections. The relation between this theory and that of finite electron theories is then analogous to the relation between quantum mechanics and the early interpretation of Schrödinger's equation. In each case we have on the one hand a picture of a continuous charge distribution and, on the other, an interpretation in terms of a probability distribution of a point particle, the probability arising from the natural limits imposed on our ability to measure, in the case of quantum mechanics, position and momentum and, in the present instance, two position coordinates, simultaneously.

One may picture the effect for a magnetic field

$$\Delta X\Delta Y\sim(l^4/e)H_z,$$

etc., by imagining at each point a small area l^4He^{-1} being drawn in a plane at right angles to the magnetic field H at that point. Then, according to the above it is impossible to measure where a particle of charge e is within this area. The area is proportional to the magnetic field strength at the point and is characteristic also of the observed particle. Suppose that through each such area is drawn e^{-1} "reciprocal flux lines" characteristic of a particle of charge e. The number of reciprocal flux lines per cm^2 drawn at right angles to H is then $(l^4H)^{-1}$, so that the product of the number of flux lines and the number of reciprocal flux lines crossing an area l^2 drawn perpendicular to H is always unity.

We note that a volume h^4 of position and momentum space corresponds to a volume

$$(h/a)^4=(2\pi(\hbar c)^{\frac{1}{2}}l^2e^{-1})^4$$

of Q^α space. For an elementary particle this is a volume l_0^8, where

$$l_0^2=2\pi(137)^{\frac{1}{2}}l^2=73.54l^2.$$

Then (3.3) becomes

$$\Delta X^k\Delta X^l\sim(l_0^2/2\pi), \tag{3.3′}$$

for field strengths of order hc/el_0^2.

PHYSICAL REVIEW VOLUME 74, NUMBER 7 OCTOBER 1, 1948

Contribution to the Theory of the Cherenkov Effect

GUIDO BECK
Córdoba Observatory, Córdoba, Argentina
(Received March 9, 1948)

The rigorous solution is given for the field of a uniformly moving point charge which, coming from vacuum, enters at $t=0$ through a plane surface into an ideal, macroscopic, homogeneous dielectric medium ($\epsilon=$const.). The solution represents a characteristic transition radiation, as the velocity of motion approaches $c/(\epsilon)^{\frac{1}{2}}$ and furnishes information about the formation of the characteristic cone if $v>c/(\epsilon)^{\frac{1}{2}}$.

1. INTRODUCTION

THE radiation discovered by Cherenkov[1] and studied in more detail by other investigators[2] represents, according to Frank and Tamm,[3] a natural consequence of relativistic electrodynamics, analogous to phenomena known in acoustics in the case of projectiles moving with velocities higher than the velocity of sound. A very brilliant and detailed study, covering all aspects of the phenomenon, has been afterwards published by Tamm, resulting from discussions on the subject with L. Mandelstamm.[4] The present paper differs from Tamm's treatment both by its method and by its aim. While Tamm admits *a priori* the existence of the Cherenkov radiation, solving a problem with boundary conditions (outgoing waves), the purpose of this paper is to show that the problem can be reduced to one with given initial conditions (electron moving uniformly in vacuum) and leads subsequently, indeed, to radiation emission, i.e., to the solution admitted by Tamm, implying retarded potentials only.

The model adopted here, represents a point charge moving with uniform velocity, coming from infinity and entering at $t=0$ a semi-infinite ideal classical dielectric. A model of this type has the advantage of permitting rigorous solutions of Maxwell's equations for given initial conditions: a point charge moving in vacuum at $t=-\infty$ at infinite distance from the dielectric and leading at $t=+\infty$ to the quasistationary field of the point charge in the dielectric.

From the physical point of view, this model is subject to several restrictions, the most important of which are the macroscopic treatment of field and dielectric and the neglection of dispersion, $\epsilon=\epsilon(\nu)$. Both restrictions limit the validity of the obtained expressions, the first one to wave-lengths greater than the thickness of the surface film (here represented simply by a discontinuous jump of ϵ) the second one to spectral regions in which ϵ is sensibly constant. Information on the influence of dispersion is, however, available from Tamm's quoted paper and from an important paper of Fermi[5] who, considering the passage of charged particles through condensed dielectrics, obtained formulae which take into account dispersion and apply also to the phenomenon observed by Cherenkov.

2. THE STATIONARY SOLUTIONS

Since our problem is, essentially, a nonstationary one, its solution will necessarily contain a radiation field. Because of the fact that we can consider here uniformly moving charges, we can, however, separate from it a stationary part of the solution, which shall be considered first.

Assuming that our point charge moves along the z-axis, our solution depends only on the coordinates $\rho=(x^2+y^2)^{\frac{1}{2}}$ and z. We suppose that the charge moves in vacuum, $\epsilon=1$, for $z<0$, $t<0$, with constant velocity v. For $z>0$, $t>0$, our charge moves in a dielectric medium, $\epsilon>1$. We have to distinguish between the solution

[1] P. A. Cherenkov, C. R. Acad. Sci. U.S.S.R. **8**, 451 (1934).
[2] G. B. Collins and B. G. Reiling, Phys. Rev. **54**, 499 (1938); H. O. Wyckoff and J. E. Henderson, Phys. Rev. **64**, 1 (1943).
[3] I. Frank and Ig. Tamm, C. R. Acad. Sci. U.S.S.R., **14**, 109 (1937).
[4] Ig. Tamm, J. Phys. U.S.S.R., **1**, 439 (1939). The author desires to thank the Editorial Board of the Physical Review for having indicated to him this paper, which was not accessible to him during the present work and which, unfortunately, was not refered to in the accessible literature.
[5] E. Fermi, Phys. Rev. **57**, 485 (1940).

outside, $\Phi^{(0)}$, $z<0$, and *inside*, $\Phi^{(i)}$, $z>0$, the medium, both solutions satisfying the boundary conditions for $z=0$,

$$E_\rho^{(0)}=E_\rho^{(i)};\quad D_z^{(0)}=D_z^{(i)}. \tag{1}$$

The solution Φ is determined by the static potential φ and the vector potential $A=A_z$, by means of which we express

$$\begin{aligned} &E_\rho=-\partial\varphi/\partial\rho;\quad D_\rho=\epsilon E_\rho\\ &E_z=-\partial\varphi/\partial z-(1/c)(\partial A/\partial t);\quad D_z=\epsilon E_z\\ &H_\varphi=-\partial A/\partial\rho;\quad B_\varphi=H_\varphi \end{aligned} \tag{2}$$

and satisfies the Lorentz condition

$$\partial A/\partial z+(\epsilon/c)(\partial\varphi/\partial t)=0. \tag{3}$$

The fact that the field of a point charge at rest, in front of the plane surface of a dielectric medium, can be represented by the superposition of the fields of several (real and virtual) point charges (electrical images), suggests that a similar superposition may be possible if we have to deal with uniformly moving point charges. We find, indeed, that Φ_1 and Φ_2 are solutions of our problem, with

$\Phi_1^{(0)}$:

$$\begin{aligned} \varphi^{(0)}&=e\left\{\frac{1}{[(1-v^2/c^2)\rho^2+(z-vt)^2]^{\frac{1}{2}}}-\frac{\epsilon-[1+(\epsilon-1)v^2/c^2]^{\frac{1}{2}}}{\epsilon+[1+(\epsilon-1)v^2/c^2]^{\frac{1}{2}}}\frac{1}{[(1-v^2/c^2)\rho^2+(z+vt)^2]^{\frac{1}{2}}}\right\},\\ A^{(0)}&=\frac{v}{c}e\left\{\frac{1}{[(1-v^2/c^2)\rho^2+(z-vt)^2]^{\frac{1}{2}}}+\frac{\epsilon-[1+(\epsilon-1)v^2/c^2]^{\frac{1}{2}}}{\epsilon+[1+(\epsilon-1)v^2/c^2]^{\frac{1}{2}}}\frac{1}{[(1-v^2/c^2)\rho^2+(z+vt)^2]^{\frac{1}{2}}}\right\}. \end{aligned} \tag{4}$$

$\Phi_1^{(i)}$:

$$\begin{aligned} \varphi^{(i)}&=\frac{2e[1+(\epsilon-1)v^2/c^2]^{\frac{1}{2}}}{\epsilon+[1+(\epsilon-1)v^2/c^2]^{\frac{1}{2}}}\frac{1}{[(1-v^2/c^2)\rho^2+\{z[1+(\epsilon-1)v^2/c^2]^{\frac{1}{2}}-vt\}^2]^{\frac{1}{2}}},\\ A^{(i)}&=\frac{2\epsilon ev/c}{\epsilon+[1+(\epsilon-1)v^2/c^2]^{\frac{1}{2}}}\frac{1}{[(1-v^2/c^2)\rho^2+\{z[1+(\epsilon-1)v^2/c^2]^{\frac{1}{2}}-vt\}^2]^{\frac{1}{2}}}, \end{aligned} \tag{5}$$

$\Phi_2^{(0)}$:

$$\begin{aligned} \varphi^{(0)}&=\frac{2e[1-(\epsilon-1)v^2/c^2]^{\frac{1}{2}}}{\epsilon[1-(\epsilon-1)v^2/c^2]^{\frac{1}{2}}+1}\frac{1}{[(1-\epsilon v^2/c^2)\rho^2+\{z[1-(\epsilon-1)v^2/c^2]^{\frac{1}{2}}-vt\}^2]^{\frac{1}{2}}},\\ A^{(0)}&=\frac{2ev/c}{\epsilon[1-(\epsilon-1)v^2/c^2]^{\frac{1}{2}}+1}\frac{1}{[(1-\epsilon v^2/c^2)\rho^2+\{z[1-(\epsilon-1)v^2/c^2]^{\frac{1}{2}}-vt\}^2]^{\frac{1}{2}}}. \end{aligned} \tag{6}$$

$\Phi_2^{(i)}$:

$$\begin{aligned} \varphi^{(i)}&=\frac{e}{\epsilon}\left\{\frac{1}{[(1-\epsilon v^2/c^2)\rho^2+(z-vt)^2]^{\frac{1}{2}}}+\frac{\epsilon[1-(\epsilon-1)v^2/c^2]^{\frac{1}{2}}-1}{\epsilon[1-(\epsilon-1)v^2/c^2]^{\frac{1}{2}}+1}\frac{1}{[(1-\epsilon v^2/c^2)\rho^2+(z+vt)^2]^{\frac{1}{2}}}\right\},\\ A^{(i)}&=\frac{v}{c}e\left\{\frac{1}{[(1-\epsilon v^2/c^2)\rho^2+(z-vt)^2]^{\frac{1}{2}}}-\frac{\epsilon[1-(\epsilon-1)v^2/c^2]^{\frac{1}{2}}-1}{\epsilon[1-(\epsilon-1)v^2/c^2]^{\frac{1}{2}}+1}\frac{1}{[(1-\epsilon v^2/c^2)\rho^2+(z+vt)^2]^{\frac{1}{2}}}\right\}. \end{aligned} \tag{7}$$

Φ_1 represents the stationary solution, while our point charge moves outside the dielectric medium, $t\leqslant 0$. It refers to one real charge e of velocity v and to two virtual charges

$$\begin{aligned} e'&=-e\frac{\epsilon-[1-(\epsilon-1)v^2/c^2]^{\frac{1}{2}}}{\epsilon+[1+(\epsilon-1)v^2/c^2]^{\frac{1}{2}}},\\ e''&=\frac{2\epsilon e}{\epsilon+[1+(\epsilon-1)v^2/c^2]^{\frac{1}{2}}},\\ v'&=-v,\\ v''&=\frac{v}{[1+(\epsilon-1)v^2/c^2]^{\frac{1}{2}}}\leqslant\frac{c}{(\epsilon)^{\frac{1}{2}}}. \end{aligned} \tag{8}$$

Φ_2 represents the stationary solution, while our point charge moves inside the dielectric medium, $t>0$. It refers to one real charge e of velocity v and to two virtual charges

$$\begin{aligned} e'&=e\frac{\epsilon[1-(\epsilon-1)v^2/c^2]^{\frac{1}{2}}-1}{\epsilon[1-(\epsilon-1)v^2/c^2]^{\frac{1}{2}}+1},\\ e''&=\frac{2e}{\epsilon[1-(\epsilon-1)v^2/c^2]^{\frac{1}{2}}+1},\\ v'&=-v,\\ v''&=\frac{v}{[1-(\epsilon-1)v^2/c^2]^{\frac{1}{2}}}. \end{aligned} \tag{9}$$

It is remarkable, that in (9) the velocity v'' becomes greater than the velocity of light c, as soon as $v>c/(\epsilon)^{\frac{1}{2}}$.

Equations (8) and (9) show that while our point charge penetrates into the medium, a rearrangement of the corresponding virtual charges takes place. This rearrangement of virtual charges gives rise to the transition radiation which becomes emitted during the considered process.

Φ_1 represents at $t=-\infty$, $z=-\infty$ a point charge e moving in vacuum with velocity v. It corresponds, therefore, to the correct initial conditions which we have to postulate. The influence of the virtual charges with increasing t accounts for the influence of the dielectric medium. We can, therefore, consider Φ_1 to be the correct solution for $t\leqslant 0$.

Φ_2 is not the correct solution for $t>0$, since, for $t=0$, it does not fit continuously with Φ_1. In order to assure continuity with time, we have to add to Φ_2 a radiation field, Φ_3, which is determined by the condition that for $t=0$ be

$$\Phi_3(0)=\Phi_1(0)-\Phi_2(0). \tag{10}$$

Satisfying the condition (10), we obtain the complete solution of our problem in the form

$$\begin{aligned}&\Phi(t)=\Phi_1(t) \text{ for } t\leqslant 0,\\ &\Phi(t)=\Phi_2(t)+\Phi_3(t) \text{ for } t\geqslant 0.\end{aligned} \tag{11}$$

3. THE RADIATION FIELD

The solution of our problem requires the determination of the radiation field Φ_3, from the condition (10). We shall proceed by representing Φ_3 by a Fourier series, determining its Fourier coefficients at $t=0$ by (10). The required solution is then obtained by summing up the Fourier series at any subsequent moment t. It is a necessary condition for (10), representing a radiation field, that the right-hand side field in (10) must not contain any real charges. It can be readily shown that this condition is satisfied.

Since the radiation field Φ_3 propagates in the dielectric medium with velocity $c/(\epsilon)^{\frac{1}{2}}$, we have to distinguish two cases:

(a) If $v<c/(\epsilon)^{\frac{1}{2}}$, the radiation field emitted in the moment $t=0$, when the charge enters the dielectric medium, will travel faster than the charge. After a sufficiently long time, the radiation field will be situated at a large distance from the charge and the field in the neighborhood of the charge will be sensibly the stationary field Φ_2. In this case, the influence of the surface of the dielectric medium leads mainly to the emission of a transition radiation, while the charge enters the medium.

(b) If $v>c/(\epsilon)^{\frac{1}{2}}$, the charge travels faster than the radiation field. This leads to the formation of the characteristic cone, already known from the elementary theory. The field is, then, given at any moment t and at any distance from the surface by $\Phi_2+\Phi_3$ and no separation into stationary and radiation part takes place.

Given the axial symmetry of our problem, we choose for the Fourier expansion an orthogonal system of cylindrical waves. Only waves not depending on the angle φ need to be taken into account. The following three sets of cylindrical waves satisfy the required conditions:

(a):

$$\begin{aligned}
E_\rho^{(0)}&=k_\rho J_1(k_\rho\rho)\cos k_z z\cdot e^{-ik_0ct},\\
E_\rho^{(i)}&=k_\rho J_1(k_\rho\rho)\cos \bar{k}_z z\cdot e^{-ik_0ct},\\
E_z^{(0)}&=-(k_\rho^2/k_z)J_0(k_\rho\rho)\sin k_z z\cdot e^{-ik_0ct},\\
E_z^{(i)}&=-(k_\rho^2/\bar{k}_z)J_0(k_\rho\rho)\sin \bar{k}_z z\cdot e^{-ik_0ct},\\
H_\varphi^{(0)}&=i(k_0k_\rho/k_z)J_1(k_\rho\rho)\sin k_z z\cdot e^{-ik_0ct},\\
H_\varphi^{(i)}&=i\epsilon(k_0k_\rho/\bar{k}_z)J_1(k_\rho\rho)\sin \bar{k}_z z\cdot e^{-ik_0ct},\\
N_a&=\left[\frac{1}{\epsilon\pi}\frac{k_z}{\epsilon k_z+\bar{k}_z}\right]^{\frac{1}{2}}\frac{\bar{k}_z}{k_0k_\rho}.
\end{aligned} \tag{12}$$

(b):

$$\begin{aligned}
E_\rho^{(0)}&=k_\rho J_1(k_\rho\rho)\sin k_z z\cdot e^{-ik_0ct},\\
E_\rho^{(i)}&=(k_\rho k_z/\epsilon k_z)J_1(k_\rho\rho)\sin \bar{k}_z z\cdot e^{-ik_0ct},\\
E_z^{(0)}&=(k_\rho^2/k_z)J_0(k_\rho\rho)\cos k_z z\cdot e^{-ik_0ct},\\
E_z^{(i)}&=(k_\rho^2/\epsilon k_z)J_0(k_\rho\rho)\cos \bar{k}_z z\cdot e^{-ik_0ct},\\
H_\varphi^{(0)}&=-i(k_0k_\rho/k_z)J_1(k_\rho\rho)\cos k_z z\cdot e^{-ik_0ct},\\
H_\varphi^{(i)}&=-i(k_0k_\rho/k_z)J_1(k_\rho\rho)\cos \bar{k}_z z\cdot e^{-ik_0ct},\\
N_b&=\left[\frac{1}{\pi}\frac{\bar{k}_z}{\epsilon k_z+\bar{k}_z}\right]^{\frac{1}{2}}\frac{k_z}{k_0k_\rho}.
\end{aligned} \tag{13}$$

(c):

$$
\begin{aligned}
E_\rho^{(0)} &= \pm k_\rho J_1(k_\rho\rho)\cdot e^{ikz}\cdot e^{-ik_0ct},\\
E_\rho^{(i)} &= \frac{[\epsilon^2\kappa^2+\bar{k}_z^2]^{\frac{1}{2}}}{\epsilon\kappa}k_\rho J_1(k_\rho\rho)\\
&\qquad\times\cos(\bar{k}_z z+\bar{\delta})\cdot e^{-ik_0ct},\\
E_z^{(0)} &= -(k_\rho^2/\kappa)J_0(k_\rho\rho)\cdot e^{ikz}\cdot e^{-ik_0ct},\\
E_z^{(i)} &= -\frac{[\epsilon^2\kappa^2+\bar{k}_z^2]^{\frac{1}{2}}}{\epsilon\kappa}\frac{k_\rho^2}{\bar{k}_z}J_0(k_\rho\rho)\\
&\qquad\times\sin(\bar{k}_z z+\bar{\delta})\cdot e^{-ik_0ct},\\
H_\varphi^{(0)} &= i(k_0k_\rho/\kappa)J_1(k_\rho\rho)\cdot e^{ikz}\cdot e^{-ik_0ct},\\
H_\varphi^{(i)} &= i\frac{[\epsilon^2\kappa^2+\bar{k}_z^2]^{\frac{1}{2}}}{\kappa}\frac{k_0k_\rho}{\bar{k}_z}J_1(k_\rho\rho)\\
&\qquad\times\sin(\bar{k}_z z+\bar{\delta})\cdot e^{-ik_0ct},\\
\operatorname{tg}\bar{\delta} &= \bar{k}_z/\epsilon\kappa,\quad N_z=\left[\frac{1}{\pi}\frac{\bar{k}_z^2}{\epsilon^2\kappa^2+\bar{k}_z^2}\right]^{\frac{1}{2}}\frac{\kappa}{k_0k_\rho}.
\end{aligned}
\tag{14}
$$

J_0 and J_1 denote Bessel functions of zero and first order. (k_ρ, k_z) and $(k_\rho, \bar{k}_z)$ are, respectively, the components of the wave vector in vacuum and in the dielectric medium,

$$
\begin{aligned}
&k_\rho^2+k_z^2=k_\rho^2-\kappa^2=k_0^2,\quad k_\rho^2+\bar{k}_z^2=\epsilon k_0^2,\\
&k_z^2=(1/\epsilon)\{\bar{k}_z^2-(\epsilon-1)\cdot k_\rho^2\}\ \text{for}\ k_\rho/\bar{k}_z\leqslant 1/(\epsilon-1)^{\frac{1}{2}},\\
&\kappa^2=(1/\epsilon)\{(\epsilon-1)\cdot k_\rho^2-\bar{k}_z^2\}\ \text{for}\ k_\rho/\bar{k}_z\geqslant 1/(\epsilon-1)^{\frac{1}{2}}.
\end{aligned}
$$

The solutions (c), (14), refer to totally reflected waves in the medium.

The normalization factors N are chosen in order to satisfy the normalization

$$
\int(\mathbf{E}_k^*\cdot\mathbf{D}_{k'}+\mathbf{H}_k^*\cdot\mathbf{B}_{k'})\cdot d\tau'=\delta_{kk'};\qquad d\tau'=\rho d\rho dz. \tag{15}
$$

If we want each wave to represent one photon,

$$
1/8\pi\int(\mathbf{E}_k^*\cdot\mathbf{D}_k+\mathbf{H}_k^*\cdot\mathbf{B}_k)\cdot d\tau'=(hc/2\pi)k_0, \tag{16}
$$

we have to renormalize (12), (13) and (14) by a factor $[4hck_0]^{\frac{1}{2}}$.

In order to determine the Fourier coefficients for each of the three sets of cylindrical waves, a_k, b_k, c_k, we have to form for $t=0$, according to (10), the difference of the vector components D_ρ, D_z and B_φ corresponding to the two stationary solutions (4), (5) and (6), (7), to multiply them by the corresponding conjugate complex components of (12), (13) and (14) at $t=0$ and to integrate over

$$
\int d\tau'=\int_0^\infty\rho d\rho\int_{-\infty}^{+\infty}dz.
$$

The computation of these somewhat long expressions, which shall not be reproduced in detail, does not present major difficulties until it leads to integrals which, by means of elementary transformations can be reduced to

$$
\begin{aligned}
&\int_0^\infty\int_0^\infty\frac{J_0(\eta)\cos\zeta}{(\alpha^2\eta^2+\zeta^2)^{\frac{1}{2}}}\eta d\eta d\zeta\\
&\quad=\int_0^\infty\int_{-\infty}^0\frac{J_0(\eta)\cos\zeta}{(\alpha^2\eta^2+\zeta^2)^{\frac{1}{2}}}\eta d\eta d\zeta=\frac{2}{\alpha^2+1},\\
&\int_0^\infty\int_0^\infty\frac{J_0(\eta)\sin\zeta}{(\alpha^2\eta^2+\zeta^2)^{\frac{1}{2}}}\eta d\eta d\zeta\\
&\quad=-\int_0^\infty\int_{-\infty}^0\frac{J_0(\eta)\sin\zeta}{(\alpha^2\eta^2+\zeta^2)^{\frac{1}{2}}}\eta d\eta d\zeta=\frac{\alpha}{\alpha^2+1},\\
&\int_0^\infty\int_{-\infty}^0\frac{J_0(\eta)e^{i\zeta}}{(\alpha^2\eta^2+\zeta^2)^{\frac{1}{2}}}\eta d\eta d\zeta=\frac{\alpha-2}{\alpha^2-1},
\end{aligned}
\tag{17}
$$

$$
\begin{aligned}
&\int_0^\infty\int_0^\infty\frac{J_0(\eta)\cos\zeta}{[-\alpha^2\eta^2+\zeta^2]^{\frac{1}{2}}}\eta d\eta d\zeta\\
&\quad=\int_0^\infty\int_{-\infty}^0\frac{J_0(\eta)\cos\zeta}{[-\alpha^2\eta^2+\zeta^2]^{\frac{1}{2}}}\eta d\eta d\zeta\\
&\quad=\frac{2}{1-\alpha^2}-i\pi\delta(1-\alpha)+i\pi\delta(1+\alpha),\\
&\int_0^\infty\int_0^\infty\frac{J_0(\eta)\sin\zeta}{[-\alpha^2\eta^2+\zeta^2]^{\frac{1}{2}}}\eta d\eta d\zeta\\
&\quad=-\int_0^\infty\int_{-\infty}^0\frac{J_0(\eta)\sin\zeta}{[-\alpha^2\eta^2+\zeta^2]^{\frac{1}{2}}}\eta d\eta d\zeta\\
&\quad=\frac{i\alpha}{1-\alpha^2}+\pi\delta(1-\alpha)-\pi\delta(1+\alpha),\\
&\int_0^\infty\int_{-\infty}^0\frac{J_0(\eta)e^{i\zeta}}{[-\alpha^2\eta^2+\zeta^2]^{\frac{1}{2}}}\eta d\eta d\zeta=\frac{2-i\alpha}{1+\alpha^2}.
\end{aligned}
\tag{18}
$$

TABLE I.

$$\frac{1}{N_a}a_\kappa = 2\epsilon e\frac{v^2}{c^2}\left\{\frac{2k_\rho^2}{k_\rho^2\{1+(\epsilon-1)v^2/c^2\}+\bar{k}_z^2(1-v^2/c^2)}-\frac{2k_\rho^2}{k_\rho^2+\bar{k}_z^2(1-\epsilon v^2/c^2)}\right.$$
$$\left.+i\pi[\delta(1-[\epsilon(v^2/c^2)-1]^{\frac{1}{2}}\bar{k}_z/k_\rho)-\delta(1+[\epsilon(v^2/c^2)-1]^{\frac{1}{2}}\bar{k}_z/k_\rho)]\right\}$$

$$\frac{1}{N_b}b_\kappa = 2ie\frac{v}{c}\frac{k_0}{\bar{k}_z}\left\{\frac{2\epsilon k_\rho^2}{k_\rho^2\{1+(\epsilon-1)v^2/c^2\}+\bar{k}_z^2(1-v^2/c^2)}-\frac{2k_\rho^2}{k_\rho^2+\bar{k}_z^2(1-\epsilon v^2/c^2)}\right.$$
$$\left.+i\pi[\delta(1-[\epsilon(v^2/c^2)-1]^{\frac{1}{2}}\bar{k}_z/k_\rho)-\delta(1+[\epsilon(v^2/c^2)-1]^{\frac{1}{2}}\bar{k}_z/k_\rho)]\right\}$$

$$\frac{1}{N_c}c_\kappa = -4ie\frac{v}{c}\frac{k_0}{\kappa}\left\{\frac{\epsilon k_\rho^2}{k_\rho^2\{1+(\epsilon-1)v^2/c^2\}+\bar{k}_z^2(1-v^2/c^2)}-\frac{k_\rho^2}{k_\rho^2+\bar{k}_z^2(1-\epsilon v^2/c^2)}\right\}$$
$$+4\epsilon e\frac{v^2}{c^2}\left\{\frac{k_\rho^2}{k_\rho^2\{1+(\epsilon-1)v^2/c^2\}+\bar{k}_z^2(1-v^2/c^2)}-\frac{k_\rho^2}{k_\rho^2+\bar{k}_z^2(1-\epsilon v^2/c^2)}\right\}$$

Fourier coefficients in the case $v>c/(\epsilon)^{\frac{1}{2}}$, $1-(\epsilon-1)(v^2/c^2)>0$.
In the case $v<c/(\epsilon)^{\frac{1}{2}}$ we have to put, for real k_ρ and $\bar{k}_z$, $\delta(1\pm i[1-\epsilon(v^2/c^2)]^{\frac{1}{2}}(\bar{k}_z/k_\rho))=0$.
All square roots denote positive, real or imaginary, values.

Dirac's symbolic function δ has, in (18), a well determined sense. It stands for

$$2\pi\delta(1-\alpha) = -i\cdot\lim_{R\to\infty} e^{i(1-\alpha)R}/1-\alpha; \quad Jm(\alpha)\gtrless 0.$$

The evaluation of the integrals (17) and (18) cannot be performed by elementary means and represents the main difficulty for the solution of our problem. The values given above, have been obtained by using properties of Poisson integrals in the complex plane. Since the mathematical method involved does not present a major interest for the physical problem we have to deal with, it shall be treated in a separate paper.[6]

In the case $v<c/(\epsilon)^{\frac{1}{2}}$ only integrals of the type (17) occur. Integrals of the type (18) appear if $v>c/(\epsilon)^{\frac{1}{2}}$. We have, therefore, to deal with the Fourier coefficients in both cases separately.

Using the values of the integrals (17) and (18) we obtain the Fourier coefficients given in Table I.

4. THE TRANSITION RADIATION

In order to obtain the radiation field, we have to multiply each set of normalized cylindrical waves (12), (13), and (14) with the corresponding Fourier coefficient from Table I and to sum up the resulting series (Fourier integrals). The result of the summation cannot, however, be expressed in closed form. It can be shown, however, that we obtain, in general, a field of finite extension, propagating with velocity c in vacuum and $c/(\epsilon)^{\frac{1}{2}}$ in the dielectric medium. The fact, that the radiation field vanishes at finite distance from the surface after infinite time flows from the time dependence of (12), (13) and (14). Indeed, if t is sufficiently large, the mentioned time factor oscillates with k_0 more rapidly than the other terms, provided that ρ and z are finite, and makes, therefore, the Fourier integrals tend to zero. The initial field distribution, given by (10) shows, that the radiation field comes from the neighborhood of the coordinate origin, i.e., of the point where our charge enters the dielectric medium. The weak transition radiation could, therefore, become observable under favorable conditions, if we focus a lens on this point.

In the case of small velocities, the transition radiation is, according to Table I, insignificant. It increases, however, as soon as v approaches the critical value $c/(\epsilon)^{\frac{1}{2}}$. The main contribution, in this case, comes from the Fourier coefficients a_κ and b_κ in Table I, from the terms which contain the denominator $\{k_\rho^2+\bar{k}_z^2(1-\epsilon v^2/c^2)\}$. The number of photons emitted, due to these terms, is given by

$$dn \cong \frac{2(\epsilon)^{\frac{1}{2}}}{\pi^2}\frac{2\pi e^2}{hc}\frac{v^2}{c^2}\frac{\sin^3\Theta d\Theta}{\{1-\epsilon(v^2/c^2)\cos^2\Theta\}^2}\frac{d\lambda}{\lambda}. \quad (19)$$

The transition radiation has, according to (19), a strong maximum in the forward direction at

$$\Theta = \left[\frac{6}{5}\left(1-\epsilon\frac{v^2}{c^2}\right)\right]^{\frac{1}{2}}.$$

The transition radiation (19) corresponds to the radiation due to the acceleration of an elec-

[6] Mathematicæ Notæ. VII, 191, (1948).

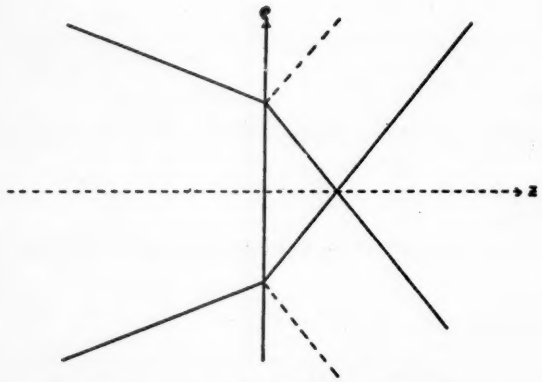

FIG. 1. The characteristic cone of the stationary solution.

tron moving in an infinite medium during a finite time, which has been determined by Tamm in his quoted paper.[7] Because of its different origin, at the surface of the medium, it differs from it both in intensity and in angular dependence, but it is of the same order of magnitude. Integrating over the angle, Tamm gives (in our notations) for the emitted energy the expression

$$dW=\frac{1}{\pi^2}\frac{2\pi e^2}{hc}\frac{1}{\epsilon(v/c)}\times\left\{\ln\frac{1+(\epsilon)^{\frac{1}{2}}(v/c)}{1-(\epsilon)^{\frac{1}{2}}(v/c)}-2(\epsilon)^{\frac{1}{2}}(v/c)\right\}h d\nu$$

while (19) leads to

$$dW=h\nu dn\rightarrow\frac{1}{\pi^2}\frac{2\pi e^2}{hc}\left\{\tfrac{1}{2}(1+\epsilon(v^2/c^2)\times\ln\frac{1+(\epsilon)^{\frac{1}{2}}(v/c)}{1-(\epsilon)^{\frac{1}{2}}(v/c)}-(\epsilon)^{\frac{1}{2}}(v/c)\right\}h d\nu.$$

Because of the logarithmic dependence on $(\epsilon)^{\frac{1}{2}}v/c$, dW increases very slowly while we approach the critical velocity $v\rightarrow c/(\epsilon)^{\frac{1}{2}}$ and amounts to the order of about one visible photon per hundred incident electrons.

As we shall see in the next paragraph, the Fourier terms taken into consideration contribute in the case $v>c/(\epsilon)^{\frac{1}{2}}$ to the formation of the characteristic cone, i.e., to a field propagation in one well-determined direction Θ. They do, then, no longer contribute to the transition radiation, though the remaining terms assure that even in this case the transition radiation does not disappear completely and becomes again important, if the velocity approaches c.

We conclude that the transition radiation shows a marked maximum in the forward direction for velocities slightly below the critical value of $c/(\epsilon)^{\frac{1}{2}}$ and weakens considerably, as soon as v exceeds the critical value.

5. THE CHERENKOV EFFECT

The case $v>c/(\epsilon)^{\frac{1}{2}}$ is characterized by the fact, that our solutions Φ_2 and Φ_3 show singularities of the field on the surface of a cone, which is given by:

Inside the medium:

$$\frac{\rho}{z}=\operatorname{tg}\vartheta^{(i)}=\frac{1}{(\epsilon(v^2/c^2)-1)^{\frac{1}{2}}};$$

$$\frac{k_\rho}{k_z}=\operatorname{tg}\Theta^{(i)}=(\epsilon(v^2/c^2)-1)^{\frac{1}{2}}, \qquad (20)$$

$$\sin\vartheta^{(i)}=\cos\Theta^{(i)}=\frac{c}{(\epsilon)^{\frac{1}{2}}v}.$$

Outside the medium:

$$\frac{\rho}{z}=\operatorname{tg}\vartheta^{(0)}=\left(\frac{1-(\epsilon-1)(v^2/c^2)}{\epsilon(v^2/c^2)-1}\right)^{\frac{1}{2}};$$

$$\frac{k_\rho}{k_z}=\operatorname{tg}\Theta^{(0)}=\left(\frac{\epsilon(v^2/c^2)-1}{1-(\epsilon-1)(v^2/c^2)}\right)^{\frac{1}{2}}, \qquad (21)$$

$$\sin\vartheta^{(0)}=\cos\Theta^{(0)}=(c/v)(1-(\epsilon-1)(v^2/c^2))^{\frac{1}{2}}.$$

ϑ denotes the angle of the singular cone, Θ the direction of its normal in which the singular cone propagates with, respectively, the velocity $c/(\epsilon)^{\frac{1}{2}}$ (inside) and c (outside).

(21) represents the refracted cone of (20), due to the change of refraction index at the surface from $(\epsilon)^{\frac{1}{2}}$ to 1. In the case

$$\epsilon>2;\quad 1-(\epsilon-1)\cdot\frac{v^2}{c^2}<0 \qquad (22)$$

the cone (20) becomes totally reflected at the surface of the medium and no characteristic cone appears outside.

The characteristic singular cone of the stationary solution (6), (7) is given by Fig. 1. It will

[7] See reference (4), p. 453, Eq. (7.10).

be advantageous in the following discussion to distinguish between the advanced and the retarded part of the cone. Frank and Tamm have shown that the advanced part of the cone corresponds to the advanced potentials in Maxwell's theory while the retarded part is given by retarded potentials. Our stationary solution is, therefore, of the well known type

$$\Phi_2=\tfrac{1}{2}\cdot(\Phi_{\text{ret}}+\Phi_{\text{adv}}).$$

In the domain outside the cone, the field becomes imaginary.

In order to study the radiation field $\Phi_3(t)$ we shall restrict our attention to the case

$$1-(\epsilon-1)(v^2/c^2)>0$$

i.e., to the case in which the Cherenkov radiation does not become totally reflected inside the medium. It will be sufficient to take into account the main terms of Table I, which are the same as the ones discussed in Section 4 plus the δ-functions. The remaining terms represent a supplementary transition radiation, which is of insignificant intensity, unless v approaches c.

The main terms of Table I lead to the following expression for the vector potential of the radiation field:

$$A_3^{(i)}=-\frac{2}{\pi}\frac{e(v/c)}{[\epsilon(v^2/c^2)-1]^{\frac{1}{2}}}\int_0^\infty J_0(k_\rho\rho)dk_\rho \times\int_{[(1-\epsilon)(\epsilon(v^2/c^2)-1)]^{\frac{1}{2}}}^\infty\left\{\frac{2}{1-\alpha^2}-i\pi\delta(1-\alpha)\right\} \times\left\{\frac{\epsilon(k_z/\bar{k}_z)}{\epsilon(k_z/\bar{k}_z)+1}\frac{v\bar{k}_z}{ck_0}\sin\bar{k}_z{}^2z +\frac{1}{\epsilon(k_z/\bar{k}_z)+1}\cos\bar{k}_zz\right\}e^{-ik_0ct}d\alpha +\text{small terms}, \quad (23)$$

with $\alpha=[\epsilon(v^2/c^2)-1]^{\frac{1}{2}}(\bar{k}_z/k_\rho)$.

$$A_3^{(i)}\cong\frac{ie(v/c)}{\rho[\epsilon(v^2/c^2)-1]^{\frac{1}{2}}}\int_0^\infty J_0(\eta)\left\{\left[\exp i\eta\frac{z-vt}{\rho[\epsilon(v^2/c^2)-1]^{\frac{1}{2}}}\right]\right. +\left.\frac{\epsilon[1-(\epsilon-1)(v^2/c^2)]^{\frac{1}{2}}-1}{\epsilon[1-(\epsilon-1)(v^2/c^2)]^{\frac{1}{2}}+1}\left[\exp-i\eta\frac{z+vt}{\rho[\epsilon(v^2/c^2)-1]^{\frac{1}{2}}}\right]\right\}d\eta,$$

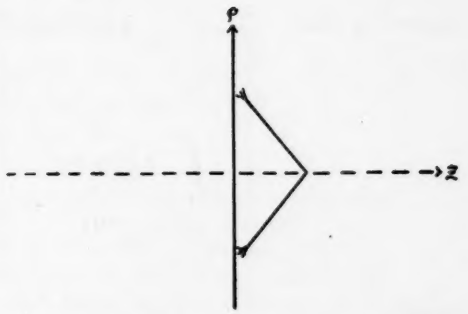

FIG. 2. The characteristic cone of the non-stationary solution for $t>0$ (formation of the Cherenkov cone).

In (23) the small contribution from the totally reflected waves, $\alpha=[(\epsilon-1)(\epsilon(v^2/c^2)-1)]^{\frac{1}{2}}$, has not been taken into account explicitly. The main contribution to the integral (23) comes from the neighborhood of the characteristic cone, $\alpha=1$. In general, (23) represents a radiation field, which shows a marked maximum of intensity in the direction of the characteristic cone. It can be evaluated rigorously at "large" distance from the surface,

$$\lim\frac{\alpha k_\rho z}{[\epsilon(v^2/c^2)-1]^{\frac{1}{2}}}\to\infty, \text{ i.e. } z\gg(\lambda/2\pi)(v/c).$$

Since, from the physical point of view, we are not interested in very long wave-lengths, we may, therefore, say that the characteristic cone of the radiation field becomes formed behind the surface, after the electron has penetrated into the medium, within a distance of the order of one average optical wave length.

Making use of the integrals

$$\lim_{S\to\infty}\int_{1-\delta}^{1+\delta}\frac{\sin\alpha S}{1-\alpha}d\alpha=-\pi e^{-iS},$$

$$\lim_{S\to\infty}\int_{1-\delta}^{1+\delta}\frac{\cos\alpha S}{1-\alpha}d\alpha=i\pi e^{-iS},^*$$

one finds easily

* The singularity on the real axis is understood to be avoided by deviating the path of integration into the *positive* imaginary half-plane of α.

and observing that

$$\int_0^\infty J_0(\eta)e^{i\beta\eta}d\eta=\begin{cases}+\dfrac{i}{(\beta^2-1)^{\frac{1}{2}}}\\ \dfrac{1}{(1-\beta^2)^{\frac{1}{2}}}\\ -\dfrac{i}{(\beta^2-1)^{\frac{1}{2}}}\end{cases}\text{for}\begin{cases}\beta>1\\ -1<\beta<+1\\ \beta<-1\end{cases}\tag{24}$$

we obtain

$$A_3^{(i)}=\bar{A}_3^{(i)}+\bar{\bar{A}}_3^{(i)},$$

with

$$\bar{A}_3^{(i)}=\begin{cases}-\dfrac{ev/c}{[(1-\epsilon(v^2/c^2))\rho^2+(z-vt)^2]^{\frac{1}{2}}}\\ +\dfrac{iev/c}{[(\epsilon(v^2/c^2)-1)\rho^2-(z-vt)^2]^{\frac{1}{2}}}\\ +\dfrac{ev/c}{[(1-\epsilon(v^2/c^2))\rho^2+(z-vt)^2]^{\frac{1}{2}}}\end{cases}\text{for}\quad\frac{z-vt}{\rho(\epsilon(v^2/c^2)-1)^{\frac{1}{2}}}\begin{cases}>+1\\ <+1\\ >-1\\ <-1\end{cases}$$

and

$$\bar{\bar{A}}_3^{(i)}=\begin{cases}\dfrac{\epsilon[1-(\epsilon-1)(v^2/c^2)]^{\frac{1}{2}}-1}{\epsilon[1-(\epsilon-1)(v^2/c^2)]^{\frac{1}{2}}+1}\dfrac{ev/c}{[(1-\epsilon(v^2/c^2))\rho^2+(z+vt)^2]^{\frac{1}{2}}}\\ \dfrac{\epsilon[1-(\epsilon-1)(v^2/c^2)]^{\frac{1}{2}}-1}{\epsilon[1-(\epsilon-1)(v^2/c^2)]^{\frac{1}{2}}+1}\dfrac{iev/c}{[(\epsilon(v^2/c^2)-1)\rho^2-(z+vt)^2]^{\frac{1}{2}}}\end{cases}\text{for}\quad\frac{z+vt}{\rho[\epsilon(v^2/c^2)-1]^{\frac{1}{2}}}\gtrless 1.$$

Comparing these expressions with the corresponding terms of the stationary solution $A_2^{(i)}$ from (7) and identifying their respective domains in Fig. 1 we find, finally, for the total solution for $t>0$ at sufficiently large distance from the surface inside the medium

$$A_2^{(i)}+A_3^{(i)}\cong\begin{cases}\dfrac{2e(v/c)}{[(1-\epsilon v^2/c^2)\rho^2+(z-vt)^2]^{\frac{1}{2}}}\\ \quad\text{inside the retarded cone,}\\ 0\text{ outside the retarded cone,}\end{cases}\tag{25}$$

(25) corresponds exactly to the solution of Tamm and Frank and is valid to the approximation to which the terms belonging to the transition radiation are negligible. Figure 2 shows the domain of the solution (25), which is identical with Cherenkov's cone.

6. CONCLUSIONS

The results of the developments given above are the following:

1. The existence of a transition radiation, of the order of one visible photon per hundred incident electrons, at electron velocities slightly below $c/(\epsilon)^{\frac{1}{2}}$, i.e., at the transition point to the Cherenkov effect (Section 4).

2. The justification and the limits of the solution given by Tamm and Frank for the Cherenkov radiation, in particular the justification for the use of retarded potentials (outgoing waves) only (Section 5).

3. The verification that the description of the phenomenon depends essentially on the behavior of non-uniform analytic functions (square roots). We may learn from this fact, that already the simple electrostatic solution, e/r, has to be written more explicitly as

$$\frac{e}{\pm(x^2+y^2+z^2)^{\frac{1}{2}}}$$

and that its singularity represents a branch point.

Generalized Virial Theorems

HARVEY EINBINDER
Pupin Laboratories, Columbia University, New York, New York

(Received March 25, 1948)

The virial theorem of Milne is extended to include frictional forces which are functions of position and time, while that of Fock and Krutov is given a much simpler derivation and is made to include non-conservative systems. The relation between PV and the moments of E, E_r, and v is derived for a general ideal relativistic gas. Finally, a proof of the mathematical equivalence between the kinetic and statistical methods of deriving the virial theorem is given.

1. INTRODUCTION

AT present there are two generalized virial theorems; one due to Milne[1] includes a viscous force $-k\dot{q}$ acting on the particle but is restricted to classical mechanics, the other given by Fock and Krutov[2] is valid for any conservative Hamiltonian system. Both can be easily generalized; the former for more general force fields and relativistic mechanics, the latter for non-conservative Hamiltonian systems.

As is well known, $PV=(2/3)E$ for any system of mechanically non-interacting field-free particles having an isotropic velocity distribution and which obey the laws of classical or non-relativistic quantum mechanics.[3] When relativistic mechanics or the Dirac equation[4] is obeyed, $PV=\langle[E(E+2mc^2)/(E+mc^2)]\rangle_{Av}$; the simple relation between the first moments of P and E, which are the corresponding thermodynamic variables, is destroyed and with it a valuable equation in statistical mechanics. Thus, for the relativistic Maxwell-Boltzmann gas, $PV=NkT$, which is the same as the non-relativistic case, but E instead of being a linear function of T is now expressed in cylindrical Hankel functions:[5] similarly for relativistic Fermi-Dirac and Bose-Einstein gases.[6] However, in the completely relativistic case ($E\gg mc^2$) it simplifies to $PV=(1/3)E$. Relativistic statistics is essential in the astrophysical treatment of white dwarf stars,[7] since for densities greater than 10^6 gm/cc. relativistic effects become important.[8]

There are two alternate ways of deriving these relations between the moments of P and E. The kinetic method views the pressure as the mean impact delivered by the gas particles in a unit time on colliding with its bounding surface, while the statistical method treates the mean behavior of the entire system employing the virial theorem, without any direct recourse to the collision process. Since these two treatments are quite different in their physical approach, a general proof of their mathematical equivalence will be given.

2. TWO GENERALIZED VIRIAL THEOREMS

The general equation of motion of the ith particle in a system of N particles is

$$\dot{p}_i=F_i(q_1, \cdots, q_n, \dot{q}_1, \cdots, \dot{q}_n, t), \tag{1}$$

where p_i is its momentum and q_i its position. Multiplying through by q_i, (1) becomes

$$d(p_iq_i)/dt=F_i\dot{q}_i+p_i\dot{q}_i, \tag{2}$$

whence

$$\langle(F_iq_i+p_i\dot{q}_i)\rangle_{Av}=0 \tag{3}$$

if

$$\lim_{t\to\infty} p_iq_i/t=0, \tag{4}$$

which will be the case if the energy and the volume of the system is bounded, although Eq. (4) holds under much more general conditions. Equation (3) is the usual statement of the

[1] E. A. Milne, Phil. Mag. **50**, 409 (1925); Fowler, *Statistical Mechanics* (Cambridge University Press, London, 1936), p. 286.
[2] V. Fock and G. Krutov, Physik. Zeits. Sowejetunion **1**, 756 (1932).
[3] B. N. Finkelstein, Zeits. f. Physik **50**, 293 (1928); Born and Jordan, *Elementare Quantenmechanik* (Springer Verlag, Berlin, 1930), p. 100.
[4] V. Fock, Zeits. f. Physik **63**, 855 (1930).
[5] F. Juttner, Ann. d. Physik **34**, 856 (1911).
[6] D. S. Kothari and B. N. Singh, Proc. Roy. Soc. London **A180**, 414 (1942); Chandrasekhar, *Introduction to the Study of Stellar Structure* (University of Chicago Press, Chicago, Illinois, 1939), Chap. 10.
[7] Chandrasekhar, *Introduction to the Study of Stellar Structure* (University of Chicago Press, Chicago, Illinois, 1939), Chap. 11.
[8] Fowler, *Statistical Mechanics* (Cambridge University Press, London, 1936), p. 648.

virial theorem. Now the most general force $\mathfrak{F}_i(q_1, \cdots q_n, \dot{q}_1, \cdots \dot{q}_n t)$ is sought that can be subtracted from the acting one but still leave the virial theorem unchanged. This requires that

$$q_i\mathfrak{F}_i(q_1, \cdots, q_n, \dot{q}_1, \cdots, \dot{q}_n, t) = d\phi_i(q_1, \cdots q_n, t)/dt = \sum_j (\partial\phi_i/\partial q_j)\dot{q}_j + \partial\phi_i/\partial t, \quad (5)$$

where ϕ_i cannot depend on $\dot{q}_j$ since on differentiation this would introduce a term $\partial^2 q_j/\partial t^2$. Thus, the most general dynamical system for which (3) holds is

$$\dot{p}_i = F_i - \{\sum_j (\partial\phi_i/\partial q_j)\dot{q}_j + \partial\phi_i/\partial t\}/q_i \quad (6)$$

provided that

$$\lim_{t\to\infty} \phi_i/t = 0. \quad (7)$$

In the case that the motion of the ith particle is independent of all the others, (6) becomes

$$\dot{p}_i = F_i(q_i, \dot{q}_i, t) - \{(\partial\phi_i/\partial q_i)\dot{q}_i + \partial\phi_i/\partial t)/q_i, \quad (8)$$

and if ϕ_i is time independent, (dropping the subscripts),

$$\dot{p} = F(q, \dot{q}) - Q(q)\dot{q}, \quad (9)$$

where $Q(q) = (\partial\phi/\partial q)/q$. $-Q(q)\dot{q}$ may be considered as a position dependent viscous force. Milne[1] derived the special case where $Q(q) = k$ and $p = m\dot{q}$, i.e., the frictional force is independent of position and the particle obeys classical mechanics. But the entire treatment holds for a relativistic particle where $p = m\dot{q}/(1-\dot{q}^2/c^2)^{\frac{1}{2}}$.

An illustration of this generalized theorem is given by the Brownian motion where, because of the viscosity of the medium, there is a resistance to the motion of the dispersed particle, which for spherical particles is $6\pi\eta a\dot{q}$. Now the virial theorem will hold even if the viscosity is a function of position, so $(3/2)\mathrm{PV} = \sum_i \langle \frac{1}{2} m\dot{q}_i^2 \rangle_{Av}$.

Fock and Krutov[2] in deriving their generalized virial theorem used Hamilton's principle, but it is much simpler to begin with Lagrange's equations which are the variational equations associated with the principle. They are

$$\frac{d}{dt}\frac{\partial \mathrm{T}}{\partial \dot{q}_i} - \frac{\partial \mathrm{T}}{\partial q_i} = Q_i, \quad (10)$$

multiplying by q_i, then

$$\frac{d}{dt}\frac{\partial \mathrm{T}}{\partial \dot{q}_i} q_i = Q_i q_i + \frac{\partial \mathrm{T}}{\partial q_i} q_i + \frac{\partial \mathrm{T}}{\partial \dot{q}_i} \dot{q}_i, \quad (11)$$

so

$$\left\langle Q_i q_i + \frac{\partial \mathrm{T}}{\partial q_i} q_i + \frac{\partial \mathrm{T}}{\partial \dot{q}_i} \dot{q}_i \right\rangle_{Av} = 0, \quad (12)$$

if

$$\lim_{t\to\infty} p_i q_i/t = 0, \quad (13)$$

since by definition $p = \partial \mathrm{T}/\partial \dot{q}$. If the system is conservative, then (12) can be written as

$$\left\langle \frac{\partial L}{\partial q_i} q_i + \frac{\partial L}{\partial \dot{q}_i} \dot{q}_i \right\rangle_{Av} = 0, \quad (14)$$

where $L = T - V$.

This is essentially the result of Fock and Krutov except that it referred to the sum over all the degrees of freedom of the system. If $\mathrm{T} = \mathrm{T}(\dot{q}_i)$ (12) reduces to Eq. (3). Finally, if $\mathrm{T}_i = \mathrm{T}_i(\dot{q}_i^{\rho})$, then

$$\langle Q_i q_i + \rho T_i \rangle_{Av} = 0, \quad (15)$$

where in general the Q_i will be nonconservative forces.

3. RELATIVISTIC CALORIC EQUATION

Consider a particle gas moving in a three-dimensional, field-free space. Assuming the distribution of velocities to be isotropic, one component of a particle's velocity will be $\frac{1}{3}$ its total velocity. Then in the usual manner

$$\mathrm{PV} = (1/3)\int \cdots \int \sum_i p_i v_i f_m \prod_i dp_i, \quad (16)$$

where f_m is distribution function per unit volume and the integration is taken over all accessible regions of momentum space, so

$$\mathrm{PV} = (1/3)\langle (\sum_i p_i v_i) \rangle_{Av} = (1/3)\langle (pv) \rangle_{Av}. \quad (17)$$

According to special relativity

$$p = mv/(1-v^2/c^2)^{\frac{1}{2}}, \quad (18) \qquad E_r^2/c^2 = p^2 + mc^2, \quad (19)$$

$$v = dE/dp = c^2 p/E_r, \quad (20) \qquad E_r = E + mc^2. \quad (21)$$

Thus

$$\mathrm{PV}=\left\langle\left[\frac{c^2p^2}{3E_r}\right]\right\rangle_{Nv}=\frac{1}{3}\left\langle\left[\frac{mv^2}{(1-v^2/c^2)^{\frac{1}{2}}}\right]\right\rangle_{Nv}$$
$$=\frac{1}{3}\left\langle\left[\frac{E_r^2-m^2c^4}{E_r}\right]\right\rangle_{Nv}$$
$$=\frac{1}{3}\left\langle\left[\frac{E(E+2mc^2)}{E+mc^2}\right]\right\rangle_{Nv}. \quad (22)$$

The form involving the velocity was derived by Tolman[9] with the kinetic method for the special case of the Maxwell-Boltzmann distribution, while Danilov[10] derived the form involving E_r for Maxwell-Boltzmann, Bose-Einstein, and Fermi-Dirac statistics by a direct use of their respective distribution functions. This general treatment, valid for any isotropic distribution function, e.g. intermediate statistics, and the corresponding relations given by Eq. (22), does not seem to have appeared in the literature before. Note that when $E\ll mc^2$, $\mathrm{PV}=(2/3)E$; $E\ll mc^2$, $\mathrm{PV}=(1/3)E$; in accordance with well known results.

[9] R. C. Tolman, Phil. Mag. **28**, 583 (1914).
[10] V. Danilov, Zeits. f. Physik **63**, 692 (1930).

4. EQUIVALENCE OF STATISTICAL AND KINETIC DERIVATIONS OF THE CALORIC EQUATION

A proof of the mathematical equivalence of the two methods is almost immediate. For generality (to allow for two dimensional statistics[11]), let the gas be moving in an n dimensional space. Then Eq. (17), based on the kinetic method, becomes

$$\mathrm{PV}=(1/n)\langle(pv)\rangle_{Nv}. \quad (23)$$

If there are no forces between the particles, the only forces being those exerted by the bounding surface, then

$$-\langle(Fq)\rangle_{Nv}=\mathrm{P}\int\cdots\int q\cdot n\,dS$$
$$=\mathrm{P}\int\cdots\int\nabla\cdot q\,d\mathrm{V}=n\,\mathrm{PV}, \quad (24)$$

whence, using the virial theorem, Eq. (3), (23) is obtained. This provides a general demonstration of the mathematical equivalence of the two methods.

[11] Fowler and Guggenheim, *Statistical Thermodynamics* (Cambridge University Press, London, 1939), p. 239; B. Singh, Ind. J. Phys. **15**, 73 (1941).

PHYSICAL REVIEW VOLUME 74, NUMBER 7 OCTOBER 1, 1948

Quantum Statistics and the ℵ Theorem

HARVEY EINBINDER
Pupin Laboratories, Columbia University, New York, New York

(Received March 25, 1948)

The thermodynamic consequences of the state equation $PV=sE$ are investigated. For such a system $E=V^{-s}\phi(TV^s)$, $S=\chi(TV^s)$ and $A=V^{-s}\psi(TV^s)$. During an adiabatic change TV^s, EV^s, and $PV^{1+1/s}$ are constant. The ℵ theorem is derived: A system of mechanically non-interacting particles in equilibrium in a field-free space, which individually obey the laws of non- or completely relativistic quantum mechanics, has $PV=sE$; as $T\to0$, then $S\to C'$; and it either has a zero-point energy, $E=CV^{-s}$, $(\partial E/\partial V)_T>0$, or it condenses, $P=CT^{1+1/s}$, $(\partial E/\partial V)_T<0$. The theorem is used to predict that a strongly degenerate gas obeying intermediate statistics will possess a zero-point energy, $E=CV^{-\frac{1}{3}}$. Further, it clarifies the statement that the third law is a quantum mechanical law, showing that it is satisfied by such a general system. If $PV=sE$, a necessary condition for it to be obeyed is $(\partial E/\partial V)_T\neq0$; a statistical attraction or repulsion must be present, i.e., $(\partial E/\partial V)_T$ greater or less than zero, respectively. Finally the ℵ theorem yields an almost intuitive demonstration of the Einstein condensation phenomenon in Bose-Einstein statistics.

1. CONSEQUENCES OF THE STATE EQUATION $PV=sE$

EVERY gas in equilibrium in a field-free space composed of mechanically non-interacting particles obeys the state equation

$$PV=sE(V,T), \quad (1)$$

where if the particles obey classical or non-relativ-

istic quantum mechanics[1] ($E \gg mc^2$), $s=\frac{2}{3}$; for completely relativistic mechanics[2] or the equivalent Dirac equation[3] ($E \gg mc^2$), $s=\frac{1}{3}$. Every system obeying (1) will be called an ideal statistical gas. The existence of this state equation imposes a restriction on the possible functional forms of $E(V, T)$, since now $H=E+PV=(1+s)E$ so

$$\partial/\partial E=(1+s)\partial/\partial H. \tag{2}$$

The form of $E(V, T)$ is found using the well known thermodynamic relation

$$(\partial E/\partial V)_T=T(\partial P/\partial T)_V-P. \tag{3}$$

Substituting for P using (1) and rearranging the equation, then

$$E=T(\partial E/\partial T)_V-(V/s)(\partial E/\partial V)_T, \tag{4}$$

which is the partial differential equation that must be satisfied by $E(V, T)$. The auxiliary equations associated with it are,[4]

$$dE/E=dT/T=-s dV/V, \tag{5}$$

whose independent solutions are $a=EV^s$ and $b=TV^s$, so the solution of (4) is

$$\Phi(a, b)=\Phi(EV^s, TV^s)=0. \tag{6}$$

or

$$E=V^{-s}\phi(TV^s), \tag{7}$$

where Φ and ϕ are arbitrary functions. Equation (7) serves as a useful check on the calculation of E for an ideal statistical gas. If the variables are further restricted by additional conditions, E may often be explicitly found. Thus, for blackbody radiation where $s=\frac{1}{3}$, general thermodynamic arguments show that $E/V=f(T)$, so the Stefan-Boltzmann law, $E/V=\sigma T^4$, follows directly from (7), or more generally $E/V=\sigma T^{1+1/s}$, as Rayleigh noted in one of his early papers on radiation pressure.

By the combined first and second laws and $PV=sE$

$$TdS=dE+PdV=dE+(sE/V)dV, \tag{8}$$

which has an integrating factor V^s, so

$$TV^s dS=d(EV^s), \tag{9}$$

applying (7), then

$$S=\chi(TV^s). \tag{10}$$

Also

$$A=E-TS=V^{-s}\psi(TV^s). \tag{11}$$

It follows from Eq. (10) that during a reversible adiabatic change, TV^s, EV^s, and $PV^{(1+s)}$ are constant. For the ordinary ideal monatomic gas, $PV^\gamma=P_0V_0^\gamma$, since $1+s=5/3$ $C_p/C_v=\gamma$, while for black body radiation[5] $VT^3=V_0T_0^3$.

2. THE N THEOREM

As $T\to 0$, E tends toward a finite limit, $E(V)$, or to zero. In the case of a zero-point energy, Eq. (6) shows that

$$E=CV^{-s}, \quad (T\approx 0). \tag{12}$$

This is illustrated by a degenerate Fermi-Dirac gas. In the case that E, which is a monotonic function of T, tends to zero, $\phi(TV^s)$ may be replaced by $(C/s)T^mV^{sm}(m>0)$ in the immediate neighborhood of absolute zero. Then

$$\lim_{T\to 0} E=\lim_{T\to 0}(C/s)T^mV^{s(m-1)}, \tag{13}$$

or

$$\lim_{T\to 0} P/T^mV^{s(m-1)-1}=C. \tag{14}$$

For dynamic stability, $(\partial P/\partial V)_T\leq 0$, whence

$$s(m-1)-1\leq 0. \tag{15}$$

Assuming that the individual gas particles obey the laws of quantum mechanics, the uncertainty principle requires that the coordinates and momenta of each of them satisfy the Heisenberg inequality

$$\Delta p\Delta q\geq h/4\pi. \tag{17}$$

Hence, if the energy of the system, and so the momentum of the individual particles, is to tend to zero, its total volume must remain finite.[6] Or, put more explicitly,

$$V=V(P, T)>0, \tag{18}$$

when $0\leq P<\infty$ and $0\leq T<\infty$. This condition

[1] B. N. Finkelstein, Zeits. f. Physik **50**, 293 (1928); M. Born, W. Heisenberg, and P. Jordan, Zeits. f. Physik **35**, 577 (1926).
[2] H. Einbinder, Phys. Rev. **74**, 803 (1948).
[3] V. Fock, Zeits. f. Physik **63**, 855 (1930).
[4] Miller, *Partial Differential Equations* (John Wiley and Sons, Inc., New York, New York, 1941), Chap. 4.
[5] In nearly all the standard thermodynamic treatises this adiabatic relation is derived with the aid of the Stefan-Boltzmann law, which is dependent on $PV=sE$ and $E/V=f(T)$; but the latter assumption is unnecessary to prove the adiabatic law.
[6] This is an argument used to show that stable electrons cannot be present in nuclei; cf. Richtmeyer and Kennard, *Introduction to Modern Physics* (McGraw-Hill Book Company, New York, New York, 1942), p. 586.

requires

$$s(m-1)-1\geq 0. \tag{19}$$

For (15) and (16) to be simultaneously satisfied,

$$s(m-1)-1=0, \tag{20}$$ or $$m=1+1/s. \tag{21}$$

From (20) and (14) it is seen that the pressure is independent of the volume in the neighborhood of $T=0$, i.e., the gas must condense, and substituting (21) into (14)

$$P=CT^{1+1/s}, \quad (T\approx 0). \tag{22}$$

This is illustrated by the degenerate Bose-Einstein gas and blackbody radiation. The ℵ (*Aleph*) *Theorem* may now be enunciated.

> *A system of mechanically non-interacting particles in equilibrium in a field-free space which individually satisfy the laws of non- or completely relativistic quantum mechanics has* $PV=sE$; *as* $T\to 0$, *then* $S\to C'$ *and either it has a zero-point energy,* $E=CV^{-s}$, *or* $(\partial E/\partial V)_T<0$, *condenses* $P=CT^{1+1/s}$, $(\partial E/\partial V)_T>0$.

The statement that at $T=0$, $S=C'$, thus obeying the third law of thermodynamics, will be proved in §3.

The ℵ theorem predicts the behavior of the system only in the neighborhood of absolute zero, having nothing to say about possible occurrences at higher temperatures. Thus, the degenerate Fermi-Dirac gas obeys the theorem only at $T=0$, the degenerate Bose-Einstein gas only when it is below its condensation temperature (3.14°K for a gas with the molecular weight and density of liquid He[7]), while blackbody radiation obeys the ℵ theorem at all temperatures.

The theorem requires that only the motion of the individual particles obey the laws of quantum mechanics. Since the particles are mechanically independent, the Hamiltonian for the system will be the sum of the N Hamiltonians referring to the N indistinguishable particles of the system; the total wave function will be a suitable linear combination of the N-product particle wave functions. To determine uniquely this linear combination some symmetry property of the total wave function must be given, e.g., Pauli's principle requiring a symmetric or antisymmetric solution, leading to Bose-Einstein and Fermi-Dirac statistics, respectively. But since the ℵ theorem is independent of the symmetry properties of the total wave function, it is valid for a much wider class of statistics.

An example is intermediate statistics, which allows a maximum occupation of d particles per cell in phase space, whose distribution function is[8]

$$\frac{N_j}{C_j}=\frac{1}{e^{(\epsilon_j-\mu)/kT}-1}-\frac{d+1}{e^{(d+1)(\epsilon_j-\mu)/kT}-1}, \tag{23}$$

which reduces to F.D. and B.E. statistics when $d=1$ and $d=\infty$, respectively, but has no discontinuity at $\epsilon_j-\mu=0$. It has been used by Gentile and his co-workers to treat the problem of He II.[9] Of greatest interest is the behavior of the system as $T\to 0$; unfortunately this strongly degenerate case has not yet been treated rigorously.[10] Since this statistics obeys the ℵ theorem, as $T\to 0$ the system must either possess a zero-point energy or condense. Since for $d=1$ the system has a zero-point energy while for $d=\infty$ it condenses; on *a priori* gounds, of the two alternatives, it is reasonable to predict that for any finite d the system will have a zero-point energy, $E=CV^{-\frac{1}{3}}$. This prediction appears correct, since Sommerfeld[8] shows, using approximate methods, that

$$E=(3/10)(h^2/m)(3/4\pi V)^{\frac{1}{3}}. \tag{24}$$

The predictions of the ℵ theorem do not arise because of the special dimensionality of the statistics; for the n dimensional case $s=2/n(E\ll mc^2)$, $s=1/n(E\gg mc^2)$.

3. THE ℵ THEOREM AND THE THIRD LAW

The third law requires that at absolute zero $S=C$ (Nernst) or alternately $S=0$ (Planck). A necessary condition that it be satisfied is that as $T\to 0$, $C_v\to 0$. If for an ideal statistical gas $(\partial E/\partial V)_T=0$, then Eq. (7) shows that $E=CT$ (Maxwell-Boltzmann statistics), clearly violating the third law. Thus, a necessary condition for an ideal statistical gas to satisfy the third law is that

[7] Mayer and Mayer, *Statistical Mechanics* (John Wiley Sons, Inc., New York, New York, 1940), p. 418.

[8] G. Gentile, Nuova Cimento **17**, 493 (1940); A. Sommerfeld, Berichte **75B**, 1988 (1942).

[9] G. Gentile, Nuova Cimento **19**, 109 (1942); C. Salvetti, Atti. Acad. Italia Mem. **13**, 651 (1942).

[10] P. Caldirola, 1st Lombardo Sci. Lett. **8**, 193 (1944); P. Urban, Akad. Wiss. Wien. **152**, 111 (1943).

$(\partial E/\partial \mathrm{V})_{\mathrm{T}} \neq 0$. This implies the existence of an attraction or repulsion between particles in phase space for any statistics valid near $\mathrm{T}=0$. From (12) and (22), as $\mathrm{T}\to 0$ if $(\partial E/\partial \mathrm{V})_{\mathrm{T}}<0$ (repulsion), the system has a zero-point energy; while if $(\partial E/\partial \mathrm{V})_{\mathrm{T}}>0$ (attraction) it condenses.

Since $\mathrm{P}=-(\partial A/\partial \mathrm{V})_{\mathrm{T}}$, then using (11)

$$A=-\int \mathrm{P}d\mathrm{V}-\varphi(\mathrm{T})=-\int \mathrm{P}d\mathrm{V}-C'\mathrm{T}, \quad (25)$$

$$S=-(\partial A/\partial \mathrm{T})_{\mathrm{V}}=\int (\partial \mathrm{P}/\partial \mathrm{T})_{\mathrm{V}}d\mathrm{V}+C'. \quad (26)$$

If the system has a zero-point energy $(\partial \mathrm{P}/\partial \mathrm{T})_{\mathrm{V}}=0$, while if it condenses $(\partial \mathrm{P}/\partial \mathrm{T})_{\mathrm{V}}=(1+1/s)C\mathrm{T}^{1/s}$. Thus, as $\mathrm{T}\to 0$, $S\to C'$ for both cases, a quantum mechanical ideal statistical gas must obey the third law, a result incorporated in the ℵ theorem. No decision can be made between the Nernst and Planck formulations, C' finite or zero, because the concept of absolute entropy has no meaning in thermodynamics.

4. CONCLUSION

The great value of the ℵ theorem is that it explicitly predicts the behavior of a quantum mechanical ideal statistical gas in the neighborhood of $\mathrm{T}=0$, giving its precise functional form; $E=C\mathrm{V}^{-s}$ for a zero-point energy and $P=C\mathrm{T}^{1+1/s}$ for condensation. It is precisely in this strongly degenerate case that theoretical difficulties often arise. Thus, it was only in 1938 that London[11] succeeded in giving a rigorous treatment of the degenerate Bose-Einstein gas demonstrating the existence of the Einstein condensation phenomenon[12] which had been previously questioned by Uhlenbeck.[13] The ℵ theorem dispels some of the remarkable character of the phenomenon; to prove its existence it is sufficient to show that the system has no zero-point energy, or that there is a statistical attraction between the particles, $(\partial E/\partial V)_T<0$. Since there is no restriction on the number of bosons which may be present in the zero energy state, it is almost intuitively evident that the system will have no zero-point energy. Quantum theory shows[14] that the number of collisions per second of a boson in a phase cell i with all other bosons is $\sum_{j,k,l} A_{kl}{}^{ij}\bar{N}_i\bar{N}_j(1+\bar{N}_k)(1+\bar{N}_l)$, indicating that the presence of a particle in a cell increases the probability that another should enter it, i.e., statistical attraction, hence $(\partial E/\partial V)_T<0$. However, since the condensation is predicted only in the neighborhood of $T=0$ where $E\to 0$, the strict use of the uncertainty principle requires that the volume and the number of particles the system tend to infinity while the volume per particle, V/N, remains finite, in agreement with conditions imposed by the statistical mechanics of condensing systems.[15]

The proof that a quantum mechanical ideal statistical gas must obey the third law helps to clarify the vague statements that it is a quantum statistical law. It holds for any system of noninteracting particles which individually obey the laws of quantum mechanics. For it to be satisfied there must be a statistical attraction or repulsion between the particles, i.e., $(\partial E/\partial V)_T\neq 0$.

In closing, the author wishes to thank L. H. Thomas for his very helpful criticism.

[11] F. London, Phys. Rev. **54**, 948 (1938).
[12] A. Einstein, Ber. Berl. Akad. p. 261 (1924); *ibid.*, p. 3 (1925).
[13] G. E. Uhlenbeck, Dissertation (Leiden, 1927).
[14] Slater, *Introduction to Chemical Physics* (McGraw-Hill Book Company, New York, 1939), p. 96; P. Jordan, Zeits. f. Physik **33**, 649 (1925).
[15] B. Kahn and G. E. Uhlenbeck, Physica **5**, 399 (1938); J. E. Mayer, J. Chem. Phys. **10**, 629 (1942).

PHYSICAL REVIEW VOLUME 74, NUMBER 7 OCTOBER 1, 1948

Elastic Scattering of High Energy Nucleons by Deuterons

GEOFFREY F. CHEW*
Department of Physics, University of Chicago, Chicago, Illinois
(Received June 21, 1948)

The elastic scattering cross section of deuterons for neutrons and protons of 90 and 350 Mev has been calculated, using the non-relativistic Born approximation. Two different approaches give roughly the same result: a total neutron-deuteron elastic cross section of about half the neutron-proton cross section at the same energy but sharply confined to small angles. The half-width at 90 Mev is about 15° in the laboratory system. The proton-deuteron elastic scattering is similar to the neutron-deuteron for large angular deflections, but at 90 Mev a difference due to the Coulomb repulsion should be noticeable within 10°. It is concluded that the assumption of a simple additivity of nucleon-nucleon cross sections for light elements is unjustified.

I. INTRODUCTION

THE scattering by deuterons of protons and neutrons of energies less than 14 Mev has been studied extensively, both experimentally and theoretically, the most complete theoretical treatment having been given by Buckingham and Massey.[1] Recently a total cross section at 90 Mev has been obtained with the Berkeley cyclotron,[2] and it should be possible in the near future to determine the angular distribution as well as the division between elastic and inelastic processes. Thus it is desirable to see what can be said theoretically about these high energy collisions.

The high energy problem differs from the low in three important features: (a) Collisions in which the deuteron disintegrates are quite probable. (b) Because the De Broglie wavelength of the incident particle is short compared to the range of the nuclear force, high angular momenta contribute strongly. Thus the computation of individual phase shifts by straightforward integration of the Schrödinger equation is impracticable. (c) The relative energy in the collision is sufficiently great that it is now reasonable to use the Born approximation. The latter will not give completely satisfactory results, as has been shown by experience with neutron-proton scattering,[3] but the order of magnitude should be correct.

The simplest theoretical guess that can be made is that for an incident particle of energy large compared to the deuteron binding, one may neglect the latter and treat the scattering as the sum of that due to a proton and an independent neutron. This idea implies negligible elastic scattering. It will be shown in this paper that the elastic scattering is never negligible, even at the highest energies, and that therefore the assumption of additivity is unjustified.

The inelastic scattering is much less easily treated since it involves the continuum wave functions of the deuteron. This problem is being attacked, however, and it is hoped that some theoretical results will be forthcoming soon.

Since the completion of the major portion of this work a paper by Wu and Ashkin[4] on the same subject has appeared. In spite of the fact that in both papers the Born approximation is used, there are important differences in the choice of the nuclear forces and of the deuteron wave function. In particular the results presented in this paper are largely independent of the detailed mechanism of the forces and can be deduced at least in part from direct data of scattering of nucleons on nucleons. Finally, the choice by Wu and Ashkin of gaussian instead of exponential wave functions seems to have affected their results to a considerable extent.

II. A SIMPLIFIED APPROACH TO THE PROBLEM

A. Theory

It is desirable, in considering the nucleon-deuteron problem, to separate as much as possible those features which have to do with the

* National Research Council Predoctoral Fellow.
[1] R. A. Buckingham and H. S. W. Massey, Proc. Roy. Soc. A179, 123 (1942).
[2] Cook, McMillen, Peterson, and Sewell, Phys. Rev. 72, 1264 (1947).
[3] M. Camac and H. Bethe, Phys. Rev. 73, 191 (1948).
[4] Ta-You Wu and J. Ashkin, Phys. Rev. 73, 986 (1948).

nature of the nuclear forces from those which reflect the presence of two of the three particles in a bound state. This is clearly not possible in an exact sense, but an understanding of the importance of the binding can only be obtained by first making such a separation. The results of a straightforward but more complicated calculation later will then be more easily interpretable.

Let us therefore think of the elastic scattering probability as the product of two separate factors: (a) The chance that the incident nucleon may suffer a collision with either of the two deuteron particles, suddenly transferring a momentum $\Delta\mathbf{p}$ to that particle. (b) The probability of finding the two deuteron particles still in their ground state after this dislocation. The first factor can be estimated from the known neutron-proton scattering, with a guess as to the corresponding neutron-neutron or proton-proton cross section. The second factor might be called the "sticking" factor, $S(\Delta p)$, and will be our principal concern in this section. If the elastic cross section is to be negligible in comparison to the total, it will be due to the smallness of $S(\Delta p)$.

To put this idea in a more definite form, the following hypothetical situation is considered: A deuteron is bombarded by a third particle of the same mass as a neutron or proton but inequivalent to either and with no spin. The third particle has an ordinary interaction with the proton, $V_p(r)$, and with the neutron, $V_n(r)$. All complications due to symmetry, spin, exchange forces, etc., are deliberately ignored. Let us also assume that the Born approximation is applicable and calculate the elastic scattering cross section.

Designate the coordinate of the neutron by $\mathbf{r}_n$, that of the proton by $\mathbf{r}_p$, and that of the incident particle by $\mathbf{r}_i$. More convenient variables are obtained by the transformation:

$$\mathbf{R}=\tfrac{1}{3}(\mathbf{r}_n+\mathbf{r}_p+\mathbf{r}_i),\quad \mathbf{r}=\mathbf{r}_n-\mathbf{r}_p,\quad \mathbf{x}=\mathbf{r}_i-\tfrac{1}{2}(\mathbf{r}_n+\mathbf{r}_p).$$

The Hamiltonian of the problem is

$$\begin{aligned}H=&\frac{\mathbf{p}_n^2}{2m}+\frac{\mathbf{p}_p^2}{2m}+\frac{\mathbf{p}_i^2}{2m}+V_{np}(|\mathbf{r}_n-\mathbf{r}_p|)\\&+V_n(|\mathbf{r}_n-\mathbf{r}_i|)+V_p(|\mathbf{r}_p-\mathbf{r}_i|)\\=&\frac{P^2}{2(3m)}+\frac{p_r^2}{2(m/2)}+\frac{p_x^2}{2(2/3)(m)}\\&+V_{np}(r)+V_n(|\mathbf{x}-\mathbf{r}/2|)+V_p(|\mathbf{x}+\mathbf{r}/2|),\end{aligned}$$

where m is the mass of the proton or neutron and $(\mathbf{p}_n, \mathbf{r}_n)$, $(\mathbf{p}_p, \mathbf{r}_p)$, $(\mathbf{p}_i, \mathbf{x}_i)$, $(\mathbf{P}, \mathbf{R})$, $(\mathbf{p}_r, \mathbf{r})$, $(\mathbf{p}_x, \mathbf{x})$, are canonically conjugate pairs of variables. $V_{np}(r)$ is the interaction between neutron and proton.

The Hamiltonian is split into two parts,

$$H=H_0+\mathcal{H},$$

where $\mathcal{H}=V_n(|\mathbf{x}-\mathbf{r}/2|)+V_p(|\mathbf{x}+\mathbf{r}/2|)$ and H_0 is the remainder, and use is made of the time dependent perturbation theory to calculate the transition probability between eigenstates of the operator H_0, due to the perturbation $\mathcal{H}$. Since the eigenstates form a continuum, we may apply the well-known formula:

$$\lambda=2\pi/h\,|\mathcal{H}_{fo}|^2\rho_E,$$

where λ is the probability per unit time of a transition from the state o into the continuum of states near f, $\mathcal{H}_{fo}$ is the matrix element of $\mathcal{H}$ between states o and f, and ρ_E is the number of final states per unit energy interval. Energy must of course be conserved.

The initial state, in the center-of-gravity system, can be written as the product of a plane wave, and the ground state of the deuteron, $\psi_0(r)$.

$$\Psi_0(\mathbf{x}, \mathbf{r})=\Omega^{-\frac{1}{2}}\exp(i\mathbf{p}_o\cdot\mathbf{x})\psi_0(r).$$

This represents the deuteron and the third particle approaching each other with relative velocity v, total momentum zero, in a box of volume Ω. The relative momentum and velocity are related by $h\mathbf{p}_o=\frac{2}{3}m\mathbf{v}$.

The final state is a similar expression with $\mathbf{p}_o$ replaced by $\mathbf{p}_f$. Energy conservation requires that $|\mathbf{p}_f|=|\mathbf{p}_o|$. The required matrix element is

$$\begin{aligned}\mathcal{H}_{fo}=&\int\int d\mathbf{x}d\mathbf{r}\,\Psi_f^*(\mathbf{x}, \mathbf{r})\mathcal{H}\Psi_o(\mathbf{x}, \mathbf{r})\\=&\Omega^{-1}\int\int d\mathbf{x}d\mathbf{r}\exp(i(\mathbf{p}_f-\mathbf{p}_o)\cdot\mathbf{x})\\&\times[V_n(|\mathbf{x}-\mathbf{r}/2|)+V_p(|\mathbf{x}+\mathbf{r}/2|)]\psi_0^*(r)\psi_0(r).\end{aligned}$$

Consider first the term involving V_n and make the change of variables $\mathbf{y}=\mathbf{x}-\mathbf{r}/2$, $\mathbf{r}=\mathbf{r}$. It may then be written, with the abbreviation,

$$\mathbf{p}_f-\mathbf{p}_o=\Delta\mathbf{p},$$

$$\Omega^{-1}\int\int dyd\mathbf{r}\exp(i\Delta\mathbf{p}\cdot(\mathbf{y}+\mathbf{r}/2))\psi_0^2(r)\,V_n(y),$$

or

$$\Omega^{-1}\left\{\int d\mathbf{y}\,\exp(i\Delta\mathbf{p}\cdot\mathbf{y})\,V_n(y)\right\}$$
$$\times\left\{\int d\mathbf{r}\,\exp(i(\Delta\mathbf{p}/2)\cdot\mathbf{r})\psi_0^2(r)\right\}.$$

Similarly, the part containing V_p may be written

$$\Omega^{-1}\left\{\int d\mathbf{y}\,\exp(i\Delta\mathbf{p}\cdot\mathbf{y})\,V_p(y)\right\}$$
$$\times\left\{\int d\mathbf{r}\,\exp(i(\Delta\mathbf{p}/2)\cdot\mathbf{r})\psi_0^2(r)\right\}.$$

In anticipation of a later result the following quantities are defined:

$$S^{\frac{1}{2}}(\Delta p)=\int d\mathbf{r}\,\exp(i(\Delta\mathbf{p}/2)\cdot\mathbf{r})\psi_0^2(r), \tag{1}$$

$$\mathcal{V}_n(\Delta\mathbf{p})=\int d\mathbf{y}\,\exp(i\Delta\mathbf{p}\cdot\mathbf{y})\,V_n(y),$$
$$\mathcal{V}_p(\Delta\mathbf{p})=\int d\mathbf{y}\,\exp(i\Delta\mathbf{p}\cdot\mathbf{y})\,V_p(y), \tag{2}$$

and the two terms are collected together again.

$$\mathcal{H}_{fo}=\Omega^{-1}\{\mathcal{V}_n(\Delta\mathbf{p})+\mathcal{V}_p(\Delta\mathbf{p})\}S^{\frac{1}{2}}(\Delta p).$$

The cross section, $\sigma_{el}d\omega$, for scattering in the direction $\mathbf{p}_f$ per unit solid angle, is related to the corresponding transition probability by

$$\lambda=\Omega^{-1}v\sigma_{el}d\omega.$$

The number of final states per unit energy is

$$\rho_E=(1/8\pi^3)\Omega p_f^2(dp_f/dE_f)d\omega,$$

and since $dE_f/dp_f=\hbar v$,

$$\rho_E=(1/8\pi^3\hbar v)\Omega p_f^2 d\omega.$$

The formula for the cross section thus becomes

$$\sigma_{el}d\omega=\lambda\Omega/v=(2\pi/\hbar)\,|\mathcal{H}_{fo}|^2(\Omega\rho_E/v)$$
$$=\frac{(2m/3)^2}{4\pi^2\hbar^4}\,|\mathcal{V}_n(\Delta\mathbf{p})+\mathcal{V}_p(\Delta\mathbf{p})|^2S(\Delta p)d\omega, \tag{3}$$

since $p_f^2/v^2=(2m/3)^2\hbar^{-2}$.

This result contains the essential feature we are looking for. The factor $S(\Delta p)$ is a function only of the deuteron configuration. It approaches zero for very weak binding and unity for very strong binding. It is always unity for zero momentum transfer. The rest of the expression, on the other hand, has nothing to do with the deuteron, depending only on the character of the forces between the projectile and the individual proton and neutron. It may be looked upon as the collision probability suggested at the beginning of this section, while $S(\Delta p)$ is the "sticking" probability.

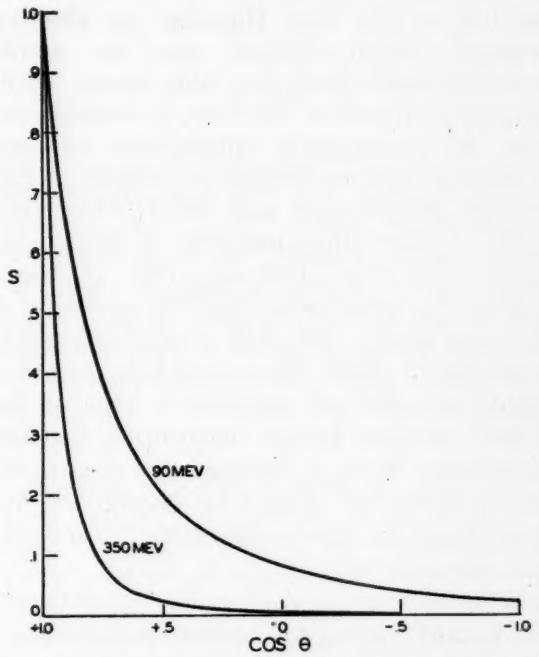

FIG. 1. The "sticking factor" S, as a function of the cosine of the scattering angle in the center-of-gravity system.

From the definition (1) of $S(\Delta p)$ one observes that it decreases monotonically with increasing magnitudes of momentum transfer. In terms of angular distribution at a given energy, this means that forward scattering is favored. In Fig. 1, S is plotted as a function of the cosine of the scattering angle in the center-of-gravity system for incident laboratory energies of 90 and 350 Mev. The wave function used in the computation (see Section III B) corresponds to a central Yukawa potential, but clearly any reasonable choice of wave function will give about the same result.

B. Estimate of Cross Section

The average value of the sticking factor over all solid angles is quite small, 0.17 at 90 Mev.

and 0.05 at 350 Mev. However, the effective average is always greater, since the simple nucleon-nucleon scattering also favors small momentum transfers. This fact, in combination with the constructive interference between neutron and proton scatterings, evident in Eq. (3), and the reduced mass effect, which contributes a factor 16/9, may give an elastic scattering cross section of the same order of magnitude as the simple neutron-proton scattering at the same energy. The ratio of elastic deuteron scattering to simple nucleon-nucleon scattering should not diminish appreciably, even at the highest energies, because momentum transfers much larger than $\hbar/a$, where a is the range of the nuclear force, will always be improbable. We now attempt to make a quantitative estimate of this ratio at 90 Mev.

We propose to use the formula (3), and insert for $\mathcal{U}_n(\Delta\mathbf{p})$ and $\mathcal{U}_p(\Delta\mathbf{p})$ matrix elements which in a corresponding simplified theory of the elementary nucleon-nucleon scattering would give the actually observed cross sections. In this way we avoid any reference to the nuclear force involved, which only confuses the issue here. In Section III a complete calculation will reveal the mistakes which this type of estimate can make.

For the sake of argument, let us assume the incident particle is a neutron. A calculation of the cross section for its scattering on a free proton, with the same simplifications as above,

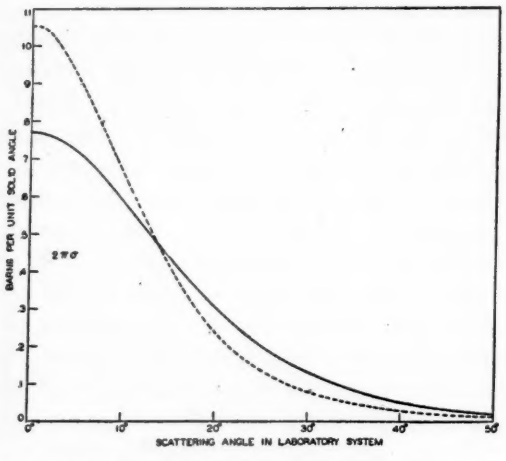

FIG. 2. Differential elastic scattering cross section for neutrons on deuterons, referred to the laboratory system of coordinates. The solid curve represents the results of Section II and the broken curve that of Section III.

yields a formula:

$$\sigma_{np}d\omega' = \frac{(m/2)^2}{4\pi^2\hbar^4}|\mathcal{U}_p(\Delta\mathbf{p}')|^2 d\omega',$$

where ω', $\Delta\mathbf{p}'$ refer to the center-of-gravity system of the two-particle problem and $\mathcal{U}_p(\Delta\mathbf{p}')$ has again the definition (2). At 90 Mev, the scattering has been observed to be roughly symmetric about 90° and to have a total value of 0.083 B.[2,5] We are clearly interested in only the forward part of the scattering here, which can be empirically fitted by choosing

$$\mathcal{U}_p(\Delta\mathbf{p}) = \frac{2\pi\mathcal{U}_0}{q}\left[\frac{1}{q^2+(\Delta p)^2}\right], \qquad (4)$$

where $\mathcal{U}_0 = 226$ Mev and $1/q = 0.578\times10^{-13}$ cm.

The corresponding neutron-neutron or proton-proton matrix element cannot be obtained so directly since there is as yet no experimental information at high energies. If we assume that the force is the same, one might guess at an expression of the form of (4) with an additional factor of about one-half in front. The argument for this is as follows: The experimentally observed symmetry implies that only even angular momenta are scattered or only the singlet spin states of identical particles. This cuts down the cross section by a factor of one-quarter due to the statistics and farther because the singlet potential is weaker than the triplet. A survey of recent calculations[3,6] would indicate the latter factor to be about one-half. Finally, we must remember the factor of two which generally appears for identical particles with spatial symmetry. The net result is a factor $\frac{1}{4}\times\frac{1}{2}\times2=\frac{1}{4}$ in the cross section or one-half in the matrix element. The effect of the Coulomb force which is present when the projectile is a proton will be considered in Section III C.

Substitution of these estimates into formula (3) leads to

$$\sigma_{el}d\omega = \frac{m^2\mathcal{U}_0^2}{\hbar^4 q^2}\left[\frac{1}{q^2+(\Delta p)^2}\right]S(\Delta p)d\omega, \qquad (5)$$

a result which is to be taken seriously only for

[5] J. Hadley, Kelly, Leith, Segrè, Wiegand, and York, Phys. Rev. **73**, 1114 (1948).
[6] J. Ashkin and Ta-You Wu, Phys. Rev. **73**, 973 (1948).

rather small angles. These small angles, of course, will include most of the total cross section.

This formula yields a total cross section of $0.045\ B$ at 90 Mev, about half the n–p cross section, and the angular distribution shown by the solid curve in Fig. 2. It may be in error by as much as a factor of two, but the state of knowledge about nuclear forces being what it is, is probably as good an estimate as can be made at this time. The neglect of possible exchange forces is not so bad as it seems, since they tend to break up the deuteron. An interesting effect not taken account of in this crude picture is an exchange of the two identical particles, leaving the deuteron intact. This will appear in the formally more correct calculation of Section III.

III. THE COMPLETE CALCULATION

A. Choice of Nuclear Forces

In this section a calculation of the elastic scattering is carried out which includes considerations of symmetry and spin but which of necessity must be based on some assumption as to the nature of the forces. It is clear from Section II that a force which gives an erroneous angular distribution for simple nucleon-nucleon scattering is likely to produce an even more misleading result for nucleon-deuteron scattering. Purely ordinary forces with a reasonable range, for example, give a strong forward maximum at high energies. When this is multiplied by the "sticking" factor, the result is an elastic cross section at 90 Mev of two to three times the observed *total* cross section. This violent dependence on the nature of the force has already been shown by Wu and Ashkin.[4] There seems no point therefore in considering a type of force which does not fairly well represent the actual high energy neutron-proton angular distribution.

The simplest acceptable force has been studied extensively by Serber's group at Berkeley.[7] It is of the type $\frac{1}{2}(1+P)V(r)$, where P is the space exchange operator and $V(r)$ is a central potential. Actually, the Berkeley study has included tensor forces, but the deuteron problem becomes unmanageable from a practical point of view if a tensor force is considered. We therefore shall take for the potential, between like as well as unlike nucleons,

$$V^{S,T}(r)=\tfrac{1}{2}(1+P)\,V_0{}^{S,T}\frac{\exp(-\mu r)}{\mu r}, \qquad (6)$$

where $V_0{}^T=-67.8$ Mev and $V_0{}^S=-46.5$ Mev, corresponding to triplet and singlet states, respectively, and $\mu^{-1}=1.18\times10^{-13}$ cm. The range and singlet depth are adjusted to fit the low energy proton-proton scattering,[8] and the triplet depth is fixed by the binding energy of the deuteron.[9] It has been shown at Berkeley that such a potential represents satisfactorily both the magnitude and the angular distribution of the 90-Mev neutron-proton scattering.

Since the Born approximation is to be used, it is advisable to consider how good the latter is when applied to the neutron-proton problem. It turns out to give a total cross section within 10 percent of the exact value at 90 Mev when used with the above potential. The angular distribution has the correct symmetry but too deep a minimum at 90° in the center-of-gravity system. The exact calculation gives a factor of 3 between the intensities at 180° and at 90°, while the Born approximation gives a factor 5.7. It is therefore expected that the deuteron elastic cross section, calculated in this way, may be too large by as much as 30 percent. At 350 Mev, the Born approximation can probably be used without reservation, but relativistic corrections will be serious.

B. Neutron-Deuteron Cross Section

The neutron case is considered first in order to avoid the Coulomb force complication. The calculation uses the same time-dependent perturbation theory as in Section II, generalized for the presence of two identical particles. Let the space and spin coordinates of the two neutrons be $(\mathbf{r}_1, \sigma_1)$, $(\mathbf{r}_3, \sigma_3)$ and that of the proton $(\mathbf{r}_2, \sigma_2)$. The symbol ξ_i denotes both space and spin variables of the ith particle. The Hamiltonian is

$$H=\frac{p_1{}^2}{2m}+\frac{p_2{}^2}{2m}+\frac{p_3{}^2}{2m}+V(\xi_1,\xi_2)+V(\xi_1,\xi_3)+V(\xi_2,\xi_3),$$

[7] R. Serber, private communication.

[8] L. E. Hoisington, S. S. Share, and G. Breit, Phys. Rev. **56**, 884 (1939).

[9] R. G. Sachs and M. Goeppert-Mayer, Phys. Rev. **53**, 991 (1938).

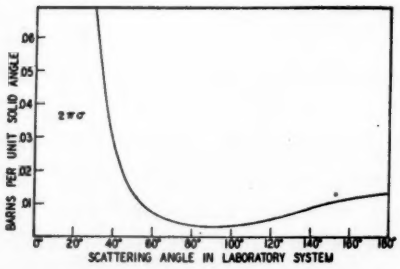

FIG. 3. Large-angle elastic scattering of 90-Mev nucleons by deuterons in the laboratory system.

where $\mathbf{p}_i$ is the momentum of particle i and $V(\xi_i, \xi_j)$ is the potential acting between particles i and j. We choose for our complete set of eigenfunctions, antisymmetric in particles 1 and 3,

$$\Psi_n(\xi_1, \xi_2, \xi_3) = 1/\sqrt{2}(1-P_{13}{}^T)\Phi_n(\xi_1, \xi_2, \xi_3),$$

where the $\Phi_n(\xi_1, \xi_2, \xi_3)$ belong to the operator $p_1{}^2/2m+p_2{}^2/2m+p_3{}^2/2m+V(\xi_1, \xi_2)$ and where $P_{13}{}^T$ interchanges all coordinates of the particles 1 and 3. The cross-section formula, as in Section II, may be written

$$\sigma_{ol}d\omega = \frac{(\frac{2}{3}m)^2\Omega^2}{4\pi^2\hbar^4}|\mathcal{H}_{fo}|^2 d\omega,$$

where now $\mathcal{H}_{fo}$ must be understood to mean

$$\mathcal{H}_{fo} = \sum_{\xi_1, \xi_2, \xi_3} [1/\sqrt{2}(1-P_{13}{}^T)\Phi_f{}^*(\xi_1, \xi_2, \xi_3)] \times [1/\sqrt{2}(1-P_{13}{}^T) \times (V(\xi_1, \xi_3)+V(\xi_2, \xi_3))\Phi_o(\xi_1, \xi_2, \xi_3)]. \quad (7)$$

This result can be obtained in a manner exactly analogous to that used to get the usual transition probability formula.[10] The sum over ξ_1, ξ_2, ξ_3 is meant to include integration over the continuous variables.

After making the usual change of variables, $\mathbf{r}=\mathbf{r}_1-\mathbf{r}_2$, $\mathbf{R}=\frac{1}{3}(\mathbf{r}_1+\mathbf{r}_2+\mathbf{r}_3)$, $\mathbf{x}=\mathbf{r}_3-\frac{1}{2}(\mathbf{r}_1+\mathbf{r}_2)$, we obtain the initial state in the center-of-gravity system by choosing

$$\Phi_0 = \Omega^{-\frac{1}{2}}\exp(i\mathbf{p}_o\cdot\mathbf{x})\psi_0(r)\chi_{1\ldots6}(\sigma_1, \sigma_2, \sigma_3),$$

and the final state by choosing a similar function with $\mathbf{p}_o$ replaced by $\mathbf{p}_t$. All symbols in these expressions have the same meaning as in Section II.

[10] See, for example, W. Heitler, *Quantum Theory of Radiation* (Oxford University Press, London, 1944), second edition, p. 88.

The spin functions $\chi_{1\ldots6}(\sigma_1, \sigma_2, \sigma_3)$ are taken as follows:

$$\left.\begin{aligned}\chi_1 &= a_1a_2a_3,\\ \chi_2 &= 3^{-\frac{1}{2}}(a_1a_2b_3+a_1b_2a_3+b_1a_2a_3),\\ \chi_3 &= 3^{-\frac{1}{2}}(b_1b_2a_3+a_1b_2b_3+b_1a_2b_3),\\ \chi_4 &= b_1b_2b_3,\end{aligned}\right\}\text{quartet states.}$$

$$\left.\begin{aligned}\chi_5 &= 6^{-\frac{1}{2}}(2a_1a_2b_3-a_1b_2a_3-b_1a_2a_3),\\ \chi_6 &= 6^{-\frac{1}{2}}(2b_1b_2a_3-a_1b_2b_3-b_1a_2b_3),\end{aligned}\right\}\text{doublet states.}$$

a_i represents z component of spin $+\frac{1}{2}$ for the ith particle and b_i represents z component $-\frac{1}{2}$.

The force chosen does not mix spin and angular momentum, so the final spin state must be the same as the initial. It is also obvious that the matrix element does not depend on the z component of the total spin. Therefore, there are only two different matrix elements to consider, one for the quartet states and one for the doublet. If expression (7) is written out in full and the spin products performed, we find for the quartet states:

$$\mathcal{H}_{fo}{}^Q = \frac{1}{2\Omega}\{I_1+I_2-2I_3\}, \quad (8)$$

and for the doublet:

$$\mathcal{H}_{fo}{}^D = \frac{1}{2\Omega}\{\tfrac{1}{4}(1+9\eta)(I_1+I_2)+I_3\}, \quad (9)$$

where

$$I_1 = \left\{\int d\mathbf{y}\exp(-i\Delta\mathbf{p}\cdot\mathbf{y})V_0{}^T\frac{\exp(-\mu y)}{\mu y}\right\} \times\left\{\int d\mathbf{r}\psi_0{}^*(r)\psi_0(r)\exp(i\Delta\mathbf{p}/2\cdot\mathbf{r})\right\},$$

$$I_2 = \int d\mathbf{y}\exp(-i(\mathbf{p}_t+\mathbf{p}_o/2)\cdot\mathbf{y})V_0{}^T\frac{\exp(-\mu y)}{\mu y} \times\int d\mathbf{r}\psi_0{}^*(r)\psi_0(|\mathbf{y}+\mathbf{r}|)\exp(-i\Delta\mathbf{p}/2\cdot\mathbf{r}),$$

$$I_3 = \left\{\int d\mathbf{y}\exp(-i(\mathbf{p}_t+\mathbf{p}_o/2)\cdot\mathbf{y})\psi_0(y)\right\} \times\left\{\int d\mathbf{r}\exp(i(\mathbf{p}_t/2+\mathbf{p}_o)\cdot\mathbf{r})\psi_0{}^*(r)V_0{}^T\frac{\exp(-\mu r)}{\mu r}\right\}$$

and $\eta = V_0{}^S/V_0{}^T$.

In the evaluation of the integrals I_1, I_2, I_3, the bound state of the deuteron $\psi_0(r)$, corresponding to the Yukawa potential, $V_0{}^T(\exp(-\mu r)/\mu r)$, must be used. This function can be approximated

with great accuracy by the difference of two exponentials, divided by r.

$$\psi_0(r)\cong A\frac{\exp(-\alpha r)-\exp(-\beta r)}{r},$$

where

$$A^2=\frac{\alpha\beta(\alpha+\beta)}{2\pi(\alpha-\beta)^2},\quad \alpha=\frac{(mB)^{\frac{1}{2}}}{\hbar},\quad \beta=5.476\alpha.$$

B is the binding energy of the deuteron, 2.18 Mev. This function has a maximum deviation from the exact function as obtained by numerical integration of 3 percent. Outside the range of the force, the two practically coincide. As a variational trial function it gives a fraction 0.999 of the binding energy.

It should be noted that I_1 is precisely the type of expression obtained for the matrix element in the simplified calculation. Of the three terms it is the most important since both of its factors have a strong maximum in the forward direction. I_3 has a weaker maximum to the back, and I_2 has a weak maximum to the back and a stronger one in front. These two terms represent the complications due to exchange forces and to the identity of the two neutrons.

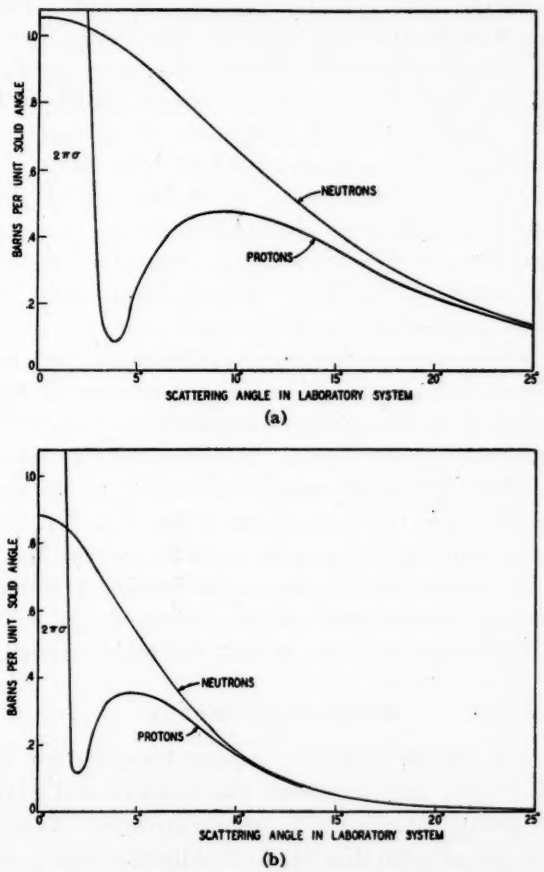

FIG. 4. Comparison of neutron-deuteron with proton-deuteron elastic scattering for small angles in the laboratory system. (a) 90-Mev incident particles, (b) 350-Mev incident particles.

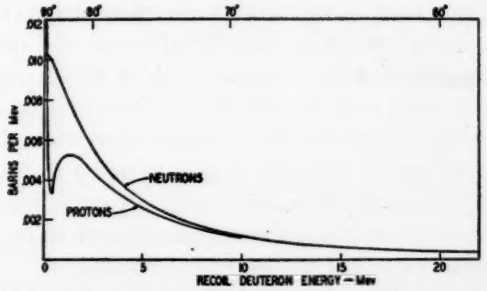

FIG. 5. Spectrum of recoil deuterons for incident nucleons of 90 Mev. The recoil angles in the laboratory system are indicated at the top of the figure.

With the above approximate wave function, I_1 can be completely evaluated analytically.

$$I_1=\frac{4\pi V_0{}^T}{\mu}\frac{1}{\mu^2+(\Delta p)^2}S^{\frac{1}{2}}(\Delta p),$$

where

$$S^{\frac{1}{2}}(\Delta p)=\frac{8\pi A^2}{\Delta p}\{\tan^{-1}\Delta p/4\alpha+\tan^{-1}\Delta p/4\beta-2\tan^{-1}\Delta p/2(\alpha+\beta)\}.$$

This is the square root of the sticking factor plotted in Fig. 1.

It is also possible to write I_3 as a fairly simple function

$$I_3=-\frac{16\pi^2\hbar^2A^2}{m}\frac{(\beta^2-\alpha^2)^2}{(\alpha^2+Q^2)(\beta^2+Q^2)^2},$$

where

$$Q=|\mathbf{p}_1+\mathbf{p}_0/2|,$$

but I_2, in which the variables of integration do not separate, can only be partially reduced. One is left finally with a single very complicated integral which can either be done numerically or, for a few special angles, by contour integration.

Having evaluated the quartet and doublet matrix elements, the total cross section is obtained by the weighted average:

$$\sigma_{el}d\omega=\frac{(\frac{2}{3}m)^2\Omega^2}{4\pi^2\hbar^4}[\tfrac{3}{4}|\mathcal{K}_{fo}{}^Q|^2+\tfrac{1}{4}|\mathcal{K}_{fo}{}^D|^2]d\omega.$$

The result is plotted as the dotted curve in Fig. 2 for 90 Mev. The total cross section of 0.059 B is slightly larger than given by the crude calculation, and the angular distribution is considerably steeper in the forward direction. Both differences are possibly attributable to the Born approximation. The one genuinely new feature is the weak backward maximum, shown in Fig. 3, a consequence of the exchange effects.

At 350 Mev the total cross section turns out to be 0.010 barn, but most of the change is due simply to the decrease in the nucleon-nucleon cross section, which is roughly inversely proportional to the energy. The angular distribution is shoved even further forward, of course, as shown in Fig. 4b.

C. Proton-Deuteron Cross Section

When the incident particle is a proton one must add to the perturbing energy the Coulomb potential between the two identical particles. The Born approximation should still be applicable, since at 90 Mev the proton velocity is half that of light. All results of part B then remain valid if one adds to both doublet and quartet matrix elements the terms

$$\Omega^{-1}\{I_1{}^C - I_2{}^C\},$$

where $I_1{}^C$ and $I_2{}^C$ are obtained from I_1 and I_2 by replacing, in the coefficients, $-V_0{}^T/\mu$ by e^2 and setting $\mu=0$ elsewhere. Since $\mu e^2/V_0{}^T=-0.018$, the additional terms are of negligible effect except for very small scattering angles and there only $I_1{}^C$ need be considered. One may easily estimate the order of magnitude of the largest angle strongly affected. $I_1{}^C$ becomes comparable to I_1 when $e^2/4p_0{}^2\sin^2\theta/2$ is no longer small compared to

$$\frac{V_0{}^T}{\mu}\,\frac{1}{\mu^2+4p_o{}^2\sin^2\theta/2}.$$

This is equivalent to $\theta\sim(\mu e^2/V_0{}^T)^{\frac{1}{2}}(\mu/p_0)$. At 90 Mev, this is an angle of 5° and at 350 Mev an angle of 2.5°, both in the center-of-gravity system. The corresponding laboratory angles are two-thirds of these.

In Figs. 4a and b the small-angle scattering of neutrons and protons is compared, showing in detail the above qualitative feature. Actually a difference between the neutron and proton scattering at 90 Mev should already be noticeable at 10° in the laboratory system. As is usual when the Coulomb force is involved, it is necessary to set a lower limit on the scattering angle if a finite total cross section is to be obtained.

IV. SUMMARY AND DISCUSSION

We have found that at high energies the cross section for the elastic scattering of neutrons on deuterons should be roughly half the neutron-proton cross section, the ratio not being a strong function of the energy. The reason for this is that in the individual nucleon-nucleon collisions momentum transfers corresponding to energies greater than 10 or 15 times the binding energy of the deuteron are unlikely, due to the finite range of the forces. Interference and the reduced mass effect then combine to give the fairly large total.

Nearly all the scattering should be confined to small angles, the angular half-width being about 15° at 90 Mev and varying inversely as the square root of the energy. There probably is a very weak backward maximum, as a result of exchange effects, which is unlikely to be observed.

The proton scattering at 90 Mev should be found to deviate appreciably from that of neutrons if the small-angle intensity can be measured at all. The Coulomb force ought to show itself quite strongly at 10°.

From an experimental standpoint, it may be easier to measure the energy spectrum of the recoil deuterons rather than the actual scattered nucleon intensity. In Fig. 5, accordingly, we have plotted the recoil energy spectrum to be expected from the calculation of Section III, for both neutron and proton projectiles at 90 Mev. The simpler considerations of Section I would predict a somewhat less steep distribution, with a half-width of about 4 Mev for the deuterons.

ACKNOWLEDGMENTS

The author wishes to express his gratitude to E. Fermi, who suggested the problem and gave frequent advice and encouragement. Many thanks are also due M. L. Goldberger who contributed invaluably to all phases of the investigation.

PHYSICAL REVIEW VOLUME 74, NUMBER 7 OCTOBER 1, 1948

The Theory of Magnetic Poles

P. A. M. DIRAC
Institute for Advanced Study, Princeton, New Jersey
(Received June 21, 1948)

If one supposes that a particle with a single magnetic pole can exist and that it interacts with charged particles, the laws of quantum mechanics lead to the requirement that the electric charges shall be quantized—all charges must be integral multiples of a unit charge e connected with the pole strength g by the formula $eg=\frac{1}{2}\hbar c$. Since electric charges are known to be quantized and no reason for this has yet been proposed apart from the existence of magnetic poles, we have here a reason for taking magnetic poles seriously. The fact that they have not yet been observed may be ascribed to the large value of the quantum of pole.

In 1931 I gave a primitive theory which described the motion of a pole in the field of a charged particle whose motion is given, or the motion of a charged particle in the field of a pole whose motion is given. The present paper sets up a general theory of charged particles and poles in interaction through the medium of the electromagnetic field. The idea which makes this generalization possible consists in supposing each pole to be at the end of an unobservable string, which is the line along which the electromagnetic potentials are singular, and introducing dynamical coordinates and momenta to describe the motion of the strings. The whole theory then comes out by the application of standard methods. There are unsolved difficulties, concerned with the interaction of a point charge or a point pole with the field it produces itself, such as occur in all dynamical theories of fields and particles in interaction.

I. INTRODUCTION

THE field equations of electrodynamics are symmetrical between electric and magnetic forces. The symmetry between electricity and magnetism is, however, disturbed by the fact that a single electric charge may occur on a particle, while a single magnetic pole has not been observed to occur on a particle. In the present paper a theory will be developed in which a single magnetic pole can occur on a particle, and the dissymmetry between electricity and magnetism will consist only in the smallest pole which can occur, being much greater than the smallest charge. This will result in an enormous energy being needed to produce a particle with a single pole, which can very well explain why such particles have not been observed up to the present.[1]

There are several kinds of particles in experimental physics for which satisfactory theories do not yet exist, and one may wonder what is the value of postulating a quite new kind of particle for which there is no experimental evidence, and thus introducing a further complication into the study of elementary particles. The interest of the theory of magnetic poles is that it forms a natural generalization of the usual electrodynamics and *it leads to the quantization of electricity*. One can set up consistent equations in quantum mechanics for the interaction of a pole of strength g with an electric charge e, only provided

$$eg=\tfrac{1}{2}n\hbar c, \tag{1}$$

where n is an integer. Thus the mere existence of one pole of strength g would require all electric charges to be quantized in units of $\frac{1}{2}\hbar c/g$ and, similarly, the existence of one charge would require all poles to be quantized. The quantization of electricity is one of the most fundamental and striking features of atomic physics, and there seems to be no explanation for it apart from the theory of poles. This provides some grounds for believing in the existence of these poles.

I first put forward the idea of magnetic poles in 1931.[2] The theory I then proposed was very incomplete, as it provided only the equations of motion for a magnetic pole in the field of charged particles whose motion is given, or the equations of motion for a charged particle in the field of magnetic poles whose motion is given. The present development provides all the equations of

[1] F. Ehrenhaft [Phys. Rev. 67, 63, 201 (1945)] has obtained some experimental results which he interprets in terms of particles with single magnetic poles. This is not a confirmation of the present theory, since Ehrenhaft does not use high energies and the theory does not lead one to expect single poles to occur under the conditions of Ehrenhaft's experiments.

[2] P. A. M. Dirac, Proc. Roy. Soc. A133, 60 (1931).

motion for magnetic poles and charged particles interacting with each other through the medium of the electromagnetic field in accordance with quantum mechanics, and is a complete dynamical theory, except for the usual difficulties of the appearance of divergent integrals in the solution of the wave equation, arising from the reaction on a particle of the field it produces itself, which difficulties are of the same nature in the present theory as in the usual electrodynamics.

II. THE CLASSICAL EQUATIONS OF MOTION

We shall work all the time with relativistic notation, using the four coordinates $x_\mu (\mu = 0, 1, 2, 3)$ to fix a point in space-time and taking the velocity of light to be unity. The electromagnetic field at any point forms a 6-vector $F_{\mu\nu} = -F_{\nu\mu}$. We shall need to use the notation of the dual $(F\dagger)_{\mu\nu}$ of a 6-vector $F_{\mu\nu}$, defined by

$$(F\dagger)_{01} = F_{23}, \quad (F\dagger)_{23} = -F_{01},$$

together with the equations obtained from these by cyclic permutation of 1, 2, 3. Note that

$$(F\dagger\dagger)_{\mu\nu} = -F_{\mu\nu} \tag{2}$$

and, with a second 6-vector $G_{\mu\nu}$,

$$(F\dagger)_{\mu\nu} G^{\mu\nu} = F_{\mu\nu} (G\dagger)^{\mu\nu}.$$

The ordinary Maxwell equations are

$$\partial F_{\mu\nu}/\partial x_\nu = -4\pi j_\mu, \tag{3}$$

where j_μ is the vector formed by the charge density and current, and

$$(F\dagger)_{\mu\nu}/\partial x_\nu = 0. \tag{4}$$

Equation (4) asserts that the divergence of the magnetic flux vanishes, and must be modified in a theory which allows single poles. The density of poles and the current of poles will form a vector k_μ which is the magnetic analog of j_μ, and Eq. (4) must be replaced by

$$(F\dagger)_{\mu\nu}/\partial x_\nu = -4\pi k_\mu. \tag{4'}$$

The world-line of a particle may be described by giving the four coordinates z_μ of a point on it as functions of the proper-time s measured along it,

$$z_\mu = z_\mu(s).$$

A particle with a point charge e gives rise to a contribution to j_μ which is infinite on the world-line and zero everywhere else. We may express it with the help of the δ-function, and then have for the charge-current vector at an arbitrary point x

$$j_\mu(x) = \sum_e e \int (dz_\mu/ds)\, \delta_4(x - z)\, ds, \tag{5}$$

where the function δ_4 is defined by

$$\delta_4(x) = \delta(x_0)\delta(x_1)\delta(x_2)\delta(x_3),$$

and $\sum_e$ denotes the sum over all charged particles. Similarly, if the poles g are concentrated at points,

$$k_\mu(x) = \sum_g g \int (dz_\mu/ds)\, \delta_4(x - z)\, ds, \tag{6}$$

where $\sum_g$ denotes the sum over all particles with poles. Equations (3), (4'), (5), and (6) fix the field when the motion of the particles and the incident radiation are known.

The motion of a charged particle is given by Lorentz's equation

$$m(d^2 z_\mu/ds^2) = e(dz^\nu/ds) F_{\mu\nu}(z).$$

We may assume the analogous equation for the motion of a pole

$$m(d^2 z_\mu/ds^2) = g(dz^\nu/ds)(F\dagger)_{\mu\nu}(z). \tag{7}$$

The field quantities $F_{\mu\nu}(z)$ occuring here are to be taken at the point z where the particle is situated and are there infinitely great and singular, so that these equations do not really have any meaning. It becomes necessary to make small changes in them to avoid the infinities. A method frequently used is to depart from the point charge model, which involves replacing the δ_4 function in (5) by a smoothed-out function approximating to it; and one could apply a similar procedure in (6) for the poles. But this method leads to an additional mass for the particles which does not transform according to the requirements of relativity. A possibly better method consists of introducing a limiting process, making a small change in the field equations in such a way that there is no additional mass for the particles in the limit. The resulting theory is not Lorentz invariant before the limit, but is Lorentz invariant in the limit. This method will

be adopted here. It will require a slightly modified field function $F_{\mu\nu}^*$ to occur instead of $F_{\mu\nu}$ in Eqs. (3) and (7), so that we have the four equations of motion

$$\partial F_{\mu\nu}^*/\partial x_\nu = -4\pi \sum_\sigma e \int (dz_\mu/ds)\delta_4(x-z)ds, \quad (8)$$

$$\partial (F\dagger)_{\mu\nu}/\partial x_\nu = -4\pi \sum_\sigma g \int (dz_\mu/ds)\delta_4(x-z)ds, \quad (9)$$

$$m(d^2z_\mu/ds^2) = e(dz^\nu/ds)F_{\mu\nu}(z) \quad (10)$$

for charged particles, and

$$m(d^2z_\mu/ds^2) = g(dz^\nu/ds)(F\dagger)_{\mu\nu}^*(z) \quad (11)$$

for particles with poles. These equations, together with the equations that connect F and F^*, which are linear and will be given later, form the complete scheme of equations of motion. They are valid with arbitrary values for the e's and g's of the various particles.

III. THE ELECTROMAGNETIC POTENTIALS

To get a theory which can be transferred to quantum mechanics we need to put the equations of motion into the form of an action principle and for this purpose we require the electromagnetic potentials. The usual way of introducing them consists of putting

$$F_{\mu\nu} = \partial A_\nu/\partial x^\mu - \partial A_\mu/\partial x^\nu, \quad (12)$$

but this is no longer possible when there are magnetic poles, since Eq. (12) leads to Eq. (4) and thus contradicts (9). Therefore, it is necessary to modify (12).

If we consider one instant of time, Eq. (12) or (4) requires that the total magnetic flux crossing any closed surface at this time shall be zero. This is not true if there is a magnetic pole inside the closed surface. Equation (12) must then fail somewhere on the surface, and we may suppose that it fails at only one point. Equation (12) will fail at one point on every closed surface surrounding the pole, so that it will fail on a line of points, which we shall call a *string*, extending outward from the pole. The string may be any curved line, extending from the pole to infinity or to another pole of equal and opposite strength. Every pole must be at the end of such a string.

The variables needed to fix the positions of the strings will be treated as dynamical coordinates and momenta conjugate to them will be introduced later. These variables are needed for the dynamical theory, but they do not correspond to anything observable and their values in a specific problem are always arbitrary and do not influence physical phenomena. They may be called *unphysical* variables.

Unphysical variables have occurred previously in dynamical theory. For example, in ordinary electrodynamics the extra variables needed to describe the potentials when the field is fixed are unphysical variables. A more elementary example is provided by the azimuthal angle of a rotating body which is symmetrical about its axis of rotation. Unphysical variables can always be eliminated by a suitable transformation, but this may introduce such a lack of symmetry into the theory as to make it not worth while. (The unphysical variables describing the strings could be eliminated by imposing the condition that the strings must always extend in the direction of the x_1-axis from each pole to infinity. With the strings fixed in this way no variables would be needed to describe them, but the symmetry of the equations under three-dimensional rotations would be completely spoilt. The physical consequences of the theory would not be affected.)

Each string will trace out a two-dimensional sheet in space-time. These sheets will be the regions where Eq. (12) fails. Each sheet may be described by expressing a general point y_μ on it as a function of two parameters τ_0 and τ_1,

$$y_\mu = y_\mu(\tau_0, \tau_1).$$

Let us suppose for definiteness that each string extends to infinity. Then the parameters τ_0 and τ_1 may be arranged so that $\tau_1 = 0$ on the world-line of the pole and extends to infinity as one follows a string to infinity, and τ_0 goes from $-\infty$ to ∞ as one goes from infinite past to infinite future.

Equation (12) must be replaced by an equation of the form

$$F_{\mu\nu} = \partial A_\nu/\partial x^\mu - \partial A_\mu/\partial x^\nu + 4\pi \sum_\sigma (G\dagger)_{\mu\nu}, \quad (13)$$

where each $(G\dagger)_{\mu\nu}$ is a field quantity which vanishes everywhere except on one of the sheets

and the summation is taken over all the sheets, one of which is associated with each pole. Substituting (13) into (9) we find, remembering (2),

$$\partial G_{\mu\nu}/\partial x_\nu = g\int (dz_\mu/ds)\delta_4(x-z)ds. \qquad (14)$$

This is the equation which determines $G_{\mu\nu}$.

It is easily verified that the solution of Eq. (14) is

$$G_{\mu\nu}(x) = g\int\int\left(\frac{\partial y_\mu}{\partial\tau_0}\frac{\partial y_\nu}{\partial\tau_1} - \frac{\partial y_\mu}{\partial\tau_1}\frac{\partial y_\nu}{\partial\tau_0}\right) \times\delta_4(x-y)d\tau_0 d\tau_1, \qquad (15)$$

integrated over the whole sheet. In fact (15) gives directly

$$\frac{\partial G_{\mu\nu}}{\partial x_\nu} = g\int\int\left(\frac{\partial y_\mu}{\partial\tau_0}\frac{\partial y_\nu}{\partial\tau_1} - \frac{\partial y_\mu}{\partial\tau_1}\frac{\partial y_\nu}{\partial\tau_0}\right)\frac{\partial\delta_4(x-y)}{\partial x_\nu}d\tau_0 d\tau_1,$$

$$= -g\int\int\left(\frac{\partial y_\mu}{\partial\tau_0}\frac{\partial y_\nu}{\partial\tau_1} - \frac{\partial y_\mu}{\partial\tau_1}\frac{\partial y_\nu}{\partial\tau_0}\right) \times\frac{\partial\delta_4(x-y)}{\partial y_\nu}d\tau_0 d\tau_1,$$

$$= -g\int\int\left(\frac{\partial y_\mu}{\partial\tau_0}\frac{\partial\delta_4(x-y)}{\partial\tau_1} - \frac{\partial y_\mu}{\partial\tau_1}\frac{\partial\delta_4(x-y)}{\partial\tau_0}\right)d\tau_0 d\tau_1.$$

From Stokes' theorem, for any two functions U and V on the sheet,

$$\int\int\left(\frac{\partial U}{\partial\tau_0}\frac{\partial V}{\partial\tau_1} - \frac{\partial U}{\partial\tau_1}\frac{\partial V}{\partial\tau_0}\right)d\tau_0 d\tau_1 = \int U\left(\frac{\partial V}{\partial\tau_0}d\tau_0 + \frac{\partial V}{\partial\tau_1}d\tau_1\right), \qquad (16)$$

the left-hand integral being taken over any area of the sheet and the right-hand integral along the rim of that area. Putting $U=\delta_4(x-y)$, $V=y_\mu$, and applying the theorem to the whole sheet, so that the only part of the rim not at infinity is the world-line of the pole, we get

$$\partial G_{\mu\nu}/\partial x_\nu = g\int \delta_4(x-y)[\partial y_\mu(\tau_0,0)/\partial\tau_0]d\tau_0,$$

which agrees with (14), since $y_\mu(\tau_0, 0)=z_\mu(s)$ with τ_0 some function of s.

With given world-lines for the particles, the solution of the field equations (8) and (9) for which there is no ingoing field is called the retarded field. It is connected by (13) with the retarded potentials. The retarded potentials consist of a contribution from each particle, depending only on the world-line of that particle and on the sheet attached to it in the case when the particle has a pole. These contributions may be conveniently expressed with the help of the Lorentz invariant function $J(x)$ defined by

$$\left.\begin{aligned} J(x) &= 2\delta(x_\mu x^\mu) \quad \text{for } x_0>0,\\ &= 0 \quad\qquad\quad \text{for } x_0<0,\end{aligned}\right\} \qquad (17)$$

or by

$$J(x) = r^{-1}\delta(x_0-r),$$
$$r = (x_1^2+x_2^2+x_3^2)^{\frac{1}{2}}.$$

The function $\Delta(x)$ of Jordan and Pauli is connected with $J(x)$ by

$$\Delta(x) = J(x) - J(-x). \qquad (18)$$

It is easily verified that

$$\Box J(x) = 4\pi\delta_4(x). \qquad (19)$$

(One can check this result in the neighborhood of the origin by expressing the integral of $\Box J(x)$ over a small four-dimensional volume around the origin as a three-dimensional surface integral over the boundary of that volume.)

The contribution of a charged particle to the retarded potentials is, according to the Lienard-Wiechert formula,

$$A_\nu^*(x)_{r\text{e}} = e\int_{-\infty}^{\infty} J(x-z)(dz_\nu/ds)ds. \qquad (20)$$

(A^* is put on the left here instead of A since the field F^* occurs in (8)). The corresponding formula for the contribution of a pole is

$$A_\nu(x)_{r\text{e}} = g\epsilon_{\nu\lambda\rho\sigma}\int\int\frac{\partial y^\lambda}{\partial\tau_0}\frac{\partial y^\rho}{\partial\tau_1}\frac{\partial J(x-y)}{\partial x_\sigma}d\tau_0 d\tau_1 \qquad (21)$$

integrated over all the sheet, where $\epsilon_{\nu\lambda\rho\sigma}$ is the antisymmetrical tensor of the fourth rank with $\epsilon_{0123}=1$. To verify (21), we note that it leads to

$$\epsilon^{\mu\nu\alpha\beta}\frac{\partial A_{\nu\sigma}}{\partial x^\mu} = g\epsilon^{\mu\nu\alpha\beta}\epsilon_{\nu\lambda\rho\sigma}\int\int\frac{\partial y^\lambda}{\partial\tau_0}\frac{\partial y^\rho}{\partial\tau_1}\frac{\partial^2 J(x-y)}{\partial y^\mu\partial y_\sigma}d\tau_0 d\tau_1.$$

Using

$$\epsilon^{\mu\nu\alpha\beta}\epsilon_{\nu\lambda\rho\sigma}=\delta_\lambda{}^\mu\delta_\rho{}^\alpha\delta_\sigma{}^\beta+\delta_\rho{}^\mu\delta_\sigma{}^\alpha\delta_\lambda{}^\beta+\delta_\sigma{}^\mu\delta_\lambda{}^\alpha\delta_\rho{}^\beta-(\alpha\beta),$$

where $-(\alpha\beta)$ means that we must subtract all the preceding terms with α and β interchanged, we get

$$\epsilon^{\mu\nu\alpha\beta}\frac{\partial A_{\nu re}}{\partial x^\mu}=g\int\int\left\{\frac{\partial^2 J(x-y)}{\partial\tau_0\partial y_\beta}\frac{\partial y^\alpha}{\partial\tau_1}+\frac{\partial^2 J(x-y)}{\partial\tau_1\partial y_\alpha}\frac{\partial y^\beta}{\partial\tau_0}+\frac{\partial y^\alpha}{\partial\tau_0}\frac{\partial y^\beta}{\partial\tau_1}\Box J(x-y)\right\}d\tau_0 d\tau_1-(\alpha\beta)$$

$$=g\int\left[\frac{\partial J(x-y)}{\partial y_\beta}\right]_{y=z}\frac{dz^\alpha}{ds}ds-(\alpha\beta)+4\pi G^{\alpha\beta},$$

with the help of Stokes' theorem (16), and (19) and (15). According to (13), this gives the retarded field

$$(F\dagger)_{re}{}^{\alpha\beta}=\epsilon^{\mu\nu\alpha\beta}\partial A_{\nu re}/\partial x^\mu-4\pi G^{\alpha\beta},$$

$$=-g\int\frac{\partial J(x-z)}{\partial x_\beta}\frac{dz^\alpha}{ds}ds-(\alpha\beta),$$

$$=-\partial B_{re}{}^\alpha/\partial x_\beta+\partial B_{re}{}^\beta/\partial x_\alpha, \qquad (22)$$

with

$$B_{re}{}^\alpha=g\int J(x-z)(dz^\alpha/ds)ds. \qquad (23)$$

This is seen to be the correct value for the retarded field produced by a pole, from the analogy of (23) to the Lienard-Wiechert potential (20).

In the usual electrodynamics the potentials are restricted by the condition

$$\partial A_\nu/\partial x_\nu=0 \quad \text{or} \quad \partial A_\nu{}^*/\partial x_\nu=0. \qquad (24)$$

This condition can be retained in the present theory, as it is satisfied by the retarded potentials (20), (21). The two forms of (24) are equivalent because of the linear connection between the starred and unstarred field (see Eq. (29)).

IV. THE ACTION PRINCIPLE

The action integral of ordinary electrodynamics may be expressed as a sum of the three terms, $I_1+I_2+I_3$, where I_1 is the action integral for the particles alone,

$$I_1=\sum_e m\int ds,$$

I_2 is the action integral for the field alone,

$$I_2=(16\pi)^{-1}\int F_{\mu\nu}F^{\mu\nu}d^4x,\ (d^4x=dx_0dx_1dx_2dx_3),$$

and I_3 is the contribution of the interaction of the charges with the field,

$$I_3=\sum_e e\int A^\nu(z)(dz_\nu/ds)ds. \qquad (25)$$

The $F_{\mu\nu}$ in I_2 are to be regarded as functions of the potentials.

The same action integral will do in the present theory, provided the sum in I_1 is extended to include the particles with poles as well as those with charges,

$$I_1=\sum_{e+g}m\int ds. \qquad (26)$$

No further term is needed to give the interaction between the poles and the field, this interaction being taken into account in I_2, in which $F_{\mu\nu}$ is now to be regarded as a function of the potentials and the string variables $y_\mu(\tau_0,\tau_1)$ given by (13) and (15).

In order to avoid infinities in the equations of motion arising from the infinite fields produced by point charges and poles, we shall make a small modification in the field equations, by replacing I_2 by

$$I_2'=(16\pi)^{-1}\int\int F_{\mu\nu}(x)F^{\mu\nu}(x')\gamma(x-x')d^4xd^4x',$$

where $\gamma(x)$ is a function which approximates to the function $\delta_4(x)$, and is made to tend to $\delta_4(x)$ in the limit. We shall assume that

$$\gamma(-x)=\gamma(x), \qquad (27)$$

and shall assume other properties for $\gamma(x)$ as they are needed, but the precise form of $\gamma(x)$ will be left arbitrary. We may write I_2' as

$$I_2'=(16\pi)^{-1}\int F_{\mu\nu}{}^*(x)F^{\mu\nu}(x)d^4x, \qquad (28)$$

using the notation that for any field quantity $U(x)$,

$$U^*(x)=\int U(x')\gamma(x-x')d^4x'. \qquad (29)$$

It will now be verified that the variation of

$$I=I_1+I_2'+I_3$$

leads to the correct equations of motion. The variation of I_1 is well known and gives

$$\delta I_1=-\sum_{s+\sigma}m\int(d^2z_\mu/ds^2)\delta z^\mu ds. \quad (30)$$

The variation of I_3 may be carried out the same as in ordinary electrodynamics and gives

$$\delta I_3=\sum_s e\int\{[(\partial A_\nu/\partial x^\mu)-(\partial A_\mu/\partial x^\nu)]_{x=z}\delta z^\mu + (\delta A_\nu)_{x=z}\}(dz^\nu/ds)ds. \quad (31)$$

The variation of I_2' gives, using (27)

$$\delta I_2'=(8\pi)^{-1}\int\int F_{\mu\nu}(x')\delta F^{\mu\nu}(x)\gamma(x-x')d^4xd^4x'$$

$$=(8\pi)^{-1}\int F_{\mu\nu}^*(x)\delta F^{\mu\nu}(x)d^4x.$$

Substituting for $F^{\mu\nu}$ its value given by (13), we get

$$\delta I_2'=-(4\pi)^{-1}\int F_{\mu\nu}^*(\partial\delta A^\mu/\partial x_\nu)d^4x + \tfrac{1}{2}\sum_\sigma\int F_{\mu\nu}^*\delta(G\dagger)^{\mu\nu}d^4x \quad (32)$$

$$=(4\pi)^{-1}\int(\partial F_{\mu\nu}^*/\partial x_\nu)\delta A^\mu d^4x + \tfrac{1}{2}\sum_\sigma\int(F\dagger)_{\mu\nu}^*\delta G^{\mu\nu}d^4x. \quad (33)$$

Using (15), the second term here becomes

$$\sum_\sigma g\int(F\dagger)_{\mu\nu}^*d^4x\delta\int\int\frac{\partial y^\mu}{\partial\tau_0}\frac{\partial y^\nu}{\partial\tau_1}\delta_4(x-y)d\tau_0d\tau_1$$

$$=\sum_\sigma g\int(F\dagger)_{\mu\nu}^*d^4x\int\int\left\{\delta\left(\frac{\partial y^\mu}{\partial\tau_0}\frac{\partial y^\nu}{\partial\tau_1}\right)\delta_4(x-y) + \frac{\partial y^\mu}{\partial\tau_0}\frac{\partial y^\nu}{\partial\tau_1}\frac{\partial\delta_4(x-y)}{\partial y^\rho}\delta y^\rho\right\}d\tau_0d\tau_1$$

$$=\sum_\sigma g\int\int\left\{(F\dagger)_{\mu\nu}^*(y)\left(\frac{\partial\delta y^\mu}{\partial\tau_0}\frac{\partial y^\nu}{\partial\tau_1}-\frac{\partial\delta y^\mu}{\partial\tau_1}\frac{\partial y^\nu}{\partial\tau_0}\right) + \frac{\partial(F\dagger)_{\mu\nu}^*(y)}{\partial y^\rho}\frac{\partial y^\mu}{\partial\tau_0}\frac{\partial y^\nu}{\partial\tau_1}\delta y^\rho\right\}d\tau_0d\tau_1$$

$$=\sum_\sigma g\int\int\left\{\frac{\partial((F\dagger)_{\mu\nu}^*\delta y^\mu)}{\partial\tau_0}\frac{\partial y^\nu}{\partial\tau_1} - \frac{\partial((F\dagger)_{\mu\nu}^*\delta y^\mu)}{\partial\tau_1}\frac{\partial y^\nu}{\partial\tau_0} - \frac{\partial(F\dagger)_{\mu\nu}^*}{\partial y^\rho}\left(\frac{\partial y^\rho}{\partial\tau_0}\frac{\partial y^\nu}{\partial\tau_1}\delta y^\mu - \frac{\partial y^\rho}{\partial\tau_1}\frac{\partial y^\nu}{\partial\tau_0}\delta y^\mu - \frac{\partial y^\mu}{\partial\tau_0}\frac{\partial y^\nu}{\partial\tau_1}\delta y^\rho\right)\right\}d\tau_0d\tau_1$$

$$=\sum_\sigma g\int(F\dagger)_{\mu\nu}^*(z)\delta z^\mu\frac{dz^\nu}{ds}ds - \sum_\sigma g\int\int\left(\frac{\partial(F\dagger)_{\mu\nu}^*}{\partial y^\rho}+\frac{\partial(F\dagger)_{\nu\rho}^*}{\partial y^\mu} + \frac{\partial(F\dagger)_{\rho\mu}}{\partial y^\nu}\right)\frac{\partial y^\rho}{\partial\tau_0}\frac{\partial y^\nu}{\partial\tau_1}\delta y^\mu d\tau_0d\tau_1 \quad (34)$$

by a further application of Stokes' theorem (16). The total variation δI is given by the sum of (30), (31), (34) and the first term in (33).

By equating to zero the coefficient of $\delta A^\mu(x)$ in δI, we get precisely Eq. (8). By equating to zero the coefficient of δz^μ for a charged particle we get

$$m(d^2z_\mu/ds^2)=e[(\partial A_\nu/\partial x_\mu)-(\partial A_\mu/\partial x^\nu)]_{x=z}(dz^\nu/ds).$$

This agrees with the equation of motion (10) provided the charged particle does not lie on any of the strings, so that $G_{\mu\nu}(z)=0$. By equating to zero the coefficient of δz^μ for a pole, we get precisely (11). Equation (9) is a consequence of Eqs. (13) and (15), which express $F_{\mu\nu}$ in terms of the potentials and string variables. Thus all the equations of motion (8), (9), (10), and (11) follow from the action principle $\delta I=0$, provided we impose the condition that *a string must never pass through a charged particle.*

By equating to zero the coefficient of the variation δy^μ in a string variable, we get

$$\partial(F\dagger)_{\mu\nu}^*/\partial y^\rho+\partial(F\dagger)_{\nu\rho}^*/\partial y^\mu+\partial(F\dagger)_{\rho\mu}^*/\partial y^\nu=0$$

or

$$\partial F_{\mu\nu}^*/\partial y_\nu=0,$$

holding at all points on the sheet. From (8) this is automatically satisfied, provided the string never passes through a charged particle. Thus the action principle leads to no equations

of motion for the string variables, in conformity with the unphysical nature of these variables.

The action integral I is a correct one and may be used as basis for a theory of electrodynamics, but it leads to some inconvenience in the Hamiltonian formulation of the equations of motion, since it makes the momentum conjugate to A_0 vanish identically. This inconvenience may be avoided by a method due to Fermi, which consists in adding on a further term to the action integral

$$I_4=(8\pi)^{-1}\int(\partial A_\nu^*/\partial x_\mu)(\partial A_\mu/\partial x_\nu)d^4x. \quad (35)$$

This gives

$$\delta I_4=(4\pi)^{-1}\int(\partial A_\nu^*/\partial x_\mu)(\partial\delta A_\mu/\partial x_\nu)d^4x \quad (36)$$

$$=-(4\pi)^{-1}\int(\partial^2 A_\nu^*/\partial x_\nu\partial x^\mu)\delta A^\mu d^4x, \quad (37)$$

and leads to a further term $-\partial^2 A_\nu^*/\partial x_\nu\partial x^\mu$ on the left-hand side of Eq. (8). This further term in (8) does not affect the equations of motion, because it vanishes when one uses the supplementary condition (24), but in the Hamiltonian formulation it is necessary to distinguish between those equations that hold only in virtue of supplementary conditions and those that are independent of supplementary conditions. Therefore, we must leave this term in (8) to have an equation of the latter kind. Equation (8) may now be written, with the help of (13) and (15),

$$\Box A_\mu^*(x)=4\pi\sum_e e\int(dz_\mu/ds)\delta_4(x-z)ds$$
$$+4\pi\sum_\sigma\partial(G\dagger)_{\mu\nu}^*/\partial x_\nu. \quad (38)$$

V. THE METHOD OF PASSING TO THE HAMILTONIAN FORMULATION

When one has the equations of motion of a dynamical system in the form of an action principle, one must put them into the Hamiltonian form as the next step in the process of quantization. The general procedure for doing this is to take the action integral previous to a certain time t and to form its variation allowing t to vary. This variation δI appears as a linear function of δt and of the variations δq in the dynamical coordinates at time t, the other terms in δI cancelling when one uses the equations of motion. One introduces the total variation in the final q's

$$\Delta q=\delta q+\dot{q}\delta t,$$

and expresses δI in terms of the Δq's and δt. One puts this equal to

$$\delta I=\sum p_r\Delta q_r-W\delta t, \quad (39)$$

(or the corresponding expression with an integral instead of a sum) and so defines the momenta p_r and the energy W. The p_r and W appear as functions of the coordinates q_r and velocities $\dot{q}_r$, and since the number of variables in the set p_r, W is one greater than the number of velocities $\dot{q}_r$, there must be a relation between the p_r, W and the coordinates, of the form

$$W-H(pq)=0. \quad (40)$$

The p's and $-W$ are the partial derivatives of I with respect to the q's and t, so (40) gives a differential equation satisfied by I, called the *Hamilton-Jacobi equation*. From this equation one can pass to the wave equation of quantum mechanics by the application of certain rules. There may be more than one equation connecting the p's, q's, and W, in which case there are more than one Hamilton-Jacobi equation, leading to more than one wave equation.

To make the above procedure relativistic, one must take the action integral over space-time previous to a certain three-dimensional space-like surface S extending to infinity. One must form its variation, making a general variation in S as well as in the dynamical coordinates previous to S, and express the result in terms of the total variation in various dynamical quantities on S. This will again give an equation of the type (39) and one can again define the coefficients in it as momenta and set up the Hamilton-Jacobi equation.

There are various ways of modifying this procedure, which may be convenient for particular problems. Instead of stopping the action integral sharply at one definite time or at one definite three-dimensional space-like surface S, one may stop different terms in it at different times. One can picture the stopping of the action integral by supposing the dynamical system to go out of existence in some unnatural way and taking the total action before it goes out of

existence. To stop different terms in the action integral at different times one must picture different parts of the dynamical system going out of existence at different times. After some parts have gone out of existence, the remaining parts continue to move in accordance with the equations of motion which follow from the surviving terms in the action integral, until they in turn go out of existence. The various ways of stopping the action integral lead to different Hamilton-Jacobi equations (40), which are equally valid and differ one from another by contact transformations.

A convenient way of stopping the action integral when one has particles interacting with a field is first to suppose the particles go out of existence at points in space-time lying outside each other's light cones, and then to stop the field at a considerably later time. One varies this stopped action integral, making variations in the points z_μ in space-time where the particles go out of existence and also in the surface S_F where the field goes out of existence. By equating to zero that part of the variation of the stopped action integral which is not connected with boundary variations, one gets the same equations of motion for the particles before they go out of existence as one had with the unstopped action integral, and one gets field equations which continue to govern the field after the particles have gone out of existence. Owing to the variations Δz_μ in the points z_μ occurring in regions of space-time completely immersed in the field, one gets equations which are more convenient to handle than those of the usual method in which one supposes the particles and the field to go out of existence together.

With the new electrodynamics let us suppose all the particles, and also the strings attached to the poles, go out of existence at a three-dimensional space-like surface S_P and the electromagnetic field goes out of existence at a much later surface S_F. This means that the integrals I_1, I_3 given by (26), (25) are to be stopped when the world-lines reach S_P and the integral over the sheet in (15) is to be stopped when the sheet reaches S_P, while I_2', I_4 given by (28), (35) are to be stopped at the boundary S_F. The stopping of these integrals will not affect the equations of motion for particles and field previous to S_P, namely (10), (11), (38), and further (38) will continue to hold through S_P and afterwards, until S_F.

Let us assume that the connection (29) between a field quantity U and U^* is such that the value of either of them at a point x is determined by the values of the other at points in space-time near x. Thus, if either of them vanishes in a certain region of space-time, the other will also vanish in that region, except possibly at points near the boundary.

Since $G_{\mu\nu}$ vanishes everywhere except on the sheets, $G_{\mu\nu}^*$ must now vanish in the region between S_P and S_F, with the exception of points near where the strings go out of existence. In this region we also have the first sum on the right-hand side of (38) vanishing, since the integrals are stopped at S_P, and hence we can infer from (38),

$$\Box A_\mu^*(x)=0. \tag{41}$$

By a similar argument we can infer

$$\Box A_\mu(x)=0 \tag{42}$$

in the region between S_P and S_F, with the exception of points near where the charged particles go out of existence.

In the regions where (42) and (41) hold we can make Fourier resolutions of $A_\mu(x)$ and $A_\mu^*(x)$ thus:

$$A_\mu(x)=\sum k_0 \int A_{k\mu} e^{i(kx)} k_0^{-1} d^3k, \tag{43}$$

$$A_\mu^*(x)=\sum k_0 \int A_{k\mu}^* e^{i(kx)} k_0^{-1} d^3k, \tag{44}$$

where

$$(kx)=k_0x_0-k_1x_1-k_2x_2-k_3x_3,$$
$$d^3k=dk_1dk_2dk_3,$$
$$k_0=\pm(k_1^2+k_2^2+k_3^2)^{\frac{1}{2}},$$

and $\sum k_0$ means the sum over both values of k_0 for given k_1, k_2, k_3. The factor k_0^{-1} is introduced because $k_0^{-1}d^3k$ is Lorentz invariant. The condition that $A_\mu(x)$, $A_\mu^*(x)$ are real gives

$$A_{-k\mu}=-\bar{A}_{k\mu}, \quad A_{-k\mu}^*=-\bar{A}_{k\mu}^*. \tag{45}$$

Let the Fourier resolution of the function $\gamma(x)$ be

$$\gamma(x)=(2\pi)^{-4}\int \gamma_l e^{i(lx)} d^4l$$

with

$$\gamma_{-l}=\bar{\gamma}_l.$$

The condition $\gamma(-x)=\gamma(x)$ gives

$$\gamma_{-l}=\gamma_l, \tag{46}$$

so γ_l is real. We now find by straightforward integration that

$$A_{k\mu}{}^*=\gamma_k A_{k\mu}. \tag{47}$$

We shall need to have the Fourier resolution (43) holding at each point z where a charged particle goes out of existence and the Fourier resolution (44) holding at each point y where a string goes out of existence. It seems probable that this can be arranged to be so by a suitable choice of the function γ, provided a point y is never very close to a point z. Let us assume that a field quantity $U(x)$ is determined by $U^*(x')$ at points x' lying close to x and outside the light cone from x. Then $A_\mu(z)$ is determined by $A_\mu{}^*(x')$ at points x' for which the Fourier resolution (44) is valid, so the Fourier resolution of $A_\mu(z)$ will be valid. Similarly, the Fourier resolution of $A_\mu{}^*(y)$ will be valid if $U^*(x)$ is determined by $U(x')$ at points x' lying close to x and outside the light cone of x.

The supplementary condition (24) gets modified in the region between S_P and S_F. With the integrals in (20) and (21) stopped at S_P, we have, writing z' for $z(s')$,

$$\frac{\partial A_\nu{}^*}{\partial x_\nu}=\sum_e e\int_{-\infty}^{s}\frac{\partial J(x-z')}{\partial x_\nu}\frac{dz_\nu'}{ds'}ds',$$

$$=-\sum_e e\int_{-\infty}^{s}\frac{\partial J(x-z')}{\partial z_\nu'}\frac{dz_\nu'}{ds'}ds',$$

$$=-\sum_e eJ(x-z). \tag{48}$$

This quantity differs from zero when x is on the future light cone of any point z where a charged particle goes out of existence. Equations (41) and (48) show that the potentials $A_\mu{}^*$ give a Wentzel type of field[8] between S_P and S_F.

VI. THE HAMILTONIAN FORMULATION

Let us form the variation of the action integral bounded as above, allowing S_P to vary but not S_F, and let us evaluate the terms in δI connected with the boundaries. The terms arising from δI_1 and δI_3 are, as in ordinary electrodynamics.

$$\sum_{e+\sigma} m(dz_\mu/ds)\Delta z^\mu+\sum_e eA_\mu(z)\Delta z^\mu, \tag{49}$$

where the Δz^μ are the total changes of the coordinates of the point where a particle goes out of existence. In forming $\delta I_2'$ we can no longer use (32), but must use instead

$$\delta I_2'=-(8\pi)^{-1}\int_{-\infty}^{S_F}\{F_{\mu\nu}{}^*(\partial\delta A^\mu/\partial x_\nu)$$

$$+F_{\mu\nu}(\partial\delta A^{\mu*}/\partial x_\nu)\}d^4x+\tfrac{1}{4}\sum_\sigma\int_{-\infty}^{S_F}\{F_{\mu\nu}{}^*\delta(G\dagger)^{\mu\nu}$$

$$+F_{\mu\nu}\delta(G\dagger)^{\mu\nu*}\}d^4x. \tag{50}$$

The second term here is equal to

$$\tfrac{1}{2}\sum_\sigma\int_{-\infty}^{\infty}F_{\mu\nu}{}^*\delta(G\dagger)^{\mu\nu}d^4x,$$

provided S_F is sufficiently far from S_P, so that $\gamma(x-x')=0$ for x earlier than S_P and x' later than S_F. We may now use the calculation which led to (34), with the integrals over the sheets extending only over the parts of the sheets previous to S_P, and we then get extra terms, coming from the application of Stokes' theorem, of the form of line integrals along the lines where the sheets meet S_P. By arranging the parametrization of the sheets so that the line where a sheet meets S_P is given by $\tau_0=$constant, and the line where the varied sheet meets the varied S_P is given by $\tau_0=$same constant, these line integrals take the form

$$\sum_\sigma g\int_0^\infty(F\dagger)_{\mu\nu}{}^*\delta y^\mu(dy^\nu/d\tau_1)d\tau_1. \tag{51}$$

The lines of integration are the positions of the strings when they go out of existence. In forming δI_4 we can no longer use (36), but must use instead

$$\delta I_4=(8\pi)^{-1}\int_{-\infty}^{S_F}\{(\partial A_\nu{}^*/\partial x^\mu)(\partial\delta A^\mu/\partial x_\nu)$$

$$+(\partial A_\nu/\partial x^\mu)(\partial\delta A^{\mu*}/\partial x_\nu)\}d^4x. \tag{52}$$

[8] The properties of this field are given, for example, in P. Dirac, Annales de l'Inst. Henri Poincaré 9, 23 (1939).

This quantity is of the same form as the first term of the right-hand side of (50), and the two together give, on integration by parts, a boundary term of the form of an integral over the three-dimensional surface S_F, which may be written

$$(8\pi)^{-1}\int\{(\partial A_\mu^*/\partial x^\nu)\delta A^\mu + (\partial A_\mu/\partial x^\nu)\delta A^{\mu *}\}dS^\nu, \quad (53)$$

dS^ν being an element of this surface. The other terms in δI all cancel when one uses the equations of motion, provided S_F is not very close to S_P, so we are left with δI equal to the sum of (49), (51) and (53).

With this expression for δI, we cannot directly introduce the momenta in accordance with formula (39), since the A^μ, $A^{\mu *}$ whose variations occur in (53) are not independent, and since we have not varied S_F. A convenient way of proceeding is to pass to the Fourier components of the potentials, for which we may use the Fourier resolutions given by (43) and (44), as we are concerned in expression (53) with the potentials on the surface S_F. Let us take a varied motion which satisfies the equation of motion, so that the Fourier resolutions (43), (44) are valid on S_F also for the varied motion. Then expression (53) becomes, with the help of (47),

$$(8\pi)^{-1}i\sum_{k_0k_0'}\int\int\int k_\nu(\gamma_k+\gamma_{k'})\times A_{k\mu}\delta A_{k'}{}^\mu e^{i(k+k',x)}k_0^{-1}d^3k k_0'^{-1}d^3k'dS^\nu.$$

If we take the surface S_F to be $x_0=$constant for simplicity (any space-like surface must give the same final result), this becomes, on integrating with respect to x_1, x_2 and x_3,

$$\pi^2 i\sum_{k_0k_0'}\int\int(\gamma_k+\gamma_{k'})A_{k\mu}\delta A_{k'}{}^\mu \times\exp[i(k_0+k_0')x_0]\delta_3(k+k')d^3k k_0'^{-1}d^3k',$$

where $\delta_3(k)$ means $\delta(k_1)\delta(k_2)\delta(k_3)$. The factor $\delta_3(k+k')$ here shows that the integrand vanishes except when $k_r'=-k_r(r=1,2,3)$, which implies $k_0'=\pm k_0$. Thus the expression reduces, with the help of (46), to

$$-2\pi^2 i\sum_{k_0}\int\gamma_k A_{k\mu}\delta A_{-k}{}^\mu k_0^{-1}d^3k + \pi^2 i\sum_{k_0}\int(\gamma_k+\gamma_{k_0,-k_r})A_{k\mu}\delta A_{k_0,-k_r}{}^\mu \times\exp[2ik_0x_0]k_0^{-1}d^3k.$$

The second term here may be written as a perfect differential,

$$\pi^2 i\delta\sum_{k_0}\int\gamma_k A_{k\mu}A_{k_0,-k_r}{}^\mu\exp[2ik_0x_0]k_0^{-1}d^3k,$$

and may therefore be discarded. The first term may be written, if we now restrict k_0 to be >0 and use (45) and (46),

$$2\pi^2 i\int\gamma_k(A_{k\mu}\delta\bar{A}_k{}^\mu-\bar{A}_{k\mu}\delta A_k{}^\mu)k_0^{-1}d^3k = 2\pi^2 i\delta\int\gamma_k A_{k\mu}\bar{A}_k{}^\mu k_0^{-1}d^3k - 4\pi^2 i\int\gamma_k\bar{A}_{k\mu}\delta A_k{}^\mu k_0^{-1}d^3k. \quad (54)$$

The first term in (54) is a perfect differential and may be discarded. We thus get the final result that δI is equal to, apart from a perfect differential, the sum of (49), (51), and the second term of (54).

We take as dynamical coordinates the coordinates z_μ of the particles when they go out of existence, the coordinates $y_\mu(\tau_1)$ of points on the strings when they go out of existence (providing a one-dimensional continuum of coordinates for each pole and each value of μ), and the Fourier components $A_{k\mu}$, with $k_0>0$, of the potentials after the particles and strings have gone out of existence. The coefficients of the variations of these coordinates in the expression for δI given by the sum of (49), (51), and the second term of (54) will be the conjugate momenta. Thus the momenta of a charged particle are

$$p_\mu=mdz_\mu/ds+eA_\mu(z), \quad (55)$$

those of a particle with a pole are

$$p_\mu=mdz_\mu/ds, \quad (56)$$

the momenta conjugate to the string variables

$y^\mu(\tau_1)$—let us call them $\beta^\mu(\tau_1)$—are

$$\beta_\mu(\tau_1)=g(F\dagger)_{\mu\nu}{}^*dy^\nu/d\tau_1, \tag{57}$$

and the momentum conjugate to $A_k{}^\mu$ is

$$-4\pi^2 i\gamma_k\bar{A}_{k\mu}k_0{}^{-1}. \tag{58}$$

The string momenta $\beta_\mu(\tau_1)$ form a one-dimensional continuum of variables, corresponding to the one-dimensional continuum of coordinates $y^\mu(\tau_1)$, and the field momenta (58) form a three-dimensional continuum, corresponding to the three dimensional continuum of field coordinates.

We may introduce Poisson brackets in the usual way. For the coordinates and momenta of each particle we have

$$[p_\mu, z_\nu]=g_{\mu\nu}. \tag{59}$$

For the coordinates and momenta of a string we have

$$[\beta_\mu(\tau_1), y_\nu(\tau_1')]=g_{\mu\nu}\delta(\tau_1-\tau_1'), \tag{60}$$

and for the field variables we have, according to (58),

$$[\bar{A}_{k\mu}, A_{k'\nu}]=i(4\pi^2)^{-1}g_{\mu\nu}\gamma_k{}^{-1}k_0\delta_3(k-k'). \tag{61}$$

The other P.B.'s all vanish.

In the limit when $\gamma(x)\to\delta_4(x)$, we have $\gamma_k\to 1$ and Eq. (61) gives the usual P.B. relation for the Fourier amplitudes of the elctromagnetic potentials. If we take $\gamma_k{}^{-1}=\cos(k\lambda)$, where λ is a small four-vector satisfying $\lambda^2>0$, and make $\lambda\to 0$, we get a limiting procedure which has already been used in electrodynamics, classical and quantum, and which gets over some of the difficulties connected with the infinite fields caused by point particles. This value for γ_k might be suitable in the present theory, but I have not investigated whether it would be compatible with all the requirements of the function $\gamma(x)$.

From Eqs. (55) and (56) we can eliminate the velocities dz_μ/ds and get

$$\{p_\mu-eA_\mu(z)\}\{p^\mu-eA^\mu(z)\}-m^2=0 \tag{62}$$

for each charged particle and

$$p_\mu p^\mu-m^2=0 \tag{63}$$

for each particle with a pole. These equations should be joined with (57) or

$$\beta_\mu(\tau_1)-g(F\dagger)_{\mu\nu}{}^*(y)dy^\nu/d\tau_1=0. \tag{64}$$

With the $A_\mu(z)$ in (62) and the $(F\dagger)_{\mu\nu}{}^*(y)$ in (64) expressed in terms of the Fourier components $A_{k\mu}$, $\bar{A}_{k\mu}$ (the validity of this was discussed near the end of the preceding section), Eqs. (62), (63), and (64) are equations involving only dynamical coordinates and momenta. They are differential equations satisfied by the action integral I, when the momenta are looked upon as derivatives of I, and they are the Hamilton-Jacobi equations of the present theory. Since they are known to have a solution, namely I itself, we can infer from the theory of differential equations that the P.B.'s of their left-hand sides all vanish, as may also be verified directly from (59), (60), and (61).

The supplementary conditions (48) should be brought in at this stage and treated as further Hamilton-Jacobi equations. The various equations (48) obtained by taking different field points x are not independent of the equations of motion or of one another, and we get a complete independent set of equations from them by making a Fourier resolution in the region between S_P and $S_{P'}$. In this region we may, from (18), replace $J(x-z)$ by $\Delta(x-z)$, whose Fourier components are given by

$$\Delta(x-z)=-i(4\pi^2)^{-1}\sum_{k_0}\int e^{i(k,\,x-z)}k_0{}^{-1}d^3k, \tag{65}$$

so the Fourier resolution of (48) in this region gives, with $k_0>0$,

$$k^\nu\gamma_k A_{k\nu}-(4\pi^2)^{-1}\sum_e ee^{-i(kz)}=0, \tag{66}$$

$$k^\nu\gamma_k\bar{A}_{k\nu}-(4\pi^2)^{-1}\sum_e ee^{i(kz)}=0. \tag{67}$$

These equations involve only dynamical coordinates and momenta, so they are of the right type to form Hamilton-Jacobi equations. One can easily verify that they and the previous Hamilton-Jacobi equations (62), (63), and (64) form a consistent set of differential equations for I, by verifying that the P.B.'s of their left-hand sides all vanish.

VII. QUANTIZATION

From the foregoing Hamiltonian formulation of classical electrodynamics one can pass over to quantum electrodynamics by applying the usual rules. One replaces the dynamical coordinates and momenta of the classical theory by opera-

tors satisfying commutation relations corresponding to the P.B. relations (59), (60), and (61), and one replaces the Hamilton-Jacobi equations by the wave equations which one gets by equating to zero the left-hand sides of the Hamilton-Jacobi equations (now involving operators for the dynamical variables) applied to the wave function ψ. The wave equations obtained in this way will be consistent with one another, since the operators on ψ in their left-hand sides commute, as may be inferred from the vanishing of the P.B.'s of the left-hand sides of the Hamilton-Jacobi equations.

This straightforward quantization leads to wave equations of the Klein-Gordon type for all particles, corresponding to their having no spins. For dealing with electrons one should replace these wave equations by the wave equations corresponding to spin $\frac{1}{2}\hbar$. We have no information concerning the spins of the poles, and may assume provisionally that they also have the spin $\frac{1}{2}\hbar$, as this gives the simplest relativistic theory. The change from zero spin to spin $\frac{1}{2}\hbar$ does not affect the mutual consistency of the wave equations.

We now have the following scheme of wave equations, expressed in terms of a set of the usual spin matrices α_1, α_2, α_3, α_m for each particle:

$$\{p_0-eA_0(z)-\alpha_r[p_r-eA_r(z)]-\alpha_m m\}\psi=0; \quad (68)$$

for each charged particle,

$$\{p_0-\alpha_r p_r-\alpha_m m\}\psi=0; \quad (69)$$

for each particle with a pole,

$$\{\beta_\mu(\tau_1)-g(F\dagger)_{\mu\nu}{}^*(y)dy^\nu/d\tau_1\}\psi=0; \quad (70)$$

for each string, and

$$\left.\begin{aligned}\{4\pi^2k^\nu\gamma_k A_{k\nu}-\textstyle\sum_e ee^{-i(kz)}\}\psi=0,\\ \{4\pi^2k^\nu\gamma_k \bar{A}_{k\nu}-\textstyle\sum_e ee^{i(kz)}\}\psi=0,\end{aligned}\right\} \quad (71)$$

for the field variables. The wave function ψ may be taken to be a function of the particle variables z_μ, suitable spin variables for each particle, the string variables $y_\mu(\tau_1)$ with $0<\tau_1<\infty$, and the field variables $A_{k\nu}$. It is defined only when all the points z_μ, $y_\mu(\tau_1)$ lie outside each other's light cones.

Equation (69) suggests at first sight that the electromagnetic field does not act on the poles. However, it acts on the strings, as shown by (70), and since the poles are constrained to be at the ends of the strings, the field does affect the motion of the poles. That it affects them in the right way can be inferred from analogy with the classical theory, in which the poles move according to Eq. (11).

VIII. THE UNIT CHARGE AND POLE

The action integral I of the classical theory may be considered as a function of the points in space-time z_μ where the particles go out of existence, of the lines $y_\mu(\tau_1)$ in space-time where the strings go out of existence, and of suitable field variables, and is defined only provided the strings do not pass through any points z_μ where charged particles go out of existence. It is, however, not a single-valued function of these variables, as may be seen in the following way.

Let us make a continuous change in the variables in I according to the following procedure. We keep all the particle points z_μ fixed, and also all the strings except one. This one we vary continuously, keeping it always in the three-dimensional surface S_P, and loop it around one of the points z_μ where a charged particle is situated just before going out of existence and bring it back to its original position. At the same time the potentials $A_\mu(x)$ are varied continuously, to keep Eqs. (13), (15) always satisfied with fixed values for the field $F_{\mu\nu}(x)$, and are brought back to their original values together with the string. We have here a continuous deformation of the variables in I which brings them all back to their starting values, and this deformation cannot be continuously shrunk up to no deformation at all, because we cannot make a string pass through a charged particle. The string will sweep out a closed two-dimensional surface, σ say, lying in S_P and enclosing the point z_μ where the charge is situated, and this surface σ cannot be continuously shrunk up to zero, since it must not pass through the charge. We may therefore expect I to vary under this deformation process, and can easily calculate its variation DI as follows.

A small variation of a string and of the potentials, with the particle points z_μ fixed, leads to a variation of I given by the sum of the right-hand sides of (50) and (52). Under the

closed deformation process described above, the first term on the right-hand side of (50) will give zero, since the $F_{\mu\nu}$, $F_{\mu\nu}^*$ are kept fixed and the A^μ, $A^{\mu*}$ are brought back to their original values. The right-hand side of (52) will also give zero, since it gives the total variation in I_4 and I_4 is brought back to its original value. We are left with the second term on the right-hand side of (50), which is equal to expression (51) and gives for the closed deformation process

$$DI=g\int (F\dagger)_{\mu\nu}^* d\sigma^{\mu\nu},$$

where $d\sigma^{\mu\nu}$ is an element of the two-dimensional surface swept out by the string. The integral here is, according to (8), just the total electric flux passing out through the closed surface σ, and is thus 4π times the charge e enclosed by the surface. Thus

$$DI=4\pi ge.$$

We may loop any string around any charge any number of times, so the total uncertainty in I is the sum

$$4\pi \sum_{ge} m_{ge} ge, \tag{72}$$

summed for all the charges e and the poles g, with an arbitrary integral coefficient m_{ge} for each term.

The phenomenon of an action integral which is not single-valued occurs frequently in mechanics. It occurs most simply with the dynamical system consisting of a rigid body rotating about a fixed axis, for which the action integral is just the angular momentum multiplied by the azimuthal angle, so that the uncertainty in the action integral is 2π times the angular momentum. The rule of quantization of Bohr's theory is given by putting the uncertainty in the action integral equal to an integral multiple of h. Applying this rule to the uncertainty (72), we get

$$4\pi ge=nh, \tag{73}$$

where n is an integer, for each pole g and charge e. This result is the same as (1), with c, the velocity of light, put equal to unity.

The result (73) may also be obtained from the quantum electrodynamics of Section VII without Bohr's rule of quantization, by using the condition that the wave function must be single-valued. The commutation relation (60) shows that $\beta_\mu(\tau_1)$ is ih times the operator of functional differentiation with respect to $y_\mu(\tau_1)$, so that the wave equation (70) is

$$ih\partial\psi/\partial y_\mu(\tau_1)=g(F\dagger)_{\mu\nu}^*(y)(dy^\nu/d\tau_1)\psi. \tag{74}$$

This equation shows how ψ varies when the position of a string is varied. If a string is displaced and sweeps out a two-dimensional surface σ, Eq. (74) shows that ψ gets multiplied by

$$\exp\left[-ig\int (F\dagger)_{\mu\nu}^* d\sigma^{\mu\nu}/\hbar\right], \tag{75}$$

provided the $(F\dagger)_{\mu\nu}^*$ occurring at different points of the integrand here all commute. (One can easily arrange to satisfy this condition accurately, in the case when σ lies in a flat three-dimensional space-like surface S_P, by a suitable choice of the function γ, and in the case of a general S_P the lack of commutation tends to zero as $\gamma(x)\rightarrow\delta_4(x)$ and does not invalidate the calculation.) Let us now apply the procedure we had before of looping the string around one of the charges and bringing it back to its original position. Since ψ is single-valued it must return to its original value, and so the factor (75) must be unity. This requires

$$g\int (F\dagger)_{\mu\nu}^* d\sigma^{\mu\nu}/\hbar=2\pi n$$

with n an integer, which gives again the condition (73).

We come to the important conclusion that *the quantization of the equations of motion of charged particles and particles with poles is possible only provided the charges and poles are integral multiples of a unit charge e_0 and a unit pole g_0 satisfying*

$$e_0g_0=\tfrac{1}{2}\hbar c. \tag{76}$$

The theory does not fix the value of e_0 or g_0, but only gives their product.

IX. DISCUSSION

The foregoing work provides a general theory of particles with electric charges and magnetic poles in interaction with the electromagnetic field. It is not a perfect theory, because the interaction of a particle with its own field is

not dealt with satisfactorily. This is shown up by the continual use in the theory of a function $\gamma(x)$ which has not been precisely specified—only certain desirable properties for it having been given. Even if a satisfactory function γ can be given, the difficulties will not all be solved because there will still be infinities appearing in the wave function when one tries to solve the wave equation. However, these difficulties occur in the ordinary electrodynamics of electrons without any poles, and if a solution of them can be found for ordinary electrodynamics, it will probably apply also for the more general electrodynamics with poles. Thus the occurrence of these difficulties does not provide an argument against the existence of magnetic poles.

The question arises as to whether an elementary particle can have both a charge and a pole. The classical equations of motion given in Section II can be immediately extended to this case, but the Hamiltonian theory meets with some difficulties connected with the precise form of γ. It does not seem possible to answer the question reliably until a satisfactory treatment of the interaction of a particle with its own field is obtained.

The theory developed in the present paper is essentially symmetrical between electric charges and magnetic poles. There is a considerable apparent difference between the treatment of charges and poles, which shows itself up in the first place through the introduction of potentials according to (13). However, one could work equally well with the rôles of the charges and poles interchanged. One would then have strings attached to the charges, and would work with potentials B_μ defined by

$$(F\dagger)_{\mu\nu}=\partial B_\nu/\partial x^\mu-\partial B_\mu/\partial x^\nu+4\pi\sum_\epsilon(G\dagger)_{\mu\nu},$$

with the $G_{\mu\nu}$ vanishing except on the sheets traced out by the new strings, instead of (13). The final result would be an equivalent quantum electrodynamics, referred to a different representation.

Although there is symmetry between charges and poles from the point of view of general theory, there is a difference in practice on account of the different numerical values for the quantum of charge and the quantum of pole. If we take the experimental value for the fine-structure constant,

$$e_0^2=(1/137)\hbar c,$$

we can infer the value of g_0,

$$g_0^2=(137/4)\hbar c.$$

Thus g_0 is much larger than e_0. It corresponds to a fine-structure constant 137/4. The forces of radiation damping must be very important for the motion of poles with an appreciable acceleration.

The great difference between the numerical values of e_0 and g_0 explains why electric charges are easily produced and not magnetic poles. Two one-quantum poles of opposite sign attract one another with a force $(137/2)^2$ times as great as that between two one-quantum charges at the same distance. It must therefore be very difficult to separate poles of opposite sign. To get an estimate of the energy needed for this purpose, we might suppose that elementary particles with poles form an important constituent of protons and have a mass μ of the order, say, half the proton mass. The binding energy of two of these particles cannot be calculated accurately without a more reliable theory of radiation damping than exists at present, but one might expect from Sommerfeld's formula for the energy levels of hydrogen with relativistic effects that this binding energy would be of the order of μc^2, or say 5×10^8 electron volts. One should look for particles with poles in atomic processes where energies of this order are available. They would appear as heavily ionizing particles and would be distinguishable from ordinary charged particles by the property that the ionization they produce would not increase towards the end of their range, but would remain roughly constant.

Letters to the Editor

PUBLICATION of brief reports of important discoveries in physics may be secured by addressing them to this department. The closing date for this department is five weeks prior to the date of issue. No proof will be sent to the authors. The Board of Editors does not hold itself responsible for the opinions expressed by the correspondents. Communications should not exceed 600 words in length.

On the Half-Life of K^{40}

T. GRÁF
L. Meitner Laboratory of Nuclear Physics, IVA:s Försöksstation, Stockholm, Sweden
August 14, 1948

IMPORTANT conclusions were drawn recently[1,2] in connection with the radioactivity of potassium by assuming for its β-decay period the value of $(7\pm1)\times10^9$ years, determined by Bleuler and Gabriel.[3] However, by examining more closely the experimental arrangement of these authors, it became apparent, that, during their absolute half-life determinations, numerous disintegration electrons, originally not directed towards the counter, must have been counted, because of back-scattering in the brass cylinder that surrounded the counter, immediately behind the source.

Special scattering experiments were carried out, suggesting that almost half the number of counts which Bleuler and Gabriel attributed to disintegration electrons may have been caused by such scattered β-particles. In fact, their detailed, unpublished report, which subsequently became available to the author through the courtesy of Mr. Gabriel, mentions no correction for this effect. Thus, a new determination of the β-decay period appeared to be highly desirable.

The aim of the present note is to report the results of such a determination, made by comparing the β-radiation of K^{40} to that of UX_2. Back-scattering was practically eliminated by mounting the foil (7μ Al), on which the active substance was evenly deposited, directly on a thin-walled Al counter, with the activated side outwards. The foils employed were 7.0 cm long and reached just around the counter. Their ends were held together with gummed Cellophane tape. A thin layer of stopcock grease (0.15 mg/cm^2) on their surface retained, firmly, 1 to 2 mg/cm^2 of the finely powdered active substances. Four different K^{40} sources and three UX_2 sources were prepared, using chemically pure KCl and K_2SO_4, specially purified UO_2, and pure uranyl nitrate. The K^{40} sources were 4.0 cm wide, the UX_2 sources 0.2, 0.8, and 1.2 cm.

In a first series of measurements a counter of 0.010-cm wall thickness and of 6.2-cm wire length was used. The results were corrected for difference in the penetrating power of the two β-radiations. This correction amounted to 9 percent. A second, experimentally determined correction of 4 percent accounted for the few UX_1 rays which penetrated through a thickness of 31 mg/cm^2 into the counter. A third correction of 1 percent was necessitated by the fact that the K^{40} sources were wider than the UX_2 sources and had their marginal parts nearer to the counter ends.

A similar run was then made with another, identical counter. Finally, a counter of 0.020-cm wall thickness was used for the purpose of eliminating the UX_1 rays. In this case the correction, because of the difference in absorption, attained 18 percent.

All the results obtained with the different counters and with the various sources agreed within the limits of the experimental error, i.e., 2 to 4 percent. Their mean value, 26.8 ± 1.2 β-particles per second per gram of potassium, yields $(13.7\pm1.5)\times10^9$ years for the β-decay period of K^{40}. This confirms the value of $(14.2\pm3)\times10^9$ years[4] generally used prior to the measurements of Bleuler and Gabriel. As a further consequence, the γ/β-ratio, previously reported as 0.07,[1] must be increased to 0.127 ± 0.012.

About half of the effect attributed by Bleuler and Gabriel to the x-rays of argon, appears to be due to the greater absorbability of the scattered β-particles in the gas layers, used by them as selective absorbers. Since the number of decay electrons is also about half that found by Bleuler and Gabriel, the branching ratio of 1.9 ± 0.4 found by them, needs to be revised only slightly. With the corrected branching ratio of 1.8 ± 0.5 and with the present result for the β-decay period, the value of $(5\pm1.5)\times10^9$ years is computed for the total half-life of K^{40}. A more extensive report will appear elsewhere.

The author wishes to express his gratitude to Professor L. Meitner, in whose laboratory this work was done.

[1] E. Gleditsch and T. Gráf, Phys. Rev. 72, 640, 641 (1947).
[2] H. E. Suess, Phys. Rev. 73, 1209 (1948).
[3] E. Bleuler and M. Gabriel, Helv. Phys. Acta 20, 67 (1947).
[4] A. Bramley and A. K. Brewer, Phys. Rev. 53, 502 (1938).

Significance of the Radioactivity of Potassium in Geophysics. II

T. GRÁF
L. Meitner Laboratory of Nuclear Physics, IVA:s Försöksstation, Stockholm, Sweden
August 14, 1948

A REVISION of the estimates of Gleditsch and Graf[1] concerning the radioactive heat production of potassium seems to be indicated, since the value assumed by them for the half-life of K^{40}, as determined by Bleuler and Gabriel,[2] was shown to be in error.[3]

A new determination yielded $(13.7\pm1.5)\times10^9$ years for the β-decay period,[3] from which, with a revised branching ratio of 1.8 ± 0.5, the value of $(5\pm1.5)\times10^9$ years is deduced for the total half-life. With these values, the radioactive heat production of K^{40}, previously given as $(38\pm7)\times10^{-6}$ cal.,[1] becomes $(22\pm3)\times10^{-6}$ cal. per year per gram of potassium, a value still far exceeding that of $(5\pm2)\times10^{-6}$ cal. given by Evans and Goodman.[4] Assuming 2.8 percent for the average potassium content of acidic igneous rocks, the heat due to the radioactivity of potassium is computed as $(0.6\pm0.1)\times10^{-6}$ cal. per year per

gram of rock, i.e., about 11 percent of the total radioactive heat.

Recent cloud-chamber observations of Franchetti and Giovanozzi[5] indicate a possible slight increase of these last figures. In fact, these authors found that about one percent of the decay electrons had energies above the previously assumed 1.35±0.05-Mev upper limit for K^{40}.[6] If these high energy tracks were not due to distortion by multiple scattering, these observations would suggest a maximum β-energy of 1.7±0.1 Mev. Since the γ-quantum of K^{40} has an energy of only 1.5 Mev, it should be possible, as pointed out by Franchetti and Giovanozzi, to attribute the γ-quantum to the β-decay. In any case, this possibility need not affect the value of the branching ratio or the present computations on the heat production of potassium.

A further suggestion concerning the disintegration scheme of K^{40} was advanced by Suess.[7] According to this, all the capture processes in K^{40} would lead to an excited argon atom, i.e., the branching ratio would equal the γ/β-ratio. However, this hypothesis is based mainly on argon determinations in soluble potassium minerals,[8] for which alterations in recent geological time cannot be excluded. Loss of argon from the investigated samples appears the more likely as even this hypothesis would require argon amounts exceeding at least 2 to 6 times those actually found. In addition, to account for the large amounts of atmospheric argon it should then be assumed that all argon was produced in a 40-kilometer deep crustal layer, since the origin of the earth has escaped into the atmosphere.

With the present values of the decay periods of K^{40}, the origin of atmospheric argon can be explained without excessive assumptions. The K^{40}/K ratio at the time of formation of the elements, say 4×10^9 years ago, becomes comparable to the Lu^{176}/Lu ratio, for example, in agreement with abundance rules advanced by Suess.[7,8] The heat produced in the earth's crust by potassium alone at the time of formation of the oldest known rocks, about 2×10^9 years ago, becomes about twice the present total radioactive heat output. This amount of heat could certainly not prevent rock formation, as might have been the case with the previous estimate,[1] according to Birch.[9]

Yet, at the time of the earth's origin, about 3.35×10^9 years ago,[10] the heat produced by the radioactivity of potassium alone probably exceeded 10 times that generated at present by the total radioactivity in the earth's crust. It seems likely that this heat, if potassium then was concentrated in the earth's crust as it is today, caused a considerable slowing down of the cooling process on the earth's surface. The very large heat production of potassium in the past may also, as suggested by Birch,[9] aid in resolving some difficulties encountered in a number of geophysical problems.

[1] E. Gleditsch and T. Gráf, Phys. Rev. **72**, 641 (1947).
[2] E. Bleuler and M. Gabriel, Helv. Phys. Acta **20**, 67 (1947).
[3] T. Gráf, previous letter.
[4] R. D. Evans and C. Goodman, Bull. Geol. Soc. Am. **52**, 459(1941).
[5] S. Franchetti and M. Giovanozzi, Phys. Rev. **74**, 102 (1948).
[6] B. Dželepov, M. Kopjova, and E. Vorobjov, Phys. Rev. **69**, 538 (1946).
[7] H. E. Suess, Phys. Rev. **73**, 1209 (1948).
[8] P. Harteck and H. Suess, Naturwiss. **34**, 214 (1947).
[9] F. Birch, Phys. Rev. **72**, 1128 (1947).
[10] A. Holmes, Nature **159**, 127 (1947).

On Models for Be^9

EUGENE GUTH AND CHARLES J. MULLIN
University of Notre Dame, Notre Dame, Indiana
August 23, 1948

THREE models for the Be^9 nucleus have been investigated.[1-4] These are: (1) the Hartree model, (2) the α-particle model ($2\alpha+n$), and (3) a two-body model in which the two α-particles are treated as a unit (Be^8), and the neutron is assumed to move in the field of the Be^8.

Of these models, the Hartree model is probably the most accurate and gives the best interpretation of the experimental data. In Table I the comparison between

TABLE I. Theoretical and experimental results for the ground state and magnetic moment of Be^9.

Model	Ground state	Magnetic moment
Hartree	$^2P_{3/2}$	-1.50
α-particle	$^2P_{3/2}$	$-0.7>\mu>-1.5$
Two body	$^2P_{3/2}$	-1.85
Experimental result	$^2P_{3/2}$	-1.18

experiment and the predictions which the three models make about the ground state and the magnetic moment of Be^9 is given. The experimental value $\mu=-1.18$ nuclear magneton is taken from the direct measurement of Kusch, Millman, and Rabi.[5] Direct evidence for spin $\frac{3}{2}$ has been obtained from hyperfine structure data obtained in Germany during the war.[6] Also, this value of the spin may be inferred with some degree of reasonableness from the experimental value of μ.[5] It should be pointed out that the two-body model makes no direct predictions concerning the ground state and magnetic moment. However, this model may be regarded as a first approximation to the α-particle model and should, therefore, lead to the same ground state as this model. If, then, it is assumed that the ground state with the two-body model is $^2P_{3/2}$ state, this model yields $\mu=-1.85$ nuclear magnetons.[7]

Although the two-body model is only a first (and sometimes poor) approximation to the more accurate models, in the explanation of certain processes, such as the photo- and electrodisintegration of Be^9, its use is probably justifiable. The justification of the use of this model for these processes is based upon the following points: (1) The binding energy for ejection of a neutron (1.63 Mev) is much less than the average binding energy per particle in the Be^9 nucleus. (2) The instability of the Be^8 nucleus is only 162 kev.[8] The lifetime of Be^8 is estimated to lie between 10^{-19} and 10^{-15} sec., corresponding to a width between 100 and 1 ev.

Very little is known about the low lying excited states of Be^9. As heretofore mentioned, the ground state should be a $^2P_{3/2}$ state. This means that the ^2P is an inverted doublet as would be predicted from relativistic spin-orbit coupling. It seems likely that the energy separation of the ^2P states should be of the same order of magnitude as the known splitting of similar states for other light nuclei. For He^5 the splitting of the P doublet is 250 kev and seems to be normal.[9] For Li^7 the ^2P splitting is 400 kev and

seems to be inverted.[10] Inglis[11] has explained the magnitude and inverted nature of the splitting in Li^7 as being due to relativistic spin-orbit coupling. Dancoff[12] has given numerical estimates for the splitting in He^5 by using a central field model. He points out that tensor forces lead to the observed normal doublet, giving the right order of magnitude for the splitting.

From the above-mentioned results for Li^7 and He^5 it seems likely that the $^2P_{\frac{1}{2}}$ state in Be^9 is a bound state. If this is the case, the $^2P_{3/2}\rightarrow{}^2P_{\frac{1}{2}}$ magnetic dipole transition should be observed in inelastic scattering experiments or by detection of the γ-ray resulting from the transition, either directly or through internal conversion. Since no empirical results on the $^2P_{\frac{1}{2}}$ level are available, it does not seem profitable, at present, to speculate about the nature of the forces which may be responsible for the ^2P splitting.

[1] E. Feenberg and E. Wigner, Phys. Rev. **51**, 95 (1937).
[2] M. E. Rose and H. A. Bethe, Phys. Rev. **51**, 205 (1937).
[3] R. G. Sachs, Phys. Rev. **55**, 825 (1939). Sachs points out that the wide limits in the magnetic moment (α-model) arise from the mixing of P and S states. This was not considered by Rose and Bethe.
[4] Eugene Guth, Phys. Rev. **55**, 411 (1939).
[5] Kusch, Millman, and Rabi, Phys. Rev. **55**, 666 (1939).
[6] Julian Schwinger, personal communication.
[7] Schmidt (Zeits. f. Physik **106**, 358 (1937)) has used this model to explain the magnetic moments of nuclei. As expected, the representation is better for medium and heavy nuclei than it is for light nuclei.
[8] This instability was first shown by Glueckauf and Paneth, Proc. Roy. Soc. **A165**, 229 (1938). The value 162 kev is due to Arthur Hemmendinger, Phys. Rev. **73**, 806 (1948).
[9] H. Staub and H. Tatel, Phys. Rev. **58**, 820 (1940). H. Staub and E. Stevens, Phys. Rev. **55**, 731 (1939).
[10] L. H. Rumbaugh and L. R. Hafstad, Phys. Rev. **50**, 681 (1936).
[11] D. R. Inglis, Phys. Rev. **50**, 783 (1936) and Phys. Rev. **56**, 1178 (1939). G. Breit and J. R. Stehn, Phys. Rev. **53**, 459 (1938). C. Kittel, Phys. Rev. **62**, 109 (1942).
[12] S. M. Dancoff, Phys. Rev. **58**, 326 (1940).

Theory of the Photo-Disintegration of Be^9

EUGENE GUTH AND CHARLES J. MULLIN
University of Notre Dame, Notre Dame, Indiana
August 23, 1948

RECENTLY the cross section for the photo-disintegration of Be^9 has been determined as a function of energy by Wattenberg and his associates.[1] Their results, as well as results of other workers, have been kindly communicated to us by Dr. Wattenberg; these results are shown in Fig. 1. It should be noted that the experimental results indicate that the photo-disintegration cross section has a maximum and a minimum in the energy range of the experimental data. Undoubtedly, there is also a second maximum beyond the range of these data.

It is possible to give a fairly accurate explanation of the observed results by applying the two-body model discussed in the preceding letter. It is assumed that the ground state is a $^2P_{3/2}$ state. Then the incident photons should produce electric dipole transitions from the ground P state to S and D states. It is also possible that a magnetic dipole transition $^2P_{3/2}\rightarrow{}^2P_{\frac{1}{2}}$ occurs. As in the case of the deuteron, the photoelectric and photo-magnetic disintegration cross sections exhibit maxima when plotted as a function of energy. For the interpretation of the experimental data, the photo-magnetic cross section does not seem necessary. Consequently, it has been assumed that the two maxima are due to the electric dipole $P\rightarrow S$ and $P\rightarrow D$ transitions, the first maximum resulting from the $P\rightarrow S$ transition. The locations and widths of the maxima are determined, at least in part, by the characteristics of the resonance levels of the states of positive energy corresponding to the final states of the disintegrated Be^9.

For simplicity, the interaction between the Be^8 and the neutron has been represented by a rectangular potential well. From general considerations, the radius of the well should probably be about $3-5\times10^{-13}$ cm. The value $r=5\times10^{-13}$ cm has been employed in the calculations; this radius determines the well depth to be 12.16 Mev for the P state. The dependence of the Be^8 neutron force upon the angular momentum has been taken into account in a schematic way by assuming that the well depth is a function of parity. For the S and D states (both with even parity) a well depth of 3 Mev has been used. (The same radius, $r=5\times10^{-13}$ cm, has been used for all states.) With this well, the first S state is bound by about 100 kev. This loosely bound state yields a resonance effect in the disintegration cross section similar to that which would be obtained with a virtual state.[2] The theoretical photo-disintegration cross section is given by the solid curve in Fig. 1. A continuation of the theoretical curve to higher energies yields a second maximum.

The theory predicts that the angular distribution of the ejected photo-neutrons should be spherically symmetric for energies near the threshold (that is, in the region of the first maximum), and should be given by $[P_2(\cos\theta)]^2$ for energies somewhat beyond the minimum of the cross-section curve. If the second peak were due to a magnetic dipole transition, the angular distribution for energies somewhat beyond the minimum would be given by $\sin^2\theta$. The angular distribution of the photo-neutrons has been found to be spherically symmetric for energies near the threshold by Goloborodko and Rosenkewitch.[3] According to Dr. Wattenberg, an investigation of the angular

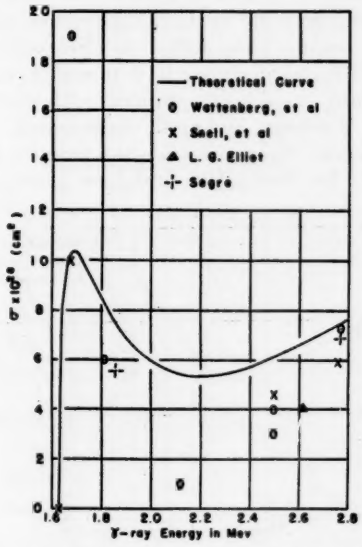

FIG. 1. Photo-disintegration cross sections for Be^9.

distribution of the photo-neutrons from Be^9 is planned by him and his group at the Argonne National Laboratories. Such an investigation would show whether or not the neglect of the $^2P_{3/2} \rightarrow {}^2P_{\frac{1}{2}}$ magnetic dipole transition is justified, or whether it must be included with the other transitions.

Very recently, in experiments on the inelastic scattering of protons on Be^9, a sharp resonance level has been found by Davis and Hafner[4] at 2.41 Mev (0.78 Mev above the photo-threshold). This resonance has been attributed by Longmire[5] to a $^2D_{3/2}$ resonance level. Such a $^2D_{5/2}$ level should be detected in the photo-disintegration measurements; however, the photo cross section has not yet been measured at the energies where this level is important. If this resonance were due to an F state, its effect on the photo cross section would probably be much less. The results of Davis and Hafner also seem to indicate the existence of an S resonance level of the type assumed to explain the first maximum in the photo-disintegration curve. However, the experimental data on this point are not conclusive.[6]

[1] Russell, Sachs, Wattenberg, and Fields, Phys. Rev. 73, 545 (1948).
[2] By using a larger radius for the potential well, it seems possible to interpret the experimental data with an "S well depth" which places the resonance state in the continuum.
[3] Goloborodko and Rosenkewitch, Physik. Zeits. Sowjetunion 11, 78 (1937). Cf. also Chadwick and Goldhaber, Proc. Roy. Soc. A151, 479 (1935).
[4] K. E. Davis and E. M. Hafner, Phys. Rev. 73, 1473 (1948).
[5] Longmire, Thesis, University of Rochester, 1948, to be published soon. The authors wish to thank Dr. Longmire and Professor Marshak for communicating their data to us.
[6] In these experiments the inelastically scattered protons were observed. It is also possible, of course, to observe the ejected neutrons.

Theory of Electrodisintegration of Be^9

E. GUTH, C. J. MULLIN, AND J. F. MARSHALL
University of Notre Dame, Notre Dame, Indiana
August 23, 1948

THE disintegration of Be^9 by electrons was first observed by Collins, Waldman, and Guth[1] in 1939. At that time, one of us[2] made an approximate calculation of the cross section right above the threshold, using the central field model discussed in a preceding letter. The value obtained was in good agreement with that observed by Collins, Waldman, and Guth. Subsequently, Wiedenbeck[3] determined the cross section as a function of energy, using a thin Be target. His results are given in Fig. 1.

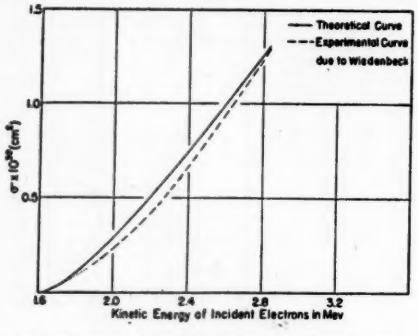

FIG. 1. Electrodisintegration cross sections for Be^9.

(The dotted part of the experimental curve is an extrapolation from Wiedenbeck's lowest point to the threshold.)

Using the theoretical cross section for photo-disintegration obtained in the preceding letter, we have calculated the cross section for electrodisintegration as a function of energy. The result, shown in the figure, agrees well with the experimental curve. If it is assumed (see the preceding letter) that the photo-disintegration cross section, $\sigma(h\nu)$, results from photoelectric transitions, then the cross section for electrodisintegration, $\sigma(E_i)$, may be written

$$\sigma(E_i)=\int_{1.63}^{E_i} \sigma(h\nu)N(E_i, h\nu)d(h\nu), \qquad (1)$$

where E_i is the kinetic energy of the incident electron, $\sigma(h\nu)$ is the cross section for photo-disintegration determined in the preceding letter, and $N(E_i, h\nu)$ is the number of virtual quanta by which the action of the field of the electron may be represented in the production of photoelectric disintegration. $N(E_i, h\nu)$ was computed by using the Born approximation. (Actually, the equivalent method due to Møller was used.) Since $\sigma(h\nu)$ is in fairly good agreement with the experimentally determined photo-disintegration cross section, it may be regarded as an empirical result. Consequently, the only assumption involved which is dependent upon the nuclear model comes in through the use of $N(E_i, h\nu)$ corresponding to a *photoelectric* transition. If $\sigma(h\nu)$ is due in part to a magnetic dipole transition, a different value of $N(E_i, h\nu)$ must be used for this transition. Assuming that $\sigma(h\nu)$ results from photoelectric transitions only, the determination of the electrodisintegration cross section is reduced to an electromagnetic, rather than a nuclear, problem. The theoretical cross section obtained from Eq. (1) is plotted in the accompanying figure. The agreement with experiment is very good and is an argument for the photoelectric nature of the photo cross section. Near the threshold, the cross section increases as the square of the energy of the ejected neutron. It should be noted that, because of the integration indicated in Eq. (1), the electrodisintegration cross section is relatively insensitive to the assumed nuclear model.

Inelastic scattering of electrons on Be^9 may reveal the S resonance level postulated in the theory of the photo-disintegration of Be^9 and may also detect the resonance level at 0.78 Mev (above threshold) found by Davis and Hafner.[4] The theory for the inelastic scattering process is included in the theory of electrodisintegration.

Mamasachlisov[5] has given a theory of the electrodisintegration of Be^9, assuming only a $P \rightarrow S$ transition. His results, which were based in part on the results of Bethe and Peierls for the electrodisintegration of the deuteron, appeared to give good agreement with the experimental measurement of Collins, Waldman, and Guth at 1.73 Mev. However, the result of Bethe and Peierls used by Mamasachlisov was marred by two algebraic errors which were subsequently corrected by Wick.[6] The correction of these errors reduced Mamasachlisov's theoretical cross section by a factor of about one-half and led to a less favorable comparison with the experimental result. Caldirola[7] tried to improve the theory of Mamasachlisov by introducing, *ad hoc*, a magnetic dipole transi-

tion between $^2P_{3/2}$ ground state and the $^2P_{\frac{1}{2}}$ state. Unfortunately, Caldirola has chosen the $^2P_{3/2}$ and $^2P_{\frac{1}{2}}$ states as eigenstates of the same potential well. Consequently, the eigenfunctions are orthogonal, and the photo-magnetic effect vanishes. Caldirola apparently did not notice this and, using approximations, obtained a non-zero value for a vanishing integral.

[1] Collins, Waldman, and Guth, Phys. Rev. **55**, 875 (1939).
[2] E. Guth, Phys. Rev. **55**, 411 (1939).
[3] Wiedenbeck, Phys. Rev. **69**, 236 (1945).
[4] K. E. Davis and E. M. Hafner, Phys. Rev. **73**, 1473 (1948).
[5] Mamasachlisov, J. Phys. U.S.S.R. **7**, 239 (1943).
[6] Wick, Ricerca Scientifica **11**, 49 (1940).
[7] Caldirola, J. de phys. et rad. **8**, 155 (1947).

Notes on Feenberg's Series—Rearrangements*

PAUL I. RICHARDS
Brookhaven National Laboratory, Upton, New York
August 20, 1948

THIS note concerns a simplified discussion of the infinite series—rearrangement procedures recently employed by Feenberg.[1] The essential point in the simplification is that, by introducing specialized notation, the expressions involved can be handled in closed form. We shall consider only the algebraic aspects of the rearrangement procedure; questions of convergence cannot be adequately handled at this level of generality.[2]

If W_{ij} is any matrix and α any list of possible index values, introduce the following notation:

$$W_{ab}{}^{n+1}(\alpha)=\sum_{i_1\cdots i_n\neq\alpha} W_{ai_1}W_{i_1i_2}\cdots W_{i_{n-1}i_n}W_{i_nb}\quad(n\geq 1). \tag{1}$$

Briefly, (1) defines $W_{ab}{}^k(\alpha)$ as the (ab) element of the matrix W^k *except* that, in all sums involved in forming W^k, the index values listed in α are omitted. It is also convenient to extend (1) to include the trivial cases where no sums are involved.

$$W_{ab}{}^1(\alpha)=W_{ab};\quad W_{ab}{}^0(\alpha)=\delta_{ab}. \tag{1a}$$

In Feenberg's notation, the basic matrix involved in the manipulations to be discussed is $W_{ab}=V_{ab}/(a)$. (His restriction $V_{ii}=0$ is of course not needed and will not be used here.)

Now choose an index value q (not already listed in α) and regroup terms on the right of (1) in the following way:

$$\begin{aligned} &i_1=q;\quad \text{others}\neq\alpha && \text{(A)}\\ &i_1\neq q \text{ or } \alpha;\quad i_2=q;\quad \text{others}\neq\alpha && \text{(B)}\\ &\cdots\\ &i_1\cdots i_{n-1}\neq q \text{ or } \alpha;\quad i_n=q && \text{(N}^{-1}\text{)}\\ &i_1\cdots i_n\neq q,\ \alpha. && \text{(N)}\end{aligned}$$

We thereby obtain:

$$W_{ab}{}^{n+1}(\alpha)=\sum_{i=0}^{n-1} W_{aq}{}^{i+1}(\alpha q)W_{qb}{}^{n-i}(\alpha)+W_{ab}{}^{n+1}(\alpha q). \tag{2a}$$

Regrouping in the reverse order ($i_n=q$, others $\neq\alpha$, etc.) we find analogously:

$$W_{ab}{}^{n+1}(\alpha)=\sum_{i=0}^{n-1} W_{aq}{}^{n-i}(\alpha)W_{qb}{}^{i+1}(\alpha q)+W_{ab}{}^{n+1}(\alpha q). \tag{2b}$$

Equations (2) are the fundamental relations on which the work below is based; they are the closed forms of [8] and [12] of Feenberg's paper.

In particular, if α does not include a and/or b

$$W_{ab}{}^{n+1}(\alpha)=\sum_{i=0}^{n} W_{ab}{}^{i+1}(\alpha b)W_{bb}{}^{n-i}(\alpha)$$

$$=\sum_{i=0}^{n} W_{ab}{}^{i+1}(\alpha a)W_{aa}{}^{n-i}(\alpha).$$

Hence, by Cauchy's rule for multiplication of infinite series, if α does not include a and/or b

$$\sum_{n=0}^{\infty} W_{ab}{}^{n+1}(\alpha)=\Big[\sum_{n=0}^{\infty} W_{ab}{}^{n+1}(\alpha b)\Big]\Big[\sum_{n=0}^{\infty} W_{bb}{}^{n}(\alpha)\Big]$$

$$=\Big[\sum_{0}^{\infty} W_{ab}{}^{n+1}(\alpha a)\Big]\Big[\sum_{0}^{\infty} W_{aa}{}^{n}(\alpha)\Big]. \tag{3}$$

This result immediately establishes[3] Feenberg's [9] and [13]. As a special use of (3), we have

$$\sum_{0}^{\infty} W_{bb}{}^{n}(\alpha)=1+\Big[\sum_{0}^{\infty} W_{bb}{}^{n+1}(\alpha b)\Big]\Big[\sum_{0}^{\infty} W_{bb}{}^{n}(\alpha)\Big].$$

Thus, either by solving for the quantity on the left or by reapplying this relation indefinitely, we find

$$\sum_{0}^{\infty} W_{bb}{}^{n}(\alpha)=\sum_{V=0}^{\infty}\Big[\sum_{n=0}^{\infty} W_{bb}{}^{n+1}(\alpha b)\Big]^V=1\Big/1-\sum_{0}^{\infty} W_{bb}{}^{n+1}(\alpha b) \tag{4}$$

which is Feenberg's formal identity [16].

All of the previous formulae break down if the list α already includes the index value to be "removed." The following devices may, however, be employed when α includes both of the matrix indices.

By definitions (1), (1a):

$$\sum_{0}^{\infty} W_{xa}{}^{n+1}(\alpha)=W_{xa}+\sum_{b\neq\alpha} W_{xb}\sum_{0}^{\infty} W_{ba}{}^{n+1}(\alpha)$$

by (3):

$$=W_{xa}+\sum_{b\neq\alpha} W_{xb}\Big[\sum_{0}^{\infty} W_{bb}{}^{n}(\alpha)\Big]\Big[\sum_{0}^{\infty} W_{ba}{}^{n+1}(\alpha b)\Big].$$

If, at this point, we use (4), we get

$$\sum_{0}^{\infty} W_{xa}{}^{n+1}(\alpha)=W_{xa}$$

$$+\sum_{b\neq\alpha}\Big\{W_{xb}\sum_{0}^{\infty} W_{ba}{}^{n+1}(\alpha b)\Big/1-\sum_{0}^{\infty} W_{bb}{}^{n+1}(\alpha b)\Big\} \tag{5}$$

which is Feenberg's [29] (last half) and [30]. Alternatively, we may repeat the process on the last factor of the last term above.

$$\sum_{0}^{\infty} W_{xa}{}^{n+1}(\alpha)=W_{xa}+\sum_{b\neq\alpha} W_{xb}\sum_{0}^{\infty} W_{bb}{}^{n}(\alpha)$$

$$\times\Big\{W_{ba}+\sum_{c\neq ab} W_{bc}\sum_{0}^{\infty} W_{cc}{}^{n}(\alpha b)\sum_{0}^{\infty} W_{ca}{}^{n+1}(\alpha bc)\Big\}.$$

Repeating indefinitely, we obtain in the limit:

$$\sum_{0}^{\infty} W_{xa}{}^{n+1}(\alpha)=W_{xa}+\sum_{b\neq\alpha} W_{xb}W_{ba}\sum_{0}^{\infty} W_{bb}{}^{n}(\alpha)$$

$$+\sum_{\substack{b\neq\alpha\\ c\neq ab}} W_{xb}W_{bc}W_{ca}\sum_{0}^{\infty} W_{bb}{}^{n}(\alpha)\sum_{0}^{\infty} W_{cc}{}^{n}(\alpha b)+\cdots. \tag{6}$$

Using (4) in (6) we have Feenberg's [21], [24], [29].

Slightly altered analogues to (5) and (6) can be obtained by using the above devices on the last element of each term, instead of the first, thus:

$$\sum_0^\infty W_{za}{}^{n+1}(\alpha) = W_{za} + \sum_{b\neq\alpha}\left[\sum_0^\infty W_{zb}{}^{n+1}(\alpha)\right]W_{b\alpha}.$$

Proceeding as before, we find

$$\sum_0^\infty W_{za}{}^{n+1}(\alpha) = W_{za} + \sum_{b\neq\alpha}\left\{W_{b\alpha}\sum_0^\infty W_{zb}{}^{n+1}(\alpha b)\Big/1-\sum_0^\infty W_{bb}{}^{n+1}(\alpha b)\right\}, \quad (5a)$$

$$\sum_0^\infty W_{za}{}^{n+1}(\alpha) = W_{za} + \sum_{b\neq\alpha} W_{zb}W_{b\alpha}\sum_0^\infty W_{bb}{}^{n}(\alpha) + \sum_{\substack{b\neq\alpha\\ c=\alpha b}} W_{zc}W_{cb}W_{b\alpha}\sum_0^\infty W_{bb}{}^{n}(\alpha)\sum_0^\infty W_{cc}{}^{n}(\alpha b) + \cdots. \quad (6a)$$

The writer is indebted to Professor Feenberg for a pre-publication copy of the paper on which this work is based.

* Research carried out at Brookhaven National Laboratory under the auspices of the Atomic Energy Commission.

[1] Eugene Feenberg, "Theory of Scattering Processes," Phys. Rev. 74, 664 (1948).

[2] It might be pointed out in this connection that one must be careful in attempting to infer the analytic properties of a function from its series representation. Consider for example $f(Z)=\sum(1/1-z)^{n+1}$; recalling Laurent series, we might be tempted to suggest that f has an essential singularity at $Z=1$. Actually, $f=-1/z$, which is analytic at $z=1$. The pole on $|z-1|=1$ is duly indicated by failure of convergence, but the series can tell us nothing about regions $|z-1|\leqslant 1$, where it does not converge.

[3] The connections between the present notation and that of Feenberg are:

$$W_{ab}=V_{ab}/(a); \quad S'_{za}=\sum_0^\infty W_{za}{}^n$$

$$(\mathfrak{E}_{\alpha\rho}-E_\rho)/(\rho)=\sum_0^\infty W_{\rho\rho}{}^{n+1}(\alpha\rho); \quad \bar{U}_{\alpha;z\alpha}=\sum_0^\infty W_{z\alpha}{}^{n+1}(\alpha).$$

The Emission of Alpha-Particles from the Different Faces of a Radioactive Crystal

J. H. J. Poole and J. W. Bremner
Physical Laboratory, Trinity College, Dublin, Eire
August 10, 1948

In a letter recently published, K. B. Mather and F. N. D. Kurie[1] state that they can find no significant difference in the α-ray emission of the various faces of a ThSO crystal. This agrees with Merton's result for uranium nitrate,[2] but differs, as they point out, from Muhlestein's experiments.[3]

Preliminary tests have been conducted here on uranium nitrate using the photographic emulsion technique, and would appear to confirm the nul result, but a small effect of the order of, say, one or two percent might not have been detected.

It is perhaps dangerous to apply naive macroscopic concepts to the structure of the nucleus, but if the above experiments had given a positive result, it would seem to imply that

(a) the nucleus in question was not spherically symmetrical but had definite axes of symmetry.
(b) the orientation of the nucleus was controlled by the crystalline forces.

It might be assumed that nuclei possessing nuclear spin and magnetic moment would fulfill the first condition. Elements of even atomic number and mass have zero spin and magnetic moment. Both U^{238} and Th^{232} fall in this class so a nul result for them might be anticipated. U^{235} has, however, a spin of either 5/2 or 7/2,[4] and presumably U^{233} and Pu^{239} would also possess spins greater than zero. It would accordingly seem to be worth while to try the same experiments using one of the above nucleides but, perhaps fortunately, the necessary material seems to be available only in America, as yet.

It may be noted that the amount of U^{235} present in natural uranium could not account for Muhlestein's result. Allowing for the fact that the equilibrium amount of U^{234} will also be present, it can be calculated from the accepted half-lives of U^{238} and U^{235} that only slightly over two percent of the α-rays from natural uranium, free from its decomposition products, would be produced by U^{235}. This could not account for Muhlestein's differences of 15 percent or more between the emission of the various faces of the uranium nitrate crystal.

[1] K. B. Mather and F. N. D. Curie, Phys. Rev. 73, 1474 (1948).
[2] Merton, Phil. Mag. 38, 463 (1919).
[3] Muhlestein, Arch-de-So. 2, 240 (1920).
[4] O. E. Anderson and H. E. White, Phys. Rev. 71, 911 (1947).

On the Motion of Point Electrons

U. Haber-Schaim
*The Hebrew University, Jerusalem**
August 16, 1948

It has been shown by Pryce[1] that it is possible to derive finite equations of motion for a point electron, as well as finite electromagnetic self-energy, by subtracting a symmetric non-divergent tensor $A^{\nu\sigma}$ ($\nu, \sigma=0, 1, 2, 3$) from Maxwell's energy-momentum tensor $T^{\nu\sigma}$. In order to assure the non-divergence of $A^{\nu\sigma}$ Pryce assumed

$$A^{\nu\sigma}=\partial K^{\mu\nu\sigma}/\partial x^\mu, \quad (1)$$

where $K^{\mu\nu\sigma}$ is antisymmetrical in μ and ν, and is a function of the variables of the electron and the four coordinates of the point under consideration $x^\mu \cdot K^{\mu\nu\sigma}$ has to be chosen so that $A^{\nu\sigma}$ will be symmetrical and will have the same singularities of the third and fourth order on the world line of the electron as Maxwell's tensor. By use of such a tensor $K^{\mu\nu\sigma}$ Pryce derived the well-known Lorentz-Dirac equations of motion,[2]

$$mv^\sigma - \tfrac{2}{3}e^2(\ddot{v}^\sigma + (\dot{v}, \dot{v})v^\sigma) = ev^\mu F^\sigma{}_{\text{ext}\mu},$$

where $F^\sigma{}_{\text{ext}\mu}$ is the external electromagnetic field.

It has been proved by Bhabha[3] that this result is independent of the particular choice of $A^{\nu\sigma}$, provided Eq. (1) is satisfied.

But as shown by Dirac[3] and Eliezer[4] there are serious difficulties in interpreting the solutions of Eqs. (2) when

applied to a free electron, an electron moving in a Coulomb field, and other cases.

While looking for new equations of motion the question arose whether there exist non-divergent tensors with singularities of the second order on the world line which do not satisfy Eq. (1). It was found that such a tensor exists. In Pryce's notation it is

$$B^{\nu\sigma}=\kappa^2 s^\nu s^\sigma/s^6. \tag{3}$$

Every other tensor which satisfies all the requirements also in respect of dimensions may be obtained from (3) by adding a tensor of the type (1).

The addition of $k\cdot e^2/\pi\cdot\kappa^2 s^\nu s^\sigma/s^6$ brings us to the generalized equations of motion of the form

$$mv^\sigma-\tfrac{2}{3}e^2(2k+1)(\dot{v}^\sigma+(v,\dot{v})v^\sigma)=ev^\mu F^\sigma{}_{\text{ext}\mu}, \tag{4}$$

which are exactly the equations obtained and discussed by Eliezer[5] generalizing Dirac's method of introducing advanced fields.

Our method of obtaining Eqs. (4) shows the physical meaning of the generalization from Pryce's point of view; for $k\neq 0$ the contribution of the additional tensor to the self-energy depends not only on the motion of the electron at that particular time, but also on its past, since the space integral of B^{00} cannot be reduced to a surface integral taken over a small sphere around the electron.

The writer is indebted to Professor G. Racah for suggesting this problem and his guidance throughout this work.

* Present address of the author: Rehovot, Israel.
[1] M. Pryce, Proc. Roy. Soc. **A168**, 389 (1938).
[2] P. A. M. Dirac, Proc. Roy. Soc. **A167**, (1938).
[3] H. J. Bhabha, Proc. Roy. Soc. **A183**, (1945).
[4] C. J. Eliezer, Proc. Camb. Phil. Soc. **39**, 173 (1943).
[5] C. J. Eliezer, Rev. Mod. Phys. **19**, 147 (1947), Eq. (61).

Directional Intensity of Cosmic Rays at High Altitudes*

J. R. WINCKLER, W. G. STROUD, AND J. SCHENCK
*Palmer Physical Laboratory, Princeton University, Princeton, New Jersey***
August 20, 1948

GEIGER counter telescopes, with and without lead filters, have been flown to atmospheric heights between 90,000 and 100,000 feet using the Office of Naval Research Project "Skyhook" balloons at Camp Ripley, Minnesota (geomagnetic latitude 56°N). The equipment consisted of five threefold coincidence telescopes with counting axes pointed to zenith angles of 0°, 22½°, 45°, 67½°, and 90°. The counters were 1″ in diameter and of 3-in. sensitive length, and in the telescopes the end members were 5½-in. apart, center to center. Extra counters were provided to detect air showers and possible multiple events produced in the lead. Lead thicknesses of 0, 1.9, 7.6, and 16.7 cm, placed in quadrants about a common center counter, were used in different flights. The azimuth of the gondola was registered by means of three groups of photo-cells. Atmospheric pressure was determined by means of an aneroid baroswitch supplemented by a mercury manometer at higher altitudes. All information, including temperature, was recorded at a ground station by a 15-channel, frequency-modulated radio telemetering system.

The measurements at zenith angles of a 0° and 67½° are given in Figs. 1 and 2, respectively, and represent averages of all azimuths. All data are normalized to the vertical ground rate at Princeton without lead, which was determined for each telescope to about 1 percent accuracy. The crosses on Fig. 1 show the comparison with results of Biehl *et al.*[1] (Rapid City, South Dakota curve, 53.3°N mag. lat.), assuming the equality of vertical ground flux at Princeton and Pasadena. The vertical rate with 1.9 cm Pb was not measured successfully; accordingly, the rate measured at 22½° zenith angle is inserted in Fig. 1, although this curve is inconsistent with the others at the highest altitudes. The 7.6-cm Pb curve represents two flights. Corresponding curves were obtained for 22½°, 45°, and 90° zenith angles, but they are not printed because of space limitations.

The $\theta=67\frac{1}{2}°$ curves reach about the same intensity as the $\theta=0°$ curves, but are displaced towards lower pressures. If the vertical curves are transformed to take into account the extra air path seen at zenith angle θ by the relation $I(p,\theta)=I(p\sec\theta,0)$, where I is the counting rate and p the pressure, they approximate the 67½° curves. The differences may be significant and are being considered further in the light of meson decay phenomena. However, looking apart from these small differences, one must conclude that the observed rays, including even the soft

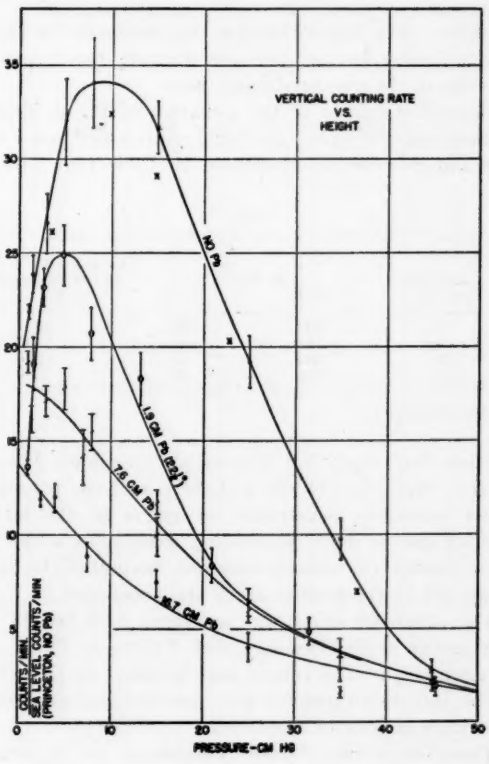

FIG. 1.

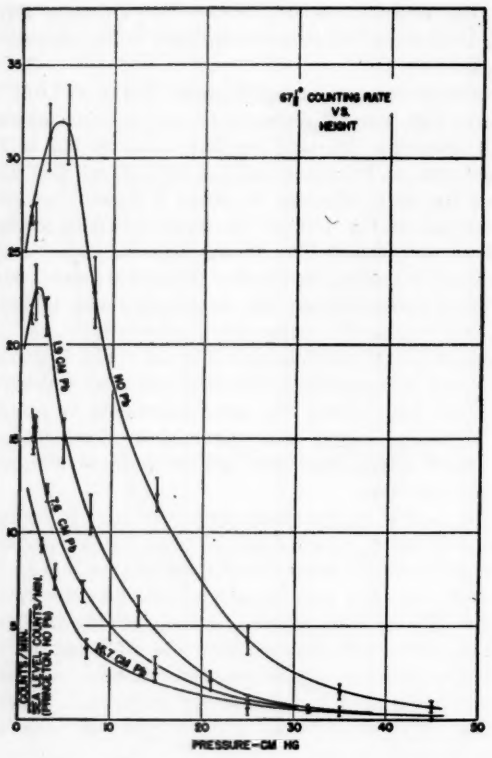

FIG. 2.

secondary rays responsible for the maximum in the intensity height curves, preserve for the most part the direction of the rays producing them.

Absorption curves of the radiation in Pb at different altitudes may be separated roughly into a soft[2] and a hard[2] part and give the results shown in Table I for μ in the

TABLE I.

Altitude cm Hg	μ, g/cm² hard*	soft*	Thickness Pb required to reduce intensity by $1/e$, cm.
1.0	400	400	>20
5.0	220	100	14.6
10	200	60	8.9
20	240	30	3.4

* See reference 2.

relation $I=I_0\exp(-\mu x)$ (for vertical direction). The data suggest that most of the radiation at 1-cm pressure is either extremely penetrating or reacts in the lead to produce one or more penetrating secondaries which continue through the counter telescope. Several of the experiments will be repeated to check this conclusion.

The azimuthal effect was measured with the 45° and 67½° zenith angle telescopes with 7.6 cm of Pb at 1-cm pressure height. The counts were summed up in each 45° sector, but no asymmetry was observed greater than the experimental error of 5 percent.

These experiments were preliminary to a proposed investigation of the directional distribution of the cosmic-ray intensity at high altitudes as a function of latitude, and will be published in greater detail.

The writers wish to express their thanks to Colonel R. A. Rossberg and the Minnesota National Guard, Mr. Henry Stinger and Mr. Thomas James of General Mills Corporation, and Lieutenant M. L. Lewis, United States Navy, for operation of the exceptional balloon facilities used for these experiments.

* See also J. R. Winckler "Directional distribution of the total cosmic radiation at atmospheric heights up to 10 cm Hg at Princeton," Bull. Am. Phys. Soc. 23 (April 29, 1948).

** Assisted by the Joint Program of the Office of Naval Research and the Atomic Energy Commission.

[1] Biehl, Montgomery, Neher, Pickering, and Roesch, Rev. Mod. Phys. 20, 360 (1948).

[2] The hard radiation is defined essentially as that capable of penetrating >4 cm Pb. The soft radiation is that penetrating <4 cm Pb.

Isotopic Shift in the Helium Line Spectrum

ALAN ANDREW AND W. W. CARTER
California Institute of Technology, Pasadena, California
August 14, 1948

USING some of the enriched He^3 mixture from the apparatus of Andrew and Smythe,[1] we have prepared a discharge tube in order to photograph the isotopic shift in the spectra.

The mass difference of the nuclei of He^3 and He^4 produces a change in the energy levels of the different states of the extra-nuclear electrons. This effect can be divided into two parts, the normal effect and the specific effect. The former applies to all energy levels and its magnitude is given by

$$\Delta W_1=(m/M)W,$$

where m is the reduced mass of the electron, M is the mass of the nucleus, and W is the term value of the energy level for a nucleus of infinite mass.

For hydrogen-like atoms the normal effect accounts for the total change; however, for more complex atoms the specific effect must be taken into account. This effect amounts to an additional change in the P levels only. Hughes and Eckart[2] have calculated this energy change to be

$$\Delta W_2=\pm(128/3)(m/M)(R_\infty)(Z_1Z_2)^5n^3(n^2-1)\frac{(Z_1n-Z_2)^{2n-4}}{(Z_1n+Z_2)^{2n+4}},$$

where R_∞ is the Rydberg constant for infinite mass, n is the quantum number of p electron, Z_1 is the effective nuclear charge for the $1s$ electron, and Z_2 is the effective nuclear charge for the np electron. The increment of energy is positive for singlets, negative for triplets.

If one considers the line 2^1P-3^1D, λ6678, the normal effect is

$$\Delta\nu_1=\frac{m}{\lambda}\left(\frac{1}{M_4}-\frac{1}{M_3}\right)$$
$$=-0.681\ \text{cm}^{-1}.$$

Eckart[3] has calculated the values of Z_1 and Z_2 and has found

$Z_1=2.003$ for the $1s$ electron,
$Z_2=0.965$ for the $2p$ electron.

The specific effect is

$$\Delta\nu_2=\left(\frac{128}{3}\right)\left(\frac{m}{M_4}-\frac{m}{M_3}\right)R_\infty(Z_1Z_2)^2n^3(n^2-1)\frac{(Z_1n-Z_2)^{2n-4}}{(Z_1n+Z_2)^{2n+4}}$$
$$=-0.364\ \text{cm}^{-1},$$

and total change is

$$\Delta\nu=\Delta\nu_1+\Delta\nu_2=-1.045\ \text{cm}^{-1},$$

or

$$\Delta\lambda=0.466\text{A}.$$

Using the Mount Wilson Observatory 15-ft. Rowland mounting with a 5-inch concave grating and a dispersion of 3.60A/mm in the first order, we photographed the line λ6678. From comparator readings, the average value of three different photographs shows

$$\Delta\lambda=0.471\pm0.009\text{A}.$$

The shift was also measured with a Fabry-Perot Interferometer. With a 3 mm etalon we obtained photographs of two interference patterns of λ6678. Measurements of the shift in six successive orders of the two microphotometer tracings give

$$\Delta\lambda=0.467\pm0.004\text{A}.$$

The agreement is well within experimental error.

We wish to express our gratitude to Professors W. R. Smythe and R. B. King for valuable discussions and suggestions.

[1] A. Andrew and W. R. Smythe, Phys. Rev. **74**, 496 (1948).
[2] D. S. Hughes and Carl Eckart, Phys. Rev. **36**, 694 (1930).
[3] Carl Eckart, Phys. Rev. **36**, 149 (1930).

Disintegration of Tc^{95} and Tc^{96}

H. MEDICUS, A. MUKERJI, P. PREISWERK, AND G. DE SAUSSURE
Swiss Federal Institute of Technology, Zurich, Switzerland
August 14, 1948

IN a preliminary note[1] we have communicated that irradiation of molybdenum with 7-Mev protons leads to the formation of several Tc isotopes, which decay by emitting γ-lines in the range between 770 and 880 kev. A 873-kev line could be assigned to 53-min. Tc^{94} [2] and another one, of 810 kev, to 62-day Tc^{95}.[3]

The Tc isotope of mass number 96 (which disintegrates by K-capture[4,5] with a 104-hr. period) has now been investigated in more detail. While the curve of the γ-ray absorption in lead seemed to suggest a homogeneous γ-line of about 800 kev, a weak component of about 1100 kev resulted from coincidence absorption measurements of the secondary electrons. A sample, chemically separated from Mo and electrolytically deposited on a foil, was used for investigating (in a magnetic lens spectrometer) the conversion electrons. This analysis showed further complexities in the γ-radiation associated with the 104-hr. period. (Fig. 1.) Three strong electron lines at 751, 786, and 822 kev were found, which correspond to γ-energies of 771±2, 806±2, and 842±2 kev, respectively. Furthermore, weak conversion lines of γ-rays of 1119±2 and 312±2 kev are present. γ−γ-coincidence measurements which were carried out with Bi cathode counters showed, in accordance with measurements performed in the same calibrated arrangement with Al cathode counters, that the γ-ray components of 771, 806, and 842 kev are emitted in threefold cascade. Both from the intensity of the 1119-kev line (which was estimated from the recoil electrons from brass in the spectrometer) and the coincidence rate, we must conclude that this γ-line is also emitted in cascade with the 771- and 842-kev γ-lines. The weak 312-kev γ-line could only be observed through its converted part and its energy fits very well the difference between 1119 and 806 kev. The ratio of K-capture X-quanta to γ-quanta was determined by measuring the absorption in aluminum with counters of known sensitivity, the electrons from the sample and the recoil electrons from the absorber being deflected magnetically. Taking into account the fluorescence yield for Mo $K\alpha$-radiation and the L-capture, one finds that the number of cascade transitions is equal to the number of orbital electron captures. No positron tracks were found on cloud-chamber photographs.—We therefore suggest a decay scheme as in Fig. 2, in which the order of succession of the last two γ-ray transitions is as yet arbitrary. The lines due to conversion electrons were backed by a weak continuous spectrum extending up to 0.8 Mev. It could not be decided whether this background is simply due to scattered electrons or to an actual β^--spectrum. The existence of a stable ruthenium isotope of mass number 96 leaves the possibility of a dual decay open.

In the course of the investigation of the 104-hr. period further details of the 20-hr. period of Tc^{95} came to light. Spectrometer measurements indicated three conversion lines corresponding to γ-energies of 762±2, 932±2, and 1071±2 kev, the strongest component being that at 762 kev. On the other hand, we were unable to detect the 200-

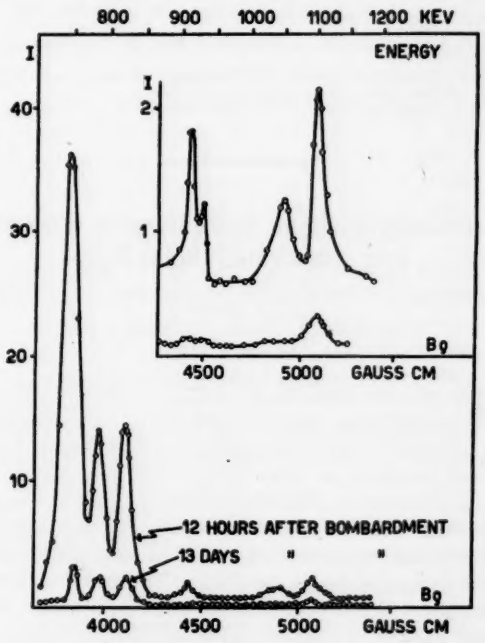

FIG. 1. Conversion electrons from 20-hr. Tc^{95} and 104-hr. Tc^{96}.

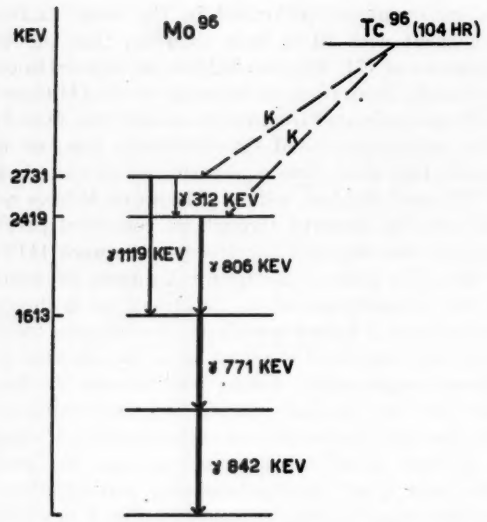

FIG. 2. Decay scheme of 104-hr. Tc^{96}.

kev electrons indicated by Eggen and Pool.[6] From the ratio of X-quanta to γ-quanta it follows that all K-captures lead to excited states. Eggen and Pool assign both the 20-hr. and the 62-day periods to an isotope of mass number 95, calling for the assumption of isomeric states in Tc^{95} decaying over different levels of Mo^{95}.

A detailed report of this work will appear in Helv. Phys. Acta. We take pleasure in thanking Professor P. Scherrer for his stimulating interest in this investigation.

[1] P. C. Gugelot, O. Huber, H. Medicus, P. Preiswerk, and R. Steffen, Helv. Phys. Acta 20, 240 (1947).
[2] O. Huber, H. Medicus, P. Preiswerk, and R. Steffen, Phys. Rev. 73, 1208 (1948).
[3] O. Huber, H. Medicus, P. Preiswerk, and R. Steffen, Phys. Rev. 73, 1211 (1948).
[4] J. E. Edwards and M. L. Pool, Phys. Rev. 69, 253 (1946); 72, 384 (1947).
[5] P. C. Gugelot, O. Huber, H. Medicus, P. Preiswerk, P. Scherrer, and R. Steffen, Helv. Phys. Acta 19, 418 (1946).
[6] D. T. Eggen and M. L. Pool, Phys. Rev. 74, 57 (1948).

Observation of a Solar Noise Burst at 9500 Mc/s and a Coincident Solar Flare

M. Schulkin, F. T. Haddock, K. M. Decker, C. H. Mayar and J. P. Hagen
Naval Research Laboratory, Washington, D. C.
August 23, 1948

ON July 29, 1948, 12:50 G.C.T. (7:50 A.M., E.S.T.), a solar noise burst on 9500 Mc/s was observed at this laboratory, and simultaneously a very bright chromospheric eruption or solar "flare" was observed at the Naval Observatory, Washington, D. C. Also, at the same time, solar noise bursts at 25, 50, 75, 110, and 480 Mc/s and the commencement of a sudden ionospheric disturbance were recorded at the National Bureau of Standards field station in Sterling, Virginia. Although similar coincidences have been observed below 3000 Mc/s,[1–6] this seems to be the first report above 3000 Mc/s.

A microwave radiometer[7] with a ten-foot paraboloid antenna, having a beam width of about 0.7°, was being used at the time to investigate atmospheric absorption, using the sun as the source of 9500 Mc/s noise. From 11:51 G.C.T. to 12:46 G.C.T. the antenna temperature[7] readings on the sun fluctuated between 2130°K to 2160°K. The sun was then allowed to drift partially out of the antenna beam for about three minutes, whereupon the antenna was again directed upon the sun. The reading then rose rapidly to normal but continued to rise at an irregular rate, taking 20 seconds to attain off-scale values of over 4000°K at 12:50:04 G.C.T. Ten seconds later the antenna was directed away from the sun, where the reading was found to be normal for the sky. At 12:53 G.C.T. the solar reading was down to 2380°K; by 13:00 G.C.T. it was 2240°K and was back to 2160°K by 13:26 G.C.T.

On this same day from 12:41 to 12:55 G.C.T., U. S. Lyons at the Naval Observatory was sketching the features of the solar disk observed through a spectrohelioscope in hydrogen alpha-light. At 12:52 G.C.T. he noticed a small, low velocity, very bright chromospheric eruption in a sunspot group at about 13° north and between 13° and 21° east of the center of the solar disk. However he feels sure that this flare commenced after 12:45 G.C.T. By 13:15 G.C.T. the flare had disappeared. The McMath-Hulbert Observatory, Pontiac, Michigan, from a photograph of the sun at 12:55 G.C.T. reported a solar flare of importance two on the I.A.U. scale arising from the same area.

G. Reber of the National Bureau of Standards informs us that a 480 Mc/s solar noise burst beginning at 12:49 G.C.T. rose in less than a minute to off-scale values of over ten times the normal antenna temperature. At 12:53 G.C.T. the reading was about twice normal, and by 13:02 G.C.T. it was normal.

J. R. Johler of the National Bureau of Standards records continuously cosmic noise received by half-wave dipoles at 25, 50, 75, and 110 Mc/s. At approximately 12:50 G.C.T. the readings on all four frequencies simultaneously went off scale for three to five minutes. These off-scale readings probably indicate a solar noise burst of over 50 or 100 times the noise power from the quiet sun.

The Coast and Geodetic Survey Magnetic Observatory at Cheltenham, Maryland, informs us that on July 29, 1948, there was no significant magnetic disturbance. Magnetograms taken near the sub-solar point have not yet been received.

The kind assistance of G. Reber, A. H. Shapley, and Miss O. E. Youngdahl of the National Bureau of Standards and U. S. Lyons and Mrs. L. T. Day of the Naval Observatory in supplying much of the above information is gratefully acknowledged.

[1] E. V. Appleton and J. S. Hey, Phil. Mag. 37, 73 (1946).
[2] Ruby Payne-Scott, D. E. Yabsley, and J. G. Bolton, Nature 160, 256 (1947).
[3] J. S. Hey, S. J. Parsons, and J. W. Phillips, Nature 160, 371 (1947).
[4] S. E. Williams, Nature 160, 708 (1947).
[5] F. J. Lehany and D. E. Yabsley, Nature 161, 646 (1948).
[6] A. E. Covington, Proc. I.R.E. 36, 454 (1948).
[7] R. H. Dicke, Rev. Inst. 17, 268 (1946).

Pulsed Second Sound in Liquid Helium II*

J. R. PELLAM
Research Laboratory of Electronics, Massachusetts Institute of Technology, Cambridge, Massachusetts
August 23, 1948

PULSE methods previously employed[1] for investigating first sound in liquid helium II have been modified to to measure the velocity and attenuation of second sound, and observe various coupling effects between ordinary sound and second sound. Piezoelectric transducers have been replaced by thermal elements, and video pulses utilized. A paper giving more details will be submitted shortly to the Physical Review. This technique has already been described in the latest M. I. T. Research Laboratory of Electronics Quarterly Progress Report[2] where block diagrams, sectional drawings of apparatus, and a condensed version of the results are given.

The oscillogram of Fig. 1 represents the time sequence involved in this pulsing process. The d.c. generating pulse appears at the extreme left, triggered simultaneously with the start of the oscilloscope time-sweep. Arrival of the second sound pulses at the temperature sensitive element (carbon resistance strip[3]) is recorded by signal pips to the right. Individual markers appearing at 61.1-μsec. intervals provide the time scale. Elapsed time delay yields velocity directly, the transmitter-receiver separation being known; for the accompanying sample this distance was 7.57 centimeters. Absence of measurable time delay during pulse formation was established with gear having variable path length.

Advantages of the pulse method acrue mainly from the fundamental directness, no recourse to resonant systems[4,5] being involved. Consequent rapid readings simplify temperature control, and the low average power inherent in pulsed signals promises ultimate lower temperature measurements. Using path lengths of a few millimeters, and motion picture recording, velocities below two meters per second have been observed as the λ-point is approached. Immediately below the λ-point, temperature control to within 0.0002°K may be realized by holding the signal position fixed on the screen for constant transmitter-receiver position.

A great number of measurements of the velocity of second sound as a function of temperature have been made in the range from the λ-point to 1.0°K and the results appear to agree generally with the results obtained by previous investigations[4,5] employing standing waves.

Attenuation measurements of video second sound pulses have been observed for the first time by means of apparatus having variable path length. Motion pictures record showing the decreased signal strength with increased path length (ambient temperature constant) provide a measure of the "exponential temperature attenuation coefficient" α.

$$\Delta T = \Delta T_0 e^{-\alpha z},$$

where ΔT is the amplitude of the temperature wave. For the pulses employed (88 per second, and 150-μsec. duration) the attenuation is small, α increasing steadily with temperature from a value of about 0.01 cm^{-1} at 1.65°K to about 0.1 cm^{-1} at 2.06°K. At still higher temperatures α increases much more rapidly, rising sharply, apparently to infinity, in the immediate vicinity of the λ-point (see plot in reference 2).

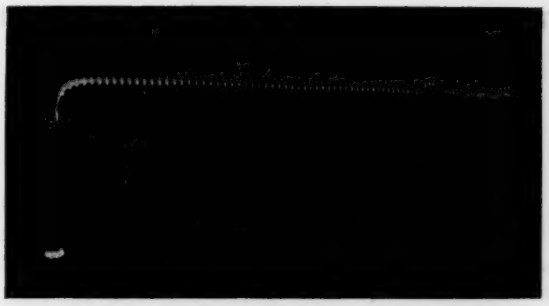

FIG. 1. Photograph of second sound pulse at 1.653°K (path length of 7.57 cm). See reference 2 for complete series.

The pulse method is particularly suitable for observing conversion phenomena between various types of sound, since the obscuring effects of system resonances are avoided. Thus quantitative data on the previously observed coupling[5] at the liquid surface has been obtained, plus evidence of two new forms of conversion for second sound. The surface coupling is observed by pulsing second sound from beneath and noting the drop in signal strength as the receiver is lifted vertically out of the liquid. The ratio of temperature fluctuations above and below the surface indicates that at 2.0°K about 5 percent of incident sound intensity is converted to vapor sound intensity (with no measurable time delay).

Substituting a classical (vibration) receiver for the temperature element reveals presence of first sound, also originating at the second sound generator, and unmistakable because of its higher wave velocity (possibly generated by internal breakdown of second sound). An even more subtle conversion is manifest in the faint signals following the original second sound signal of Fig. 1. The additional time delay corresponds to first sound transit time, though the events and their sequence are not clear.

After most of the data for the present research were obtained, word was received that similar experiments are in progress at the Royal Mond Laboratory in Cambridge, England. It is understood their results in the velocity of second sound are in general agreement with the present measurements.

Of those aiding in this work, particular thanks are extended R. Cavileer and P. Nicholas for their technical assistance.

* This research has been supported in part by the Signal Corps, the Air Materiel Command, and O. N. R.

[1] J. R. Pellam and C. F. Squire, Phys. Rev. 72, 1245 (1947).
[2] J. R. Pellam, "Investigations of second sound in liquid helium II," M. I. T. Research Laboratory of Electronics Quarterly Progress Report, July 15, 1948, p. 16.
[3] H. Fairbanks and C. T. Lane, Rev. Sci. Inst. 18, 525 (1947).
[4] V. Peshkov, J. Phys. 10, 389 (1946).
[5] Lane, Fairbank, Schultz, and Fairbank, Phys. Rev. 70, 431 (1946).

Temperature Dependence of Penetration Depth of a Magnetic Field in Superconductors

J. G. DAUNT
Mendenhall Laboratory, Ohio State University, Columbus, Ohio
AND
A. R. MILLER, A. B. PIPPARD, AND D. SHOENBERG
Royal Society Mond Laboratory, Cambridge, England
August 9, 1948

IN view of conflicting statements in recent discussions[1,2] of the temperature variation of λ (penetration depth of a magnetic field into a superconductor), it is worth reviewing the available experimental data. The only evidence providing a sensitive test of any proposed law is that from the magnetic properties of the small particles in colloids,[3] which gives essentially $\lambda(T)/\lambda(0)$ (the absolute value of $\lambda(0)$ could not be deduced since the particle size was not accurately known). So far results have been obtained only for mercury and these show (Fig. 1) that

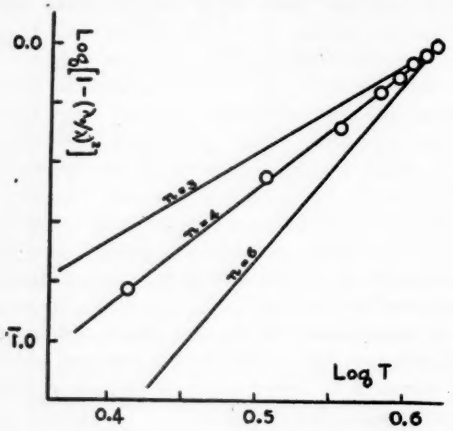

FIG. 1. $\text{Log}[1-(\lambda_0/\lambda)^2]$ *vs.* log$T$ for Hg.

the law

$$[\lambda(0)/\lambda(T)]^2=1-(T/T_c)^n \qquad (1)$$

with $n=4$ is very well obeyed, provided it is assumed (as is probably justified) that the spread in particle size in the colloid used was not sufficient to affect the results. This law is consistent with the Gorter-Casimir theory[4] if it is combined with the London theory[5] and the superconductor is assumed to have a parabolic H_c-T relation or a specific heat proportional to T^3. The relation (1) and this theoretical interpretation were first pointed out by Daunt[1] but owing to a misprint, only recently noticed, the n in (1) appeared as 3 instead of 4; a discussion has also been given by Miller.[6]

Other experiments have been of three kinds, (a) various measurements of $\Delta\lambda=(\lambda(T)-\lambda(T_0))$, with T_0 usually about 2.1°K,[7-10] (b) measurements of r-f resistance[11-13] from which λ can be deduced, but only indirectly and on the basis of an assumed model of the resistive process, and (c) measurements of the critical fields of thin wires[14] and thin films.[15] The measurements of $\Delta\lambda$ are all consistent within experimental error with (1), but they are not sufficiently accurate to prove the truth of (1) or to indicate more than a rough value of n, unless $\lambda(0)$ is already known. It should be noted that the full curves of $\Delta\lambda$ against T for mercury published by Désirant and Shoenberg and by Laurmann and Shoenberg in preliminary notes[8,9] are curves *calculated* from the colloid data (using a value of $\lambda(0)$ deduced by combining the colloid data with the $\Delta\lambda$ data from thin wires[8]); it is therefore impossible to deduce from these curves anything regarding n that is not already contained in the original colloid data. A detailed discussion of experiments on $\Delta\lambda$ was given at the recent conference on metals in Amsterdam.[16] As regards the r-f resistance measurements, it should be emphasized that any derivation of λ from them is only as reliable as the theoretical model of the resistive mechanism assumed; recent measurements at a higher frequency[17] suggest that the frequency dependence is not in accord with the theoretical model used by Pippard to derive values of λ. Thus it is unsafe as yet to use r-f resistance measurements as evidence for any particular law of temperature variation of λ. It may be noticed that the same theoretical model is partially involved also in Pippard's method[7] for $\Delta\lambda$, but since the specific theoretical assumptions enter only in a correction term, the results of this method should be reliable except very close to T_c. The critical field measurements again lead only indirectly to information about λ and, as has been discussed elsewhere,[8] their interpretation must await the development of a detailed theory.

[1] J. G. Daunt, Phys. Rev. **72**, 89 (1947).
[2] de Launay and Steele, Phys. Rev. **73**, 1450 (1948).
[3] D. Shoenberg, Proc. Roy. Soc. **A175**, 49 (1940).
[4] Gorter and Casimir, Physik. Zeits. **35**, 963 (1934).
[5] F. and H. London, Proc. Roy. Soc. **A149**, 71 (1935).
[6] Miller, Australian J. Sci. **10**, 172 (1948).
[7] Pippard, Nature **159**, 434 (1947).
[8] Désirant and Shoenberg, Nature **159**, 201 (1947) and Proc. Phys. Soc. **60**, 413 (1948).
[9] Laurmann and Shoenberg, Nature **160**, 474 (1947).
[10] Shalnikov and Sharvin, J. Exper. Theor. Phys. U.S.S.R. **18**, 102 (1948).
[11] H. London, Proc. Roy. Soc. **A176**, 522 (1940).
[12] Pippard, Proc. Roy. Soc. **A191**, 399 (1947).
[13] Maxwell, Marcus, and Slater, Bull. Am. Phys. Soc. **23**, 40 (1948).
[14] Pontius, Phil. Mag. **24**, 787 (1937).
[15] Appleyard, Bristow, Misener, and H. London, Proc. Roy. Soc. **A170**, 540 (1939).
[16] D. Shoenberg, Communication to the Conference on Metals, Amsterdam (1948).
[17] Pippard, Nature **162**, 68 (1948).

Frictional Electricity

E. W. B. GILL
Electrical and Clarendon Laboratory, Oxford, England
August 14, 1948

IN Phys. Rev. 66, 9–16 (1944) you published a paper by Mr. D. E. Debeau on frictional electricity. He got the remarkable result that the charge produced on small insulating particles sliding down a metal depended very much on the pressure of the air. At very low pressures of the order of 10^{-4} mm of mercury the charge is large; as the pressure is increased up to about 1 mm it gets less and less and thereafter increases again with further pressure increase. The charge at 1 mm was only about 1/7 of that at 10^{-4}. He explains this result as being due to adsorbed layers of gas but to explain the minimum he is driven to the conclusion there must be two adsorbed layers.

A much simpler explanation seems worth investigating. The frictional charges are very large and after the stream has slid some distance over the metal the charge per unit volume is sufficient to create a large potential difference between the particles and the metal. If this gets high enough to produce a discharge through the air round the particles, it will put an automatic limit on the final charge on the particles. In this case we should expect the curve charge against pressure to resemble the well-known curve of sparking potential against pressure, which it does.

Additional confirmation is that, taking his experimental results for the charges at 1 mm pressure, it is easy to calculate that in the stem of the metal funnel down which the particles pass the P.D. between the center and the sides is of the order of 400 volts which is of the order of the minimum sparking potential.

Microwave Magnetic Dispersion in Carbonyl Iron Powder

J. B. Birks
Department of Natural Philosophy, The University, Glasgow, Scotland
August 16, 1948

MEASUREMENTS have been made of the complex permeability of mixtures of carbonyl iron powder and paraffin wax at microwave frequencies, using the dual impedance wave guide method.[1] Typical results for the modulus of permeability $|\mu|$ and the magnetic loss angle δ_μ of specimens containing 18 percent by volume of iron powder are given in Table I. The modulus of permittivity

TABLE I.

λ (cm)	58.4	39.6	29.9	22.4	15.4	9.1	5.95	3.09
$\|\mu\|$	2.28	2.23	2.17	2.05	1.91	1.70	1.53	1.40
δ_μ	6.8°	9.0°	12.2°	13.3°	17.7°	17.7°	18.1°	21°

$|\epsilon|$ of the mixture and its dielectric loss angle δ_ϵ remained constant, within the experimental error, over the complet wave-length range, at 5.60 (±2 percent) and 1.0° (±0.1°), respectively.

The magnetic dispersion and absorption of iron does not display any of the resonance characteristics, attributable to internal anisotropy fields, observed in the iron oxides.[1,2] This marked difference in behavior is due to the high conductivity of iron, and the consequent skin effect which restricts the penetration of the microwave field into the iron, to a depth of 10^{-4} to 10^{-5} cm. The skin effect masks any *natural* resonance effects resulting from the anisotropy field, although the much more pronounced *induced* resonances can be observed, when the electron spins are aligned by an applied saturation magnetostatic field.[3,4]

Kittel[5] has pointed out that the skin depth in iron at microwave frequencies is only a small fraction of the domain thickness, so that the applied h.f. magnetic field only penetrates a little way down a surface domain boundary. The force on this boundary is consequently less than at low frequencies, so that the domain boundary shift and the resultant magnetization are correspondingly

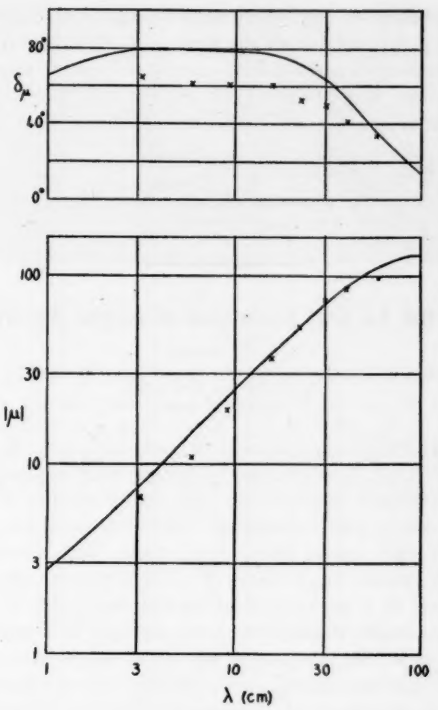

FIG. 1.

reduced, leading to a decrease in permeability with increase in frequency. Kittel has considered a thin film, one domain thick, as a theoretical model, and he has derived and evaluated expressions for its magnetic dispersion.

It is of interest to compare the experimental results with Kittel's theoretical curves. It has been found for carbonyl iron mixtures up to 50 percent concentration, that $|\mu|$ and $\tan\delta_\mu$ obey similar logarithmic and linear concentration laws to those observed for γ-ferric oxide mixtures.[1] Above this concentration, deviations from the laws become apparent, as a result of particle agglomeration. The measurements on mixtures below 50 percent concentration have been extrapolated to zero dilution, and the results are plotted together with the curves for Kittel's film model (see Fig. 1).

The extrapolated permeability values are not in general equivalent to observations on solid iron, since the majority of the particle surfaces responsible for the dispersion disappear into the bulk of the material as the concentration is increased. On the other hand, the extrapolation corresponds much more closely to a thin film, in which the particle surfaces remain exposed to the applied h.f. field. This presumably accounts for the good agreement between the extrapolated experimental data and Kittel's thin film model. The average particle size of the carbonyl iron was 5.5 microns compared with 2.5 microns for Kittel's model.

The results appear to substantiate the validity of the theory, and it is likely that an elaboration of the model, to take account of the eddy currents induced in the material behind the surface film, would lead to better agreement with the observations on solid iron. At wave-

lengths below 10 cm, where such an elaboration becomes less necessary because of the very small field penetration, the extrapolated permeability values are found to approach closely the measurements on iron wires by Arkadiew and others.[5]

[1] J. B. Birks, Proc. Phys. Soc. 60, 282 (1948).
[2] J. B. Birks, Nature 160, 535 (1947).
[3] J. H. E. Griffiths, Nature 158, 670 (1946).
[4] W. A. Yager and R. M. Bozorth, Phys. Rev. 72, 80 (1947).
[5] C. Kittel, Phys. Rev. 70, 281 (1946).

On the Lateral Extension of Auger Showers

S. F. SINGER
Applied Physics Laboratory, Johns Hopkins University, Silver Spring, Maryland
August 12, 1948

A SHOWER experiment has been carried out by Skobeltzyn, Zatsepin, and Miller[1] in which they measured the coincidence rate between two sets of counter trays as a function of their separation. They conclude that their experimental results give a much higher coincidence rate at large counter separations than the curve calculated on the basis of a primary electron shower model. Possible reasons for this discrepancy have recently been examined by Cocconi.[2] He points out that good agreement can be reached between theory and experiment if one takes into account the effect of showers incident at large zenith angles. Particularly for large tray separations, this effect cannot be neglected; for a shower whose axis is at zenith angle θ in the vertical plane joining the counter trays, the effective separation between the trays is reduced by a factor $\cos\theta$, thereby increasing the probability for the shower to be detected. It is the purpose of this note (a) to extend Cocconi's argument, and (b) to report on an experimental confirmation.

(a) A shower striking the experimental arrangement at an angle θ not only sees a smaller separation but—depending on the geometry of the counter tray—a smaller area as well. This decrease in area reduces the sensitivity of the equipment to low density showers, and thereby lowers the counting rate. The net effect is an increase in counting rate smaller than calculated in reference 2.

(b) To check this point, the following experiment, suggested by Professor J. A. Wheeler, was carried out at Silver Spring, Maryland (altitude 120 meters). The coincidence rate of two Geiger counters was measured. The counters were 29.2 cm long and 2.4 cm in diameter; their separation in the horizontal plane was 40 meters. In arrangement A, the counter axes were parallel to each other and perpendicular to their line of separation. In arrangement B (see Fig. 1), the counters were rotated through 90° about a vertical axis so that their axes were along their line of separation. Evidently, arrangement B is subject to the effect discussed in (a) to a much greater degree than arrangement A. This is borne out by the result of the experiment: the counting rate under arrangement A was greater than the corresponding rate for arrangement B by 32 percent±13 percent.

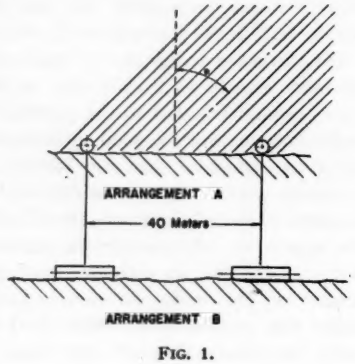

FIG. 1.

The experiment was repeated with the separation reduced from 40 meters to 20 meters. Within the statistics of the experiment (10 percent) there was no difference in counting rate between arrangements A and B.

From the experimental results, it appears reasonable to conclude (i) that non-vertical showers contribute greatly to the coincidence rate of arrangement A for large counter separations; (ii) arrangement B has a lower counting rate than arrangement A since it does not record many non-vertical showers of low particle density because of the decrease of counter area discussed above.

[1] D. V. Skobeltzyn, G. T. Zatsepin, and V. V. Miller, Phys. Rev. 71, 315 (1947).
[2] G. Cocconi, Phys. Rev. 72, 350 (1947).

The Specific Charge of the Positron

J. BARNÓTHY
Institute for Experimental Physics, University of Budapest, Budapest, Hungary
August 11, 1948

SEVERAL considerations regarding the properties of elementary particles[1] seem to suggest that the mass of an elementary particle is composed of intrinsic mass and mass-defect. The positron as a free particle has a positive intrinsic mass equal to the intrinsic mass of the electron, i.e., to m_0, whereas its mass-defect $-0.00177m_0$ has equal size but opposite sign. Accordingly, the mass of the positron would be with 0.354 percent less than the mass of the electron, entailing the consequence that the specific charge of the positron would be higher by the same amount.

Spees and Zahn[2] report measurements in which they compared the specific charge of electron and positron. A close scrutiny of the position of the peaks upon the curves seems to indicate that the specific charge of the positron slightly exceeds that of the electron. Unfortunately, the accuracy of the measurement does not permit a determination with greater accuracy than one percent. It would seem to be worth while to investigate this point with an improved method of greater accuracy.

A further consequence of this mass difference is that the g value of the positron will slightly differ from that of the electron:

$$g_p = 1.99636, \quad \text{while} \quad g_e = 2.00343.^{3}$$

[1] J. Barnóthy, Terr. Mag. No. 2 (1947).
[2] A. H. Spees and C. T. Zahn, Phys. Rev. 58, 861 (1940).
[3] J. Barnóthy, Phys. Rev. 73, 113 (1948).

Nuclear Evaporations Produced by Cosmic Rays

G. BERNARDINI, G. CORTINI, AND A. MANFREDINI
Instituto de Fisica dell'Università, Centro di Fisica Nucleare del C.N.R., Roma, Italy
August 14, 1948

WITH the photographic emulsion technique,[1] the well-known processes discovered by Blau and Wambacher,[2] i.e., the so-called "stars" produced by cosmic radiation, were investigated.

The experiments, which were performed partly at the Laboratorio della Testa Grigia (3500 m.s.l.) and partly with balloon flights,[3] have yielded results which, though provisional, are, we feel, not without significance.

In a first series of experiments (carried out at 3500 m.s.l.) the plates were exposed under varying thicknesses of several materials. Up to now 10 plates exposed under lead have been completely scanned. The results concerning those stars, which show at least three clearly observable prongs, are summarized in Table I.

TABLE I.

cm of Pb	0	2	9	13
No. of stars / cm²·day	15.3±1	18.0±0.9	13.1±1.15	9.7±1

These results are perhaps consistent with the assumption that there is a small transition effect in the first two centimeters of lead. This is also borne out by the results reported by Heitler, Powell, and Heitler[4] in connection with single proton tracks.

From the data summarized in Table I it is also possible to give a rough estimate of the absorption coefficient of lead for the radiation which produces the stars. Neglecting the transition effect, we find an absorption coefficient

$$K_{Pb}=1/300\ \text{g}^{-1}\cdot\text{cm}^2.$$

To take into account the finite size of the lead blocks, this value should be enlarged by about 20 percent.

Let us now turn to the results of the balloon flights. The first of these balloons reached an altitude of about 18 km and the second 22 km. In the plates exposed during these balloon flights (see Fig. 1) we found π- and σ-mesons, and a relatively great number of stars.

We have attempted to evaluate the absorption coefficient for the star-producing radiation, comparing the number of stars in the first balloon flight plates and in the L.T.G. ones. We obtained an absorption coefficient for air:

$$K_A=1/(141\pm12)\ \text{g}^{-1}\cdot\text{cm}^2.[5]$$

This result is in quite good agreement with that of Perkins from single proton tracks.[6]

In Fig. 2 the stars are classified according to the number of their prongs. In spite of the large statistical errors there is reasonable evidence for saying that the shape of the distribution does not vary greatly in the very different cases represented by the histograms.[7] This appears to support the assumption that the processes by which the stars arise are roughly independent of the energy of the radiation which produces them.

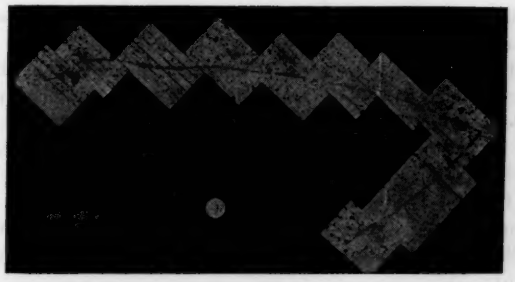

FIG. 1. Mosaic of photomicrographs of a $\pi\rightarrow\mu$-disintegration process, observed in one of the balloon plates.

It is quite evident that there is a close correlation between the observations concerning stars and the burst experiments.[8] As a matter of fact, below 200 g/cm² under the top of the atmosphere, the curve of the burst rate *versus* depth is very well represented by the relation

$$I=I_0\exp[-K^x]$$

with

$$K=1/138\ \text{g}^{-1}\cdot\text{cm}^2$$

in very good agreement with our result.

The relatively low absorption coefficient in lead excludes the possibility that any appreciable fraction of the stars are due to the electron-photon component. The same conclusion is reached by considering the lack of maximum in the burst curve obtained in the atmosphere.

The stars can similarly not be produced in an appreciable measure by mesons of mass 200. In fact, the ratio between the number of stars registered at 3500 m and at s.l. is

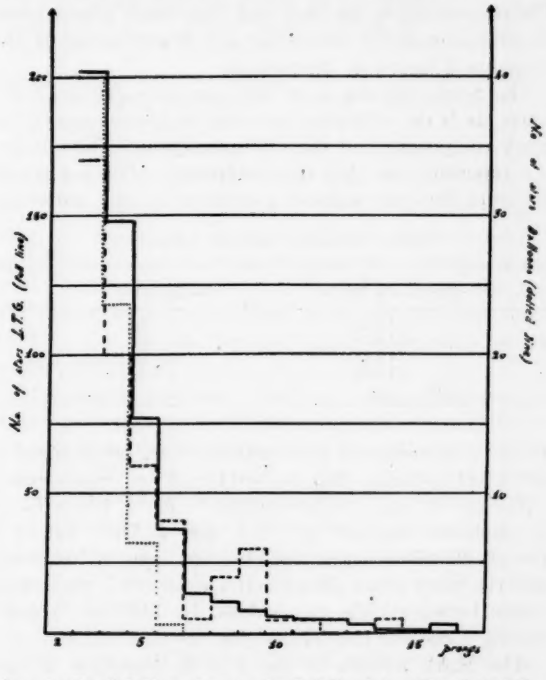

FIG. 2. The full line refers to the L.T.G. plates. The dotted line refers to the balloon plates. The finely dotted line describes the stars produced by 400-Mev α-particles (see reference 7)

about 15/1, while the corresponding ratio of meson intensity is only 2/1.

Hence we may say that it appears almost certain that high energy nucleons and σ-mesons play the principal role in the creation of these stars. The latter may be spoken of as "local indicator" of these components of cosmic radiation.

If this assumption is justified, we may deduce, by comparing the measurements under air and lead, the following value for the total cross section of this component:

$$\sigma \leqq 3A^{\frac{2}{3}} \times 10^{-26} \text{ cm}^2.$$

[1] C. F. Powell, G. P. S. Occhialini, and C. M. G. Lattes, Nature 159, 186 (1947); 159, 694 (1947); 160, 453 (1947); 160, 486 (1947).
[2] H. Wambacher, Sitz. Akad. Wiss. Wien, IIA, 149, 157 (1940).
[3] We are very indebted to Dr. A. Persano for his invaluable help in the performance of the flights.
[4] W. Heitler, C. F. Powell, and H. Heitler, Nature 146, 65 (1940).
[5] G. Cortini, A. Manfredini, and A. Persano, Nuovo Cimento, in press.
[6] D. H. Perkins, Nature 160, 707 (1947).
[7] Communication by Professor L. W. Alvarez at the Zurich Congress, July 1948.
[8] H. Bridge and B. Rossi, Phys. Rev. 71, 379 (1947); H. Bridge, B. Rossi, and R. Williams, Phys. Rev. 72, 257 (1947); H. E. Tatel and J. A. Van Allen, Phys. Rev. 73, 87 (1948).

Preliminary Analysis of the Microwave Spectrum of Ethylene Oxide*

R. G. Shulman, B. P. Dailey, and C. H. Townes
Columbia University, New York, New York
August 23, 1948

FOUR strong lines of the pure rotational spectrum of the asymmetric rotor, ethylene oxide, have been observed in the region near 24,000 Mc/sec. (see Table I). The frequencies of the lines and their Stark effects allow identification of the transitions and determination of the moments of inertia of the molecule.

The Stark splitting is of the form $\Delta\nu = \mu^2 E^2 (A + BM^2)$ where $\Delta\nu$ is the difference between the frequencies of the Stark component and the undisplaced line. The number of components and their relative spacings allow a determination of the lower value of J involved in each transition.

Table I. Ethylene oxide absorption lines.

Frequency Mc/sec.	Designation
23,160	$3_1 - 3_2$
23,614	$3_{-1} - 3_1$
24,855	$4_0 - 4_2$
24,948	$2_{-2} - 2_0$

Relative intensities of the components are proportional to M^2, which indicates that $\Delta \cdot J = 0$ for all four transitions.[1]

For $\Delta J = 0$, $\nu_{J\tau;J\tau'} = (a-c)/2(E_\tau^J - E_{\tau'}^J)$, where E_τ^J is a tabulated function[2] of J, τ, and κ. Only values of $\kappa = \pm 0.395$ allow fitting the observed lines in frequency, and the Stark effect shows that $\kappa = +0.395$ is the correct choise between these two values. In addition to determining κ, the line frequencies give $(a-c)/2 = 0.1898$ cm^{-1}.

The Stark pattern of the $2_{-2} - 2_0$ transition is very sensitive to the ratio of $(a-c)/(a+c)$. Changes of 1 percent in the value of this ratio vary the ratio of the Stark effect coefficients A/B by 3 percent, giving $(a-c)/(a+c) = 0.2756 \pm 0.003$, and $(a+c)/2 = 0.689 \pm 0.007$ cm^{-1}.

For the analysis, ethylene oxide was considered to be rigid and the effective moments of inertia rather than the equilibrium moments are determined. They are:

$$I_A = 31.9 \times 10^{-40} \text{ g cm}^2,$$
$$I_B = 36.7 \times 10^{-40} \text{ g cm}^2,$$
$$I_C = 56.7 \times 10^{-40} \text{ g cm}^2.$$

As a check on the structure, the Stark patterns of the $3_3 - 3_1$, $3_1 - 3_{-1}$, and $4_2 - 4_0$ transitions were calculated and the ratios of various coefficients involved were compared with the experimental values (see Table II).

Table II. Ratios of Stark effect coefficients for observed lines. [Stark displacement $\Delta\nu = \mu^2 E^2 (A + BM^2)$.]

Ratio	Calculated	Observed
$A_{3_1 - 3_2}/B_{3_1 - 3_2}$	0.69	0.69
$A_{3_{-1} - 3_1}/B_{3_{-1} - 3_1}$	−0.20	−0.18
$B_{3_1 - 3_2}/B_{3_{-1} - 3_1}$	0.67	0.66
$A_{4_0 - 4_2}/B_{4_0 - 4_2}$	0.002	0.01
$A_{2_{-2} - 2_0}/B_{2_{-2} - 2_0}$	0.233	0.233
$B_{4_0 - 4_2}/A_{2_{-2} - 2_0}$	−0.62	−0.62

If the C−H distance is assumed to be 1.09A, then the H−C−H angle is 121°.

Further work is contemplated to study isotopic species and to obtain more accurate molecular constants.

* Work supported by the Signal Corps.
[1] S. Golden and E. B. Wilson, Jr., J. Chem. Phys. 16, 669 (1948).
[2] G. W. King, R. M. Hainer, and P. C. Cross, J. Chem. Phys. 11, 27 (1943).

On the Production of Showers of Penetrating Particles

H. A. Meyer, G. Schwachheim, and Andrea Wataghin
Departamento de Física, Universidade de São Paulo, Brasil
August 26, 1948

THE purpose of the present experiments[1] was to study the cross section for the production of penetrating showers in various materials.

The penetrating showers were detected by a pair of "telescopes" shielded by lead from all sides (of the type used by G. Wataghin[2]). The registered radiation had a minimum range of 18 cm Pb. The telescopes were separated by 16 cm Pb.

Two series of measurements were planned. In the first one we distributed an equal number of nucleons (equal masses) of different materials in the same volume, and we obtained the frequencies of showers produced in these materials as the difference of the frequencies of the showers registered with and without the materials. In the second series (which is being performed) equal numbers of nuclei of two different elements are distributed in equal volumes. In this case the frequencies of the showers produced in the materials are proportional to the average cross sections of the respective nuclei.

In the present note we give the results of the first series, which consisted of experiments A and B. The shower-

producing materials were water and iron-filing located above the counter arrangement (equal masses in equal volumes). In experiment *A* the upper counters of the telescopes had an area of 400 cm² each and the lower ones an area of 250 cm². In experiment *B* all counters had an area of 600 cm² each. The resolving time of the circuit was 10^{-6} sec. The results are given in the table below.

TABLE I. Frequencies of penetrating showers in h^{-1}.

	Exp. *A*	Exp. *B*
No material	0.412±0.045	1.06±0.08
H_2O (57 g cm^{-2})	0.783±0.074	2.07±0.12
Fe (57 g cm^{-2})	0.592±0.049	1.37±0.14
H_2O (120 g cm^{-2})		2.02±0.11
Fe (120 g cm^{-2})		1.34±0.12

We see from these data that (a) the registered cross section per nucleon is larger in the case of water than in the case of iron, indicating that either the absorption coefficient of primaries or the constitution and multiplicity of the produced showers depends on the nuclear structure;[3] (b) with 57 g cm^{-2} of water or iron we observed saturation; (c) the existence of a difference between the frequencies at saturation in the case of water and iron suggests that the constitution, multiplicity, or angular divergence of the produced showers are different in the two cases. (d) The intensity of the shower-producing radiation is reduced by a factor $\gtrsim 1/e$ in a thickness of 57 g cm^{-2} in both H_2O and Fe. We conclude that the lower limit of the cross sections of this radiation is in both cases of the order of the geometrical cross sections of the nuclei.[4]

We thank Prof. G. Wataghin for the suggestion of this problem and for his kind, constant help during the performance of the measurements.

[1] A preliminary account of this work was presented at the meeting on July 13 of the Academia Brasileira de Ciencias.
[2] G. Wataghin, Phys. Rev. **71**, 453 (1947).
[3] Similar conclusions can be drawn from a recent work of Cocconi and Greisen, Phys. Rev. **74**, 62 (1948).
[4] For further work on the production of penetrating showers we refer to: V. Regener, Phys. Rev. **64**, 250 (1943); W. Hasen, Phys. Rev. **64**, 257 (1943); L. Janossy and Rochester, Proc. Roy. Soc. **A183**, 183 (1944); L. Janossy and D. Broadbent, Proc. Roy. Soc. **A190**, 497 (1947); O. Sala and G. Wataghin, Phys. Rev. **70**, 430 (1946); E. George and A. Jason, Nature **161**, 248 (1948). We finally mention experiments on the production of penetrating showers in paraffin and lead made by Professor Clay (private communication to Professor Wataghin).

The Beta-Spectrum of S^{35}

R. D. ALBERT AND C. S. WU
Columbia University, New York, New York*
August 19, 1948

RECENTLY Cook, Langer,[1] and Price[2] have published results on S^{35} negatrons and both positrons and negatrons from Cu^{64} which show an increase in number over that predicted by the Fermi theory at low energies. Because it is difficult to understand theoretically why such deviations should occur at low energy after the Coulomb correction has been made, an attempt was made to check these results with thinner sources. The Columbia University solenoid β-ray spectrometer[3,4] was used with eight

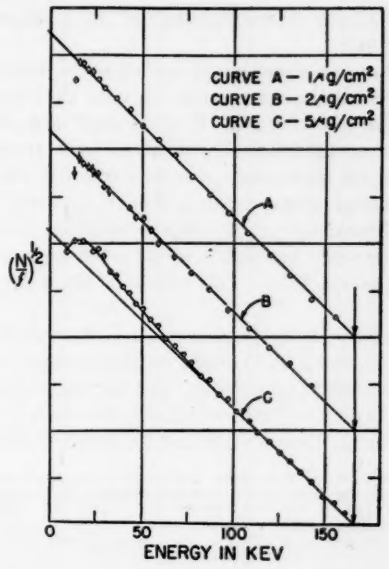

FIG. 1.

different S^{35} sources. These measurements all show straight-line Fermi plots for the upper half of the energy spectrum. Some show straight-line plots from the upper energy limit down to 16 kev, while others showed deviations from the straight line at much higher energies, similar to the curve given by Cook and Langer.[2] The solenoid spectrometer possesses advantages over the other type instruments in that it has a high geometric efficiency (~1 percent) and can use a large effective source area. This permits the use of extremely thin sources with as low as ~1 microcurie of total activity and a resolution of 1.25 percent.

Figure 1, curves *A* and *B*, show the results for two of the best sources prepared. Curve *C* shows the results for a somewhat thicker source. These Fermi plots are corrected for the Coulomb effect, using the non-relativistic correction factor which agrees within ~2 percent or better with the relativistic correction for S^{35}. The best straight line in each case was made to meet the axis at 166 kev; this value was obtained on each of several runs when the high energy region was investigated. The points of curves *A* and *B* do not deviate significantly from the straight-line plot above 16 kev. The drop at lower energies is probably instrumental and will be investigated further.

The counter windows consist of four thicknesses of collodion films prepared by spreading one drop of collodion solution (one part collodion, two parts amylacetate) over a pan of water in the usual manner. The total thickness is probably <30 micrograms/cm² and will transmit electrons down to 4 kev. The source backings were also collodion about 3 micrograms/cm². The sources were prepared by placing a drop of solution of carrier free S^{35} (from Oak Ridge) on the backing and drying in such a manner that it spread over a suitable area. The deposit did not form a perfectly uniform layer, so that the maximum local thicknesses were hard to estimate. Assuming uniform spreading, the sources for Fig. 1A, B, C were

about 1, 2, and 5 micrograms/cm² in addition to the backing film.

These are considerably thinner than the sources previously reported. It is important to note that a source as thin as that used for Fig. 1C gives such large deviations from the straight-line Fermi plot, and these results emphasize the importance of using extremely thin sources for low energy measurements. Rough data also indicate that additional source backing (a collodion film of ~10 micrograms/cm²) noticeably distorts the low energy portion of the spectrum. This effect is being investigated further.

We wish to thank Professors L. J. Rainwater, W. W. Havens, Jr., and J. R. Dunning for the constant encouragement and valuable discussion. The document is based on work performed under Contract AT-30-1-Gen 72 with the Atomic Energy Commission and Columbia University.

* This letter is based on work performed under Contract AT-30-1-Gen-72, and the information covered therein will appear in the Manhattan Project Technical Series, as part of the contribution of Columbia University.

[1] C. S. Cook and L. M. Langer, Phys. Rev. 73, 601 (1948).
[2] C. S. Cook, L. M. Langer, and H. C. Price, Jr., Phys. Rev. 73, 1395 (1948).
[3] C. M. Witcher, Phys. Rev. 60, 32 (1941).
[4] C. S. Wu, W. W. Havens, Jr., R. Albert, and G. Grimm, Phys. Rev. 73, 1259 (A) (1948).

Secondary Electron Emission by Fast Neutral Molecules and Neutralization of Positive Ions*

H. W. BERRY
Syracuse University, Syracuse, New York
August 4, 1948

WHEN a beam of positive ions passes through a gas at rest there occurs a weakening of the beam by a charge exchange with the gas atoms.[1] For most of these charge collisions the now fast atom undergoes little deviation. As a result there is little transfer of kinetic energy and we have, on removing any unneutralized ions, a beam of fast atoms with an energy equivalent to that of the original ion beam. One method of detection of such a neutral beam is to allow the atoms to strike a metal surface and measure the secondary electrons emitted under this bombardment.[2] The investigation here reported concerns the measurement of the number of these secondary

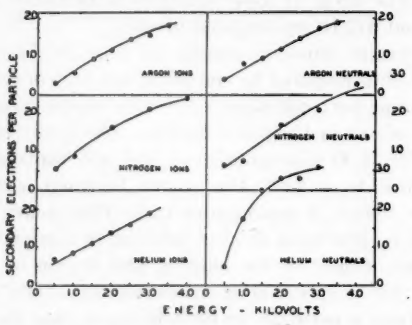

FIG. 1. Number of secondary electrons emitted from a tantalum surface per particle as a function of the energy of the particle in electron volts.

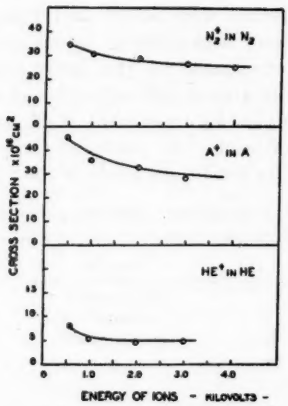

FIG. 2. Cross section for neutralization of ions in their own gas as a function of the ion energy in electron volts.

electrons removed from a tantalum surface by argon, helium, and nitrogen ions and molecules with energies ranging from 500 to 4000 electron volts.

A beam of positive ions of the desired energy is directed into a region where the same gas as that from which the positive ions are formed is present at a pressure of 10^{-4} to 10^{-3} mm of Hg. If in this neutralizing chamber a charge exchange collision should occur, the fast ion now becomes a neutral atom and a gas atom an ion. Most of these charge exchange collisions will be glancing, as is indicated by the much larger cross section for collisions obtained from various kinetic theory measurements. Hence most of the ions resulting from this charge exchange will be slow. These slow ions can be collected on an electrode by a small potential difference between the ends of the neutralizing chamber. In confirmation of this, it is found that as the potential difference between the electrodes at the ends of the neutralizing chamber is increased, the slow positive ion current collected by the electrodes increases rapidly with the voltage up to 40 or 50 volts. From 50 to 80 volts the current remains practically constant but beyond 80 volts rises again. The now neutralized fast atom may continue through a hole in the end of the neutralizing chamber and strike the tantalum surface from which the secondary electron emission occurs.

If E_+ = the ion current to the tantalum surface when it is positive, thus holding secondary electrons, E_- = the current to the tantalum surface (positives arriving, electrons leaving) when the surface is negative, and A = the slow positive ion current collected in the neutralizing chamber; then $E_- - E_+$ = the number of secondary electrons removed from the tantalum surface.

$$E_- - E_+ = k_+ E_+ + k_0 A,$$

where k_+ = number of electrons removed per positive ion striking the surface and k_0 = number of electrons removed per neutral atom striking the surface; so

$$(E_- - E_+)/E_+ = k_+ + k_0(A/E_+).$$

Now if the pressure in the neutralizing chamber is increased the slow positive ion current A will increase; since more ions are neutralized and since there are now,

proportionately, more atoms than ions in the beam, $(E_- - E_+)/E_+$ will also increase. When $(E_- - E_+)/E_+$ is plotted against A/E_+ (as abscissa) straight lines are obtained. The intercept of the line with the ordinate is the value of k_+, and the slope is k_0. Argon, nitrogen, and helium were investigated, and the values of k_+ and k_0 are shown in Fig. 1.

Since the current A is a measure of the number of neutralizing collisions occurring, it is possible with the same arrangement to measure the cross section for neutralization of each ion in its own gas for various ion energies. The cross section as a function of the ion energy is shown in Fig. 2.

* This work was supported in part by the Office of Naval Research under Contract N6Onr-248 T.O.I.

[1] Kallmann and Rosen, Zeits. f. Physik 61, 61 (1930).

[2] Rostagni, Zeits. f. Physik 88, 55 (1934).

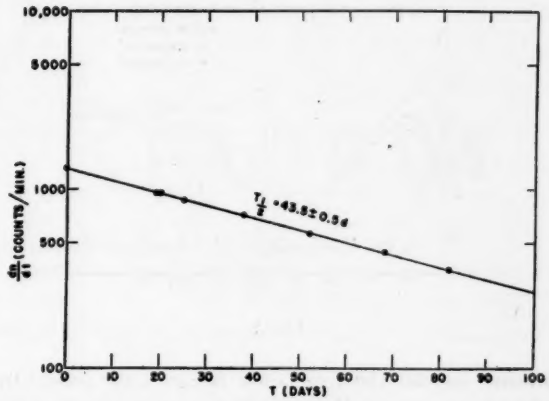

FIG. 1.

The Beta-Spectrum of $Hg^{(203)}_{(205)}$

D. SAXON
Argonne National Laboratory, Chicago 80, Illinois
August 19, 1948

THE 180° β-spectrometer has been used to measure the long-lived $Hg^{(203)}_{(205)}$ activity. In their final work, G. Friedlander and C. S. Wu[1] found 51.5±1.5 days for the half-file, 460 kev for the β-end point by absorption in Al, and a γ-ray of 300 kev by absorption in Pb. L. C. Miller and L. F. Curtiss,[2] using a thin lens spectrometer, obtained the β-end point as <0.3 Mev and the γ-energy as 0.28 Mev.

The sample, in the form of the oxide, was irradiated in the Argonne heavy-water pile. After allowing a month for the shorter activities to decay, the half-life measurements were started; at present they indicate a single activity of 43.5±0.5 days (see Fig. 1). The sample is still being followed to see if a longer-lived tail exists, possibly explaining the large difference between the present value and that of Friedlander and Wu.

The source for the spectrometer was of thickness ~2.4 mg/cm², mounted on Nylon backing of 0.54 mg/cm². The resolution $\Delta H\rho/H\rho$ finally used was 2 percent; a previous source used at 1 percent proved to be too weak.

In Fig. 2 the spectrum shape is shown for two values of window thickness—the first 0.05 mg/cm², the second ~0.2 mg/cm², both of Nylon. It is clear that the true β-end point is hidden in the K and L conversion lines of the γ-ray. The previous β-end-point measurements included these lines and are, accordingly, much too high. In that of Miller and Curtiss, the source was quite thick, 20 mg/cm² mounted on 3-mg/cm² backing, with the counter window 2.36 mg/cm². This means that, essentially, the continuous β-spectrum was not counted in their measurement.

To get the true end point, and a comparison for spectrum shape, the Kurie plot of the Fermi theory is shown in Fig. 3. Below the K line the plot is linear back to 40 kev, then falls rapidly as a result of window absorption. Extrapolating the linear portion through the base of the K line, the end point is obtained as 205±10 kev. Using this end point, with the half-life of 43.5 days, the ft value was computed at 2.6×10^6. This places the activity in the first forbidden empirical classification. However, from the linearity of the Kurie plot, the spectrum shape, where visible, is allowed. Thus the total forbidden correction factor is constant with energy, the theory giving this for $\Delta J=0, \pm1$, with any of the interactions for heavy elements.[3]

From the K and L conversion lines, the energy of the γ-ray is 286±5 kev, correction for the resolution having been made. This agrees well with the value of Miller and Curtiss.

The present result assumes the γ-ray after the simple β-transition to $Tl^{(203)}_{(205)}$, checked by the decay of the conversion lines with the Hg period.

The conversion coefficients are as follows:

$E(\gamma)$	K	L	M	K/L	L/M
286	18%	6%	≤0.5%	3	≥12

Assuming the radiation to be electric multipole, and extrapolating the theoretical ratio[4] for K/L to high Z, it is found that the γ-ray has $\Delta l=2$.

Friedlander and Wu produced the Hg activity with both fast and slow neutrons, and thus suggested the mass assignment of 203. No check on this was made with the

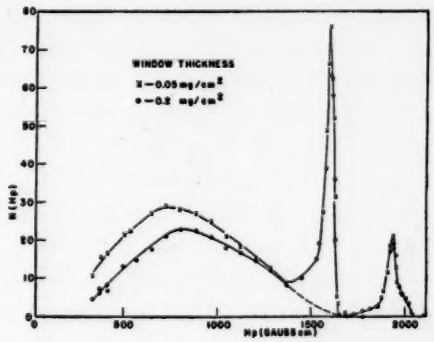

FIG. 2.

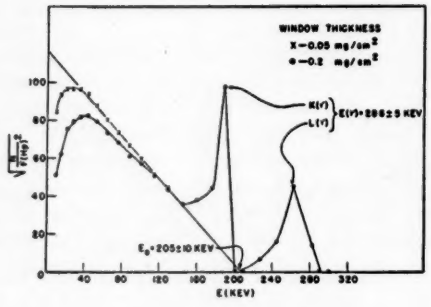

FIG. 3.

present sample, the irradiation being made essentially with slow neutrons. However, the recent analysis of the Hg isotopes by Inghram, Hess, and Hayden[5] makes almost certain the 203 mass assignment.

The author wishes to thank W. Woelf for help in taking the spectrometer data.

[1] G. Friedlander and C. S. Wu, Phys. Rev. **63**, 227 (1943).
[2] L. C. Miller and L. F. Curtiss, Phys. Rev. **70**, 983 (1946).
[3] E. J. Konopinski and S. E. Uhlenbeck, Phys. Rev. **60**, 308 (1941).
[4] M. H. Hebb and E. Nelson, Phys. Rev. **58**, 486 (1940).
[5] M. S. Inghram, D. C. Hess, Jr., and R. J. Hayden, Phys. Rev. **71**, 561 (1947).

Erratum: A Rapid Method for the Determination of the Maximum Energies of β-Emitters with Simple Spectra

[Phys. Rev. **73**, 1400 (1948)]

L. YAFFE AND KATHARINE M. JUSTUS
Chemistry Branch, Division of Atomic Energy, National Research Council of Canada, Chalk River, Ontario, Canada

June 18, 1948

Line 5 should read "50 micrograms/cm²," *not* "50 milligrams/cm²."

Erratum: An Example of the Beta-Decay of the Light Meson

E. C. FOWLER, R. L. COOL, AND J. C. STREET
Lyman Laboratory of Physics, Harvard University, Cambridge, Massachusetts

[Phys. Rev. **74**, 101 (1948)]

THE photograph of Fig. 1 on page 101 has been inverted. The separate views of the cloud chamber were mounted as a single photograph so that the proper orientation can be obtained by rotating the figure through 180°.